Molecular basis of HS memory in
Arabidopsis thaliana

Vicky Oberkofler

publikationsbasierte Univ.-Diss.

zur Erlangung des akademischen Grades
"doctor rerum naturalium"
(Dr. rer. nat.)
in der Wissenschaftsdisziplin "Molekulare Pflanzenphysiologie"

eingereicht an der
Mathematisch-Naturwissenschaftlichen Fakultät
Institut für Biochemie und Biologie
der Universität Potsdam

Ort und Tag der Disputation: Potsdam, 14.10.2022

Hauptbetreuerin: Prof. Dr. Isabel Bäurle
Gutachter*innen: Prof. Dr. Isabel Bäurle
                   Prof. Dr. Tina Romeis
                   Prof. Dr. Daniel Schubert

Acknowledgements

Statement of authorship

I hereby declare that this thesis is the result of my own work. My work was carried out independently and exclusively with the specified means. This thesis has exclusively been submitted to the University of Potsdam as part of the examination process for a doctoral degree.

Potsdam, June 2022

Vicky Oberkofler

Abstract

Plants can be primed to survive the exposure to a severe heat stress (HS) by prior exposure to a mild HS. The information about the priming stimulus is maintained by the plant for several days. This maintenance of acquired thermotolerance, or HS memory, is genetically separable from the acquisition of thermotolerance itself and several specific regulatory factors have been identified in recent years.

On the molecular level, HS memory correlates with two types of transcriptional memory, type I and type II, that characterize a partially overlapping subset of HS-inducible genes. Type I transcriptional memory or sustained induction refers to the sustained transcriptional induction above non-stressed expression levels of a gene for a prolonged time period after the end of the stress exposure. Type II transcriptional memory refers to an altered transcriptional response of a gene after repeated exposure to a stress of similar duration and intensity. In particular, enhanced re-induction refers to a transcriptional pattern in which a gene is induced to a significantly higher degree after the second stress exposure than after the first.

This thesis describes the functional characterization of a novel positive transcriptional regulator of type I transcriptional memory, the heat shock transcription factor HSFA3, and compares it to HSFA2, a known positive regulator of type I and type II transcriptional memory. It investigates type I transcriptional memory and its dependence on HSFA2 and HSFA3 for the first time on a genome-wide level, and gives insight on the formation of heteromeric HSF complexes in response to HS. This thesis confirms the tight correlation between transcriptional memory and H3K4 hyper-methylation, reported here in a case study that aimed to reduce H3K4 hyper-methylation of the type II transcriptional memory gene *APX2* by CRISPR/dCas9-mediated epigenome editing. Finally, this thesis gives insight into the requirements for a heat shock transcription factor to function as a positive regulator of transcriptional memory, both in terms of its expression profile and protein abundance after HS and the contribution of individual functional domains.

In summary, this thesis contributes to a more detailed understanding of the molecular processes underlying transcriptional memory and therefore HS memory, in *Arabidopsis thaliana*.

Table of Contents

List of abbreviations

This list contains, in alphabetical order, all abbreviations that are used in the sections General Introduction, General Discussion and Perspectives. Abbreviations used in the three presented manuscripts are excluded.

°C	degree Celsius
5'	five-prime
ABA	abscisic acid
ABF	abscisic acid-responsive transcription factor
ACC	acclimation
ADP	adenosine diphosphate
AHA	aromatic and large hydrophobic amino acids embedded in acidic context
AHG3	abscisic acid-hypersensitive germination 3
APX	ascorbate peroxidase
AREB	abscisic acid-responsive element binding protein
ARP6	actin-related protein 6
ASF1	anti-silencing function 1
ASH2R	*Arabidopsis* ASH2 relative
aTT	acquired thermotolerance
ATX	*Arabidopsis* trithorax
ATXR	*Arabidopsis* trithorax-related
bHLH	basic helix-loop-helix
BiFC	bimolecular fluorescence complementation
bp	base pair
BRM	brahma
BRU1	brushy1/tonsoku/mgoun3
BTH	acibenzolar-S-methyl
bTT	basal thermotolerance
bZIP	basic leucine zipper
Ca²⁺	divalent calcium ion
CaM3	calmodulin 3
CAT	catalase
ChIP-qPCR	chromatin immunoprecipitation followed by quantitative PCR
ChIP-seq	chromatin immunoprecipitation followed by sequencing
CHR	chromatin remodeling protein
CLF	curly leaf
Col-0	*Arabidopsis* ecotype Columbia-0
COMPASS	complex proteins associated with SET1
COR15A	cold-regulated 15A
CRISPR/Cas9	clustered regularly interspaced short palindromic repeats/ CRISPR associated protein 9
DBD	DNA-binding domain
dCas9	catalytically dead Cas9

dJMJ	catalytically dead Jumonji
DNA	deoxyribonucleic acid
DREB	dehydration-responsive element binding protein
e.g.	exempli gratia, for example
EMS	ethyl methanesulfonate
ER	endoplasmic reticulum
E(Z)	enhancer of zeste
FAD	flavin adenine dinucleotide
FAO	Food and Agriculture Organization of the United Nations
Fe(II)	element iron in its +2 oxidation state
FGT	forgetter
FLC	flowering locus C
FLD	flowering locus D
FT	flowering locus T
FWA	flowering Wageningen
GAL1	galactokinase 1
GO	gene ontology
h	hour
H	histone
H2Bub	histone 2B monoubiquitination
H3K4me	histone 3 lysine 4 (mono-, di-, or tri)methylation
H3K4me1	histone 3 lysine 4 monomethylation
H3K4me2	histone 3 lysine 4 dimethylation
H3K4me3	histone 3 lysine 4 trimethylation
H3K9ac	histone 3 lysine 9 acetylation
H3K9me2	histone 3 lysine 9 dimethylation
H3K27me3	histone 3 lysine 27 trimethylation
H3K36me3	histone 3 lysine 36 trimethylation
H4K12ac	histone 4 lysine 12 acetylation
HAC	histone acetyltransferase
HDAC	histone deacetylase
HKDM	histone lysine demethylase
HKMT	histone lysine methyltransferase
HKT1	high-affinity K^+ transporter
HLP1	hikeshi-like protein 1
HR-A/B	hinge region A/B
HS	heat stress
HSA32	heat stress-associated 32-kD protein
HSE	heat shock element
HSF	heat shock transcription factor
HSP	heat shock protein
HY5	hypocotyl elongation 5
HYH	HY5-homolog
i.e.	id est, that is
IFN-γ	interferon gamma
INO1	inositol-1-phosphate synthase
IPCC	Intergovernmental Panel on Climate Change
JA	jasmonic acid
JMJ	Jumonji
JmjC	Jumonji C
K	lysine

K⁺	monovalent potassium ion
KYP	kryptonite
LBD	lateral organ boundaries domain
LDL	lysine specific demethylase 1 like
LSD	lysine specific demethylase
LTP	lipid transfer protein
LUC	luciferase
maTT	maintenance of acquired thermotolerance
MBF1C	multiprotein bridging factor 1C
MED	mediator
min	minute
MLL1	mixed-lineage leukemia 1
NAC	NAM (no apical meristem), ATAF1,2 and CUC2 (cup-shaped cotyledon)
NCED3	9-*cis*-epoxycarotenoid dioxygenase 3
NES	nuclear export signal
NLS	nuclear localization signal
NO	nitric oxide
NPC	nuclear pore complex
OD	oligomerization domain
P5CS1	Δ^1-pyrroline-5-carboxylate synthetase 1
PCR	polymerase chain reaction
PHD	plant homeodomain
PIC	preinitiation complex
PLDα2	phospholipase D alpha 2
PP2C	protein phosphatase 2C
PRC2	polycomb repressive complex 2
RAB18	responsive to ABA
RBBP5	retinoblastoma-binding protein 5
RD	responsive to desiccation
RNA	ribonucleic acid
RNA Pol II	RNA polymerase II
RNA-seq	RNA sequencing
ROF1	rotamase FK506 binding protein 1
ROS	reactive oxygen species
SA	salicylic acid
SAG	senescence-associated gene
SAM	S-adenosylmethionine
SDG	SET-domain group
Ser5P Pol II	polymerase II phosphorylated at serine 5
SET	suppressor of variegation 3-9, enhancer of zeste, trithorax
SFL1	suppressor gene for flocculation 1
sgRNA	single guide RNA
sHSP	small heat shock protein
SPP1	subunit of COMPASS (SET1C) PHD finger protein 1
SUV	suppressor of variegation
SWN	swinger
SWR1	SWI2/SNF2-related 1 chromatin remodeling
TAF3	TATA-box binding protein associated factor 3
TBP	TATA-binding protein
TDR	temperature-dependent repression domain

TET1	ten-eleven translocation1
TF	transcription factor
TFIID	transcription factor II D
TSS	transcriptional start site
UPR	unfolded protein response
UTR	untranslated region
VIN3	vernalization insensitive 3
VP64	virus protein 64
VRN5	vernalization 5
WDR5A	human WDR5 (WD40 repeat) homolog A
WRKY	WRKY transcription factor
Ws-0	*Arabidopsis* ecotype Wassilewskija-0

List of figures and tables

This list contains all figures and tables that are part of the sections General Introduction and General Discussion. Figures and tables used in the three presented manuscripts are excluded.

Fig. 1: Transcriptional memory and transcription pattern of non-memory genes in response to heat stress

Fig. 2: HSF domain organization in plants

Fig. 3: Distribution of H3K4 methylation of plant genes

Fig. 4: Molecular mechanisms of HS memory associated with transcriptional memory

Supplementary Table 1: Results of mutant screen of HKMTs and HKDMs for altered physiological HS memory

General Introduction

The work presented in this thesis aimed to contribute to the understanding of molecular mechanisms governing maintenance of acquired thermotolerance, or heat stress (HS) memory, in *Arabidopsis thaliana* (*Arabidopsis*). I will first introduce the general concept of plant heat stress responses including HS memory and the associated transcriptional memory. I will then introduce the family of heat shock transcription factors (HSFs), which are key components of the HS response. I will give an overview of how plant chromatin responds to HS, with a particular focus on histone lysine methylation, and will summarize current knowledge about the relationship between transcription factors, chromatin, and transcriptional memory. I will introduce the CRISPR/Cas9 system as a powerful tool to modify chromatin status at individual loci. Finally, I will summarize current knowledge about the molecular mechanisms of transcriptional memory in *Arabidopsis*.

Heat stress responses in plants

During their life time, plants are exposed to a variety of abiotic and biotic stressors, such as temperature extremes, drought, flooding, hypersalinity, as well as phytopathogen and herbivore attacks. Anthropogenic climate change is exacerbating the frequency and intensity at which most of these events occur (IPCC, 2021). HS refers to the exposure of organisms to a temperature above their optimum range for growth, at which development and reproduction, and therefore survival, are negatively affected (Richter, Haslbeck and Buchner, 2010). HS negatively affects structural integrity and function of different macromolecules in the cell, leading to a state of imbalance (Mittler, Finka and Goloubinoff, 2012). The HS response of plants involves profound changes of the transcriptome, proteome, metabolome, and lipidome (Kaplan *et al.*, 2004; Larkindale and Vierling, 2008; Yángüez *et al.*, 2013; Li *et al.*, 2015). These changes aim to increase the synthesis of protective and damage-repairing compounds, to optimize photosynthesis, to adjust homeostasis in order to maintain osmotic and ionic balance, and to optimize cross-talk with other stress and hormone signaling pathways (De Vos *et al.*, 2005; Mahajan and Tuteja, 2005; van Hulten *et al.*, 2006; Ding *et al.*, 2013). The universal core

response to HS of prokaryotic and eukaryotic organisms involves the transcriptional activation of *HEAT SHOCK PROTEINS* (*HSPs*) by HSFs. HSPs can be divided into different functional classes such as molecular chaperones and metabolic enzymes, and are involved in restoring/maintaining cellular homeostasis (Richter, Haslbeck and Buchner, 2010). Molecular chaperone HSPs have the primary role of stabilizing partially folded protein intermediates. They do not contain specific information about the correct folding of a certain substrate but rather prevent formation of aggregates by interfering with unproductive interactions between substrates (Baniwal *et al.*, 2004). Chaperone HSPs are divided into different families based on their molecular weight: HSP100, HSP90, HSP70, HSP60, and small HSPs (sHSPs) (Kotak *et al.*, 2007). The precise substrates and catalytic modes of action of the different HSP families are not known. Members of different HSP families likely interact with each other in a concerted manner to maintain or restore protein homeostasis in the cell (Baniwal *et al.*, 2004). An example of metabolic enzyme HSPs are reactive oxygen species (ROS) scavengers such as ASCORBATE PEROXIDASES (APX) and CATALASES (CAT) (Vanderauwera *et al.*, 2011; Ohama *et al.*, 2017).

Plants have evolved distinct responses to different types of HS. These responses are mediated by both common and distinct molecular factors, and include basal thermotolerance and acquired thermotolerance (Mittler, Finka and Goloubinoff, 2012; Yeh *et al.*, 2012). Basal thermotolerance is defined as tolerance towards severe HS (generally 44 °C for *Arabidopsis thaliana* seedlings) without prior exposure to elevated temperature. Acquired thermotolerance is defined as increased ability to withstand severe HS achieved by prior exposure to moderate HS (36-38 °C for *Arabidopsis thaliana* seedlings). Acquisition of thermotolerance is an example of priming, which defines a process that is set in motion after exposure to a first, priming stimulus, in order to positively impact an organism's performance upon exposure to a second, triggering stimulus (Hilker *et al.*, 2016). In *Arabidopsis*, the primed state after acquisition of thermotolerance is maintained over time as priming and triggering HS can be spaced several days apart before the plants' performance in response to the triggering HS returns to baseline thermotolerance levels (Charng *et al.*, 2006; Stief *et al.*, 2014). This maintenance of acquired thermotolerance, or HS memory, is an active process and several specifically required factors have been characterized (Charng *et al.*, 2006, 2007; Meiri and Breiman, 2009; Brzezinka *et al.*, 2016; Lämke *et al.*, 2016; Brzezinka, Altmann

and Bäurle, 2019; Urrea Castellanos *et al.*, 2020). HS memory positively correlates with transcriptional memory. The term transcriptional memory refers to particular transcription patterns of genes in response to single or multiple stress exposures (reviewed in Bäurle, 2018). Here, I distinguish between type I transcriptional memory or sustained induction, and type II transcriptional memory, in particular enhanced re-induction (**Fig. 1**). Sustained induction refers to the differential expression (upregulation) of a gene relative to non-stressed baseline expression level that is maintained for several days after the end of stress exposure. Type II transcriptional memory in general describes the altered transcriptional response of a gene to repeated stress exposure, where the stress is of similar duration and intensity each time. An important feature of type II transcriptional memory is that gene expression returns to baseline expression levels in the recovery phase in between stresses. Enhanced re-induction refers to a particular subtype of type II transcriptional memory in which a gene, which is induced above baseline expression upon a first stress treatment, is induced significantly higher upon a second stress exposure. These type II memory genes are variously referred to in literature as (+/+) memory genes (e.g. Ding *et al.*, 2013) or (+/++) memory genes (e.g. H. Liu *et al.*, 2018). Another subtype of type II transcriptional memory is sensitization, which describes genes that are only induced after repeated exposure to stress, but not after a single stress exposure (Friedrich *et al.*, 2019). These genes are also referred to as (0/+) memory genes (e.g. H. Liu *et al.*, 2018).
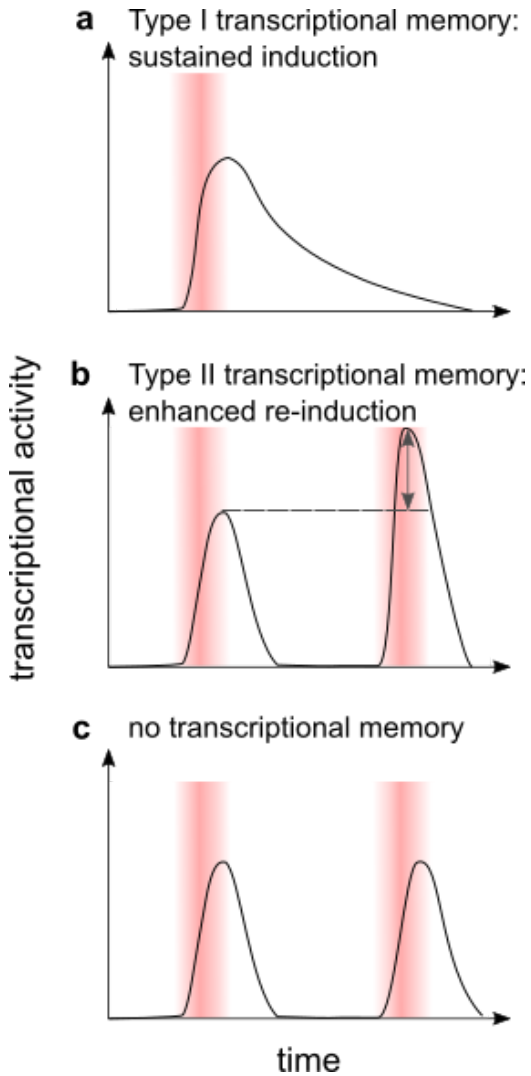
Fig. 1: Transcriptional memory and transcription pattern of non-memory genes in response to heat stress. HS memory in *Arabidopsis thaliana* is associated with two types of transcriptional memory, type I (sustained induction) (**a**), and type II (**b**). (**a**) Sustained induction describes transcriptional activity that exceeds non-stressed baseline expression levels for an extended period after initial HS (red) has ceased. (**b**) Type II transcriptional memory describes altered transcriptional activity in response to two temporally separated stresses of similar intensity and duration. The stress exposures are separated by a stress-free interval during which transcriptional activity returns to baseline levels. In the case of enhanced re-induction, transcriptional activity is induced after both stresses, and to a higher degree after the second stress exposure. (**c**) HS-inducible genes that have no transcriptional memory are induced to a similar degree after each re-occurring stress exposure. Figure from Oberkofler, Pratx and Bäurle, 2021.

The plant heat shock transcription factor family

Changes in gene expression due to binding and activation of target genes by HSFs are key to the eukaryotic HS response (Wu, 1995; Nover, Bharti and Scharf, 2001). Compared to other eukaryotes, the number of HSFs in the plant kingdom is notably high, likely reflecting gene and whole genome duplication events followed by both gene loss and subfunctionalization (Wang *et al.*, 2018). For example, the yeast (*Saccharomyces cerevisiae*) genome encodes 1 HSF protein and 3 HSF-related proteins, *Caenorhabditis elegans* and *Drosophila melanogaster* both encode a single HSF, and vertebrates have 4 HSFs (Scharf *et al.*, 2012), while monocot and eudicot species encode an average number of almost 30 HSFs (Wang *et al.*, 2018). There are 21 *HSF*-encoding genes in the *Arabidopsis* genome (Nover, Bharti and Scharf, 2001).

Domain architecture of HSFs is modular and well conserved (**Fig. 2**). They have a DNA-binding domain (DBD) located at the N-terminus which consists of 3 α-helixes (H1, H2, H3) and one β-sheet with 4 antiparallel β-strands (β1, β2, β3, β4). The central helix-turn-helix (H2-T-H3) motif binds to heat shock element (HSE) sequence motifs with consensus sequence 5'-AGAAnnTTCT-3' (Damberger *et al.*, 1994; Harrison, Bohm and Nelson, 1994; Vuister *et al.*, 1994; Nover, Bharti and Scharf, 2001). Genome-wide analyses of direct targets and binding kinetics of HSFs are still largely lacking. The DBD is connected to the hinge region (HR-A/B) or oligomerization domain (OD) by a flexible linker of varying length. The OD consists of 2 heptameric repeats of hydrophobic amino acids which form a coiled-coil-like structure (Peteranderl and Nelson, 1992; Peteranderl *et al.*, 1999; Scharf *et al.*, 2012). In general, the OD is subjected to low evolutionary selective pressure compared to the DBD (Wang *et al.*, 2018). So far, little research activity has focused on investigating formation and functional specialization of the potentially very large number of heteromeric HSF complexes. Tomato HSFA1A and HSFA2 heterodimerize and synergistically promote the expression of HS-responsive genes (Chan-Schaminet *et al.*, 2009). Tomato HSFA1A and HSFB1 interact to recruit HISTONE DEACETYLASE 19 (HDAC19) to target gene promoters (Bharti *et al.*, 2004). In *Arabidopsis*, HSFA4 and HSFA5 preferentially form heterodimers, whereas neither protein interacts with HSFA1 or HSFA2 (Baniwal *et al.*, 2007). Most HSFs possess a nuclear localization signal (NLS) and a nuclear export signal (NES) for shuttling between

cytosol and nucleus. The NLS consists of one or two clusters of basic amino acids and the NES is a hydrophobic, usually leucine-rich sequence motif (Scharf *et al.*, 2012). The C-terminus of most HSFs contains AHA (aromatic and large hydrophobic amino acids embedded in acidic context) activator motifs. They are crucial for the activator function and likely interact with basal transcriptional machinery as this type of activator motif is common among different types of eukaryotic transcription factors (Döring *et al.*, 2000).
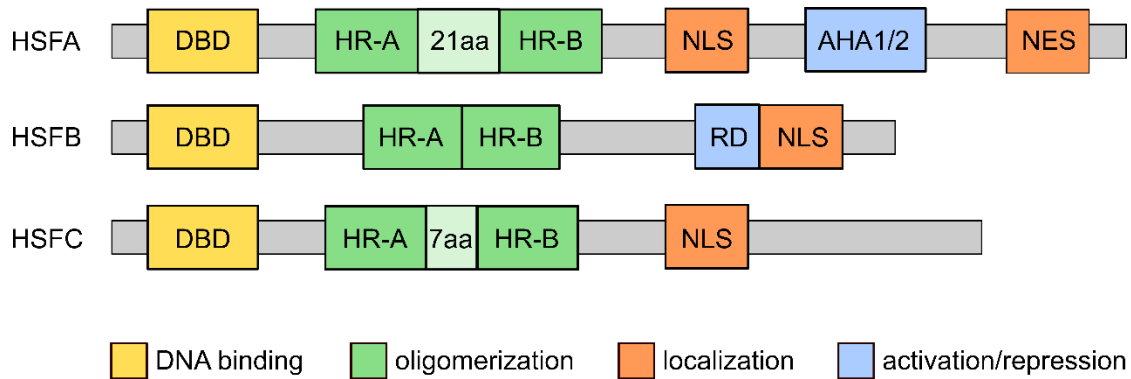
Fig. 2: HSF domain organization in plants. Plant HSFs are divided into 3 classes (A, B, C) and are characterized by the presence of specific domains that determine DNA binding, oligomerization, subcellular localization, and activation/repression function. DBD, DNA-binding domain; HR-A/B, hinge region A/B; NLS, nuclear localization signal; AHA1/2, aromatic and large hydrophobic amino acids embedded in acidic context motif 1/2; NES, nuclear export signal; RD, repression domain. Figure adapted from Scharf *et al.*, 2012.

Based primarily on the presence and length of an amino acid insertion in between the 2 heptameric repeats in the OD, as well as on the length of the flexible linker, plant HSFs are divided into 3 classes (**Fig. 2**). In *Arabidopsis*, there are 15 class A HSFs (A1-A9), 5 class B HSFs (B1-B4), and 1 class C HSF (C1) (Nover, Bharti and Scharf, 2001). Class A HSFs represent the evolutionarily youngest class and have evolved only after plants moved to land. They are also the most diverse group of HSFs as they were under less selective pressure than classes B and C (Wang *et al.*, 2018). Recently, a novel conserved region localized C-terminally of the NLS of HSFA1s of different plant species, including *Arabidopsis*, was identified (Ohama *et al.*, 2016). Based on deletion experiments with AtHSFA1D, this region was termed the temperature-dependent

repression domain (TDR). The TDR interacts with HSP70/90 and truncated HSFA1D proteins lacking the TDR localize to the nucleus and transcriptionally activate a subset of HSFA1D target genes in the absence of HS (Ohama *et al.*, 2016). A particular characteristic of class B HSFs is the presence of a LFGV tetrapeptide repressor domain close to the NLS (Ikeda and Ohme-Takagi, 2009). *Arabidopsis* HSFB1 and HSFB2B are transcriptional repressors, but also positive regulators of acquired thermotolerance (Kumar *et al.*, 2009; Ikeda, Mitsuda and Ohme-Takagi, 2011). Class C HSFs do not possess AHA motifs and their function has not been elucidated (Scharf *et al.*, 2012).

Signaling network of the plant heat stress response

HS generates signals that are perceived and transduced to activate different transcription factors (TFs) which mediate HS-induced changes of gene expression in the context of a complex transcriptional regulatory network (reviewed in (Ohama *et al.*, 2017)). HSFA1s are often considered the master regulators of the HS response. Several signaling pathways converge on HSFA1s. Post-translational modification, especially phosphorylation, of HSFs is widely postulated, but experimental evidence is scarce. HSFA1s interact with various protein kinases and phosphatases that are regulators of the HS response (Reindl *et al.*, 1997; H.-T. Liu *et al.*, 2007), but it is not known if, when, where, and which percentage of the total HSFA1 protein pool is phosphorylated. It is postulated that CALMODULIN 3 (CaM3) may be a central regulator of these kinases and phosphatases, and it is in turn a key transducer of Ca^{2+} fluxes and ROS/ nitric oxide (NO) signaling pathways that are activated upon HS (H.-T. Liu *et al.*, 2007; Liu *et al.*, 2008; W. Zhang *et al.*, 2009; Xuan *et al.*, 2010; Wang *et al.*, 2014). An additional layer of HSFA1 regulation is mediated by the accumulation of misfolded and unfolded proteins in the cytosol and in the endoplasmic reticulum (ER) during HS. According to the chaperone titration model, these folding intermediates sequester part of the HSP chaperone pool in the cell, leading to the dissociation and activation of previously bound HSF proteins (Richter, Haslbeck and Buchner, 2010). In the cytosol, these chaperones include HSP70 and HSP90 (Richter, Haslbeck and Buchner, 2010). In the ER, an analogous regulatory mechanism acts on the master regulators of the local unfolded

protein response (UPR), basic leucine zipper (bZIP) transcription factors bZIP28 and bZIP60 (Iwata and Koizumi, 2005; J.-X. Liu *et al.*, 2007; Song *et al.*, 2015).

In *Arabidopsis*, the 4 existing HSFA1s (A, B, D, and E) are partially redundant as different types of HS tolerance are only affected in higher order mutants (Liu, Liao and Charng, 2011). HSFA1s directly induce the transcription of other transcriptional (co)activators which are involved in the HS response, such as *HSFA2*, *HSFA7A*, *HSFB1*, *HSFB2B*, *DEHYDRATION-RESPONSIVE ELEMENT BINDING PROTEIN 2A* (*DREB2A*), and *MULTIPROTEIN BRIDGING FACTOR 1C* (*MBF1C*) (Ohama *et al.*, 2017). *HSFA3* expression upon HS is in turn induced by several DREB2 isoforms (Sakuma *et al.*, 2006; Schramm *et al.*, 2007; Yoshida *et al.*, 2008; Chen *et al.*, 2010).

Plant chromatin and stress responses

Chromatin is the complex of DNA and various proteins in the nucleus. The basic building block of eukaryotic chromatin is the nucleosome, which consists of approximately 146 bp of DNA wrapped around a histone octamer which contains two histone proteins H2A, H2B, H3, and H4, each (Luger, 1997). Histones, in particular their N-terminal tails which protrude from the globular core, are targets of post-transcriptional modifications such as acetylation, methylation, phosphorylation, ubiquitination, sumoylation, and ADP-ribosylation (Rothbart and Strahl, 2014). By changing the net charge of histones, these modifications can alter the affinity between negatively charged DNA and generally positively charged histones. Post-translational modification of histones can create or occlude binding sites of multiple chromatin and transcriptional regulators, so called "readers". Readers recognize these modifications through several specific domains, e.g. the PLANT HOMEODOMAIN (PHD) or the chromodomain (reviewed in Scheid, Chen and Zhong, 2021). Post-translational histone modifications alter the accessibility and the transcriptional potential of the chromatin environment. Certain histone variants, histone modifications, and DNA methylation tend to preferentially co-localize, forming up to nine distinct chromatin landscapes in the plant genome with specific biochemical and functional properties (Roudier *et al.*, 2011; Sequeira-Mendes *et al.*, 2014). For example, promoter and 5' UTR regions that are actively transcribed tend to be enriched in histone H3 lysine 4 tri- and dimethylation (H3K4me3 and H3K4me2), histone H3 acetylation,

histone H3 lysine 36 trimethylation (H3K36me3), histone H2B monoubiquitination (H2Bub), and histone variant H2A.Z (Sequeira-Mendes *et al.*, 2014). In plants, all forms of H3K4 methylation are predominantly associated with genes (**Fig. 3**). H3K4me3 and H3K4me2 are enriched in the promoter and 5' region of genes around the transcriptional start site (TSS), while H3K4me1 is distributed within the gene body (X. Zhang *et al.*, 2009).
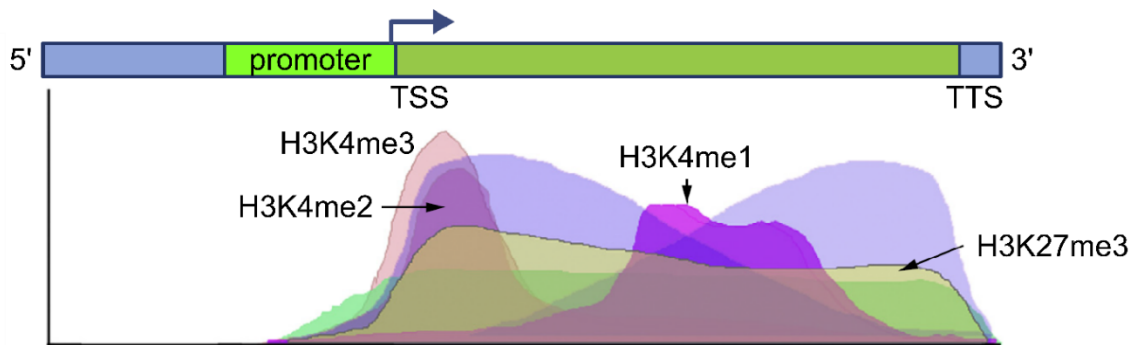
Fig. 3: Distribution of H3K4 methylation of plant genes. While di- and trimethylated lysine K4 (H3K4me2, H3K4me3) are mostly enriched in promoter and 5' regions of genes, monomethylated lysine K4 (H3K4me1) is distributed within the gene body. TSS, transcriptional start site; TTS, transcription termination site. Figure adapted from Xiao, Lee and Wagner, 2016.

Histone lysine methyltransferases and demethylases

In plants, histone lysine methylation has been shown for histones H3 and H4. H4 lysine methylation takes place at K20 (Naumann *et al.*, 2005). H3 lysine methylation takes place at K4, K9, K27, and K36. In general, H3K4 and H3K36 methylation are associated with gene expression, while H3K9 and H3K27 methylation are associated with transcriptional repression (Pfluger and Wagner, 2007). Lysine can be mono-, di-, or trimethylated (Xiao, Lee and Wagner, 2016; Hyun *et al.*, 2017).

Histone lysine methylation is catalysed by HISTONE LYSINE METHYLTRANSFERASES (HKMTs) (Xiao, Lee and Wagner, 2016). Catalytic activity of HKMTs is based on the transfer of a methyl group from donor S-adenosylmethionine (SAM) to the amine group of the acceptor lysine residue and resides in the SET domain (Qian and Zhou, 2006).

The SET domain is named after the three *Drosophila melanogaster* HKMTs SUPPRESSOR OF VARIEGATION 3-9 (SUV39), ENHANCER OF ZESTE (E(Z)), and TRITHORAX (Ng *et al.*, 2007). Hence, HKMTs are part of the superfamily of SET DOMAIN GROUP (SDG) proteins. The *Arabidopsis* genome contains approximately 49 SDG family genes. Not all of them are predicted to be functional and functionality has been proven experimentally for only a small number of putative HKMTs (Liu *et al.*, 2010; Pontvianne, Blevins and Pikaard, 2010; Xiao, Lee and Wagner, 2016). SDG proteins are divided into five main classes based on their substrate specificity and domain architecture (reviewed in Pontvianne, Blevins and Pikaard, 2010). Class I HKMTs have H3K27 methyltransferase activity. Class II HKMTs have H3K36 methyltransferase activity. Class V HKMTs have H3K9 methyltransferase activity. Class III HKMTs methylate H3K4. In *Arabidopsis*, class III has five members, ARABIDOPSIS TRITHORAX 1/ SET DOMAIN GROUP 27 (ATX1/SDG27), ATX2/SDG30, ATX3/SDG14, ATX4/SDG16, and ATX5/SDG29. Class III SDG enzymes have been implicated in development and stress response. In the *atx3/4/5* triple mutant, genome-wide levels of H3K4me2 and H3K4me3 are decreased. It has delayed vegetative and reproductive development, whereas the single and double mutants are aphenotypic (Chen *et al.*, 2017). On the other hand, both *atx4* and *atx5* single mutants are more drought stress-tolerant than wild type plants (Y. Liu *et al.*, 2018). In the same study, ATX4 and ATX5 were found to jointly and directly promote H3K4me3 deposition, RNA Pol II occupancy, and expression of *ABA-HYPERSENSITIVE GERMINATION 3* (*AHG3*), a protein phosphatase which negatively regulates ABA signaling (Nishimura *et al.*, 2004; Yoshida *et al.*, 2006). ATX1 is a positive regulator of dehydration stress tolerance, promoting the expression of several dehydration stress-responsive genes (Ding, Avramova and Fromm, 2011a). Among its targets is *9*-CIS-*EPOXYCAROTENOID DIOXYGENASE 3* (*NCED3*), which encodes the enzyme catalyzing the rate-limiting step of endogenous ABA production (Qin and Zeevaart, 1999). ATX1 directly binds *NCED3* and in the *atx1* mutant, RNA Pol II occupancy and H3K4me3 levels are decreased (Ding, Avramova and Fromm, 2011a).

In addition to the five ATX enzymes, the *Arabidopsis* genome encodes seven additional enzymes with a possible role in H3K4 methylation: ATX-RELATED1 (ATXR1)/SDG35, ATXR2/SDG36, ATXR3/SDG2, ATXR4/SDG38, ATXR5/SDG15, ATXR6/SDG34, and ATXR7/SDG25 (Avramova, 2009). ATXR2, ATXR3, and ATXR7 have been functionally characterized. ATXR2 promotes callus formation through H3K36me3 deposition at

LATERAL ORGAN BOUNDARIES DOMAIN (LBD) genes (Lee, Park and Seo, 2017) and promotes lateral root formation (Lee, Park and Seo, 2018). ATXR3 controls a large part of genome-wide H3K4me3 (Guo *et al.*, 2010). ATXR7 is involved in flowering time regulation through H3K4me3 deposition at *FLOWERING LOCUS C* (*FLC*) locus (Berr *et al.*, 2009; Tamada *et al.*, 2009). ATXR7 and ATX1 contribute to H3K4 hyper-methylation and transcription of several transposable element genes in the recovery period after prolonged, medium-intensity HS (Song *et al.*, 2020).

Histone lysine demethylation is catalysed by two different classes of HISTONE LYSINE DEMETHYLASES (HKDMs), JUMONJI C (JmjC) domain containing enzymes (JMJ), and plant homologues of LYSINE SPECIFIC DEMETHYLASE 1 (LSD1), called LSD1 LIKE (LDL) (Shi *et al.*, 2004; Xiao, Lee and Wagner, 2016). JMJ enzymes demethylate tri-, di-, and monomethylated lysine in the presence of Fe(II) and α-ketoglutarate, generating formaldehyde and succinate (Tsukada *et al.*, 2006). Substitution of the histidine which is critical for Fe(II) interaction disrupts demethylase activity of the JmjC domain (Chen, Hu and Zhou, 2011). In plants, six JMJ proteins, JMJ14-19, potentially target H3K4 methylation (Hong *et al.*, 2009). JMJ14 regulates flowering time through direct H3K4 demethylation of *FLOWERING LOCUS T* (*FT*) (Jeong *et al.*, 2009; Lu *et al.*, 2010; Yang *et al.*, 2010). Overexpression of *JMJ15* increases salt stress tolerance through downregulation of stress signaling genes (Shen *et al.*, 2014). Overexpression of *JMJ15* and *JMJ18* resulted in early flowering and reduced H3K4me3 levels at *FLC* (Yang, Han, *et al.*, 2012; Yang, Mo, *et al.*, 2012). Recently, *JMJ16* was identified as negative regulator of leaf senescence as its progressive downregulation during the plant life cycle leads to induction of positive regulators of senescence *WRKY TRANSCRIPTION FACTOR 53* (*WRKY53*) and *SENESCENCE-ASSOCIATED GENE 201* (*SAG201*) through lack of H3K4 demethylation (Liu *et al.*, 2019). H3K27me3 demethylases JMJ11, JMJ12, JMJ30, and JMJ32 have recently been characterized as positive regulators of heat acclimation and HS memory through regulation of the expression of *HSP22* and *HSP17.6C* (Yamaguchi *et al.*, 2021).

LDL proteins are amino-oxidases that demethylate di- and monomethylated lysine using flavin adenine dinucleotide (FAD) as cofactor. In plants, four homologues of LSD1 exist: FLOWERING LOCUS D (FLD), LDL1, LDL2, and LDL3 (Xiao, Lee and Wagner, 2016). FLD, LDL1, and LDL2 have been implicated in flowering time regulation through *FLC*

repression by removal of H3K4 di- and monomethyl groups (F. Liu *et al.*, 2007; Jiang *et al.*, 2007).

In summary, a single HKMT/HKDM enzyme can play multiple roles in different developmental and stress-response processes, and there is often functional redundancy between different enzymes.

Recruitment of histone lysine methyltransferases and demethylases to target loci and mechanism of positive regulation of transcription

In animals, H3K4 HKMTs exercise their catalytic activity as part of the evolutionarily conserved COMPLEX PROTEINS ASSOCIATED WITH SET1 (COMPASS)-like complex (Xiao, Lee and Wagner, 2016). In *Arabidopsis*, COMPASS-like complex subunits are ARABIDOPSIS ASH2 RELATIVE (ASH2R), HUMAN WDR5 (WD40 REPEAT) HOMOLOG A (WDR5A), and RETINOBLASTOMA-BINDING PROTEIN 5 (RBBP5) (Jiang *et al.*, 2011). The *ash2r* mutant shows genome-wide decrease of H3K4me3 (Jiang *et al.*, 2011), suggesting that at least one of the additional COMPASS-like complex subunits is required for the function of HKMTs. Targeting of the COMPASS-like complex to specific loci to mediate H3K4 methylation could be achieved by sequence-specific chromatin components (transcription factors) through specific recruitment of the HKMT enzyme, or by recruitment of the other COMPASS-like complex subunits. It was shown that bZIP28 and bZIP60 interact with ASH2 and WDR5A (Song *et al.*, 2015).

Sustained H3K4 hyper-methylation of a subset of heat-stress responsive genes is promoted by HSFA2 (Lämke *et al.*, 2016). Transcription factors HYPOCOTYL ELONGATION 5 (HY5) and HY5-HOMOLOG (HYH) promote H3K4 hyper-methylation at Δ^1-*PYRROLINE-5-CARBOXYLATE SYNTHETASE 1* (*P5CS1*) in response to osmotic stress (Feng *et al.*, 2016). In all these cases, it is not clear which HKMTs catalyze H3K4 hyper-methylation. For HKDM enzymes, it is known that transcription factors NAC DOMAIN CONTAINING PROTEIN 50 (NAC50) and NAC52 directly interact with, and are functionally associated with, JMJ14, regulating flowering time through facilitation of H3K4 demethylation and gene repression (Ning *et al.*, 2015; Zhang *et al.*, 2015).

H3K4me3 enrichment is associated with transcriptionally active genes in yeast, mammals, and plants (X. Zhang *et al.*, 2009), though the promotion of transcription is likely based on different mechanisms. In yeast, initiation of transcription precedes HKMT SET1 recruitment to the promoter region by RNA Pol II (Ng *et al.*, 2003). Contrarily, in mammalian cells, MIXED-LINEAGE LEUKEMIA 1 (MLL1) establishes H3K4me3 at promoters and this chromatin mark is subsequently bound by the PHD finger domain of the TAF3 subunit of the basal transcription factor TFIID (Vermeulen *et al.*, 2007). *Arabidopsis* lacks the TAF3 subunit completely (Lawit *et al.*, 2007), while yeast TAF3 lacks the PHD finger domain which recognizes H3K4me3 (Gangloff *et al.*, 2001). In plants, the binding of ATX1 to the promoter regions of *WRKY DNA-BINDING PROTEIN 70* (*WRKY70*), *LIPID TRANSFER PROTEIN 7* (*LTP7*), and *NCED3* does not induce H3K4me3. In this case, it is hypothesized that the initial binding of ATX1 facilitates PREINITIATION COMPLEX (PIC) assembly through direct interaction between ATX1 and TATA-BINDING PROTEIN (TBP), and that ATX1 induces H3K4me3 further downstream after being recruited to the locus by phosphorylated RNA Pol II (Ding, Avramova and Fromm, 2011b). Here, it is not clear how ATX1 is specifically recruited to these promoters. H3K4me3 enrichment due to interaction of bZIP28/bZIP60 with COMPASS-like complex is also thought to facilitate PIC assembly (Song *et al.*, 2015).

In summary, although individual interactions between TFs, HKDMs/HKMTs, and components of the COMPASS-like complex have been described, a generalized model for enzyme recruitment to specific target loci is still lacking. Similarly, the functional connection between H3K4 hyper-methylation and positive transcriptional regulation remains speculative in many cases.

Plant chromatin dynamics associated with response to temperature stimulus or stress

The transcriptional response to high and low ambient temperature or to heat and cold stress correlates with nucleosome remodeling, incorporation of histone variants, and post-translational histone modifications (Avramova, 2019; Friedrich *et al.*, 2019; Bäurle and Trindade, 2020). Some of these chromatin changes are transient; others persist after the original stimulus or stress has ceased and may contribute to the future expression potential of a gene (Avramova, 2019).

Both euchromatin and heterochromatin are responsive to environmental changes. Prolonged exposure to HS, cold stress, or a combination of the two results in transient loss of transcriptional silencing of several types of transposable elements in heterochromatic regions in *Arabidopsis* (Lang-Mladek *et al.*, 2010; Pecinka *et al.*, 2010; Tittel-Elmer *et al.*, 2010). These regions are characterized by high levels of DNA methylation and accumulation of H3K9me2. Release of transcriptional silencing is not associated with a decrease of these repressive chromatin marks or with an increase of the active H3K4me3 mark, but with reduced nucleosome occupancy and increase of H3K9/K14 acetylation. In plants, the histone variant H2A.Z is distributed across the gene body of inactive genes as well as in the promoter region of actively transcribed genes (Lei and Berger, 2020). Plants lacking ACTIN-RELATED PROTEIN 6 (ARP6), a component of the SWR1 chromatin remodeling complex which deposits H2A.Z (Mizuguchi *et al.*, 2004), are depleted in H2A.Z accumulation at +1 nucleosomes and, grown at 17 °C, phenocopy plants that are shifted from 17 °C to 27 °C. The phenotype of *arp6* mutants at low temperature correlates with the deregulation of the ambient temperature transcriptome. The temperature-dependent displacement of H2A.Z from the +1 nucleosome was shown for *HSP70*, leading to the hypothesis that H2A.Z functions as a thermosensor which regulates the transcriptional response to a shift in growth temperature (Kumar and Wigge, 2010). The H3-H4 histone chaperone ANTI-SILENCING FUNCTION 1 (ASF1) promotes expression of some HS response genes, among which *HSFA2* and several *HSPs* through H3K56 acetylation-facilitated nucleosome remodeling (Weng *et al.*, 2014). Winter annual *Arabidopsis* accessions require a prolonged exposure to low temperature during winter in order to flower in the following spring, a phenomenon called vernalization (reviewed in Amasino, 2010; Luo and He, 2020). Vernalization is by far the best studied example of cold-induced chromatin changes. At the molecular level, exposure to cold silences *FLC* which encodes a MADS-box transcription factor functioning as a repressor of flowering. *FLC* silencing is achieved by POLYCOMB REPRESSIVE COMPLEX 2 (PRC2)-mediated H3K27me3 deposition at the locus and involves both the CURLY LEAF (CLF) and SWINGER (SWN) catalytic subunits. PRC2 is recruited to the locus by PHD domain-containing proteins VERNALIZATION INSENSITIVE 3 (VIN3) and VERNALIZATION 5 (VRN5), and *VIN3* expression itself is induced upon long-term cold exposure. Additionally, exposure to cold generates *FLC* antisense long non-coding

RNAs (lncRNAs) COOLAIR (Swiezewski *et al.*, 2009; Csorba *et al.*, 2014; Tian *et al.*, 2019), COLDAIR, and COLDWRAP (Heo and Sung, 2011; Kim and Sung, 2017; Kim, Xi and Sung, 2017), which promote *FLC* silencing upstream of H3K27me3 deposition.

Epigenetic and transcription factor-based mechanisms associated with transcriptional memory in plants

Much of the current understanding of the molecular basis of type II transcriptional memory in plants was obtained by repeated dehydration stress experiments performed on *Arabidopsis* seedlings (reviewed in Avramova, 2019). Repeated dehydration stress induces four types of type II transcriptional memory, abbreviated as (+/+), (+/-), (-/+), and (-/-), respectively. The first sign refers to transcription levels upon the first stress, which can be significantly up- (+) or downregulated (-) compared to baseline transcription in a non-stressed state. The second sign compares transcription levels upon a subsequent stress exposure to first stress transcription levels.

In *Arabidopsis*, (+/+) and (+/-) dehydration stress responsive genes have been studied in detail. Initial characterization of (+/+) memory genes such as *RESPONSIVE TO DESICCATION 29B* (*RD29B*), *RESPONSIVE TO ABA 18* (*RAB18*), *P5CS1*, *LTP3*, and *LTP4*, revealed that enrichment of H3K4me3 and RNA polymerase II phosphorylated at serine 5 (Ser5P Pol II) remains elevated during the recovery phase in between stresses and increases further upon second stress exposure (Ding, Fromm and Avramova, 2012). In follow-up work, it was shown that these genes differ in their transcription state during the recovery phase. For example, transcription of *RD29B* decreases to non-stressed baseline levels during recovery after first stress exposure, while transcription of *LTP4* in the recovery phase is at intermediate levels between first stress exposure and the subsequent stress (Liu *et al.*, 2014). In contrast, non-memory genes *RD29A* and *COLD-REGULATED 15A* (*COR15A*) are induced to similar levels upon each dehydration stress and also accumulate similar amounts of H3K4me3 and Ser5P Pol II, which return to baseline levels in the recovery phase (Ding, Fromm and Avramova, 2012). Transcription of *RD29B*, *RAB18*, *LTP3*, and *LTP4* is primeable (Liu and Avramova, 2016). Exposure to jasmonic acid (JA) triggers bHLH transcription factor MYC2 binding to these loci, which recruits the Mediator complex through interaction with subunit MED25. The Mediator complex recruits PIC, and stalled Ser5P Pol II and H3K4me3

accumulate. Transcription is however only initiated in the presence of ABF transcription factors, which are only activated upon dehydration stress. For (+/-) memory genes, neither H3K4me3 nor H3K27me3 function as epigenetic marks (Liu *et al.*, 2014). In this case, their transcription upon second stress exposure is impeded by the absence of MYC2, which is itself a (+/-) memory gene (Liu *et al.*, 2014; Liu and Avramova, 2016; Liu, Staswick and Avramova, 2016). It is not clear what determines this transcriptional pattern of *MYC2*.

Priming of transcription in Arabidopsis has also been observed in response to treatment with acibenzolar S-methyl (BTH), a synthetic analogue of the plant hormone salicylic acid (SA), as well as in distal leaf tissue after local infection with *Pseudomonas syringae* pv. *Maculicola* (*Psm*) (Jaskiewicz, Conrath and Peterhänsel, 2011). More precisely, while BTH treatment itself does not induce *WRKY DNA-BINDING PROTEIN 29* (*WRKY29*) expression, it establishes H3K4me3, H3K9ac, H4K12ac and several other epigenetic modifications at the locus. Upon a challenging stress, *WRKY29* is induced to a higher extent if the plant has previously been treated with BTH. Furthermore, both *WRKY29* and *WRKY6* accumulate H3K4me3 and H3K4me2 and show trainability in response to *Psm* infection. Therefore, while the presence of chromatin marks is not sufficient to induce these genes, they could function as epigenetic marks and may be important for stronger induction upon recurring stress.

Plant roots primed by osmotic stress hyper-induce the root-specific sodium transporter *HIGH-AFFINITY K$^+$ TRANSPORTER 1* (*HKT1*). H3K27me3 is slowly but persistently lost at the *HKT1* locus following priming treatment in accordance with genome-wide loss of H3K27me3 and increase of H3K4me3/2 (Sani *et al.*, 2013). *P5CS1* also shows enhanced re-induction in response to osmotic stress which correlates with sustained accumulation of H3K4me3 in the 5' UTR and intragenic region (Feng *et al.*, 2016).

CRISPR/dCas9: a novel tool to engineer plant chromatin

The prokaryotic clustered regularly interspersed short palindromic repeats (CRISPR)/CRISPR-associated 9 (Cas9) system mediates RNA-guided site-specific double-stranded cleavage of DNA (Jinek *et al.*, 2012). A single point mutation in each of the two catalytic domains of Cas9, RuvC and HNH, generates a catalytically dead

enzyme (dCas9) (Qi *et al.*, 2013). The CRISPR/(d)Cas9 system can be repurposed to alter specific loci in a plant genome by single guide RNA (sgRNA)-mediated targeting of (d)Cas9 protein (Kumlehn *et al.*, 2018). dCas9-based fusion proteins can also be used to manipulate DNA methylation or chromatin modifications. In *Arabidopsis*, CRISPR/dCas9-based targeting of the catalytic domain of the demethylase TEN-ELEVEN TRANSLOCATION1 (TET1) of *Homo sapiens* has been used to demethylate DNA at the *FLOWERING WAGENINGEN* (*FWA*) locus (Gallego-Bartolomé *et al.*, 2018). Similarly, a DNA methyltransferase of prokaryotic origin was targeted to *FWA* to successfully methylate the locus (Ghoshal *et al.*, 2021). CRISPR/Cas9-based targeting of SET domain of *Arabidopsis* KRYPTONITE (KYP), an H3K9 methyltransferase, leads to downregulation of *FT* (Lee *et al.*, 2019). *ABSCISIC ACID (ABA)-RESPONSIVE ELEMENT BINDING PROTEIN 1* (*AREB1*) is transcriptionally activated by targeting of Arabidopsis HISTONE ACETYLTRANSERASE 1 (HAC1) to the locus (Roca Paixão *et al.*, 2019).

Current model of the contribution of transcriptional memory to HS memory in *Arabidopsis*

In *Arabidopsis*, acquired thermotolerance is maintained for several days. This duration correlates well with the duration of type I transcriptional memory (Stief *et al.*, 2014; Lämke *et al.*, 2016), which correlates with the presence of gene products encoded by memory genes throughout the lag phase between priming and triggering HS (Lämke *et al.*, 2016). The presence of these protective components, e.g. sHSP chaperones and ROS scavenging enzymes, upon exposure to triggering HS likely contributes to improved survival of primed plants compared to non-primed plants. *Arabidopsis* plants defective in one single memory gene are not always more susceptible to HS or can have pleiotropic phenotypes. Mutants in the type I transcriptional memory genes *HEAT STRESS-ASSOCIATED 32-kD PROTEIN* (*HSA32*) and *HSP21*, however, show specific phenotypic defects in maintenance of acquired thermotolerance (Charng *et al.*, 2006; Sedaghatmehr, Mueller-Roeber and Balazadeh, 2016). Our lab has successfully used a *pHSA32::HSA32-LUCIFERASE* (*LUC*) reporter line to employ genetic forward screens aimed at identifying novel regulators of maintenance of acquired thermotolerance. This

line allows efficient luciferase-based screening of multiple progeny of EMS-mutagenized seeds for altered type I transcriptional memory of the reporter gene. With this reporter line, two novel regulators of HS memory have previously been characterized by our lab, nucleosome remodeler FORGETTER 1 (FGT1), and a type 2C protein phosphatase, FGT2 (Brzezinka *et al.*, 2016; Urrea Castellanos *et al.*, 2020). The mode of action of FGT2 remains unclear (Urrea Castellanos *et al.*, 2020). FGT1 directly binds to memory genes and maintains low nucleosome occupancy close to the TSS of memory genes in the lag period after priming HS. It interacts with chromatin remodelers CHROMATIN-REMODELING PROTEIN 11 (CHR11), CHR17, and BRAHMA (BRM) (Brzezinka *et al.*, 2016). Type I and type II transcriptional memory are mediated by heat shock transcription factor HSFA2, which is specifically required for HS memory (Charng *et al.*, 2007; Lämke *et al.*, 2016; H. Liu *et al.*, 2018). HSFA2 directly binds memory gene targets and promotes sustained H3K4 hyper-methylation in the promoter region (Lämke *et al.*, 2016; H. Liu *et al.*, 2018), though the molecular mechanism and identity of the responsible HKMT is not known. It is also unclear whether H3K4 hyper-methylation contributes to transcriptional potential of memory genes or is rather a by-product of transcription. Current knowledge about mechanisms governing transcriptional memory in response to HS in *Arabidopsis* is summarized in **Fig. 4**.
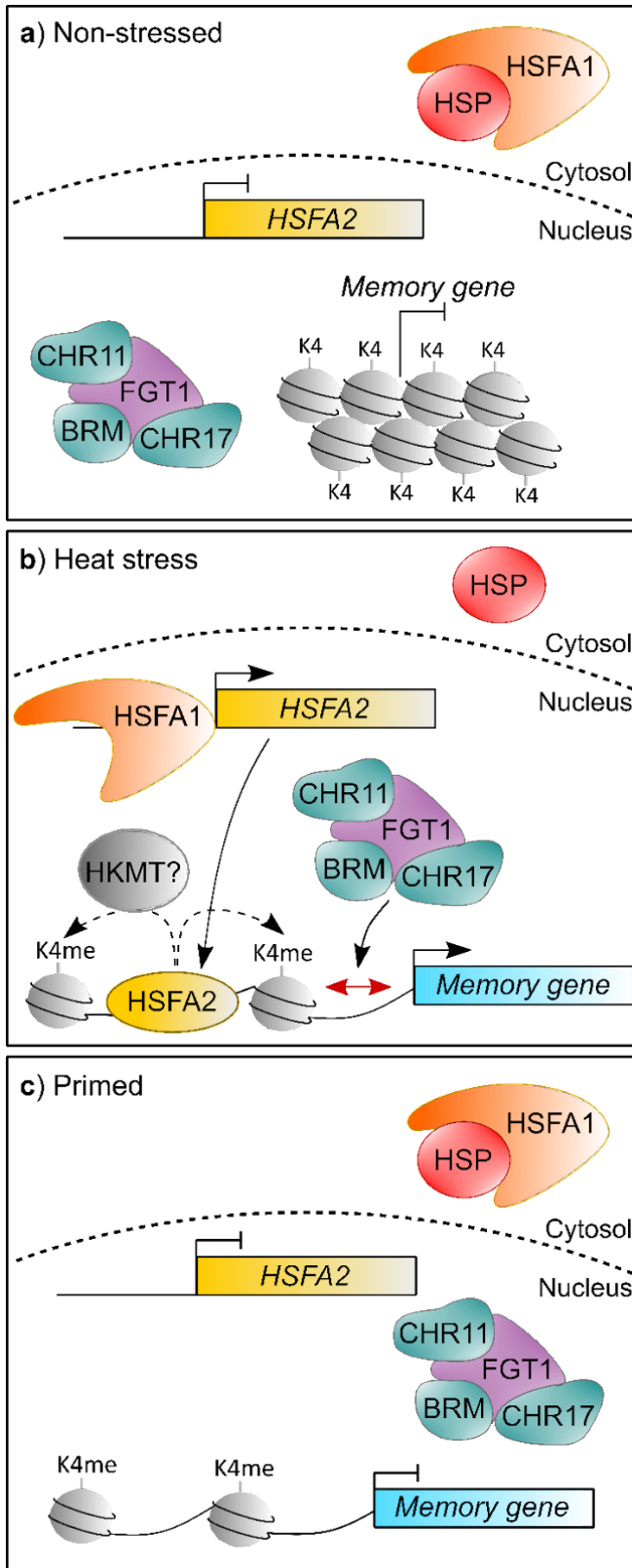
Fig. 4: Molecular mechanisms of HS memory associated with transcriptional memory. (**a**) In non-stressed conditions, target genes of the HS response, such as *HSFA2*, and memory genes, are not expressed. Memory genes are characterized by high nucleosome occupancy and low H3K4 methylation. HSFA1s are sequestered through interaction with HSP chaperones. (**b**) Upon HS, HSFA1s are released and transcriptionally activate target genes. HSFA2 and FGT1 directly bind promoters of memory genes and promote their expression. HSFA2 promotes H3K4 methylation, the HKMT enzyme which catalyzes methylation remains unknown. FGT1 forms complexes which contain BRM, CHR11, and CHR17, and reduces nucleosome occupancy around the TSS of memory genes. (**c**) After HS has ceased, the chromatin environment of memory genes remains in an open state characterized by low nucleosome occupancy and high levels of H3K4 methylation. Gene expression is primed for future stress exposure. Figure adapted from Oberkofler, Pratx and Bäurle, 2021.

24

Aim of this thesis

I present two published manuscripts and one manuscript draft which aim to elucidate different molecular aspects of HS memory.

Manuscript 1 describes the discovery by forward genetic screening and subsequent characterization of a novel positive regulator of HS memory, HSFA3. After HSFA2, HSFA3 is the second characterized HSF specifically required for HS memory. Therefore, we investigated how similar these two HSFs were in promoting type I and type II transcriptional memory and sustained H3K4 hyper-methylation after HS, as well as to which degree they could substitute for each other in absence of the respective other HSF. We investigated type I transcriptional memory and its dependence on HSFA2 and HSFA3 for the first time on a genome-wide level. Furthermore, we investigated whether HSFA2 and HSFA3 interact directly and with which other HSFs, with the aim of shedding light on HSF complex formation during HS memory.

Manuscript 2 summarizes the findings of a case study on the contribution of sustained H3K4 hyper-methylation to type II transcriptional memory of endogenous *APX2*, as well as of the reporter gene *pAPX2::LUC*, which mimics type II transcriptional memory. This was investigated by targeting dCas9 fused to catalytically active or inactive JMJ to the promoter region of these genes with the aim of interfering with H3K4me3 deposition after priming HS. The approach was developed as complementary approach to targeted screening of HKMT and HKDM mutants for altered maintenance of acquired thermotolerance with the aim to find the enzyme(s) depositing H3K4me3. This approach is further discussed in the General Discussion.

Manuscript 3 describes the results of a promoter and domain swap experiment between HSFA2, which is required for HS memory, and HSFA1D, which contributes to the general HS response. After initial findings that HSFA1D could not replace HSFA3 during HS memory (reported in **Man. 1**), I was interested to see whether this was also true for HSFA2. In a second step, I exchanged single functional domains between HSFA2 and HSFA1D to see to which degree HSFA1D domains could replace their HSFA2 counterpart, with the overarching goal to gain insight on which are the defining characteristics of a memory HSF.

Manuscript overview and candidate contributions

This section lists the three manuscripts that are included in this thesis and specifies my individual contributions to each of them.

Manuscript 1: Heteromeric HSFA2/HSFA3 complexes drive transcriptional memory after heat stress in *Arabidopsis*

Authors: Thomas Friedrich, **Vicky Oberkofler**, Inês Trindade, Simone Altmann, Krzysztof Brzezinka, Jörn Lämke, Michal Gorka, Christian Kappel, Ewelina Sokolowska, Aleksandra Skirycz, Alexander Graf, Isabel Bäurle

Status: Published in *Nature Communications*, Volume **12**, Article number 3426, 08 June 2021, https://doi.org/10.1038/s41467-021-23786-6

Candidate contributions: I generated the *pHSFA2::FLAG-HSFA2* complementation line in *hsfa2* background used in Figure 8 and Supplementary Table 3. I generated the *pHSFA3::FLAG-HSFA1D* promoter swap line in *hsfa3* background and created data shown in Figure S8e-g. Together with TF I planned the RNA-seq experiment and grew, harvested, processed and prepared samples. I then used data provided by CK to make Figure 6. I contributed to critical review of the manuscript.

Manuscript 2: Inducible epigenome editing probes for the role of histone H3K4 methylation in Arabidopsis heat stress memory

Authors: **Vicky Oberkofler**, Isabel Bäurle

Status: Published in *Plant Physiology*, 14 March 2022, kiac113, https://doi.org/10.1093/plphys/kiac113

Candidate contributions: IB and I conceived experiments. I performed experiments and analyzed them with input from IB. I created the figures. IB and I wrote the manuscript.

Manuscript 3: Promoter and domain swap analysis between Arabidopsis HSFA1D and HSFA2 gives insight into the requirements for HS memory HSFs

Authors: **Vicky Oberkofler**, Witold Szymanski, Isabel Bäurle

Status: Expected to be ready for submission within 2022

Candidate contributions: IB and I conceived experiments. I performed experiments except protein mass spectrometry and pertinent data analysis, which were performed by WS. I analyzed data with input from IB. I created the figures. I wrote the manuscript with input from IB.

Manuscript 1: Heteromeric HSFA2/HSFA3 complexes drive transcriptional memory after heat stress in *Arabidopsis*

Thomas Friedrich[1], Vicky Oberkofler[1], Inês Trindade[1], Simone Altmann[1,3], Krzysztof Brzezinka[1], Jörn Lämke[1], Michal Gorka[2], Christian Kappel[1], Ewelina Sokolowska[2], Aleksandra Skirycz[2], Alexander Graf[2] & Isabel Bäurle[1✉]

[1] Institute for Biochemistry and Biology, University of Potsdam, Potsdam, Germany

[2] Max-Planck-Institute for Molecular Plant Physiology, Potsdam, Germany

[3] Present address: School of Life Sciences, University of Dundee, Dundee, UK

✉ email: isabel.baeurle@uni-potsdam.de

T.F., V.O., S.A., K.B., and I.B. conceived and designed experiments, T.F., V.O., I.T., S.A., K.B., J.L., E.S., A.S., M.G., A.G., and C.K. performed experiments and analyzed the data. T.F. and I.B. wrote the manuscript with contributions from all authors.

ORCID:

TF: 0000-0003-2038-3670; CK: 0000-0002-1450-1864; AS: 0000-0002-7627-7925; IB: 0000-0001-5633-8068;

Abstract

Adaptive plasticity in stress responses is a key element of plant survival strategies. For instance, moderate heat stress (HS) primes a plant to acquire thermotolerance, which allows subsequent survival of more severe HS conditions. Acquired thermotolerance is actively maintained over several days (HS memory) and involves the sustained induction of memory-related genes. Here we show that *FORGETTER3/ HEAT SHOCK TRANSCRIPTION FACTOR A3* (*FGT3/HSFA3*) is specifically required for physiological HS memory and maintaining high memory-gene expression during the days following a HS exposure. *HSFA3* mediates HS memory by direct transcriptional activation of memory-related genes after return to normal growth temperatures. HSFA3 binds HSFA2, and in vivo both proteins form heteromeric complexes with additional HSFs. Our results indicate that only complexes containing bothHSFA2 and HSFA3 efficiently promote transcriptional memory by positively influencing histone H3 lysine 4 (H3K4) hyper-methylation. In summary, our work defines the major HSF complex controlling transcriptional memory and elucidates the in vivo dynamics of HSF complexes during somatic stress memory.

Introduction

Many organisms are frequently exposed to adverse environmental conditions that interfere with their development and growth and are referred to as stress. Plants can acclimate to stress conditions, and a transient stress cue can prime plants for a modified defense response upon exposure to a recurring stress after a stress-less interval[1–3]. This so-called somatic stress memory has been described in response to a number of different biotic and abiotic stress cues (reviewed in refs. [3–5]). Occasionally, stress-memory may also extend into future generations[6–8]. Somatic transcriptional memory based on enhanced re-induction of stress-induced genes following a second stress exposure has been reported for drought stress[9,10], salt stress[11] and for defense-related priming[12–14]. In these cases, chromatin modifications, in particular histone H3 lysine 4 (H3K4) methylation, have been correlated with transcriptionalmemory[9,11–13]. However, the mechanistic basis of stress-induced transcriptional memory and its conservation across different phenomena remains poorly understood. A major factor limiting global crop yields is heat stress (HS), and it is predicted that its prevalence will increase with climate change[15,16]. In response to acute HS, plants acquire thermotolerance and this is molecularly very similar to the HS response (HSR) of yeast and metazoans[17–20]. However, in nature, HS is often recurring, and plants can be primed by one HS for an improved response to a recurring HS after a stress-less lag phase of several days[3,21,22]. This HS memory is an active process as it is genetically separable from the acquisition of thermotolerance, and several genes have been identified that function specifically in HS memory[21–25]. An essential component of transcriptional HS responses across kingdoms is their activation through HEAT SHOCK FACTOR (HSF) transcription factors. Interestingly, the activity of HSF proteins is also highly relevant for aging and tumorigenesis[18,19]. While yeast only has one HSF and vertebrates have up to 4, this gene family has radiated massively in higher plants[26]. Of the 21 HSF genes in *Arabidopsis thaliana*, seven have been implicated in the HSR, among them three isoforms of *HSFA1*; *A1A*, *A1B*, and *A1D*[26–31]. The *HSFA1* genes are considered as master regulators that function in a largely analogous manner to yeast and metazoan HSF1[20]. *HSFA1* isoforms are constitutively expressed and are posttranslationally activated upon HS. They induce a suite of target genes, including many heat shock proteins (HSPs) that act as chaperones. HSFA2 specifically functions in HS memory[22] and it is very strongly induced after HS by HSFA1 proteins[28,29]. HSFA2

in turn amplifies the transcriptional induction of a subset of HS-response genes, but is not required for their initial activation. This subset overlaps with the genes that have been classified as HS memory-related genes due to their sustained induction after HS, lasting for at least two days[23]. Interestingly, HSFA2 binds only transiently to these HS memory-related genes, while HSFA2-dependent differences in transcriptional activity are mostly observed after binding of HSFA2 has decreased[32]. Chromatin profiling of HS memory-related genes revealed that HSFA2 recruits H3K4 hyper-methylation at these loci, and this correlates with the duration of the memory phase (at least 5 d)[32,33]. This HS-induced enrichment likely extends the phase of active transcription at these genes and was not present in highly HS-inducible "non-memory" genes such as *HSP70* and *HSP101*. Thus, the current model is that HSFA2 sustains transcriptional activation through the memory phase by recruiting sustained H3K4 methylation. This mediates a transcriptional memory (type I) that sustains transcriptional activity of certain genes for several days after the end of a short HS. After transcription has subsided, a second type of transcriptional memory remains active at a subset of genes. This causes enhanced transcriptional re-induction upon a recurring HS (type II transcriptional memory) and is active for 6 d after the priming HS[33]. HSFA2 is required for both types of transcriptional memory after HS[32]. However, the mechanistic basis of how HSFA2 promotes HS memory remains poorly understood. It is well established that HSF proteins form trimeric and hexameric complexes in yeast, metazoans and plants[18,34,35]. Yet, major unresolved questions are (1) whether HSFA2 is the only HSF protein in *A. thaliana* that mediates HS memory, and (2) what the composition of the HSFA2-containing HSF complexes is. (3) More generally, the composition of HSF complexes in vivo at endogenous expression levels is virtually unknown, as is the function of many of the different HSF family members in *A. thaliana*. To identify additional components required for regulation of HS memory, we have employed a reporter-based genetic screen where the HS memory gene *HSA32* was translationally fused to the *LUCIFERASE* reporter gene[24]. *HSA32* shows sustained induction after HS and the corresponding mutant is specifically defective in HS memory at the whole plant level[21,24]. Screening for mutants with normal activation but reduced maintenance of *HSA32-LUC* expression, we identified the *forgetter1* (*fgt1*) mutant[24]. *FGT1* encodes the *A. thaliana* orthologue of Drosophila *strawberry notch*, a highly conserved helicase protein that is required to maintain an open chromatin conformation through cooperation with chromatin remodeling complexes of the SWI/SNF family[24,36]. Here, we describe the isolation and characterization of the

FGT3 gene from the above screen. We show that *FGT3* encodes the *HSFA3* gene and that the *fgt3* mutant has a HS memory-specific phenotype, comparable to *hsfa2*. We provide evidence that *HSFA3* is a second key HSF underlying HS memory and that it forms heteromeric complexes with HSFA2 that efficiently promote transcriptional memory. These findings serve not only to assign function to a further important HSF family member, but also provide information about the in vivo composition of HSF complexes in *A. thaliana*.

Results

FORGETTER3 (*FGT3*) is required for HS memory and sustained induction of HSA32. To identify factors that are implicated in HS memory, we performed a mutagenesis screen for modifiers of HS-induced sustained expression of *pHSA32::HSA32-LUC*[24]. In *fgt3* mutants *HSA32-LUC* induction was normal at 1 d after a two-step HS treatment ("acclimation", ACC, Fig. 1a), but declined prematurely during the following two days at normal growth temperature (Fig. 1b). In line with this finding *fgt3* mutants also had a defective HS memory at the physiological level (Fig. 1c, Supplementary Fig. 1a). However, the immediate HS responses - as assayed by basal thermotolerance and acquired thermotolerance - were not affected in *fgt3* (Supplementary Fig. 1b-c). Thus, *FGT3* is specifically required for HS memory.

FGT3 encodes HSFA3. The *fgt3* mutant segregated as a single recessive locus with no apparent morphological defects under normal growth conditions. To identify the genetic mutation underlying the HS memory phenotype, we combined recombination breakpoint mapping and genome re-sequencing, and identified a single nucleotide polymorphism in exon 2 of *At5g03720* that introduces a premature stop codon in the *HSFA3* gene (Fig. 1d). To confirm that *fgt3* is allelic to *hsfa3*, we crossed *fgt3* to *hsfa3-1* and assayed HSA32-LUC activity in the F1 progeny after HS. The progeny of the *fgt3* x *hsfa3-1* cross, but not the control cross, showed strongly reduced maintenance of HSA32-LUC activity and loss of physiological HS memory, similar to *fgt3* (Fig. 1b, Supplementary Fig. 2a). In addition, genomic constructs expressing *HSFA3* under the control of the endogenous promoter (1.3 kb promoter fragment) with or without an N-terminal FLAG tag complemented *HSA32-LUC* expression and survival phenotypes of *fgt3* (Supplementary Figs. 1a, 2b). The *hsfa3-1* allele displayed similar HS memory defects as *fgt3* and was also complemented by *pHSFA3::FLAG-HSFA3* (Fig. 2a–d). Thus, the loss of *HSFA3* function is causative for the *fgt3* mutant phenotypes and we renamed *fgt3* as *hsfa3-3*. Under our conditions, *HSFA3* induction peaked at 4 h after the end of ACC (Fig. 2e). We also tested the expression pattern of the two *pHSFA3::FLAG-HSFA3* lines. Line #1 expressed *FLAG-HSFA3* similarly as *HSFA3* in Col. Line #12, however, showed a several-fold stronger induction of *FLAG-HSFA3* after ACC, suggesting that this line acts as a native overexpressor (Fig. 2e). Interestingly, line #12 displayed enhanced HS memory compared to Col (Fig. 2b). Further extending the recovery phase between the

priming and triggering HS for up to 6 d and reducing the dose (duration) of the triggering HS revealed that HS memory in wild type was still detected after 5 d of recovery, albeit at decreasing levels (Supplementary Fig. 3a, b). This observation extends the memory period regarding physiological effects by 2 d compared to previous reports[23,24]. Notably, the native overexpressing line retained some HS memory 6 d after ACC, when primed Col plants no longer had enhanced survival compared to unprimed Col plants. Thus, HSFA3 protein levels control HS memory.

HSFA3 and HSFA2 interact genetically and have redundant and non-redundant functions. *HSFA3* was induced by ACC, albeit more slowly than *HSFA2*, which peaked right at the end of the ACC treatment (Fig. 3a, b). *HSFA3* was suggested to be induced by the HS-activated DEHYDRATION-RESPONSIVEELEMENT BINDING PROTEIN 2 A (DREB2A), which in turn is activated by HSFA1 isoforms[37–39]. Indeed, under our HS regime *HSFA3* but not *HSFA2* expression depended on DREB2A, consistent with the predicted presence of more DREB binding elements in the *HSFA3* promoter than in the *HSFA2* promoter (Supplementary Fig. 3c, Supplementary Table 1). This two-step activation may account for the slower induction kinetics of *HSFA3*. Consistent with both genes being downstream of HSFA1s, induction of either *HSFA2* or *HSFA3* was independent of the respective other protein (Fig. 3a, b). *HSFA2* and *HSFA3* are both required for HS memory, with *hsfa2* having a slightly stronger defect (Fig. 3c, d). To test whether both genes interact genetically, we generated the *hsfa2 hsfa3-1* double mutant and analyzed physiological HS memory. The double mutant was more sensitive to a triggering HS that was applied 3 d after ACC than either single mutant (Fig. 3c, d). None of the mutants or native overexpressing lines showed any defects in basal or acquired thermotolerance, indicating that the observed phenotypes are specific to HS memory (Supplementary Fig. 4). In summary, despite the already strong phenotypes of the single mutants, double mutant analysis indicates that HSFA2 and HSFA3 act partially redundantly.

HSFA3 is required for sustained induction of HS memory-related genes. Two types of HS-related transcriptional memory have been described; type I memory (sustained induction) and type II memory (enhanced re-induction)[5,32]. We asked whether *HSFA3* is required for type I memory (sustained induction) by analyzing transcript levels of the endogenous *HSA32* gene as well as three other genes of this group, *HSP18.2*, *HSP22*, and *HSP21*[23,24,32]. Starting from 28 h after ACC, transcript levels of these genes in

hsfa3-1 were lower compared to wild type, indicating a defect in sustained induction, but not initial upregulation (Fig. 4). In contrast, the native overexpressing line #12 showed increased expression levels of *HSA32*, *HSP22*, and *APX2* from 28 h onwards (Supplementary Fig. 5a), in line with the stronger *HSFA3* expression after ACC and the enhanced HS memory (Fig. 2). In the *hsfa2 hsfa3-1* double mutant, *HSA32*, *HSP22*, and *HSP21* had further reduced transcript levels starting from 28 h compared to either single mutant (Fig. 4). This is in line with the further reduced HS memory in the double mutant and suggests that both proteins act in HS memory and cannot replace each other. In addition, we observed similar changes at the level of unspliced transcripts (Supplementary Fig. 5b), which are often used as a proxy for transcriptional activity[23,24,40], indicating that the observed changes in transcript levels reflect changes in (ongoing) gene transcription. The expression of HS-induced non-memory genes *HSP101* and *HSP70* was unaltered in all of the mutants (Fig. 4). Consistent with previous findings[33], *HSFA2* was required for type II memory at *APX2*, *HSFA1E*, *MIPS2*, *LACS9*, *LPAT5*, *TPR1*, *MYB86*, and *DGS1* (Fig. 5). In contrast, *hsfa3-1* mutants showed wild type-like enhanced re-induction of these genes. Expression of *HSP101*, which does not show type II transcriptional memory, was unaffected in all mutant backgrounds (Fig. 5). Thus, while *HSFA2* is required for both types of transcriptional memory, *HSFA3* appears specifically required for the sustained induction of HS memory-related genes (type I). To globally assess the effects of the mutants on heat-induced gene expression during the memory phase, we performed RNA-seq on Col, *hsfa2*, *hsfa3*, and double mutant seedlings that were subjected to an ACC treatment and recovered for 4 h, 28 h, or 52 h or control samples without ACC. In Col, we identified 156 genes that showed differential gene induction ($\log_2$ FC > 1 and p < 0.05) at all three time points ("1-1-1 up"), and that we therefore call HS memory genes (Supplementary Data 1). In contrast, 3225 genes were induced specifically at 4 h after ACC ("1-0-0 up"). Among the memory genes, 18.6%/13.5%/23.7% were not induced in *hsfa2*/ *hsfa3*/ *hsfa2 hsfa3* at 4 h after ACC (Fig. 6a, Supplementary Data 1). These numbers progressively increased to 37.2%/30.8%/53.2% at 28 h and 62.2%/55.8%/74.4% at 52 h after ACC. Thus, HSFA2 and HSFA3 are partially redundantly required for sustained induction of HS memory genes and their effect becomes more pronounced as the recovery phase progresses. In contrast, of the 3225 early HS genes (1-0-0 up), 22.3%/21.4%/24.2% were not induced at 4 h in *hsfa2*/ *hsfa3*/ *hsfa2hsfa3*. For both groups of genes and at all three time points there was a large overlap between the genes with loss of upregulation in the mutants,

confirming that their functions are largely overlapping (Fig. 6b). For the memory genes only, the number of genes with loss of overexpression was increased in the double mutant, confirming the cooperative effect of HSFA2 and HSFA3.The overall similar but stronger effect of the double mutant was also apparent from looking at the effect size of individual genes (Fig. 6c). Among the HS memory genes, all differentially expressed genes showed reduced induction, with the exception of two genes. In contrast, among the early HS genes, enhanced induction was more prevalent (Fig. 6c). In summary, global analysis confirmed that HSFA2 and HSFA3 function as transcriptional activators on an overlapping set of HS memory genes, where they are required for sustained induction of gene expression (type I memory).

HSFA3 and HSFA2 proteins interact. HSF proteins form multimeric complexes[34,41]. With the plethora of HSF proteins in *A. thaliana*, there is the potential for multiple combinations; however, which of these occur in vivo remains unresolved. We hypothesized that HSFA3 and HSFA2 may directly interact. We confirmed the interaction of HSFA2 and HSFA3 in the yeast-two-hybrid system (Fig. 7a). The C-terminus of HSFA2 and HSFA3, which we truncated in the BD constructs to prevent auto activation, was dispensable for the interaction. This is consistent with the notion that the interaction is mediated by the oligomerization domain (OD, Fig. 1d). We next confirmed the interaction by *in planta* co-immunoprecipitation from stable transgenic lines using HSFA2-YFP[32] and FLAG-HSFA3, both expressed from their own promoters in the *hsfa2 hsfa3-1* double mutant background. Both proteins were strongly induced after ACC with a peak around 4 h into the recovery phase and they were still detectable at 76 h after ACC (Fig. 7b, c). FLAG-HSFA3 precipitated HSFA2-YFP at all time points where both proteins were detectable (Fig. 7b). Conversely, HSFA2-YFP was able to pull down HSFA3 (Fig. 7c). In summary, HSFA2 and HSFA3 form heteromers *in planta* that persist for several days after HS/ACC.

Interaction with other HSFs. Our genetic analysis indicated that in the absence of the respective other "memory" HSF, the remaining HSF still retains some activity. Thus, both HSFA2 andHSFA3 may have other binding partners. To investigate this we purified FLAG-HSFA3 and interacting proteins under no-HS conditions, 4 h after HS (1 h at 37 °C), or 4 h after ACC from the complementing *pHSFA3::FLAG-HSFA3* line and subjected them to mass spectrometry analysis (Co-IP/MS). The most frequent interacting protein as estimated by unique peptide numbers in all heat-treated samples was HSFA2 (Fig.

7d, Supplementary Table 2), indicating that HSFA2 is the preferred binding partner of HSFA3. In addition, we also identified HSFA1D, HSFA1B, HSFA6B, HSFA7A, and HSFA1A as interacting proteins (Fig. 7d,Supplementary Table 2). Thus, HSFA3 forms multimeric complexes with other HSF proteins, providing a tentative explanation for the residual activity of HSFA3 in the absence of HSFA2. Interestingly, we also detected interactions of HSFA3 with HSFA1 isoforms before applying any heat treatment, suggesting that the formation of HSFA1-HSFA3 complexes does not depend on a HS stimulus. Correspondingly, we isolated HSFA2-YFP protein complexes for mass spectrometry (Fig. 7e). Since *HSFA2* expression is induced faster than *HSFA3* (Fig. 3a, b), samples were taken 45 min and 3 h after 1 h HS at 37 °C treatments. HSFA3 was detected with very low peptide numbers under no-HS conditions but increased at 45 min and 3 h after HS in line with the induction of *HSFA3*; at 3 h after HS HSFA3 was the second most frequent interacting protein after HSFA7A. At all time points other HSFs were recovered as HSFA2 interacting proteins. They were HSFA7A, HSFA1B, HSFA1D, HSFA1A, HSFA6B, and HSFA7B (Fig. 7e, Supplementary Table 2). With the exception of HSFA7B, we identified all HSFA2-interacting HSFs also as interactors of HSFA3, suggesting that both proteins share a common set of interactors after HS. Using in vitro pulldowns we confirmed that each HSFA2 and HSFA3 interact directly with HSFA1A, B, D, and HSFA7A (Fig. 7f). We next asked which proteins (if any) HSFA2 and HSFA3 bind to in the absence of the respective other memory HSF. To this end, we repeated the Co-IP/MS analysis of HSFA2 or HSFA3 in the respective other mutant background in the absence of HS or 4 h after ACC treatment. Besides the memory HSFs, the previously identified additional interacting HSFA1s and HSFA7B were rediscovered (Supplementary Table 3). In the *hsfa2* mutant HSFA3 complexes also contained HSFA1D, HSFA1B and HSFA1A. Conversely, in the *hsfa3* mutant HSFA2 complexes contained HSFA1D, HSFA1B, HSFA1A and HSFA7B. This is consistent with the idea that either memory HSF still forms complexes with additional HSF proteins in the absence of the other memory protein. However, our mutant analysis clearly indicates that these alternative complexes are less efficient in promoting HS memory.

HSFA3 and HSFA2 bind with overlapping kinetics to the same target genes. To test whether HSFA3 sustains the expression of HS memory-related genes directly, we performed time-course chromatin immunoprecipitation (ChIP) with sampling from the end of ACC until 28 h into the recovery phase. Indeed, we detected HS-dependent enrichment of FLAG-HSFA3 in the promoters of *HSP22*, *HSP18.2*, *HSA32*, and *APX2* at

HSE-containing sequences (Fig. 8a, Supplementary Fig. 6a). The binding of HSFA3 peaked 4 h into the recovery phase, and was still detected at 28 h. This is consistent with HSFA3 promoting transcription for at least 24 h after the end of ACC. We previously found that HSFA2 is associated with these loci early after the HS[32]. We confirmed this in the present study using a *pHSFA2::FLAG-HSFA2* line that was grown and sampled side-by-side with the *FLAG-HSFA3* line (Fig. 8a, Supplementary Fig. 6a). After ACC HSFA3 and HSFA2 were also associated with the HS-inducible non-memory gene *HSP101* (Fig. 8a), where they did not have any impact on gene expression (Figs. 4 and 5). Thus, while HSFA3 and HSFA2 bind to the same loci after HS, their binding kinetics differ with HSFA3 showing a delayed peak. This suggests that both proteins bind these loci with overlapping kinetics, partially together and partially using alternative HSFs as binding partners.

HSFA3 binds target loci independently of HSFA2. Given the interaction between HSFA2 and HSFA3 we wondered whether binding of HSFA3 to the promoters of target genes depends on HSFA2. We thus performed time-course ChIP with FLAG-HSFA3 in the *hsfa2* background. Overall, the HSFA3 binding dynamics to *HSP22*, *HSP18.2*, *HSA32*, *APX2*, and *HSP101* were very similar to those in the wild type background (Fig. 8b, Supplementary Fig. 6b). This suggests that HSFA2 is not required to recruit HSFA3 to its target loci. Moreover, these findings indicate that the loss of HS memory in *hsfa2* is not due to concomitant loss of HSFA3 for transcriptional activation; rather, it reinforces the idea that alternative HSF complexes have differential capacity to activate HS memory.

HSFA3 and HSFA2 jointly recruit histone H3K4 methylation. We previously found that *HSFA2* is required for sustained enrichment of H3K4 trimethylation (H3K4me3) at memory-related genes after HS[32]. In *hsfa2* mutants, H3K4me3 enrichment was strongly reduced but not completely abolished. To test the role of HSFA3 in sustained H3K4me3 enrichment, we analyzed H3K4me3 levels in the double mutant and either single mutant at 28 h and 52 h after ACC. Indeed, in either single mutant H3K4me3 enrichment after ACC was reduced to an intermediate level at *HSP22*; at *APX2*, HSFA3 was dispensable for H3K4me3 enrichment, however, at both loci H3K4me3 was more strongly reduced in the *hsfa2 hsfa3-1* double mutant (Fig. 9). In contrast, H3K4me3 enrichment at *HSP101* was not affected in either of the genotypes tested. Over all genotypes and assayed regions, histone H3 enrichment decreased after ACC (Supplementary Fig. 7), consistent

with previous findings[24]. In summary, our findings suggest that HSFA2 and HSFA3, despite the strong phenotypes of the single mutants, show functional redundancy at the level of physiological HS memory, sustained memory-related gene activation, and hyper-methylation of H3K4me3.

HSFA2 and HSFA3 can substitute for each other. The strong phenotypes of the single mutants may be caused by partially non-overlapping expression domains or by sub-functionalization at the protein level. To discriminate between these possibilities, we performed complementation analyses with HSFA2 and HSFA3 proteins that were expressed under the control of the respective other promoter. We first expressed the *FLAG-HSFA3* coding region from the *pHSFA2* promoter, which is activated earlier after HS than *pHSFA3* (cf. Fig. 3a, b). This construct was able to partially complement the physiological HS memory phenotype of *hsfa2* (Fig. 10a, Supplementary Fig. 8a, d), suggesting that the HSFA3 protein can (partially) take over HSFA2 function, when supplied from the *HSFA2* promoter. The *pHSFA2::FLAG-HSFA3* construct also partially complemented the *hsfa3-1* mutant (Fig. 10a). We conversely asked whether the early induction of *HSFA2* is required for HS memory by expressing the complementing *HSFA2-YFP* coding region under the control of *pHSFA3*. Indeed, *pHSFA3*- and *pHSFA2*-driven *HSFA2-YFP*, respectively, rescued the *hsfa2* mutant phenotype in part (Fig. 10a). Finally, expression of *HSFA2-YFP* from *pHSFA3* was sufficient to restore HS-memory in *hsfa3-1*, suggesting that both proteins carry out the same function. In contrast, expressing *FLAG-HSFA1D* from the *pHSFA3* promoter failed to complement the *hsfa3-1* mutant (Supplementary Fig. 8e–g), indicating that HSFA2 and HSFA3 have a specialized protein function that is absent from HSFA1D. *HSFA2* but not *HSFA3* is required for type II transcriptional memory after HS (Fig. 5). This is surprising in light of the above finding that both proteins appear to carry out the same functions. To further investigate this, we tested whether HSFA3 could substitute for HSFA2 regarding type II memory if expressed from *pHSFA2*. Introduction of *pHSFA2::FLAG-HSFA3* into *hsfa2* restored the enhanced re-induction of *APX2* after recurring HS, suggesting that *HSFA3* is able to mediate type II memory when supplied under the correct promoter (Fig. 10b, c). Conversely, *pHSFA3::HSFA2-YFP* rescued type II transcriptional memory defects of *APX2* in the *hsfa2* mutant. In summary, the promoter swapping experiments indicate that there is no clear qualitative difference between HSFA2 and HSFA3 protein functions. In

the absence of HSFA2-HSFA3 heteromers, increased protein levels and correct timing of expression partially compensate for the missing partner.

Discussion

Here, we identified *HSFA3* as an essential component of HS memory in *A. thaliana*. We show that HSFA3 is required for sustained induction of several HS memory-related genes through direct gene activation and recruitment of histone H3K4 hyper-methylation. Previously, only HSFA2 was implicated in HS memory. We demonstrate that HSFA3 binds to HSFA2 to form heteromeric complexes that are highly effective at promoting HS memory. *HSFA2* and *HSFA3* show different expression dynamics and this may allow fine-tuning of HS (memory) responses according to the actual environmental conditions. HSFA2 is a direct target gene of HSFA1 and induced very rapidly after the onset of HS[22,30]. In contrast, HSFA1s or HSFA2 do not directly induce HSFA3 (Fig. 10d). Rather, HSFA3 is activated by DREB2A, which in turn is activated by HSFA1A, and the related DREB2B and DREB2C[30,37–39]. DREB2A and DREB2B are also induced by drought and high salinity stress, and DREB2A is in addition regulated at the posttranslational level[39,42,43]. Under our conditions, *HSFA3* expression is primarily induced during the recovery phase, which is in full agreement with its function during HS memory. HSFA3 and its presumed activator DREB2B were reported as the only two transcription factors specifically enriched in acclimated plants, but not by direct exposure to acute HS[37,44]. Another study reported *HSFA3* expression peaking after 10 h of continuous 37 °C treatment[38]. These studies provided inconclusive evidence regarding the functional involvement of HSFA3 in HS responses. Our finding that HSFA3 has a specific role in HS memory unifies these studies and assigns a clear function to HSFA3. To further assess the significance of the different expression dynamics, we performed promoter swapping experiments. Both *HSFA2* and *HSFA3* rescued the other respective mutant when expressed from the corresponding promoter at least partially. While *HSFA3* was not required for enhanced re-induction after a second HS (type II memory), it was able to partially complement the type II memory defects of *hsfa2* when expressed from *pHSFA2*, suggesting that the early induction of *HSFA2* contributes to type II memory. Importantly, HSFA1D was not able to rescue the *hsfa3* mutant, indicating functional specialization at the protein level. Thus, HSFA2 and HSFA3 appear to have similar protein properties enabling them to recruit specific transcriptional co-activators or H3K4 methyltransferases, and these appear distinct from the remainder of the HSF family. It remains an open question whether this recruitment occurs through direct protein-protein

interactions or through other proteins, e. g. components of the general transcriptional machinery. H3K4 methylation is deposited by the COMPASS complex and is required for efficient transcriptional elongation[45–48]. This is critical for transcriptional regulation in development and stress response in animals, where release of paused RNA Pol II into elongation is a limiting step[49,50]. Understanding the molecular basis for the memory-specific function of HSFA2 and HSFA3 will be an important goal of future work. In yeast and animals, HSFs are present as trimers or hexamers (where two trimers combine), and a similar structure has been proposed for plant HSF complexes[18,20,34,35,51]. HSFA2 and HSFA3 associate with each other during the three days following a priming HS. HSFA3 binding to its target sites was independent of HSFA2, suggesting that it also forms functional complexes with other HSFs that may also be represented in the trimeric HSFA2/HSFA3/X complexes. We identified several HSFA1s (1A, 1B, 1D) as well as HSFA7A, and HSFA6B as direct interactors of both HSFA2 and HSFA3. Indeed, we showed that binding partners of both memory HSFs in the absence of the respective other memory HSF contained the same HSFs that were found in the presence of the other memory HSF. This supports the notion that despite their overall promiscuity, only complexes that contain both HSFA2 and HSFA3 have full capacity to activate HS memory (Fig. 10e). If HSFs assemble in heteromeric trimers with varying components, these complexes may vary in their temporal regulation, co-activator activity and target specificity; they may serve to integrate responses to different environmental cues. Noteworthy, *HSFA3* responds to oxidative stress and both *HSFA2* and *HSFA3* are activated by excess light, while *HSFA6B* is activated by salt stress, osmotic stress and ABA[52–54]. This work has started to unravel the in vivo complexity and dynamics of plant HSF complexes. HSFA2 and HSFA3 share a specific ability to recruit transcriptional co-activators and histoneH3K4 methyltransferases during HS memory, which other HSFA proteins cannot do in their absence. HSFA2 and HSFA3 are found in heteromeric complexes together with additional HSFs, in particular HSFA1s. Maximal HS memory activation likely depends on the formation of heteromeric HSFA2/HSFA3/X trimers (Fig. 10e). The surprisingly strong single mutant phenotypes of *hsfa2* and *hsfa3* support this model; in the mutant backgrounds, trimers only contain a single memory HSF, resulting in much less efficient activation of transcriptional memory (Fig. 10e). The partial complementation of *hsfa2* single mutants by an additional copy of *HSFA3* and vice versa would then be due to a higher overall abundance of such less efficient, single-memory HSF-containing complexes. In summary, our work has begun to shed light on the

composition and specialized functions of in vivo HSF complexes in *A. thaliana*, resulting in testable predictions about a super-memory HSF complex. Ultimately, understanding the function of HSF complexes in heat shock response and transcriptional memory at a detailed biochemical level will provide targets for engineering crop plants that are more resilient to temperature extremes.

Methods

Plant material and growth conditions. All *A. thaliana* lines used in this study are in the Col-0 background. The *pHSA32::HSA32-LUC*[24] and *pHSFA2::HSFA2-YFP* lines[32], the *hsfa2-1*[22], *hsfa3-1* (Salk_011107)[38], *dreb2a-1* (379F02 GABI-KAT)[39] and *hsp101*[23] mutants have been described. Seedlings were grown on GM medium (1% [w/v] glucose) under a 16 h/8 h light/dark cycle at 23/21 °C[23]. Primer sequences for genotyping are listed in Supplementary Table 4.

HS treatments. 4 d-old seedlings were exposed to 44 °C for 25–45 min to examine basal thermotolerance (bTT); to examine acquired thermotolerance (aTT) they were exposed to 37 °C for 1 h, 23 °C for 90 min and 44 °C for 160–250 min[23]. For HS memory assays, 4 d-old seedlings were primed with a two-step acclimation (ACC) protocol consisting of 37 °C for 1 h, 23 °C for 90 min and 44 °C for 45min[23]. Primed seedlings were exposed to a triggering HS at 44 °C for 70–130 min on day 7 or 44 °C for 30–80 min on day 8–10.

Construction of HSFA3 complementation and promoter swap constructs. To obtain a genomic fragment containing the *HSFA3* gene as well as flanking regions until the borders of the neighboring genes, PCR with primers 2410 containing an *Asc*I site and 2418 containing a *Pac*I site was performed and the resulting product was subcloned into pJET1.2 (Thermo Fisher). After sequencing, the genomic *HSFA3* fragment was introduced using *Asc*I and *Pac*I into a *pGreenII* binary vector harboring a Norflurazone resistance (kindly provided by T. Laux). To obtain a FLAG-tagged version of *HSFA3* driven by the native promoter the promoter flanked by *Asc*I and *Age*I (primers 2410 and 2420) and *3xFLAG-HSFA3* flanked by *Age*I until the beginning of the downstream neighboring gene flanked by a *Pac*I-site (Primers 2417 and 2418) were amplified and the resulting fragments subcloned into pJET1.2. After sequencing, the two fragments were combined in pJET1.2 via *Age*I and *Pac*I and the final fragment introduced into *pGreenII* with Norflurazone resistance. In order to generate promoter swap constructs, either *pHSFA2* (primers 2624/2625), *HSFA2-YFP* (primers 2786/2787), or *3xFLAG-HSFA1D* (primers 2810/2811) were amplified, subcloned into *pJET1.2* and sequenced. *pHSFA2* replaced *pHSFA3* and *HSFA2-YFP* or *3xFLAG-HSFA1D* replaced *3xFLAG-HSFA3* in the *pHSFA3::3xFLAG-HSFA3* construct to obtain *pHSFA2::3xFLAG-HSFA3*, *pHSFA3::HSFA2-YFP* and *pHSFA3::3xFLAG-HSFA1D*. All constructs were introduced

into the *GV3101* strain of *Agrobacterium tumefaciens* and transformed using the floral dip method[55]. Primer sequences are listed in Supplementary Table 4.

RNA extraction and qRT-PCR. To examine sustained induction of gene expression, 4 d-old seedlings were exposed to an ACC treatment and samples were taken during the following 3 d as indicated. To study enhanced re-induction of memory genes, seedlings were treated for 1 h at 37 °C on day four and again on day six or day seven as indicated. Samples including non-treated controls were taken at the end of the last HS. RNA was extracted from seedlings using hot-phenol RNA extraction: frozen tissue was ground to a powder and resuspended in 500 µl homogenization buffer (100mM Tris pH 8.0, 5mM EDTA, 100mM NaCl, 0.5% SDS), 250 µl phenol and 5 µl ß-mercaptoethanol and incubated for 15 min at 60 °C. 250 µl chloroform was added and samples were incubated for 15 min at 60 °C before spinning 10 min at 13000 rpm. 550 µl aqueous phase was transferred into a new tube containing 550 ul phenol:chloroform:isoamylalcohol (25:24:1), mixed and centrifuged as above. 500 µl aqueous phase was transferred into a new tube containing 50 µl 3M sodium acetate and 400 µl isopropanol and precipitated at−80 °C. After 30 min of centrifugation at 4 °C and 13000 rpm, pellets were dried and resuspended in 500 µl H_2O. 500 µl 4M LiCl was added and RNA was precipitated overnight at 4 °C. RNA was pelleted, washed in 80% EtOH, dried, and resuspended in 40 µl H_2O. For quantitative RT-PCR, total RNA was treated with TURBO DNA-free (Ambion) and reverse transcribed with SuperScript III (Invitrogen) according to manufacturer's instructions. 0.1 µl cDNA was used per 10 µl QPCR reaction with GoTaq qPCR Master Mix (Promega) and LightCycler480 (Roche)[23]. All data were normalized to the reference gene *At4g26410*[56] using the comparative CT method. Primers are listed in Supplementary Table 4.

RNA-seq. For RNA-seq analysis, total RNA was extracted from Col-0, *hsfa2*, *hsfa3-1*, and *hsfa2, 3-1* seedlings with RNeasy Plant Mini kit (Qiagen). On-column DNase digest of RNA was performed with RNase-Free DNase (Qiagen). RNA quality control, library preparation, and sequencing were performed by BGI Genomics (http://www.bgi.com) with the DNBseq platform generating 2 × 150 bp paired-end sequencing reads. Three biological replicates were generated and analyzed per treatment and genotype. Reads were mapped against the *Arabidopsis thaliana* reference genome (TAIR10) using STAR[57] version 2.5.1a. Quantification at gene level was done using STAR with the quantMode GeneCounts option. Differential gene expression analysis was done using

the R (https://www.r-project.org) package DESeq2[58]. Only protein-coding genes were analyzed, transposable element genes were excluded. Col 1-1-1 up genes were defined as being induced above baseline non-heat stressed level (defined as $\log_2$(fold change)>1, $p < 0.05$) at 4 h, 28 h, and 52 h after ACC treatment. 156 such genes were identified in the Col-0 background. Col 1-0-0 up genes were defined as being induced above baseline non-heat stressed level (defined as $\log_2$(fold change)>1, $p < 0.05$) at 4 h after ACC treatment, but not at 28 h or 52 h after ACC treatment. 3225 such genes were identified in the Col-0 background. Genes were counted as "not upregulated in mutant" at 4 h, 28 h, or 52 h after ACC treatment relative to no-HS level when either one of the following conditions was met: $\log_2$(fold change)≤1 or $\log_2$(fold change)>1, $p > 0.05$. Data visualizations were done using the R package ggplot2 (https://ggplot2.tidyverse.org).

Chromatin immunoprecipitation. All heat-treated samples were exposed to an ACC treatment, seedlings harvested at the indicated time points after ACC and cross-linked under vacuum in ice-cold MC buffer/ 1% (v/v) formaldehyde[59] for 2 × 5 min for histone ChIP or 2 × 10 min for 3xFLAG-HSFA2 or 3xFLAG-HSFA3ChIP. Chromatin was extracted as follows;[59] frozen tissue was ground up and resuspended in 25 ml M1 buffer, washed five times in 5ml M2 buffer, and once in 5 ml M3 buffer with centrifugation for 10 min, 1000 g for each washing step. The resulting chromatin pellet was taken up in 1 ml of sonication buffer (buffer recipes described in [59]). Chromatin was sonified using a Diagenode Bioruptor (17 cycles/30sec on/off) on low-intensity settings. For histone ChIP, equal amounts of chromatin from the same preparation were immunoprecipitated at 4 °C overnight using antibodies against H3 (ab1791, Abcam) or H3K4me3 (ab8580, Abcam). For 3xFLAG-HSFA2/3-ChIP, chromatin was incubated with anti-DYKDDDDK paramagnetic beads for 1 h at 4 °C and chromatin was recovered using a DYKDDDDK isolation kit (both Miltenyi Biotec). Immunoprecipitated DNA was quantified by qPCR (LightCycler480, Roche).

Yeast-two-hybrid analysis. *HSFA2* and *HSFA3* full and truncated (without AHA domains) coding regions were amplified and inserted into pGBKT7 and pGADT7 (Clontech), through either Gateway® technology (Invitrogen) or restriction enzyme (*BamH*I and *EcoR*I) digestion. Yeast cultures (MaV203 strain) were grown at 28 °C on Yeast Peptone Dextrose (YPD) or Synthetic Dextrose (SD) media supplemented with selective Drop-out (DO) aminoacid mixtures. Double transformation with both pGBKT7 (bait) and pGADT7 (prey) constructs was performed according to standard protocols.

Transformants were selected on SD medium supplemented with DO–Trp–Leu (SD–WL) and protein interaction was analyzed by growth on SD medium supplemented with DO–Trp–Leu–His (SD–WLH) and 50 mM 3-Amino-1,2,4-triazole (3-AT).

Co-IP, immunoblotting, and mass spectrometry. Total native protein complexes were isolated from 1 g of seedlings in 4 ml of Extraction buffer (50mM Tris–HCl pH7.5, 150mM NaCl, 2% Triton X-100, 1 Tablet complete mini Protease inhibitor cocktail (Roche)/25 ml) and centrifuged 4 times at 4 °C and maximum speed for 10 min. 100 µl input was taken from the supernatant and 2 ml protein extract were incubated with 50 µl of α-DYKDDDDK paramagnetic beads for 1.5 h at 4 °C. Protein complexes were recovered using a DYKDDDDK isolation kit (Miltenyi Biotec) and 3 washes with wash buffer (50mM Tris–HCl pH7.5, 150mM NaCl, 0.1% Triton X-100, 1 Tablet complete mini Protease inhibitor cocktail (Roche) /25ml). For mass spectrometry, 3 more washes with 20 mM Tris–HCl were performed. Proteins were eluted in 50 µl 8 M urea and used for immunoblotting[32] with anti-GFP (ab290, Abcam, 1:2000), anti-FLAG (M2, F1804, Sigma, 1:2500), anti H3 (ab1791, Abcam, 1:5000) or anti-Tubulin (T5168, Sigma, 1:4000) antibodies. For mass spectrometry, eluates were further processed as described[24]. Briefly, eluates were diluted and digested with Trypsin (Fig. 7) or Trypsin/Lys-C Mix (SupplementaryTable 3, Promega). Peptides were desalted, lyophilized and re-suspended in 20 µl 3% (v/v) acetonitrile, 0.1% (v/v) formic acid. Measurements were performed on a Q Exactive Plus Orbitrap mass spectrometer coupled with an EasynLC1000 HPLC (Thermo Fisher Scientific, Fig. 7) a Q Exactive HF (Thermo Fisher Scientific) mass spectrometer coupled with an Aquity M class UPLC (Waters, Supplementary Table 3).

In vitro pulldown assay. Coding sequences of HSFA proteins were inserted into the pIX-HALO expression vector by Gateway cloning. Primers are listed in Supplementary Table 4. For HSFA2 and HSFA3, the Halo tag was replaced by a 3xFLAG tag to yield pIX-FLAG expression vectors. For each pulldown reaction, 500 ng of each plasmid were mixed and transcription and translation were carried out in TNT wheat germ expression kits (Promega) according to manufacturer's instructions. Proteins were incubated overnight with Magne HaloTag beads (Promega), washed three times in PBS/ 0.1% NP-40, and eluted in SDS loading buffer. Samples were analyzed by SDS-page and immunoblotting using anti-FLAG (M2, F1804, Sigma, 1:2500) and monoclonal anti-Halo (G9211, Promega, 1:2000) antibodies.

Promoter analysis. The sequences for HSFA2 and HSFA3 promoters were analyzedusing JASPAR[60]. The profiles for Arabidopsis HSF (MA1664.1, MA1665.1, MA1666.1, MA1667.1) and DREB2 (MA0986.1, MA1258.1) binding sites were selected for promoter analysis and analyzed with standard settings (profile score threshold 80%).
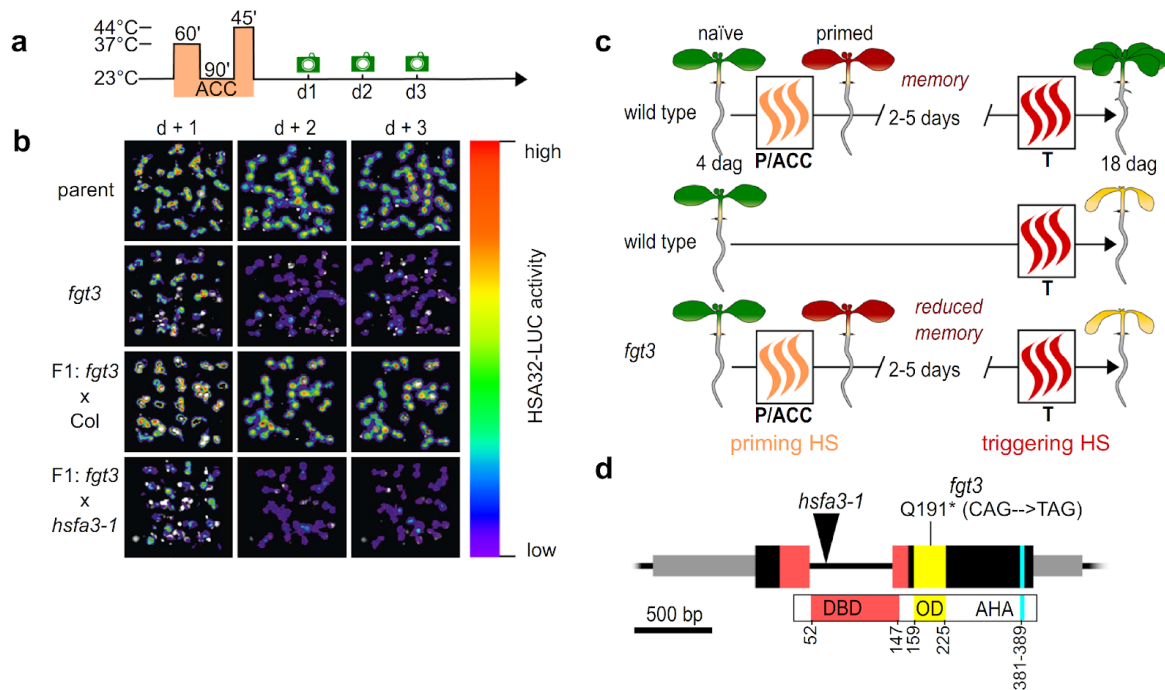
Main figures

Fig. 1 *FGT3/HSFA3* **is required for HS memory. a** Treatment scheme for LUC-based HS memory assay: 4 d-old seedlings were exposed to a two-step acclimation treatment (ACC; 60 min 37 °C, 90 min 23 °C and 45 min 44 °C). Activity of the HS memory marker *pHSA32::HSA32-LUC* was scored on the following three days (green camera symbols). **b** LUC-based HS memory assay shows reduced maintenance of *pHSA32::HSA32-LUC* induction in *forgetter 3* (*fgt3*) mutants. Crossing to Col but not to the *hsfa3-1* mutant complements the defect of *fgt3* in the F1 progeny. **c** Schematic representation of physiological HS memory: Plants that have not experienced any HS (naïve plants) can be primed by a non-lethal HS (P or ACC), leading to an enhanced capacity to withstand a triggering HS (T). This enhanced thermotolerance results in increased survival of T in a primed plant compared to a naïve plant for up to 5 d (HS memory). *Fgt3* mutants are defective in HS memory and do not survive the T despite prior priming. **d** Schematic representation of the *HSFA3* locus (*At5g03720*) with location of the *fgt3* (Q191*) and *hsfa3-1* mutations. Exons are shown as large black boxes with protein domains overlaid in color (DBD: DNA-binding domain, OD: oligomerization domain, AHA: AHA motif), aa numbers are given to depict the positions of protein domains. UTRs are shown as gray boxes and the intron as a black line.
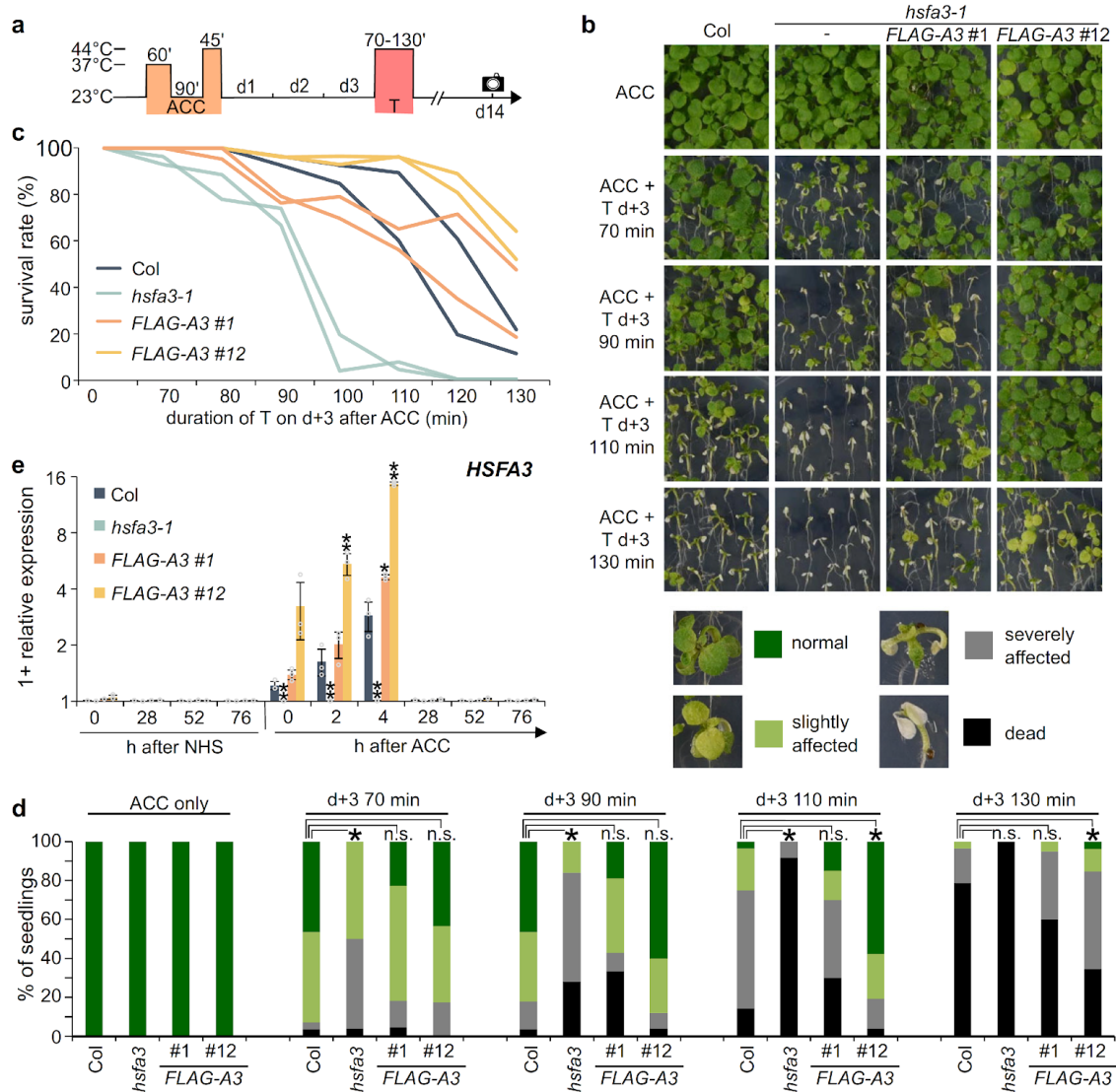
Fig. 2 *FGT3/HSFA3* **is required for physiological HS memory. a** Treatment scheme for HS memory assays: plants are exposed to a triggering HS (T, 44 °C for 70–130 min) 3 d after ACC (which was applied 4 d after germination) and survival is scored 14 d after ACC (black camera symbol). **b–d** HS memory assay of *hsfa3-1* and two complementing lines of *pHSFA3::FLAG-HSFA3* in the *hsfa3-1* background. **b** Representative images of HS memory assay, with legend showing examples of phenotype categories used for the quantification in **d**. **c** Survival rates of the different genotypes in HS memory assay. Data are from 2 independent replicates with n ≥ 19 seedlings for each time point and genotype. **d** Distribution of phenotypic categories observed in the HS memory assay shown in **b**. Asterisks depict significant differences to Col ($p < 0.01$, Fisher's exact test, n ≥ 19 seedlings for each time point and genotype). **e** Transcript levels of *HSFA3* in Col, *hsfa3-1* and two *pHSFA3::FLAG-HSFA3* lines in the *hsfa3-1* background as measured by qRT-PCR. Expression values are relative to the *At4g26410* reference gene, as in all following qRT-PCR figures. Data are mean ± SD of three independent experiments and asterisks indicate significant differences to Col (*, $p < 0.05$; **, $p < 0.01$; unpaired two-sided t-test).
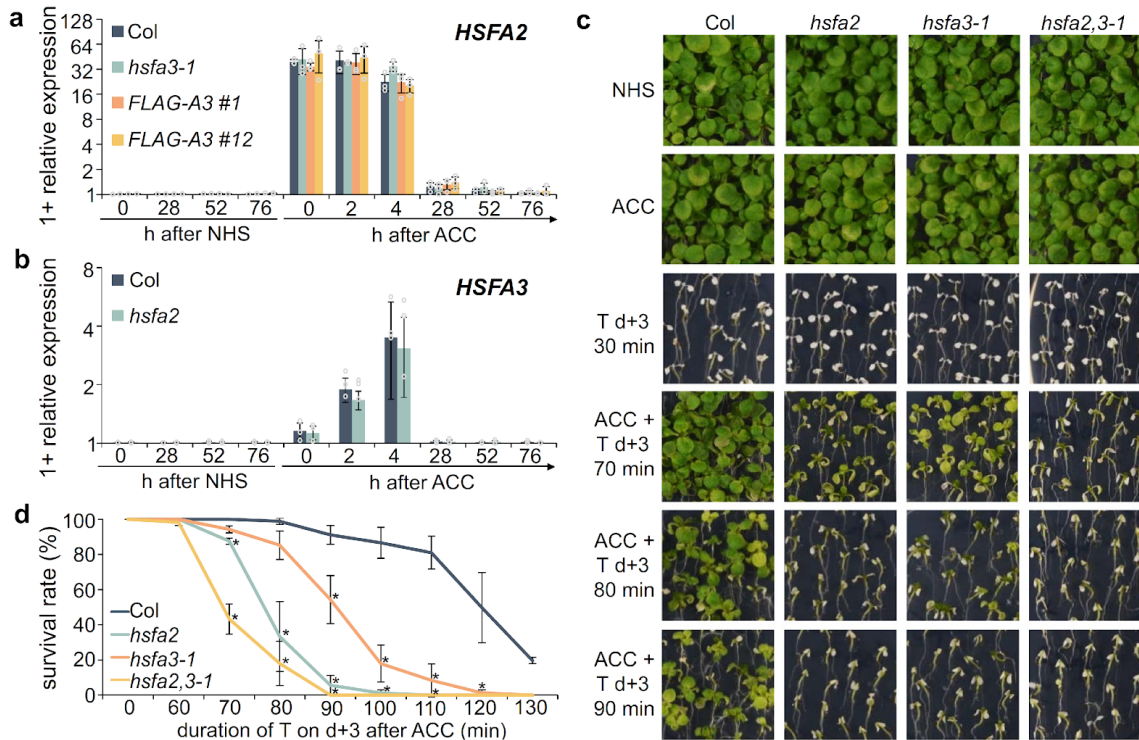
50

Fig. 3 *HSFA2* and *HSFA3* are independently induced by HS and interact genetically. a Relative transcript levels of *HSFA2* in Col, *hsfa3-1* and *pHSFA3::FLAG-HSFA3* lines in *hsfa3-1* background as measured by qRT-PCR. **b** Relative transcript levels of *HSFA3* in Col and *hsfa2* as measured by qRT-PCR. Data are mean ± SD of three independent experiments (**a**, **b**). **c**, **d** HS memory assay for *hsfa2*, *hsfa3-1* and *hsfa2 hsfa3-1* double mutants. 4 d-old seedlings were exposed to ACC treatment and 3 d later to a triggering HS at 44 °C for 70–130 min. NHS, no-HS control; ACC, plants primed with an ACC treatment. Representative images (**c**) and survival rates (**d**) were recorded 14 d after ACC. Error bars indicate SD of three independent experiments. Asterisks mark significant differences to Col ($p < 0.05$, unpaired two-sided t-test).
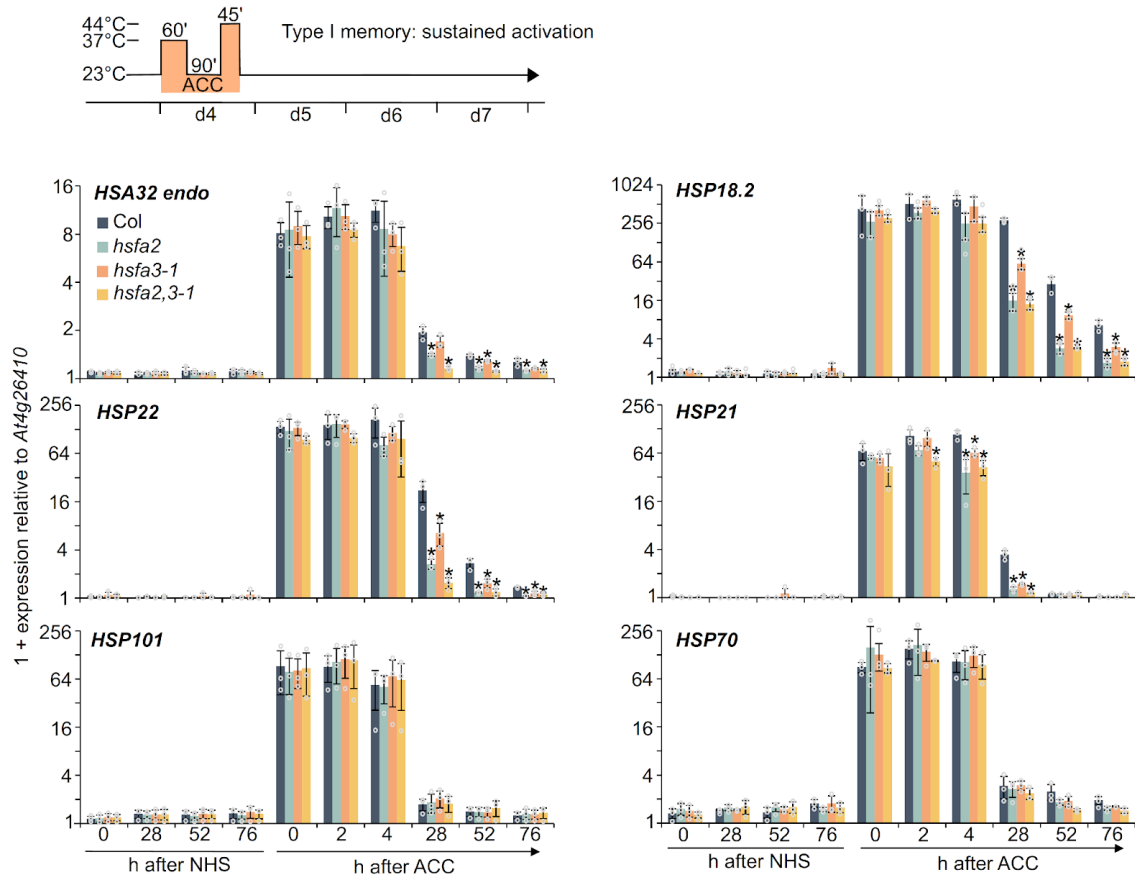
Fig. 4 Sustained induction of HS memory genes depends on *HSFA2* and *HSFA3*. Type I transcriptional memory (sustained induction): Memory gene expression is induced by a priming ACC treatment and expression is sustained above baseline for several days. Plants were exposed to an ACC treatment and samples taken at the indicated time points during the following 76 h. Relative transcript levels of 4 memory genes (*HSA32*, *HSP18.2*, *HSP22*, *HSP21*) and 2 HS-inducible non-memory genes (*HSP101* and *HSP70*) were measured by qRT-PCR. Time points depict hours after end of ACC. Data are mean ± SD of three independent experiments. Asterisks mark significant differences to Col ($p < 0.01$, unpaired two-sided t-test).
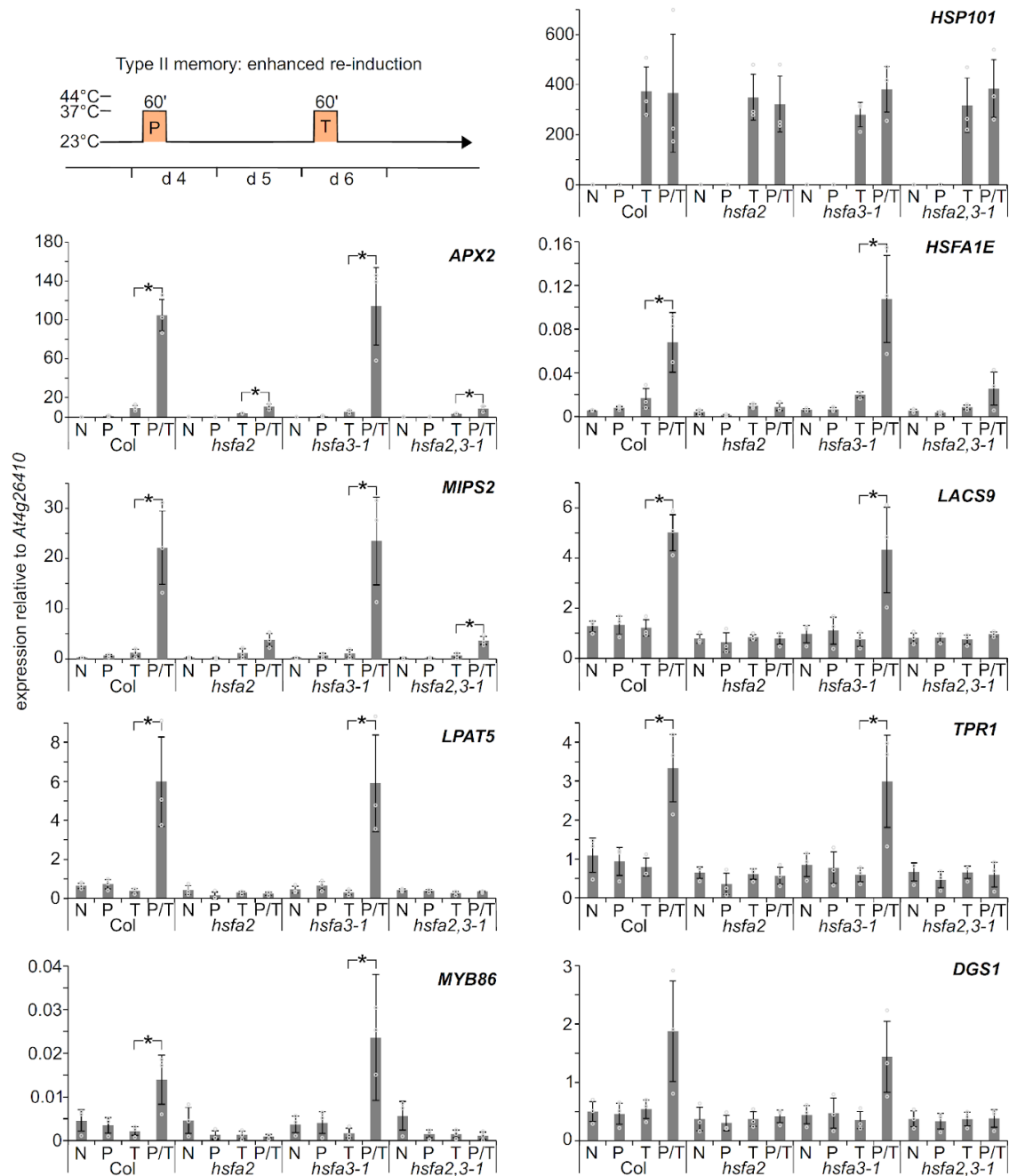
Fig. 5 Enhanced re-induction of HS memory genes depends on *HSFA2* but not *HSFA3*. Type II transcriptional memory (enhanced re-induction): Memory gene expression is activated by a priming treatment (P), and more highly activated by a second triggering treatment (T) 2 d later. P and T treatments consist of 37 °C for 1 h. Relative transcript levels in enhanced re-induction experiments of eight memory genes (*APX2*, *HSFA1E*, *MIPS2*, *LACS9*, *LPAT5*, *TPR1*, *MYB86*, and *DGS1*) and one non-memory gene (*HSP101*) were measured by qRT-PCR. Plants were either not treated (N), only primed on d 4 (P), only triggered on d 6 (T), or primed on d 4 and triggered on d 6 (P + T). Regardless of their treatment, all samples were harvested on d 6 at the end of the T treatment. Data are mean ± SD of three independent experiments. Asterisks mark significant differences to Col (*p* < 0.01, unpaired two-sided t-test).
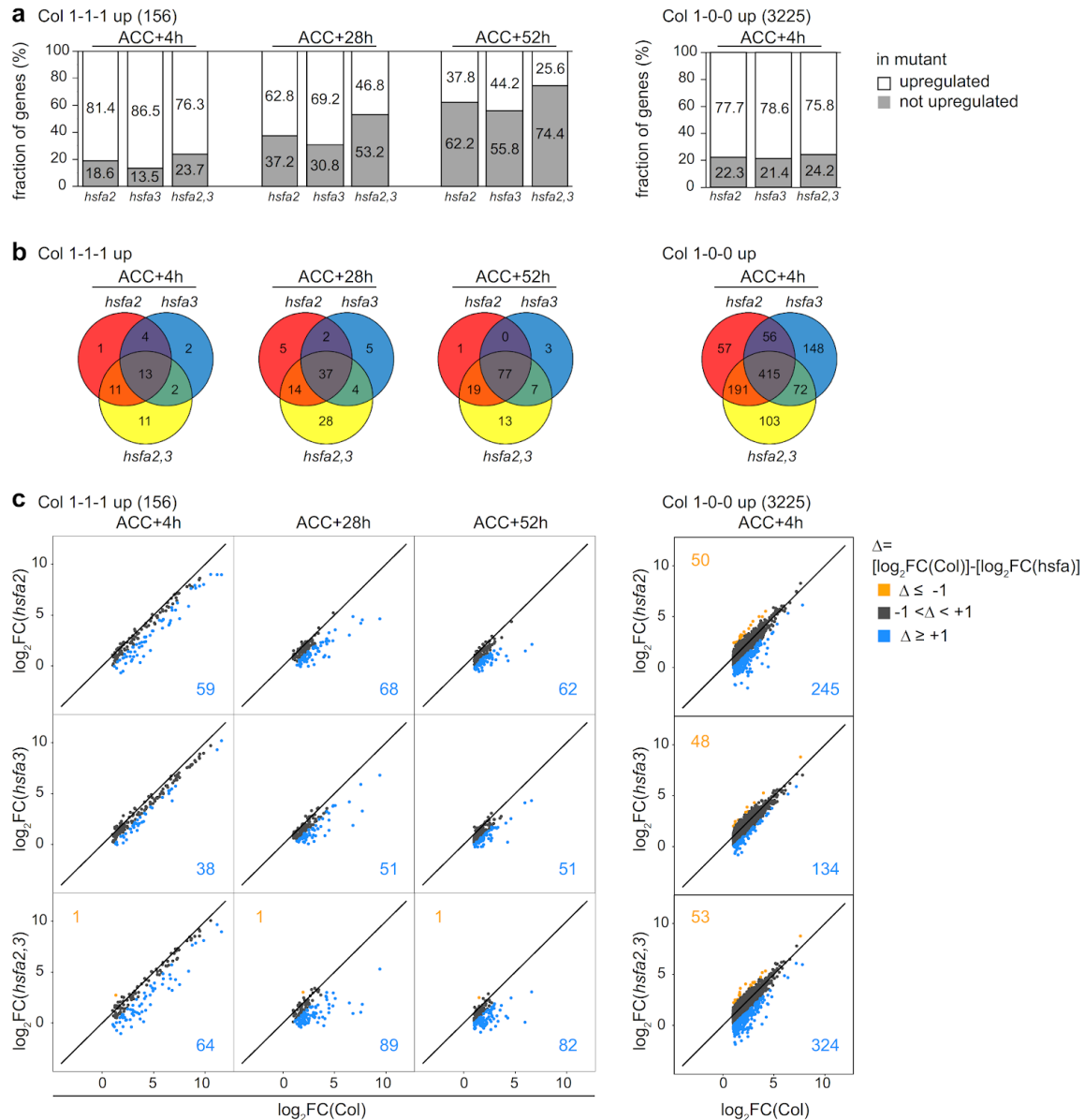
Fig. 6 HSFA2 and HSFA3 jointly promote type I transcriptional memory in a genome-wide manner. Genome-wide transcriptome profiling by RNA-seq analysis identifies 156 HS memory genes with sustained induction above no-HS levels ($\log_2$FC > 1, p < 0.05) at 4 h (ACC + 4 h), 28 h (ACC+ 28 h), and 52 h (ACC + 52 h) after end of ACC treatment in Col (1-1-1 up) and 3225 genes that are induced above no-HS levels only 4 h after end of ACC treatment in Col (1-0-0 up). **a** Fraction of 1-1-1 up (Col) and of 1-0-0 up (Col) genes that are no longer upregulated in *hsfa2*, *hsfa3-1* (*hsfa3*), and *hsfa2 hsfa3-1* (*hsfa23*) mutants relative to their no-HS expression ($\log_2$FC ≤ 1 OR $\log_2$FC > 1 AND p > 0.05, blue; $\log_2$FC > 1 AND p > 0.05, gray). **b** Overlap of genes with loss of upregulation relative to no-HS expression ($\log_2$FC ≤ 1 OR $\log_2$FC > 1 AND p > 0.05) in *hsfa2*, *hsfa3-1* (*hsfa3*), or *hsfa2 hsfa3-1* (*hsfa23*) mutants among 1-1-1up (Col) and 1-0-0 up (Col) genes. **c** Pairwise comparison of $\log_2$FCs relative to no-HS expression between Col and *hsfa2*, *hsfa3-1* (*hsfa3*) or *hsfa2 hsfa3-1* (*hsfa23*) mutants of 1-1-1 up (Col) and 1-0-0 up (Col) genes. Genes in orange are more strongly induced in the mutant, genes in blue are less induced in the mutant. Colored numbers indicate the number of genes in the respective group.
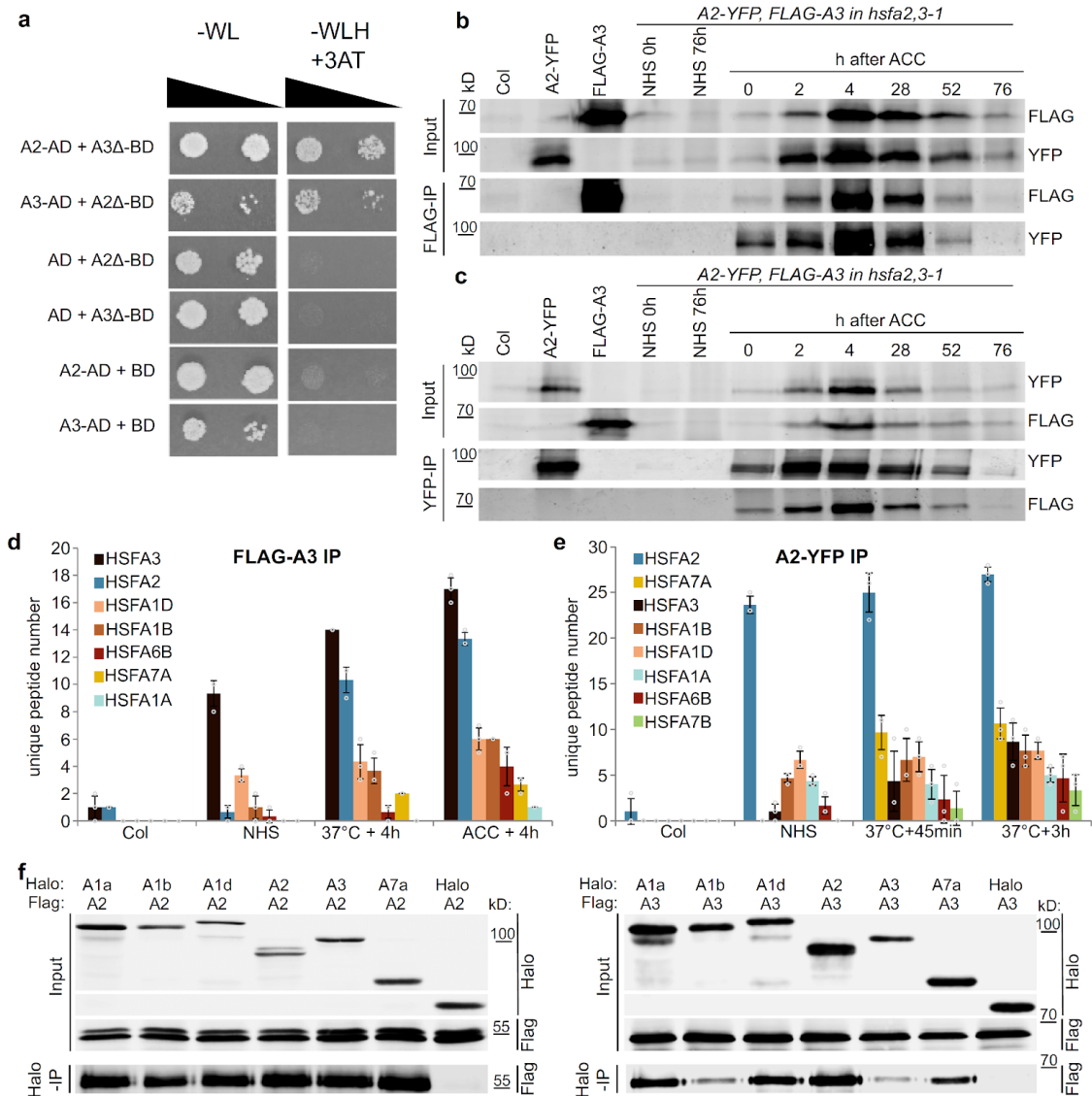
54

Fig. 7 HSFA2 and HSFA3 form protein complexes during HS memory. a HSFA2 and HSFA3 interact in the yeast-two-hybrid assay. The C-terminal transactivating domains of HSFA2 and HSFA3 were deleted (A2Δ aa 1-269, A3Δ aa 1-275) when fused to the GAL4-DNA-binding domain (BD) to prevent auto activation. Serial dilutions were grown on –WL medium (not selecting for interaction) or on –WLH medium supplemented with 50 mM 3-AT to check for protein-protein interactions. **b**, **c** HSFA2 and HSFA3 interact *in planta* as shown by co-immunoprecipitation experiments: transgenic lines carrying both *pHSFA2::HSFA2-YFP* and *pHSFA3::FLAG-HSFA3* constructs in the *hsfa2 hsfa3-1* double mutant background were subjected to an ACC treatment and samples were taken at the indicated time points. Immunoprecipitation of FLAG-HSFA3 yielded the HSFA2-YFP protein (**b**) and immunoprecipitation of HSFA2-YFP yielded the FLAG-HSFA3 protein (**c**) at all time points examined. No bands of similar size were co-purified in non-treated plants (NHS 0 h and NHS 76 h), single transgenic lines or Col plants sampled at 4 h after ACC. A representative experiment from 3 independent experiments is shown. **d**, **e** Interacting HSF proteins as identified by co-immunoprecipitation of FLAG-HSFA3 (**d**) or HSFA2-YFP (**e**) followed by mass spectrometry after the indicated treatments (37 °C treatment was for 1 h). Average numbers of unique peptides

55

are given for all HSF proteins identified (cf. Supplementary Table 2). Data are mean ± SD of three independent experiments. Note that the HSF proteins are sorted according to the number of peptides recovered and this differs for HSFA2- andHSFA3-co-purified proteins, the same color code is used in (**d**) and (**e**). **f** In vitro pulldown of HSFA proteins. Pairs of the indicated Halo-tagged and FLAG-tagged HSF proteins were co-translated in vitro and purified with anti-Halo beads. The Halo-tag alone was used as a negative control. A representative experiment from 3 independent experiments is shown.
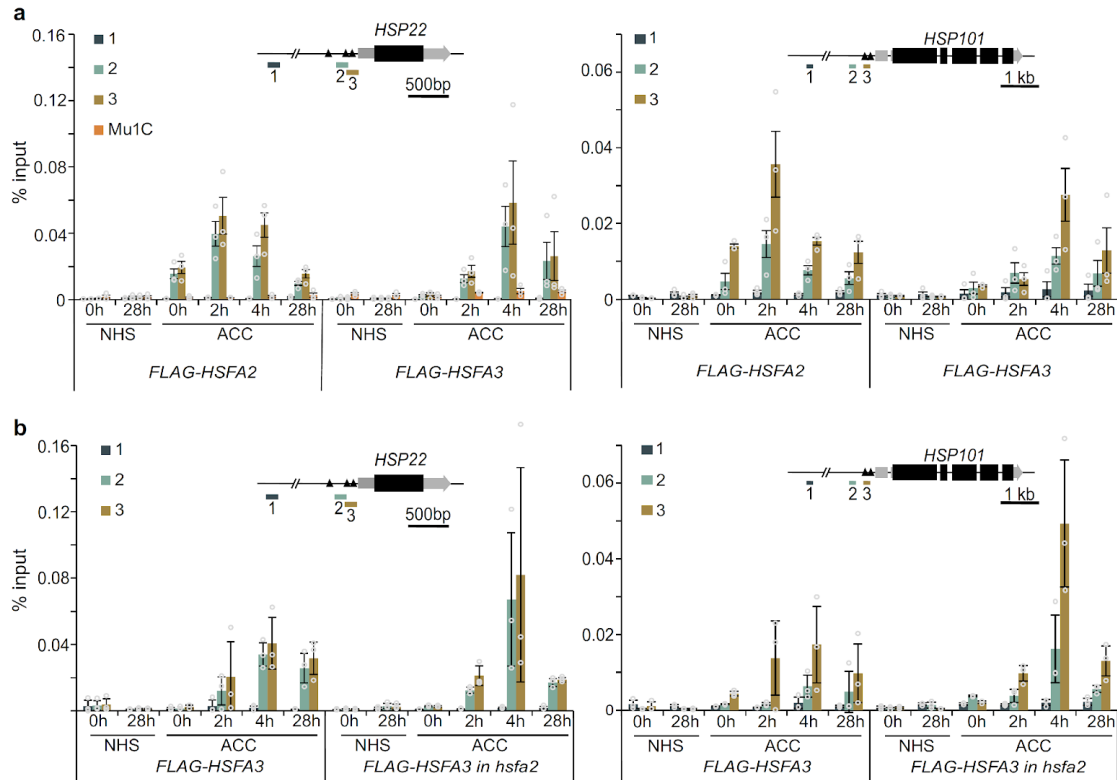
Fig. 8 HSFA2 and HSFA3 bind to memory gene promoters directly and independently. a Occupancy of HSFA2 and HSFA3 as determined by ChIP-qPCR from *pHSFA2::FLAG-HSFA2* and *pHSFA3::FLAG-HSFA3*. **b** Occupancy of HSFA3 as determined by ChIP-qPCR from *pHSFA3::FLAG-HSFA3* in the wild type or *hsfa2* mutant background. Enrichment normalized to Input (Data are mean ± SD) from three independent experiments is shown for the HS memory gene *HSP22* and the non-memory gene *HSP101*. The transposon *Mu1c* is shown as a non HS-responsive locus. Time points are given in h after end of ACC treatment. For each locus one control amplicon situated approximately 3 kb upstream is shown alongside the amplicon covering heat shock elements (black triangles) in the promoter (inset gene models).
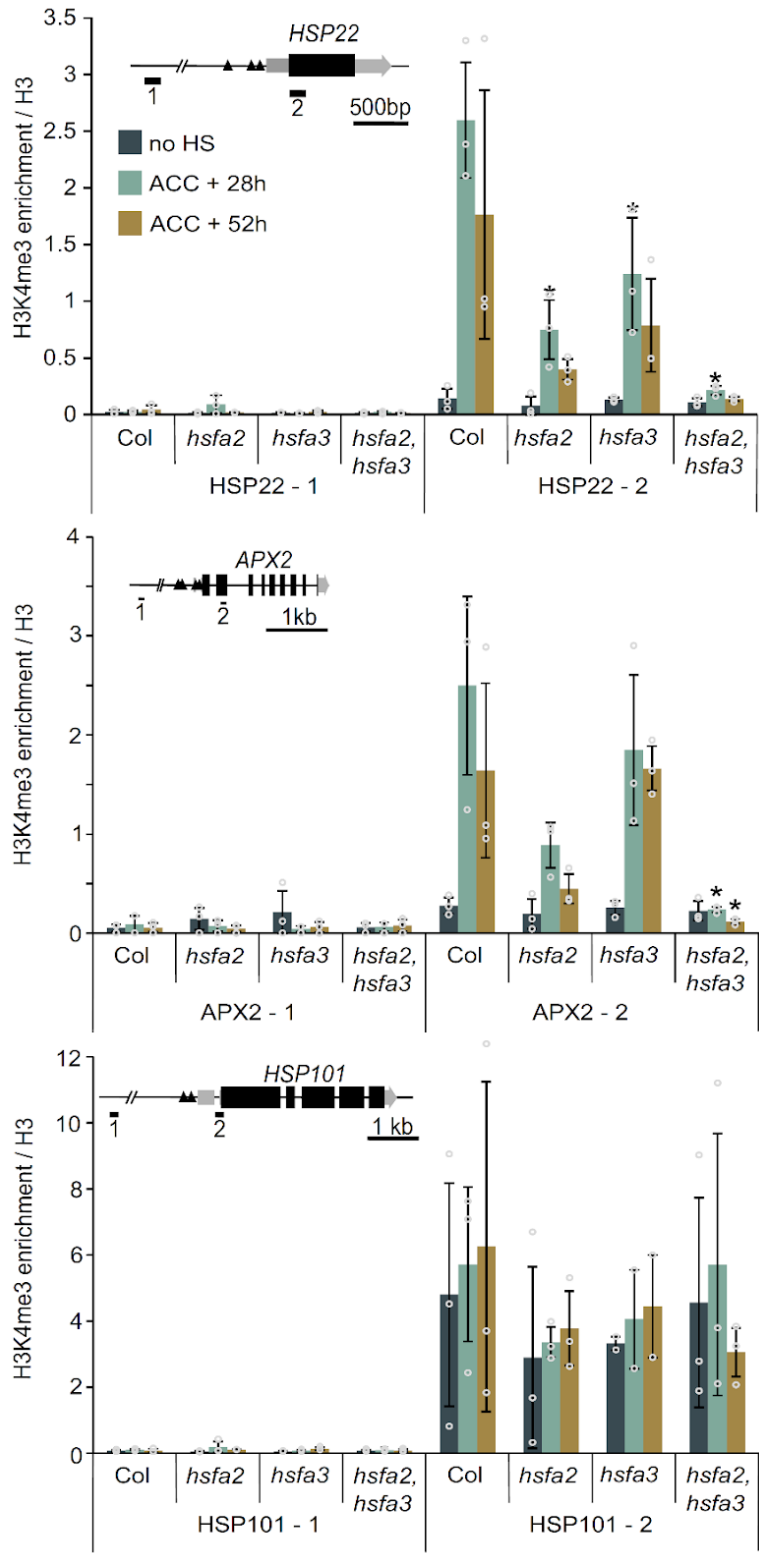
Fig. 9 H3K4me3 deposition depends on HSFA2 and HSFA3. Enrichment of H3K4me3 over H3 for the HS memory genes *HSP22* and *APX2*, and the non-memory gene *HSP101* as determined by ChIP-qPCR from three independent experiments. For each locus one control amplicon situated approximately 3 kb upstream is shown alongside the amplicon covering the transcriptional start site (inset gene models). Time points are given in h after end of ACC treatment. Data are mean ± SD. Asterisks mark significant differences relative to Col (*p* < 0.05, unpaired two-sided t-test).
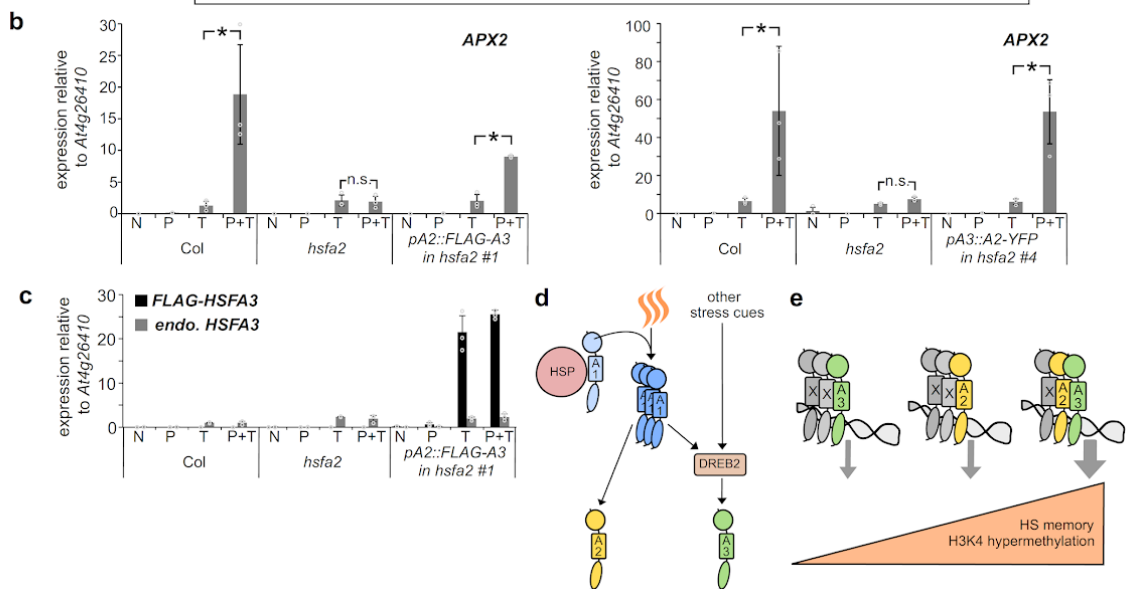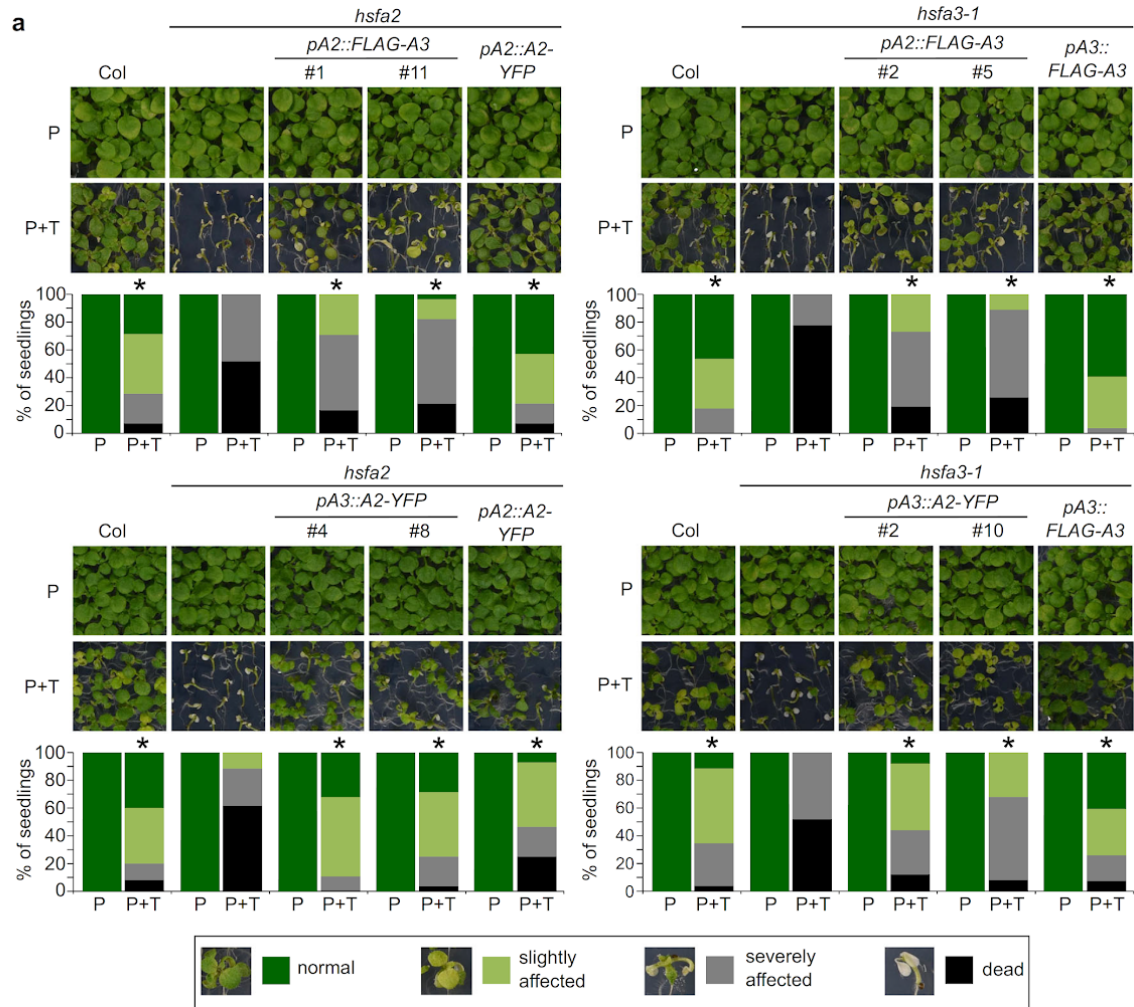
Fig. 10 Promoter swapping indicates that HSFA2 and HSFA3 proteins carry out the same functions and working model. a *FLAG-HSFA3* expressed from the *HSFA2* promoter complements *hsfa2* and *hsfa3-1* mutants in HS memory assays. *HSFA2-YFP* expressed from the *HSFA3* promoter complements *hsfa2* and *hsfa3-1* mutants in HS memory assays. Asterisks mark significant differences to the mutant background ($p < 0.05$, Fisher's exact test, n ≥ 24 seedlings for each time point and genotype). Phenotype categories used for quantification are indicated. **b**, **c** *pHSFA2::FLAG-HSFA3* and *pHSFA3::HSFA2-YFP* are each sufficient to rescue the type II memory defect of *hsfa2*. Relative transcript levels in enhanced re-induction experiments shown for the memory gene *APX2* (**b**) and endogenous HSFA3 or FLAG-HSFA3 (**c**) as measured by qRT-PCR. Samples were either not treated at all (N), only primed on d 4 (P), only triggered on d 7 (T) or primed on d 4 and triggered on d 7 (P+ T). All samples were harvested at the end of the triggering HS (T) on d 7. Data are mean ± SD of three independent experiments. Asterisks mark significant differences for the indicated comparisons ($p < 0.01$, unpaired two-sided t-test). **d**, **e** Working model for HS memory regulation by HSFA2 and HSFA3. **d** Differential regulation of *HSFA2* and *HSFA3* fine-tunes HS responses and integrates different environmental cues. A priming HS activates HSFA1 proteins through the release from HSPs and formation of active trimers. Active HSFA1s promote the expression of *HSFA2* and *DREB2* genes. DREB2 in turn promotes the expression of *HSFA3*; since DREB2s are also induced and activated at the posttranslational level by other stress cues, this may serve to integrate different cues into the HS memory response through HSFA3. **e** Different HSF complexes containing HSFA2 and/or HSFA3 form after a priming HS. They vary in their capacity to activate HS memory. The most efficient HSF complex to promote HS memory contains both HSFA2 and HSFA3, while complexes with only one of the two proteins have a reduced capacity for the recruitment of H3K4 hyper-methylation and for HS memory.

Data availability and supplementary material

RNA sequencing data have been deposited at NCBI GEO under accession number GSE162434. All raw data underlying the individual figures are provided as Supplementary Data. The plant materials generated and analyzed during the current study are available from the corresponding author upon request. Source data are provided with this paper.

The online version contains supplementary material available at https://doi.org/10.1038/s41467-021-23786-6:

- Fig. S1: *FGT3* is required for HS memory, but not basal thermotolerance or acquired thermotolerance
- Fig. S2: *FGT3* encodes *HSFA3*
- Fig. S3: Physiological HS memory lasts for 5 days and depends on *HSFA2* and *HSFA3*
- Fig. S4: HSFA2 and HSFA3 are not required for basal or acquired thermotolerance
- Fig. S5: *pHSFA3::FLAG-HSFA3* rescues the sustained induction defects of memory genes in *hsfa3-1* and sustained induction of unspliced transcripts in mutants
- Fig. S6: HSFA2 and HSFA3 bind to memory gene promoters (additional target genes, cf. Fig. 8)
- Fig. S7: Histone H3 enrichment after ACC (cf. Fig. 9)
- Fig. S8: Protein expression of promoter-swap constructs (cf. Fig. 10) and HSFA1D protein cannot functionally replace HSFA3
- Table S1: HSF- and DREB-binding motifs in *HSFA2* and *HSFA3* promoters identified by JASPAR (http://jaspar.genereg.net/)
- Table S2: Unique peptide numbers of HSF-proteins identified in IP-MS experiments
- Table S3: Unique peptide numbers of HSF-proteins identified by Co-IP/MS experiments of 3xFLAG-HSFA2, 3xFLAG-HSFA3 in wild type and *hsfa* mutant backgrounds

- Table S4: Oligonucleotides used in this study
- Dataset S1: Log$_2$ fold change relative to no-HS expression of 1-0-0 up (Col) and 1-1-1 up (Col) genes in Col, *hsfa2*, *hsfa3-1*, *hsfa2 hsfa3-1*

References

1. Conrath, U. Molecular aspects of defence priming. *Trends Plant Sci.* **16**, 524–531 (2011).

2. Hilker, M. et al. Priming and memory of stress responses in organisms lacking a nervous system. *Biol. Rev. Camb. Philos. Soc.* **91**, 1118–1133 (2016).

3. Lämke, J. & Bäurle, I. Epigenetic and chromatin-based mechanisms in environmental stress adaptation and stress memory in plants. *Genome Biol.* **18**, 124 (2017).

4. Conrath, U., Beckers, G. J., Langenbach, C. J. & Jaskiewicz, M. R. Priming for enhanced defense. *Annu. Rev. Phytopathol.* **53**, 97–119 (2015).

5. Bäurle, I. Can't remember to forget you: Chromatin-based priming of somatic stress responses. *Semin. Cell Dev. Biol.* 133–139 (2017) https://doi.org/10.1016/j.semcdb.2017.09.032.

6. Rasmann, S. et al. Herbivory in the previous generation primes plants for enhanced insect resistance. *Plant Physiol.* **158**, 854–863 (2012).

7. Slaughter, A. et al. Descendants of primed Arabidopsis plants exhibit resistance to biotic stress. *Plant Physiol.* **158**, 835–843 (2012).

8. Wibowo, A. et al. Hyperosmotic stress memory in Arabidopsis is mediated by distinct epigenetically labile sites in the genome and is restricted in the male germline by DNA glycosylase activity. *eLife* **5**, e13546 (2016).

9. Ding, Y., Fromm, M. & Avramova, Z. Multiple exposures to drought 'train' transcriptional responses in Arabidopsis. *Nat. Commun.* **3**, 740 (2012).

10. Kim, J. M. et al. Transition of chromatin status during the process of recovery from drought stress in Arabidopsis thaliana. *Plant Cell Physiol.* **53**, 847–856 (2012).

11. Feng, X. J. et al. Light affects salt stress-induced transcriptional memory of P5CS1 in Arabidopsis. *Proc. Natl Acad. Sci. USA* **113**, E8335–E8343 (2016).

12. Jaskiewicz, M., Conrath, U. & Peterhänsel, C. Chromatin modification acts as a memory for systemic acquired resistance in the plant stress response. *EMBORep.* **12**, 50–55 (2011).

13. Singh, P. et al. Environmental history modulates Arabidopsis pattern-triggered immunity in a HISTONE ACETYLTRANSFERASE1-dependent manner. *Plant Cell* **26**, 2676–2688 (2014).

14. Mozgova, I. et al. Chromatin assembly factor CAF-1 represses priming of plant defence response genes. *Nat. Plants* **1**, 15127 (2015).

15. Battisti, D. S. & Naylor, R. L. Historical warnings of future food insecurity with unprecedented seasonal heat. *Science* **323**, 240–244 (2009).

16. Lobell, D. B., Schlenker, W. & Costa-Roberts, J. Climate trends and global crop production since 1980. *Science* **333**, 616–620 (2011).

17. Richter, K., Haslbeck, M. & Buchner, J. The heat shock response: life on the verge of death. *Mol. Cell* **40**, 253–266 (2010).

18. Li, J., Labbadia, J. & Morimoto, R. I. Rethinking HSF1 in stress, development, and organismal health. *Trends cell Biol.* **27**, 895–905 (2017).

19. Gomez-Pastor, R., Burchfiel, E. T. & Thiele, D. J. Regulation of heat shock transcription factors and their roles in physiology and disease. *Nat. Rev. Mol.Cell Biol.* **19**, 4–19 (2018).

20. Ohama, N., Sato, H., Shinozaki, K. & Yamaguchi-Shinozaki, K. Transcriptional regulatory network of plant heat stress response. *Trends Plant Sci.* **22**, 53–65 (2017).

21. Charng, Y. Y., Liu, H. C., Liu, N. Y., Hsu, F. C. & Ko, S. S. Arabidopsis Hsa32, a novel heat shock protein, is essential for acquired thermotolerance during long recovery after acclimation. *Plant Physiol.* **140**, 1297–1305 (2006).

22. Charng, Y. Y. et al. A heat-inducible transcription factor, HsfA2, is required for extension of acquired thermotolerance in Arabidopsis. *Plant Physiol.* **143**, 251–262 (2007).

23. Stief, A. et al. Arabidopsis miR156 regulates tolerance to recurring environmental stress through SPL transcription factors. *Plant Cell* **26**, 1792–1807 (2014).

24. Brzezinka, K. et al. Arabidopsis FORGETTER1 mediates stress-induced chromatin memory through nucleosome remodeling. *eLife* **5**, e17061 (2016).

25. Brzezinka, K., Altmann, S. & Baurle, I. BRUSHY1/TONSOKU/MGOUN3 is required for heat stress memory. *Plant Cell Environ.* **42**, 765–775 (2019).

26. Scharf, K. D., Berberich, T., Ebersberger, I. & Nover, L. The plant heat stress transcription factor (Hsf) family: structure, function and evolution. *Biochim. Biophys. Acta* **1819**, 104–119 (2012).

27. Ikeda, M., Mitsuda, N. & Ohme-Takagi, M. Arabidopsis HsfB1 and HsfB2b act as repressors of the expression of heat-inducible Hsfs but positively regulate the acquired thermotolerance. *Plant Physiol.* **157**, 1243–1254 (2011).

28. Nishizawa-Yokoi, A. et al. HsfA1d and HsfA1e involved in the transcriptional regulation of HsfA2 function as key regulators for the Hsf signaling network in response to environmental stress. *Plant Cell Physiol.* **52**, 933–945 (2011).

29. Liu, H. C., Liao, H. T. & Charng, Y. Y. The role of class A1 heat shock factors (HSFA1s) in response to heat and other stresses in Arabidopsis. *Plant Cell Environ.* **34**, 738–751 (2011).

30. Yoshida, T. et al. Arabidopsis HsfA1 transcription factors function as the main positive regulators in heat shock-responsive gene expression. *Mol. Genet Genomics* **286**, 321–332 (2011).

31. Yeh, C. H., Kaplinsky, N. J., Hu, C. & Charng, Y. Y. Some like it hot, some like it warm: phenotyping to explore thermotolerance diversity. *Plant Sci.: Int. J. Exp. Plant Biol.* **195**, 10–23 (2012).

32. Lämke, J., Brzezinka, K., Altmann, S. & Bäurle, I. A hit-and-run heat shock factor governs sustained histone methylation and transcriptional stress memory. *EMBO J.* **35**, 162–175 (2016).

33. Liu, H. C. et al. Distinct heat shock factors and chromatin modifications mediate the organ-autonomous transcriptional memory of heat stress. *Plant J.* **95**, 401–413 (2018).

34. Chan-Schaminet, K. Y., Baniwal, S. K., Bublak, D., Nover, L. & Scharf, K. D. Specific interaction between tomato HsfA1 and HsfA2 creates hetero-oligomeric superactivator complexes for synergistic activation of heat stress gene expression. *J. Biol. Chem.* **284**, 20848–20857 (2009).

35. Clos, J. et al. Molecular cloning and expression of a hexameric Drosophila heat shock factor subject to negative regulation. *Cell* **63**, 1085–1097 (1990).

36. Majumdar, A., Nagaraj, R. & Banerjee, U. strawberry notch encodes a conserved nuclear protein that functions downstream of Notch and regulates gene expression along the developing wing margin of Drosophila. *Genes Dev.* **11**, 1341–1353 (1997).

37. Schramm, F. et al. A cascade of transcription factor DREB2A and heat stress transcription factor HsfA3 regulates the heat stress response of Arabidopsis. *Plant J.* **53**, 264–274 (2008).

38. Yoshida, T. et al. Functional analysis of an Arabidopsis heat-shock transcription factor HsfA3 in the transcriptional cascade downstream of the DREB2A stress-regulatory system. *Biochem. Biophys. Res. Commun.* **368**, 515–521 (2008).

39. Sakuma, Y. et al. Dual function of an Arabidopsis transcription factor DREB2A in water-stress-responsive and heat-stress-responsive gene expression. *Proc. Natl Acad. Sci. USA* **103**, 18822–18827 (2006).

40. Bäurle, I., Smith, L., Baulcombe, D. C. & Dean, C. Widespread role for the flowering-time regulators FCA and FPA in RNA-mediated chromatin silencing. *Science* **318**, 109–112 (2007).

41. Sandqvist, A. et al. Heterotrimerization of heat-shock factors 1 and 2 provides a transcriptional switch in response to distinct stimuli. *Mol. Biol. Cell* **20**,1340–1347 (2009).

42. Sakuma, Y. et al. Functional analysis of an Arabidopsis transcription factor, DREB2A, involved in drought-responsive gene expression. *Plant Cell* **18**,1292–1309 (2006).

43. Morimoto, K. et al. BPM-CUL3 E3 ligase modulates thermotolerance by facilitating negative regulatory domain-mediated degradation of DREB2A in Arabidopsis. *Proc. Natl Acad. Sci. USA* **114**, E8528–E8536 (2017).

44. Larkindale, J. & Vierling, E. Core genome responses involved in acclimation to high temperature. *Plant Physiol.* **146**, 748–761 (2008).

45. Ding, Y. et al. ATX1-generated H3K4me3 is required for efficient elongation of transcription, not initiation, at ATX1-regulated genes. *PLoS Genet.* **8**, e1003111 (2012).

46. Zhou, K., Kuo, W. H. W., Fillingham, J. & Greenblatt, J. F. Control of transcriptional elongation and cotranscriptional histone modification by the yeast BUR kinase substrate Spt5. *Proc. Natl Acad. Sci. USA* **106**, 6956–6961(2009).

47. Lu, C. et al. Phosphorylation of SPT5 by CDKD;2 Is Required for VIP5 Recruitment and Normal Flowering in Arabidopsis thaliana. *Plant Cell* **29**, 277–291 (2017).

48. Leng, X., Thomas, Q., Rasmussen, S. H. & Marquardt, S. A G(enomic)P(ositioning)S(ystem) for Plant RNAPII Transcription. *Trends Plant Sci.* **25**, 744–764 (2020).

49. Zeitlinger, J. et al. RNA polymerase stalling at developmental control genes in the Drosophila melanogaster embryo. *Nat. Genet.* **39**, 1512–1516 (2007).

50. Jonkers, I. & Lis, J. T. Getting up to speed with transcription elongation by RNA polymerase II. *Nat. Rev. Mol. Cell Biol.* **16**, 167–177 (2015).

51. Liu, X. et al. Crystal structure of the hexamer of human heat shock factor binding protein 1. *Proteins* **75**, 1–11 (2009).

52. Jung, H. S. et al. Subset of heat-shock transcription factors required for the early response of Arabidopsis to excess light. *Proc. Natl Acad. Sci. USA* **110**, 14474–14479 (2013).

53. Nishizawa, A. et al. Arabidopsis heat shock transcription factor A2 as a key regulator in response to several types of environmental stress. *Plant J.* **48**, 535–547 (2006).

54. Huang, Y.-C., Niu, C.-Y., Yang, C.-R. & Jinn, T.-L. The heat stress factor HSFA6b connects ABA signaling and ABA-mediated heat responses. *Plant Physiol.* **172**, 1182–1199 (2016).

55. Clough, S. J. & Bent, A. F. Floral dip: a simplified method for Agrobacterium-mediated transformation of Arabidopsis thaliana. *Plant J.* **16**, 735–743 (1998).

56. Czechowski, T., Stitt, M., Altmann, T., Udvardi, M. K. & Scheible, W. R. Genome-wide identification and testing of superior reference genes for transcript normalization in Arabidopsis. *Plant Physiol.* **139**, 5–17 (2005).

57. Dobin, A. et al. STAR: ultrafast universal RNA-seq aligner. *Bioinformatics* **29**,15–21 (2013).

58. Love, M. I., Huber, W. & Anders, S. Moderated estimation of fold change and dispersion for RNA-seq data with DESeq2. *Genome Biol.* **15**, 550 (2014).

59. Kaufmann, K. et al. Chromatin immunoprecipitation (ChIP) of plant transcription factors followed by sequencing (ChIP-SEQ) or hybridization to whole genome arrays (ChIP-CHIP). *Nat. Protoc.* **5**, 457–472 (2010).

60. Fornes, O. et al. JASPAR 2020: update of the open-access database of transcription factor binding profiles. *Nucleic Acids Res.* **48**, D87–D92 (2020).

Acknowledgements

Manuscript 2: Inducible epigenome editing probes for the role of histone H3K4 methylation in *Arabidopsis* heat stress memory

Vicky Oberkofler[1] and Isabel Bäurle[1,*,†]

[1] Institute for Biochemistry and Biology, University of Potsdam, Potsdam, 14476, Germany

[*] Author for correspondence: isabel.baeurle@uni-potsdam.de

[†] Senior author

Abstract

Histone modifications play a crucial role in the integration of environmental signals to mediate gene expression outcomes. However, genetic and pharmacological interference often causes pleiotropic effects, creating the urgent need for methods that allow locus-specific manipulation of histone modifications, preferably in an inducible manner. Here, we report an inducible system for epigenome editing in Arabidopsis (*Arabidopsis thaliana*) using a heat-inducible dCas9 to target a JUMONJI (JMJ) histone H3 lysine 4 (H3K4) demethylase domain to a locus of interest. As a model locus, we target the *ASCORBATE PEROXIDASE2* (*APX2*) gene that shows transcriptional memory after heat stress (HS), correlating with H3K4 hyper-methylation. We show that dCas9–JMJ is targeted in a HS-dependent manner to *APX2* and that the HS-induced overaccumulation of H3K4 trimethylation (H3K4me3) decreases when dCas9–JMJ binds to the locus. This results in reduced HS-mediated transcriptional memory at the *APX2* locus. Targeting an enzymatically inactive JMJ protein in an analogous manner affected transcriptional memory less than the active JMJ protein; however, we still observed a decrease in H3K4 methylation levels. Thus, the inducible targeting of dCas9–JMJ to *APX2* was effective in reducing H3K4 methylation levels. As the effect was not fully dependent on enzyme activity of the eraser domain, the dCas9–JMJ fusion protein may act in part independently of its demethylase activity. This underlines the need for caution in the design and interpretation of epigenome editing studies. We expect our versatile inducible epigenome editing system to be especially useful for studying temporal dynamics of chromatin modifications.

Introduction

Recent years have seen great progress in our knowledge of the distribution and regulation of histone modifications and their involvement in various plant processes including development, as well as short- and long-term adaptation to changing environments (Lämke and Bäurle, 2017; Xiao et al., 2017; Cheng et al., 2020; Ueda and Seki, 2020; Samo et al., 2021). While the dynamics of histone modifications are well characterized, it remains challenging to establish causal relationships between histone modifications and changes in gene expression or epigenetic states. Such analyses require the knockout of a specific histone modification, ideally in a locus-specific manner. In plants, this is often hampered by functional redundancy of writer/eraser enzymes and/or their lack of specificity (Cheng et al., 2020; Ueda and Seki, 2020). The known writer/eraser mutants affect many genes, causing pleiotropic effects that may be difficult to disentangle. For example, at least eight histone H3 lysine 4 (H3K4) methyltransferases (SET DOMAIN GROUP [SDG] 4, 8, 25; ARABIDOPSIS TRITHORAX [ATX] 1, 2, 3, 4, 5) have been described in Arabidopsis (*Arabidopsis thaliana*) (Cheng et al., 2020; Ueda and Seki, 2020). In addition, these enzymes are not necessarily specific toward histone H3K4, making genetic analysis and its interpretation difficult. Clustered regularly interspaced short palindromic repeats (CRISPR)/CRISPR-associated 9 (Cas9) provides a powerful method to selectively manipulate individual loci by targeting them with the help of specific single-guide RNAs (sgRNAs) (Doudna and Charpentier, 2014; Kumlehn et al., 2018). Targeting of heterologous proteins can be achieved by fusing an enzymatically inactive version of Cas9 (dCas9) with an effector protein of interest (Hilton et al., 2015; Kearns et al., 2015; Kwon et al., 2017; Lee et al., 2019; Papikian et al., 2019). In plants, the CRISPR/dCas9-editing system has been previously used to manipulate DNA methylation at individual loci including the imprinted *FLOWERING WAGENINGEN* (*FWA*) locus by expressing DNA methyltransferases (Ghoshalet al., 2021; Liu et al., 2021) or the TEN–ELEVEN TRANSLOCATION1 (TET1) DNA demethylase (Gallego-Bartolomé et al., 2018). For histone modifications, it has been used to target the HISTONE ACETYLTRANSFERASE1 and the H3 lysine 9 methyltransferase KRYPTONITE to an abscisic acid-response gene (*AREB1*) and the flowering time gene *FLOWERING LOCUS T*, respectively (Lee et al., 2019; Roca Païxao et al., 2019). While moderate effects on gene expression have been observed in both

cases, neither study provided evidence that the effect on gene expression was due to modification of histones at the locus of interest following the binding of the dCas9-effector fusion protein. Moderate heat stress (HS) primes a plant to acquire thermotolerance and better withstand a subsequent HS (Bäurle, 2016; Ohama et al., 2017; Oberkofler et al., 2021). A short HS pulse induces the acquisition of thermotolerance, but also activates a lasting stress memory that is maintained for several days after the HS has subsided (referred to as recovery phase). At the physiological level, this HS memory mediates enhanced survival upon a second HS that would be lethal to a naïve plant (Charng et al., 2007; Stief et al., 2014). At the molecular level, HS induces two types of transcriptional memory at partially overlapping sets of genes (Lämke et al., 2016; Liu et al., 2018); first, it induces sustained induction of gene expression that is actively maintained during several days of recovery at normal growth temperatures (Type I). Second, HS induces enhanced transcriptional reactivation upon a recurrent HS in certain genes, after their expression has returned to baseline levels during the recovery phase (Type II). In our experimental setup to analyze Type II memory, we refer to the first HS as priming HS (P) and to the second HS as triggering HS (T). Notably, P and T consist of an identical HS treatment (1 h at 37°C). Types I and II transcriptional memory require the HEAT SHOCK FACTOR A2 (HSFA2) transcription factor and correlate with enhanced H3K4 methylation (Charng et al., 2007; Lämke et al., 2016; Liu et al., 2018). Notably, the H3K4 hyper-methylation is maintained at elevated levels even after active transcription has subsided. The *ASCORBATE PEROXIDASE2* (*APX2*) gene displays Type II transcriptional memory (Lämke et al., 2016). While the current model posits that HSFA2 recruits a histone methyltransferase that sets and maintains H3K4 hyper-methylation, the identity of this methyltransferase is still elusive. Although SDG25 and ATX1 have been implicated in HS-induced H3K4 trimethylation (H3K4me3), it is unclear, whether they target *APX2* or other memory genes (Song et al., 2021). Thus, it remains an open question whether H3K4 methylation mediates the transcriptional memory or whether it is only correlated with the state of activated memory in Arabidopsis. In yeast and mammalian cells, H3K4 hyper-methylation marks recent transcriptional activity of a locus and may cause modified re-activation after a second stimulus (Ng et al., 2003; D'Urso et al., 2016). In plants, H3K4 hyper-methylation was also associated with somatic stress memory in response to dehydration stress and salt stress (Ding et al., 2012; Sani et al., 2013; Feng et al., 2016). Thus, we were curious to investigate the effects of perturbing H3K4 methylation at *APX2* after HS. Histone

demethylation is an enzymatically mediated process, and two families of histone demethylases are present in eukaryotes (Dimitrova et al., 2015; Cheng et al., 2020). While LYSINE-SPECIFIC DEMETHYLASE1 (LSD1)-like amine oxidases only demethylate dimethylated and monomethylated lysines, JUMONJI (JMJ) demethylases are active on trimethylated, dimethylated, and monomethylated lysines (Dimitrova et al., 2015). In Arabidopsis, there are four LSD1-like genes that all act on H3K4me2/1 (*LSD1-LIKE1* [*LDL*]*1*, *LDL2*, *LDL3*, *FLOWERING LOCUS D*) (Jiang et al., 2007; Liu et al., 2007; Ishihara et al., 2019), while the JMJ family consists of 21 members (Liu et al., 2010; Chen et al., 2011; Cheng et al., 2020). Typically, JMJ proteins show a high specificity toward the lysine that they demethylate (Ueda and Seki, 2020). Based on experimental and phylogenetic analysis, at least five JMJ proteins act on H3K4, namely JMJ14, JMJ15, JMJ16, JMJ17, and JMJ18 (Lu et al., 2010; Yang et al., 2012b, 2012a; Huang et al., 2019; Liu et al., 2019). These proteins are at least partially functionally redundant, rendering genetic analyses cumbersome. We selected the well-characterized JMJ18 as a demethylase for use in targeted epigenome editing (Yang et al., 2012a). To our knowledge, a histone demethylase has not been used in an epigenome editing experiment in plants. In animals, this has been done with an LSD family demethylase (Kearns et al., 2015), and with the H3K9 demethylase JMJD2 (Baumann et al., 2019). Targeting dCas9–JMJD2 together with a transcriptional activator was evaluated for its ability to enhance gene activation and found to have no substantial effect on target gene expression (Baumann et al., 2019). In addition, when targeted by a customized Zinc finger protein the H3K4me3 demethylase KDM5A/RBP2/JARID1A was able to reduce transcript levels of the targeted gene in a cancer cell line (Horton et al., 2016; Cano-Rodriguez et al., 2017). To create an inducible system for H3K4 demethylation, we expressed the dCas9–JMJ18 fusion under the control of a HS-inducible promoter. In summary, we report epigenome editing by expressing a histone H3K4-specific demethylase in Arabidopsis to evaluate the role of H3K4 methylation in HS memory. We show that the effector construct binds to the targeted *APX2* locus, where it decreases HS-induced transcriptional memory and H3K4 methylation. We highlight a need for careful design of controls, including enzyme-dead versions of the constructs, to be able to ascribe effects to the enzymatic activity of the targeted protein. Our HS-inducible epigenome editing system is widely applicable to address the role of epigenetic modifications for various processes such as stress responses and cell differentiation.

Results

Design and construction of inducible locus-specific epigenome editing for H3K4me demethylation. We have previously shown that HS-induced transcriptional memory is tightly correlated with H3K4me3 hyper-methylation at several loci including *APX2* (Lämke et al., 2016; Liu et al., 2018). To establish whether H3K4 methylation is required for Type II transcriptional memory (enhanced re-induction), we sought to target an H3K4 demethylase specifically after HS to *APX2*. We first created a construct where the HS-inducible *pHSP21* promoter drives expression of a fusion protein consisting of an inactive Cas9 (dCas9) and the catalytically active domain of JMJ18, referred to as JMJ in the following (Figure 1, A–C; Yang et al., 2012a; Stief et al., 2014; Hilton et al., 2015; Kearns et al., 2015). This domain of JMJ18 was previously shown to be sufficient to specifically demethylate histone H3K4me3/me2 (Yang et al., 2012a). To be able to test whether the catalytic activity of JMJ18 is necessary for any potential effects, we also generated a construct with a catalytically inactive JMJ18, dJMJ, where we mutated the highly conserved histidine 395 to alanine. In JMJ14, the corresponding point mutation (H397A) abolishes binding of the essential Fe(II)-cofactor and renders the enzyme catalytically inactive (Lu et al., 2010). Three sgRNA cassettes consisting of three individual sgRNAs each were designed and evaluated (Figure 1, A and B; Table 1). SgRNA cassette a binds just upstream of the heat shock elements (HSEs) (Nover et al., 2001; Schramm et al., 2006) between –113- and –205-bp relative to the transcriptional start site (TSS) of *APX2* (Table 1). Previous analyses indicated that HSFA2 and other HSFs bind to these HSEs (Schramm et al., 2006; Friedrich et al., 2021). Cassette b binds the promoter further upstream in a region that overlaps with the 5'-end of H3K4 hyper-methylation after HS (between –238- and –387-bp relative to the TSS). We chose this location because a previous epigenome editing study reported that effector complexes were most efficient when targeted to the boundaries of histone modification domains (Kwon et al., 2017). The third cassette (c) was designed by scrambling the cassette a sequences, resulting in no predicted target sequences in the genome.

Selection and validation of sgRNAs in a transient assay. To evaluate the efficiency of sgRNA cassettes a–c in targeting dCas9 to *APX2*, we took advantage of a transient transformation system, where we combined the *pAPX2::LUCIFERASE* (*LUC*) reporter gene, the respective sgRNA cassette, and a *35S::dCas9–VP64* effector construct

(Figure 1A). VP64 is a transcriptional activator consisting of four tandem repeats of herpes simplex virus early transcriptional activator VP16 that mediates transcriptional activation if bound to the promoter of a gene (Sadowski et al.,1988; Beerli et al., 1998). SgRNA-targeted dCas9–VP64 has been successfully used for transcriptional activation of protein-coding and noncoding genes in Arabidopsis and *Nicotiana benthamiana* (Lowder et al., 2015). Targeting of the dCas9–VP64 activator to the *APX2* promoter via the sgRNAs can be monitored by LUC-dependent bioluminescence. Three days after co-infiltrating the constructs into *N. benthamiana* leaves, LUC activity was analyzed (Figure 2). Cassette a promoted high LUC activity upon co-infiltration with the effector and reporter constructs. In contrast, co-infiltration of cassettes b (distal promoter) and c (scrambled), respectively, did not induce LUC activity above baseline levels (Figure 2), suggesting that these sgRNAs are not efficient in targeting dCas9–VP64 for transactivation. Thus, we selected cassette a for further studies.

dCas9–JMJ affects *pAPX2::LUC* expression after recurrent HS. We next generated transgenic plants that carried cassette a, *pAPX2::LUC*, and *pHSP21::dCas9–JMJ* or *pHSP21::dCas9–dJMJ*, respectively. We selected two representative lines from 20 primary transformants for detailed analysis of LUC expression after HS. In the absence of the dCas9–JMJ effector, expression of LUC after a priming HS (P d4, 1 h 37°C) was low and was slightly increased after 2 d of recovery (P d6, Figure 3, A and B). Similarly, expression of LUC after only a triggering HS (T, 1 h 37°C) was low. However, LUC expression was strongly increased in seedlings that received both the P and T treatments (P + T, Figure 3). For plants expressing *pHSP21::dCas9–JMJ*, LUC expression was similar to plants without the effector in either P or T conditions (P d4, T, Figure 3), and it was lower in seedlings that received P treatment and 2 d of recovery before imaging (P d6). The strongest difference, however, was observed after P + T treatment, where the dCas9–JMJ seedlings had similar LUC signal to plants that only received the T treatment, while plants lacking this construct showed a much stronger LUC activity (Figure 3B). LUC expression after a two-step acclimation (ACC) treatment, which induces more persistent type I memory than the P treatment described above, was reduced throughout the recovery phase (Supplemental Figure S1). Together, these findings suggest that dCas9–JMJ expression interferes with both, Types I and II transcriptional memory after HS. To investigate the function of the JMJ domain, we analyzed transgenic plants expressing the presumably inactive dCas9–dJMJ fusion. In contrast to the active JMJ, where all transformants showed a very similar *LUC*

75

expression phenotype, the dJMJ transformants fell into two phenotypic classes with respect to this phenotype. One class was indistinguishable from the plants that did not carry any dCas9 construct (dJMJ#2), while the second class was more similar to dCas9–JMJ plants (dJMJ#1) (Figure 3B; Supplemental Figures S1 and S2A). Both dJMJ phenotypic classes were equally frequent among independent transformants (n = 8; four lines dJMJ#1-like, four lines dJMJ#2-like).

dCas9–JMJ affects *APX2* expression after recurrent HS. We next sought to confirm and extend the findings of the bioluminescence assay at the transcript level of *pAPX2::LUC* and the endogenous *APX2* gene by reverse transcription-quantitative PCR (RT-qPCR, Figure 4). Compared to plants without a *dCas9* construct, *LUC* transcript levels after T treatment of naïve plants (Figure 4A) were slightly lower in *dCas9–JMJ* plants, and similar to the control in *dCas9–dJMJ* (Figure 4B). However, if the T treatment was preceded by a priming treatment (P) 2 d earlier (P + T), *LUC* transcript levels were strongly and significantly reduced in *dCas9–JMJ*. For *dCas9–dJMJ* plants, in contrast, *LUC* transcript levels were reduced in the dJMJ#1-like class, but not in the dJMJ#2-like class (Figure 4B; Supplemental Figure S2B). We next analyzed transcript levels of the endogenous *APX2* gene (Figure 4B; Supplemental Figure S2B). All genotypes showed similar induction after T treatment; however, the dCas9–JMJ lines showed a strongly reduced expression after P + T treatment, suggesting that transcriptional memory is impaired in these plants. For the dCas9–dJMJ lines, the results were heterogeneous, but in full agreement with the LUC bioluminescence assay, with *dCas9–dJMJ #1*-class showing a reduced and #2-class showing parent-like *APX2* expression levels. For the non-memory HS-inducible *HSP101* gene, expression was similar in all lines. Thus, transcript analyses confirm that the *dCas9–JMJ* lines show decreased expression after P + T treatment, consistent with the notion that these lines are impaired in HS-induced transcriptional memory. We selected two *dCas9–JMJ* lines (*JMJ#1*, *#2*) and one representative lines of each *dJMJ* class (*dJMJ#1*, *#2*) for further analyses. The four selected *dCas9–JMJ* and *dCas9–dJMJ* lines had similar protein expression levels, as confirmed by immunoblotting protein extracts from HS-treated plants (Supplemental Figure S3).

The dCas9–(d)JMJ fusion proteins bind to the *APX2* promoter. To test whether the reduced transcriptional memory is mediated by direct binding of dCas9–JMJ to the *APX2* promoter, we performed chromatin immunoprecipitation (ChIP) using the Flag epitope in

the dCas9–(d)JMJ fusion protein (Figure 1). We found enrichment of Flag-dCas9–(d)JMJ relative to the control amplicon outside the *APX2* locus (amplicon 2) after heat treatment (P, T, P + T, Figure 5, A and B). However, dJMJ line #2 had a weaker signal compared to the others. All lines showed the strongest enrichment after P + T treatment. The enrichment peaked at the TSS-160 amplicon (4, Figure 5, A and B), overlapping with the location of the sgRNAs of cassette a. The signal decreased shortly after the TSS, consistent with the idea that dCas9–JMJ does not spread far beyond the targeted binding site. Very slight but significant binding was also found in N conditions, indicating a basal activity of *pHSP21* under no-HS conditions. We did not find any enrichment at the *ACTIN* locus, which we included as a negative control (Figure 5B). Thus, dCas9–(d)JMJ is expressed and targeted to *pAPX2*.

dCas9–JMJ reduces H3K4me3 at *APX2*. We next studied the effect of dCas9–(d)JMJ expression on H3K4 methylation at *APX2* using ChIP. H3K4me3 is induced after HS at *APX2*, and is maintained for at least 3 d, thus corresponding with the duration of the transcriptional memory (Lämke et al., 2016; Liu et al., 2018). Fully consistent with previous reports, H3K4me3 was enriched in P, T, and P + T conditions relative to N in the control line without the dCas9 fusion protein (Figures 4A and 6; e.g. amplicon 6, P versus N, $P = 0.025$, unpaired two-sided t test). The enrichment of H3K4me3 was strongest around the TSS and in the coding region (amplicons 5, 6 in Figure 6). As expected, after P (HS + 2 d recovery) the signal was stronger than after T (45min after HS). The strongest enrichment, was observed in P + T conditions, which was significantly higher than the enrichment in T (amplicon 6, P + T versus T, $P = 0.003$, unpaired two-sided t test). Here, a reduction in H3K4me3 levels was observed in both *dCas9–JMJ* lines (#1, $P = 0.004$, unpaired two-sided t test). A slight reduction in H3K4me3 levels was also observed in the P condition, but not in the T condition (Figure 6). Thus, dCas9–JMJ is effective in reducing H3K4me3 levels at *APX2* after HS. However, due to the use of a HS-inducible system, the demethylation function may not yet be active at the time when T was sampled. In contrast, we did not find any consistent changes at the *ACTIN* locus. For *pAPX2::LUC*, H3K4me3 was overall less enriched, however, we nevertheless observed a significant decrease in the enrichment around the TSS in *dCas9–JMJ* #1. For *dCas9–dJMJ*, the overall pattern was similar to *dCas9–JMJ*, but with nonsignificant reductions after P and P + T relative to the parent at the same treatment. Thus, we found that dCas9–JMJ reduced H3K4 methylation at *APX2*, strongly suggesting that the demethylase activity of JMJ18 causes reduced transcriptional

77

memory. However, we cannot exclude that this is mediated by non-enzymatic effects of the JMJ fusion protein since similar phenotypes were observed with the catalytically inactive dJMJ18 domain.

Discussion

We have developed an inducible epigenome editing system for H3K4 methylation that can be easily adapted to other chromatin modifiers. We provide a framework of how the functional relevance of histone methylation may be tested in a locus-specific manner, thus avoiding pleiotropic effects of other approaches. The system may not only be useful for studying environmentally mediated chromatin modifications, but also for studying the role of histone methylation in the determination of cell fates during cell differentiation. For example, our system may be easily adapted to study the effect of removing the Polycomb mark H3K27me3 in flowering time or flower development (Xiao et al., 2017; Pelayo et al., 2021). Our results are consistent with the notion that H3K4 hyper-methylation marks the chromatin of *APX2* and mediates enhanced transcriptional re-induction upon a recurrent HS. Histone demethylation was detected in a region close to the binding site of cassette a. H3K4me3 typically peaks at the 5'-end of genes and we found the strongest enrichment just downstream of the TSS. Dynamic H3K4me3 has been observed in many contexts, however, its biological function is still not fully clear. The transient removal of this mark may shed light onto this function in an unprecedented manner. We evaluated the efficiency of the sgRNA cassettes using a rapid transient *N. benthamiana* assay. Only one of the two sgRNA cassettes that we tested was efficient in targeting dCas9–VP64 to *APX2*. Thus, we focused further analysis on this cassette. However, we cannot exclude that the nonfunctional cassette was located simply too far from the TSS to provide efficient transactivation. Thus, this cassette might have been efficient in targeting dCas9–JMJ as the methylation is enriched also in the promoter (Figure 6). A previous study in mammalian cells found that epigenome editing of the p300 acetyl transferase was most efficient if the sgRNAs were located just outside the acetylated region (Kwon et al., 2017). Further studies will be needed to test whether this requirement is generally applicable also for histone (de-)methylation in plants. The use of a HS-inducible promoter allowed us to minimize effects in the noninduced condition. The *HSP21* promoter was previously characterized to have very low baseline expression and very high induction levels (Stief et al., 2014). It also shows sustained induction during the recovery phase, thus boosting protein levels during this phase. We did not precisely determine the lag time until functional dCas9–(d)JMJ protein is generated. However, the observed H3K4me3 dynamics (Figure 6) suggest that 45 min of recovery

time may be too short to detect effects of the editing if plants were only triggered (T). On the other hand, this recovery time was sufficient if plants were primed before the triggering HS (P + T). We included an inactive JMJ domain in our study to be able to assess whether the effects are linked to the demethylase activity of the JMJ domain. The mutated residue is required for binding of the Fe(II)-cofactor and was previously shown to be essential for enzymatic activity of JMJ14 (Lu et al., 2010). The inactive dJMJ construct reduced the transcriptional memory to some extent and caused a reduction in H3K4me3 levels. This may be explained by at least two different scenarios. First, it is possible that the dJMJ domain has a scaffolding function that is able to recruit endogenousH3K4 demethylases. While demethylase activity was shown for JMJ18 (Yang et al., 2012a), it is possible that it also fulfills structural functions for which the demethylase activity is dispensable. Second, the effect may be caused by steric hindrance or interference with the binding and functioning of gene-specific and general components of the transcriptional machinery. The size of the dCas9–JMJ fusion protein (dCas9 + (d)JMJ = 180 kDa) is roughly the same as that of the presumed trimeric HSF complex (Friedrich et al., 2021). It may be helpful for future studies to include a fusion of dCas9 to an unrelated protein of a similar size as the effector protein (here: (d)JMJ) to disentangle steric effects from effects caused by the active or inactive JMJ protein. Protein size is a highly relevant consideration for construct design, as several available epigenome editing systems (such as SunTag) target multiple effector proteins to one target site (Tanenbaum et al., 2014; Morita et al., 2016; Papikian et al., 2019). Steric effects may be minimal when using a system that mediates binding of only one effector protein per target site. Thus, our data indicate the need to carefully design epigenome editing studies, at least those in which mechanistic insights are desired in addition to effects on expression levels of the modified gene. In summary, we developed an inducible epigenome editing system to modify H3K4 methylation, which can be easily adapted to other histone modifications. We report an efficient system to evaluate sgRNA cassettes and provide guidelines for study design. Our results demonstrate that H3K4 hyper-methylation is tightly connected with transcriptional memory of *APX2*. This versatile system is widely applicable to modify histone modification levels in both basic research questions and applied settings.

Materials and methods

Plant materials, growth conditions, and HS treatments. All Arabidopsis (*A. thaliana*) lines generated and used in this study harbor the *pAPX2$_{600bp}$::LUC* transgene (Liu et al., 2018) in Col-0 background; hence, we refer to this line as parent. Seedlings were grown on GM medium (1% (w/v) glucose) under 16-h/8-h light/dark cycle at 23°C/21°C. For the analysis of Type II transcriptional memory, seedlings were exposed to HS at 37°C for 1 h either on Day 4 (priming, P), or on Day 6 (triggering, T), or on Days 4 and 6 (priming and triggering, P + T), or not at all (no HS, NHS). For the analysis of type I transcriptional memory by LUC imaging, 4-d-old seedlings were exposed to a two-step acclimation (ACC) protocol as follows: 37°C for 1 h, 23°C for 1.5 h, 44°C for 45 min.

Construction of transgenic lines. To generate dCas9–JMJ constructs, pHEE401E (Wang et al., 2015) was used as backbone. *3xFLAG-dCas9* was amplified from pHSN6A01 (Wang et al., 2015) with primer 3197 containing *Xba*I restriction site and primer 3198 containing *Asc*I and *Sac*I restriction sites. *pHSP21* was amplified from genomic DNA with primers 3033/34 containing *Nco*I and *Xba*I restriction sites. The JmjC domain of JMJ18 (*JMJ*) was amplified from cDNA with primers 3203/04 containing *Asc*I and *Sac*I restriction sites and stop codon. To generate the catalytically inactive JMJ, site-directed mutagenesis was performed on the *JMJ* fragment, corresponding to H395A substitution of the full-length JMJ18 protein. sgRNA cassettes flanked by *Hind*III and *Nco*I restriction sites were obtained from BioCat (Heidelberg, Germany) in pUC57 and subcloned into pHEE401E vector. To generate dCas9–VP64 constructs, *dCas9–VP64* and *2x35S* promoter were amplified from pHSN6A01. *dCas9–VP64* was amplified using primers 3459/60 containing *Xba*I and *Sac*I restriction sites, *2x35S* was amplified using primers 3035/36 containing *Nco*I and *Xba*I restriction sites. Both fragments were subcloned into pHEE401E containing the sgRNA cassette. All constructs were introduced into *Agrobacterium tumefaciens* GV3101 for plant transformation. For generation of stable transgenic lines, *pAPX2::LUC* plants were transformed using the floral dip method (Clough and Bent, 1998). Primer sequences are listed in Supplemental Table S1.

LUC imaging and immunoblotting. For LUC imaging in the transient transactivation assay, 4-week-old leaves of *N. benthamiana* were co-infiltrated (Sparkes et al., 2006) with the following *A. tumefaciens* GV3101 suspensions: pGreenII binary vector

81

containing *pAPX2::LUC* (kindly provided by Y. Pan) and pHEE401E binary vector containing *p2x35S::dCas9–VP64* and either one of the three sgRNA cassettes, or no sgRNA cassette. After 3 d, leaves were infiltrated with 2-mM firefly luciferin (Promega, Madison, WI, USA) and immediately imaged with NightOWL In Vivo Imaging System (Berthold Technologies) using standard settings. For LUC imaging of seedlings, they were sprayed with 2-mM luciferin and imaged as above. For immunoblotting, total protein was extracted from frozen tissue (Smaczniak et al., 2012). An amount of 40 mg of total protein was separated by sodium dodecylsulfate-polyacrylamide gel electrophoresis (SDS–PAGE) on a 4% (v/v) gel and immunoblotted with anti-Flag or anti-histone H3 antibodies (F1804, Sigma, ab1791, Abcam, Cambridge, UK) and secondary anti-mouse antibody (926-32210) on an Odyssey imaging system (both LI-COR Biosciences Lincoln, NE, USA).

RT-qPCR. To examine enhanced re-induction of gene expression, seedlings were exposed to 37°C for 1 h on Day 4 and/or Day 6 after germination. All samples, including nontreated controls, were snap-frozen 6 d after germination at a time corresponding to the end of the Day 6 HS treatment. To extract RNA frozen tissue was ground to a fine powder and resuspended in 500-µL RNA extraction buffer (100-mM Tris–HCl pH 8.5, 5-mM EDTA, 100-mM NaCl, 0.5% (w/v) SDS), 250-µL phenol, and 5-µL b-mercaptoethanol. Samples were incubated at 60°C for 15 min. An aliquot of 250-µL chloroform was added and samples were incubated at RT for 15 min, followed by centrifugation at RT for 10 min at 16,000 g. An aliquot of 550-µL of the aqueous phase were recovered and mixed with 550-µL phenol:chloroform:isoamyl alcohol (25:24:1), incubated and centrifuged as above. Then 500-µL of the aqueous phase was recovered and mixed with 400-µL isopropanol and 50-µL 3-M sodium acetate and precipitated at –80°C for 15 min, followed by centrifugation at 4°C for 30 min at 20,500 g. RNA was precipitated overnight at 4°C in 2-M LiCl. RNA was pelleted by centrifugation at 4°C for 30 min at 20,500g, washed in 80% (v/v) EtOH, dried, and resuspended in 40-µL H_2O. For RT-qPCR, total RNA was treated with TURBO DNA-free (Ambion, Austin, TX, USA) and reverse transcribed with SuperScript III (Invitrogen, Waltham, MA, USA) according to manufacturer's instructions. For each 13.33-µL RT-qPCR reaction, 0.167-µL cDNA was used with GoTaq qPCR Master Mix (Promega Madison, WI, USA) on a LightCycler480 II system (Roche, Basel, Switzerland). All analyzed transcripts were normalized to the reference gene *At4g26410* (Czechowski et al., 2005) using the comparative Cq method. Primer sequences are listed in Supplemental Table S1. To

perform multiple comparison of gene expression results between transgenic lines, one-way ANOVA with post-hoc Tukey's HSD analysis (confidence level = 0.95) were performed using the TukeyHSD() function of the R package multcompView (https://cran.r-project.org/web/packages/multcompView/index.html).

ChIP. For dCas9–JMJ and histone modification ChIP, seedlings were exposed to 37°C for 1 h on Day 4 and/or Day 6 after germination. All samples, including nontreated controls, were harvested 6 d after germination at a time corresponding to 45min after the d6 HS treatment. Cross-linking of samples was done under vacuum in ice-cold MC buffer with 1% (v/v) formaldehyde for 2 x 10 min. Chromatin was extracted as follows (Kaufmann et al., 2010): frozen tissue was ground to a fine powder, resuspended in 25-mL M1 buffer, filtered through Miracloth mesh (Merck Kenilworth, NJ, USA), washed five times in 5-mL M2 buffer, and once in 5-mL M3 buffer, with a centrifugation step at 4°C, 10 min,1,000 g in between each wash. The resulting chromatin pellet was resuspended in 1-mL Sonication buffer and sheared with a Bioruptor Pico (Diagenode Denville, NJ, USA) for 17 cycles (30 s on/30 s off) on low-intensity settings. Equal chromatin amounts of chromatin from each sample were immunoprecipitated over night at 4°C using antibodies against Flag (F1804, Sigma-Aldrich), H3 (ab1791, Abcam), and H3K4me3 (ab8580, Abcam). Immunoprecipitated DNA was quantified by qPCR on a LightCycler480 II system (Roche). Primer sequences are listed in Supplemental Table S1. To statistically evaluate dCas9–(d)JMJ and H3K4me3 enrichment, independent t tests were performed (https://www.graphpad.com/quickcalcs/ttest1.cfm).

Accession numbers. Accession numbers for genes mentioned in this work are as follows: *APX2* (*AT3G09640*), *JMJ18* (*AT1G30810*), and *HSP101* (*AT1G74310*).
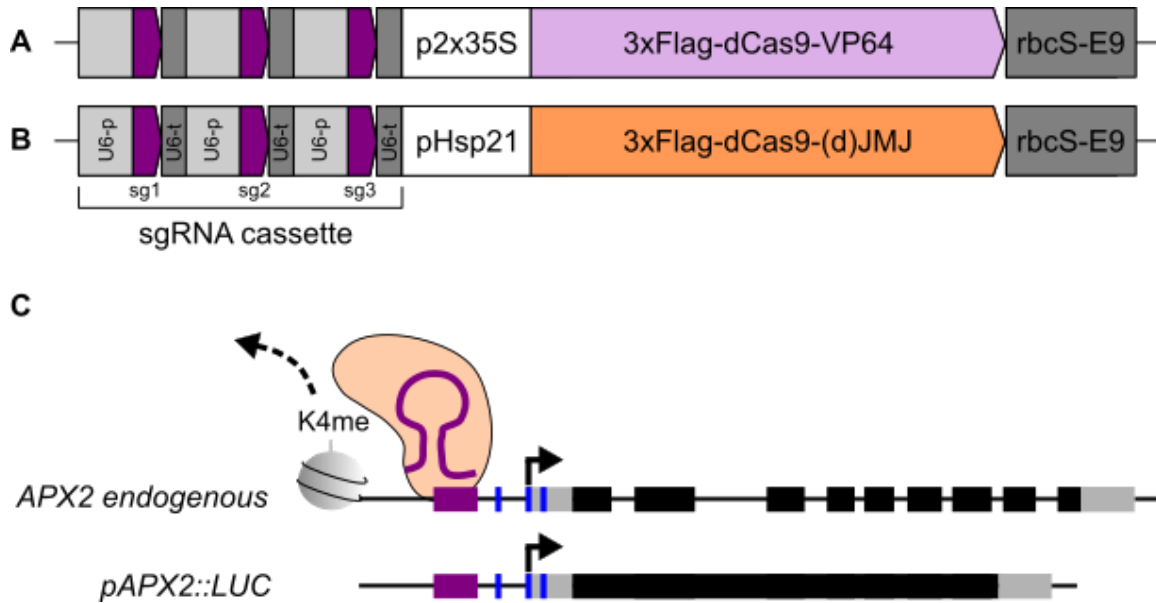
Main figures and tables

Figure 1 Principle and design of JMJ epigenome editing constructs targeting *APX2*. Schematic representation of generated constructs for validation of sgRNA design by transient transactivation in *N. benthamiana* (**A**) and for generation of stable lines (**B**) in the *pHEE401E* vector backbone. Both types of constructs contain an sgRNA cassette, which is consisting of three repeats of a U6 promoter variant (light gray box) driving expression of three different sgRNA + scaffold sequence (purple arrow) followed by a U6 terminator variant (dark gray box). To validate sgRNA targeting efficiency, constitutively expressed 3xFlag-dCas9 was translationally fused to VP64 (A, light purple arrow), followed by the rbcS-E9 terminator sequence. To generate stable lines, 3xFlag-dCas9–(d)JMJ (**B**, orange arrow) was expressed under the HS-inducible *pHSP21* promoter, followed by the rbcS-E9 terminator sequence. **C**, sgRNA (purple line)-mediated targeting of 3xFlag-dCas9–(d)JMJ (orange) to the promoter region of *APX2* is expected to affect histone H3 lysine K4 demethylation (dashed arrow) and type II transcriptional memory of *APX2 endogenous* and *pAPX2::LUC* genes. Both genes show enhanced re-induction of transcription after repeated HS. Purple box, sgRNA-targeted region; blue insets, HSEs; gray box, untranslated region; black box; coding region exon; black line, DNA.
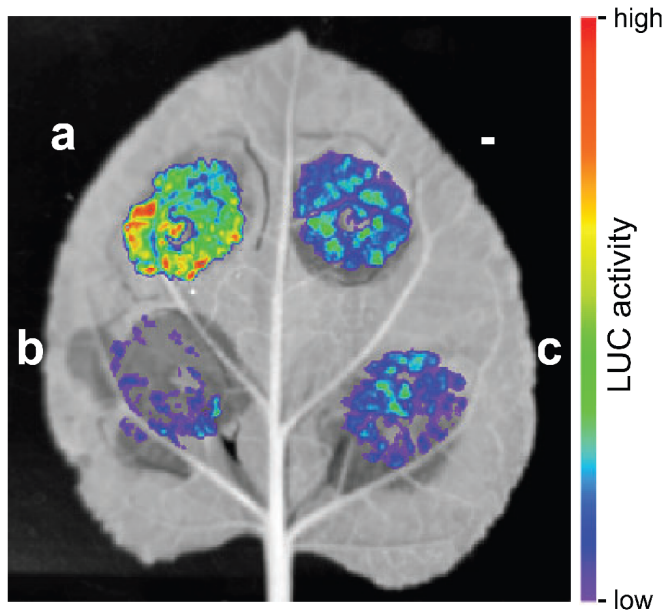
Figure 2 Validation of sgRNA targeting of *pAPX2* in a transient transactivation assay in *N. bentha-miana*. LUC-based assay to validate targeting efficiency of sgRNA cassettes to $APX2_{600bp}$ promoter fragment. Luciferin-infiltrated *N. ben-thamiana* leaf 3 d after co-infiltration with $pAPX2_{600bp}::LUC$ and *p2x35S:: 3xFlag-dCas9-VP64* in combination with sgRNA cassette a (a), cassette b (b), or scrambled cassette (c), or without any cassette (–). High LUC activity in presence of cassette a indicates binding of 3xFlag-dCas9–VP64 to $pAPX2_{600\ bp}$ and trans-activation of *LUC* expression by transcriptional activator VP64. The image is representative of three independent experiments.
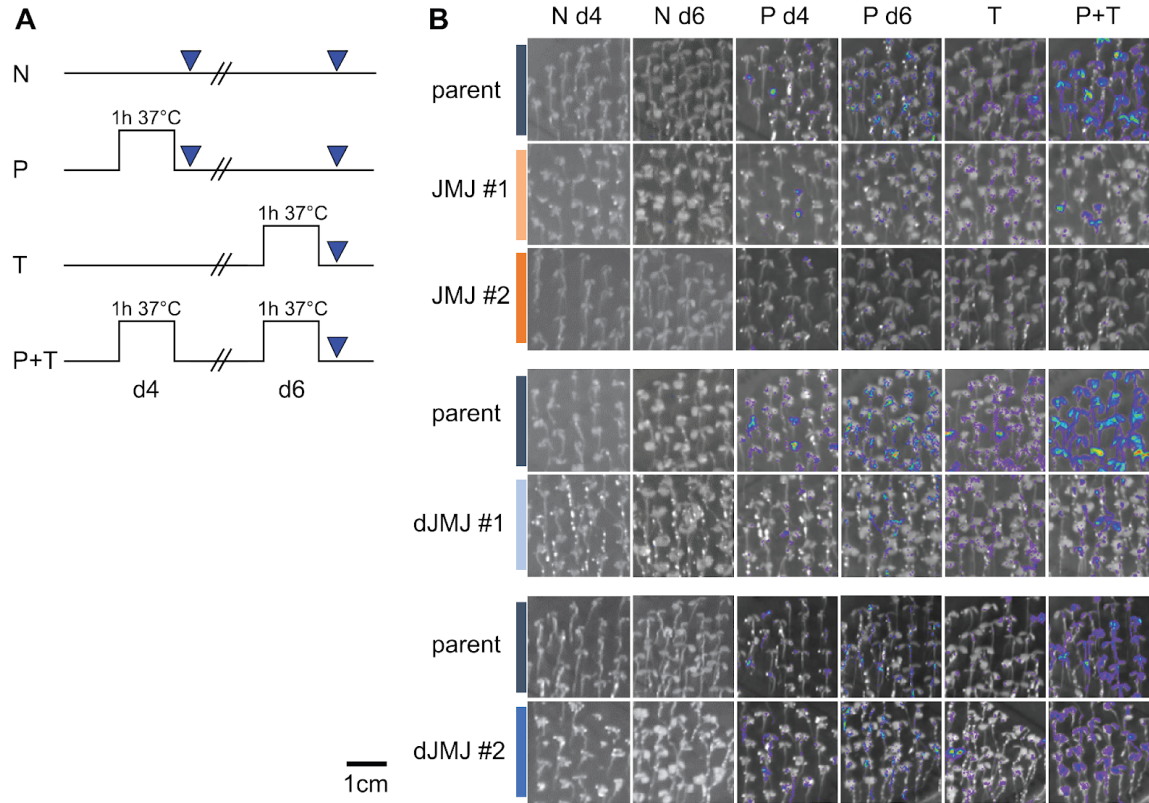
Figure 3 Effect of dCas9–(d)JMJ on type II transcriptional memory of *pAPX2::LUC*. A, Treatment scheme for LUC-based type II transcriptional memory assay. Four-day-old seedlings were either exposed to priming HS (P) on Day 4 and imaged on Day 4 (P d4) or on Day 6 (P d6), exposed to a triggering HS (T) on Day 6 and imaged on Day 6 (T), exposed to priming HS on Day 4 and a triggering HS on Day 6 (P + T) and imaged on Day 6 (P + T), or not exposed to any HS and imaged on Day 4 (N d4) or on Day 6 (N d6). **B**, LUC-based type II transcriptional memory assay shows reduced transcriptional activity of the *pAPX2 $_{600\,bp}$::LUC* reporter in *dCas9-JMJ* lines (top panel, JMJ #1 and JMJ #2) compared to the parent, as well as different behavior of two *dCas9–dJMJ* lines (middle and bottom, dJMJ #1 and dJMJ #2). For images within one panel the indicated genotypes were grown and treated side-by-side on the same set of plates. Images are representative of three independent experiments.
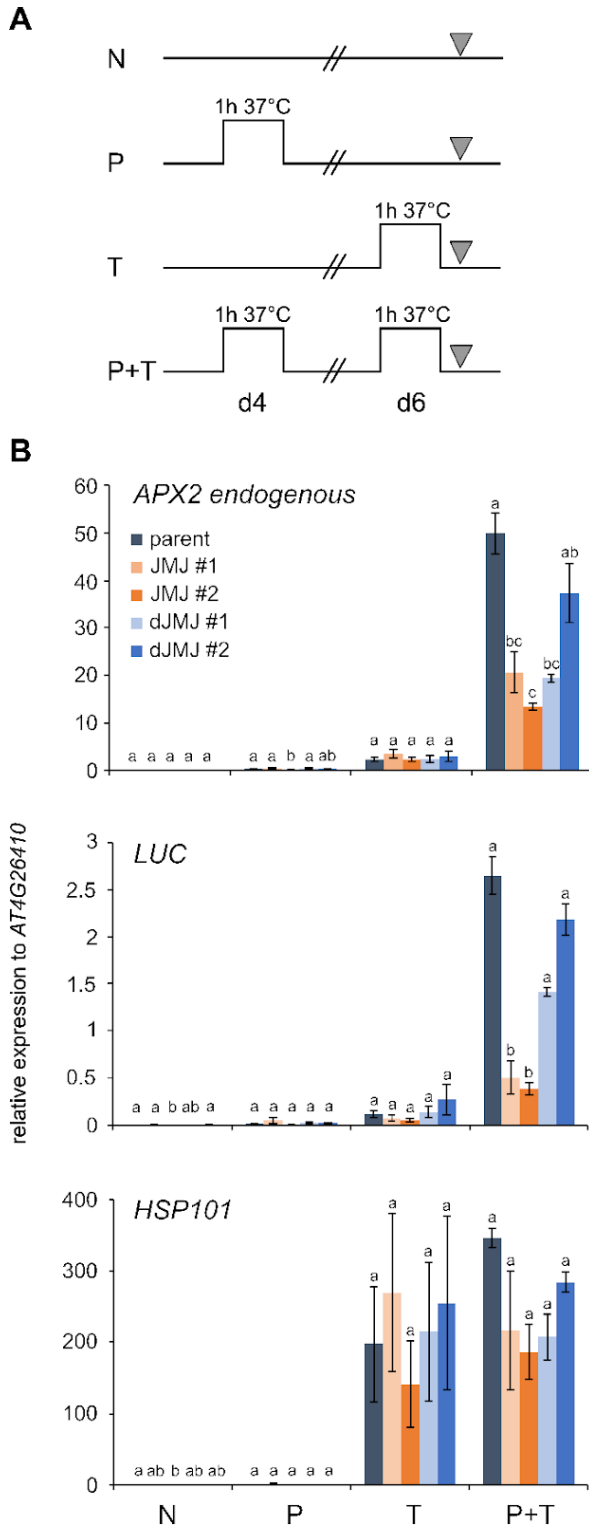
Figure 4 Type II transcriptional memory of endogenous *APX2* and *pAPX2::LUC* after recurrent HS is reduced in *dCas9–JMJ* lines. A, Treatment scheme for RT-qPCR-based type II transcriptional memory assay. Four-day-old seedlings were either exposed to priming HS (P) on Day 4, exposed to a triggering HS (T) on Day 6, exposed to a priming and a triggering HS (P + T), or not exposed to any HS (N). All samples were taken on d 6 corresponding to the end of the HS treatment. **B**, Transcript levels of endogenous *APX2* (*At3g09640*), *LUC* (*pAPX2*$_{600\ bp}$*::LUC*), and *HSP101* (*At1g74310*) in parent, two *dCas9–JMJ* lines (JMJ #1 and JMJ #2), and two *dCas9-dJMJ* lines (dJMJ #1 and dJMJ#2) as measured by RT-qPCR. Expression values are relative to *At4g26410*. Data are mean ± SEM of three independent experiments. Transcript levels were statistically evaluated for all genotypes within each time point by Tukey's HSD (*P* < 0.05). Genotypes are assigned one or more letters based on their statistical group. Genotypes sharing one letter are not significantly different.
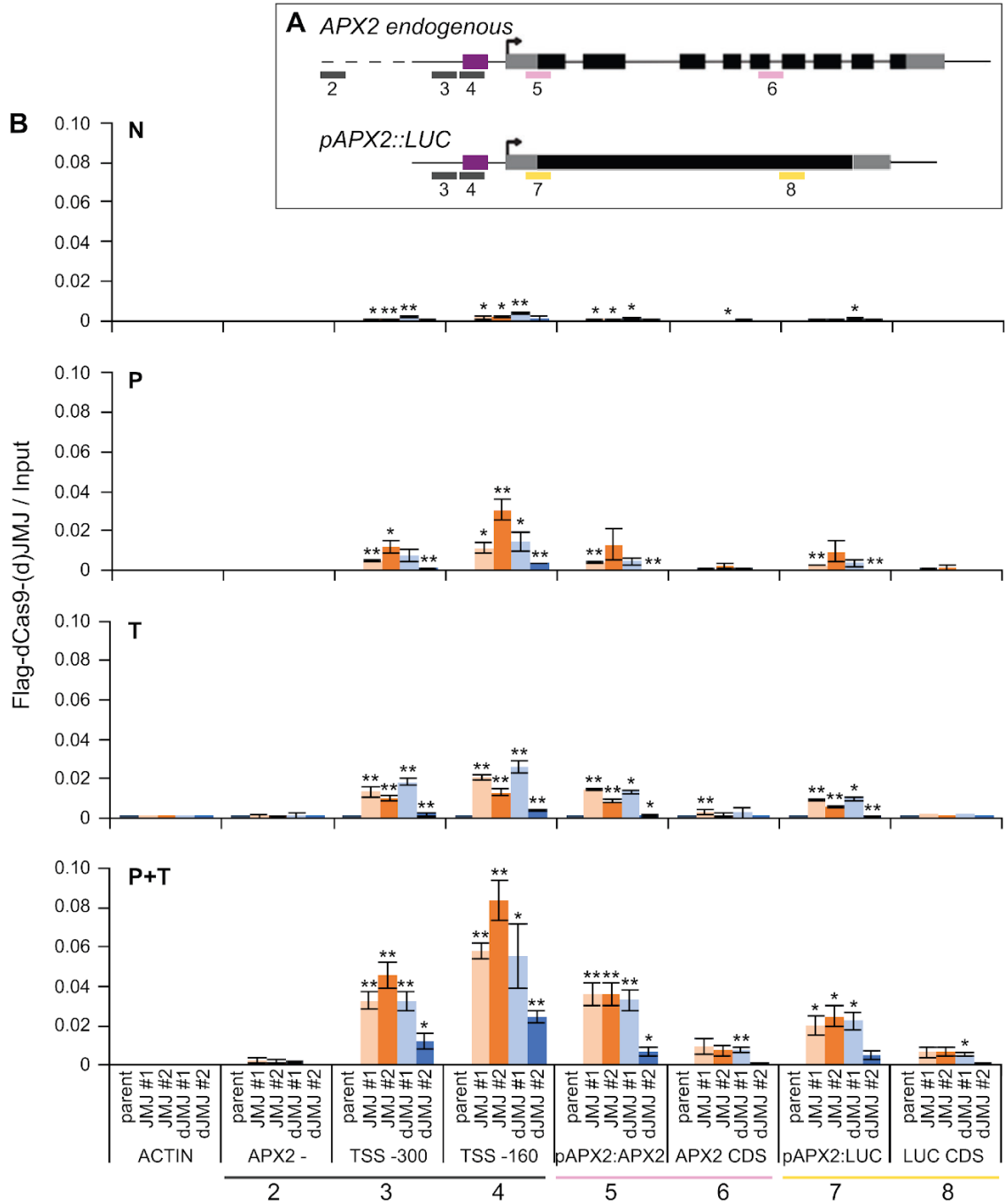
Figure 5 dCas9–(d)JMJ proteins bind *APX2* after HS. A, Schematic representation of positions of analyzed amplicons by ChIP-qPCR. For the *APX2 endogenous* locus and the *pAPX2$_{600\ bp}$::LUC* transgene, the TSS is shown with a black arrow, UTRs are shown as gray boxes, exons are shown as black boxes, and the introns of the endogenous *APX2* are shown as black lines. The sgRNA cassette a binding area is shown as purple box. Amplicons are shown as colored lines below the gene models. Pink amplicons are specific for *APX2 endogenous*, yellow amplicons are specific for *pAPX2$_{600\ bp}$::LUC*, and gray amplicons are not specific, that is, amplicons 3 and 4

amplify both the endogenous *APX2* and the transgene. 2, APX2– (3 kb upstream of *At3g09640*); 3, TSS –300 bp; 4, TSS –160 bp; 5, *pAPX2-APX2*; 6, *APX2 CDS*; 7, *pAPX2-LUC*; 8, *LUC CDS*. **B**, Occupancy of dCas9–JMJ and dCas9–dJMJ as determined by ChIP-qPCR. Sampling time points as described in Figure 4. Amplicons shown on the *x*-axis as indicated in (**A**), an amplicon of the *ACTIN* locus is shown as control. Enrichment normalized to Input. Data are mean ± SEM of three independent experiments. Asterisks mark significant differences to amplicon 2 (APX2–) of the same genotype (unpaired two-sided *t* test, *$P < 0.05$, **$P < 0.01$).
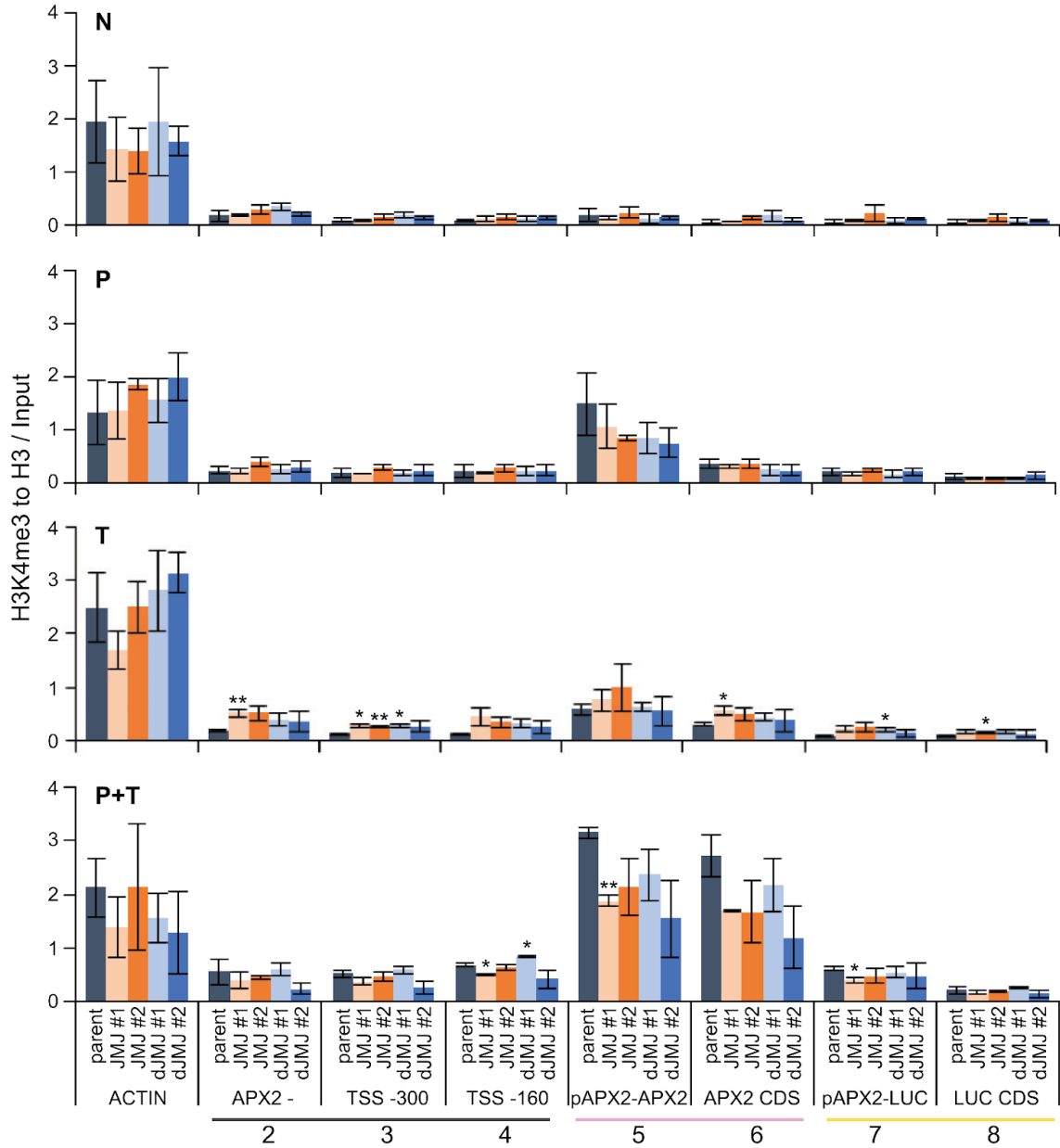
Figure 6 Epigenome editing reduces H3K4me3 enrichment after HS. Enrichment of H3K4me3 as determined by ChIP-qPCR. Sampling time points as described in Figure 4A. Amplicons shown on the *x*-axis as indicated in Figure 5A, an amplicon of the *ACTIN* locus is shown as control. Enrichment is normalized to histone H3 and Input. Data are mean ± SEM of three independent experiments. Asterisks mark significant differences to parent (unpaired two-sided *t* test, *$P < 0.05$, **$P < 0.01$).

Cassette	sgRNA sequences (5′–3′)	Position rel. to TSS (bp)
a	GGACGGTCATGATTTGTAGA	−113
	GACTATGGATGGTTTCTGGA	−160
	GACACGTGGTGTGTATCTGT	−205
b	GAGTTGGTACAACATACTCG	−238
	GATCGAGCACAAAAACGTTA	−326
	GAACCCTTAAGTCTTTTTGG	−387
c	GGTATAGGCATTAAGTGGTC	NA (Scrambled sequences of cassette a)
	GGTAGGTCGTTAGGTATACT	
	GGTTGTATACTGTCGGCGTA	

Table 1 Sequences and positions of sgRNAs relative to TSS of *APX2*.

Supplemental data

The following materials are available in the online version of this article (https://doi.org/10.1093/plphys/kiac113):

- Fig. S1: Effect of (d)JMJ on type I transcriptional memory of *pAPX2::LUC*
- Fig. S2: Type II transcriptional memory of additional dCas9–dJMJ lines
- Fig. S3: Immunoblot detection ofdCas9– (d)JMJ proteins
- Table S1: Oligonucleotides used in this study

References

Baumann V, Wiesbeck M, Breunig CT, Braun JM, Köferle A,Ninkovic J, Götz M, Stricker SH (2019) Targeted removal of epigenetic barriers during transcriptional reprogramming. Nat Commun **10**: 2119

Bäurle I (2016) Plant heat adaptation: priming in response to heat stress. F1000Res **5**: 694

Beerli RR, Segal DJ, Dreier B, Barbas CF (1998) Toward controlling gene expression at will: specific regulation of the erbB-2/HER-2promoter by using polydactyl zinc finger proteins constructed from modular building blocks. Proc Natl Acad Sci USA **95**:14628–14633

Cano-Rodriguez D, Campagnoli S, Grandi A, Parri M, Camilli ED,Song C, Jin B, Lacombe A, Pierleoni A, Bombaci M, et al. (2017) TCTN2: a novel tumor marker with oncogenic properties. Oncotarget **8**: 95256–95269

Charng YY, Liu HC, Liu NY, Chi WT, Wang CN, Chang SH, Wang TT (2007) A heat-inducible transcription factor, HsfA2, is required for extension of acquired thermotolerance in Arabidopsis. Plant Physiol **143**: 251–262

Chen X, Hu Y, Zhou DX (2011) Epigenetic gene regulation by plant Jumonji group of histone demethylase. Biochim Biophys Acta **1809**: 421–426

Cheng K, Xu Y, Yang C, Ouellette L, Niu L, Zhou X, Chu L, Zhuang F, Liu J, Wu H, et al. (2020) Histone tales: lysine methylation, a protagonist in Arabidopsis development. J Exp Bot **71**: 793–807

Clough SJ, Bent AF (1998) Floral dip: a simplified method for Agrobacterium-mediated transformation of Arabidopsis thaliana. Plant J **16**: 735–743

Czechowski T, Stitt M, Altmann T, Udvardi MK, Scheible WR (2005) Genome-wide identification and testing of superior reference genes for transcript normalization in Arabidopsis. Plant Physiol **139**: 5–17

Dimitrova E, Turberfield AH, Klose RJ (2015) Histone demethylases in chromatin biology and beyond. EMBO Rep **16**: 1620–1639

Ding Y, Fromm M, Avramova Z (2012) Multiple exposures to drought "train" transcriptional responses in Arabidopsis. Nat Commun **3**: 740

Doudna JA, Charpentier E (2014) The new frontier of genome engineering with CRISPR-Cas9. Science **346**: 1258096

D'Urso A, Takahashi YH, Xiong B, Marone J, Coukos R, Randise-Hinchliff C, Wang JP, Shilatifard A, Brickner JH (2016) Set1/COMPASS and Mediator are repurposed to promote epigenetic transcriptional memory. eLife **5**: e16691

Feng XJ, Li JR, Qi SL, Lin QF, Jin JB, Hua XJ (2016) Light affects salt stress-induced transcriptional memory of P5CS1 in Arabidopsis. Proc Natl Acad Sci USA **113**: E8335–E8343

Friedrich T, Oberkofler V, Trindade I, Altmann S, Brzezinka K, Lämke J, Gorka M, Kappel C, Sokolowska E, Skirycz A, et al. (2021) Heteromeric HSFA2/HSFA3 complexes drive transcriptional memory after heat stress in Arabidopsis. Nat Commun **12**: 3426

Gallego-Bartolomé J, Gardiner J, Liu W, Papikian A, Ghoshal B, Kuo HY, Zhao JM-C, Segal DJ, Jacobsen SE (2018) Targeted DNA demethylation of the Arabidopsis genome using the human TET1catalytic domain. Proc Natl Acad Sci USA **115**: E2125–E2134

Ghoshal B, Picard CL, Vong B, Feng S, Jacobsen SE (2021) CRISPR-based targeting of DNA methylation in Arabidopsis thaliana by a bacterial CG-specific DNA methyltransferase. Proc Natl Acad Sci USA **118**: e2125016118

Hilton IB, D'Ippolito AM, Vockley CM, Thakore PI, Crawford GE, Reddy TE, Gersbach CA (2015) Epigenome editing by aCRISPR-Cas9-based acetyltransferase activates genes from promoters and enhancers. Nat Biotechnol **33**: 510–517

Horton JR, Engstrom A, Zoeller EL, Liu X, Shanks JR, Zhang X, Johns MA, Vertino PM, Fu H, Cheng X (2016) Characterization of a linked jumonji domain of the KDM5/JARID1 family of histoneH3 lysine 4 demethylases. J Biol Chem **291**: 2631–2646

Huang S, Zhang A, Jin JB, Zhao B, Wang TJ, Wu Y, Wang S, Liu Y, Wang J, Guo P, et al. (2019) Arabidopsis histone H3K4 demethylaseJMJ17 functions in dehydration stress response. New Phytol **223**: 1372–1387

Ishihara H, Sugimoto K, Tarr PT, Temman H, Kadokura S, Inui Y, Sakamoto T, Sasaki T, Aida M, Suzuki T, et al. (2019) Primed histone demethylation regulates shoot regenerative competency. Nat Commun **10**: 1786

Jiang D, Yang W, He Y, Amasino RM (2007) Arabidopsis relatives of the human lysine-specific Demethylase1 repress the expression of FWA and FLOWERING LOCUS C and thus promote the floral transition. Plant Cell **19**: 2975–2987

Kaufmann K, Muino JM, Osteras M, Farinelli L, Krajewski P, Angenent GC (2010) Chromatin immunoprecipitation (ChIP) of plant transcription factors followed by sequencing (ChIP-SEQ) or hybridization to whole genome arrays (ChIP-CHIP). Nat Protocol **5**: 457–472

Kearns NA, Pham H, Tabak B, Genga RM, Silverstein NJ, Garber M, Maehr R (2015) Functional annotation of native enhancers with a Cas9-histone demethylase fusion. Nat Methods **12**: 401–403

Kumlehn J, Pietralla J, Hensel G, Pacher M, Puchta H (2018) The CRISPR/Cas revolution continues: From efficient gene editing for crop breeding to plant synthetic biology. J Integr Plant Biol **60**: 1127–1153

Kwon DY, Zhao YT, Lamonica JM, Zhou Z (2017) Locus-specific histone deacetylation using a synthetic CRISPR-Cas9-based HDAC. Nat Commun **8**: 15315

Lämke J, Bäurle I (2017) Epigenetic and chromatin-based mechanisms in environmental stress adaptation and stress memory in plants. Genome Biol **18**: 124

Lämke J, Brzezinka K, Altmann S, Bäurle I (2016) A hit-and-run heat shock factor governs sustained histone methylation and transcriptional stress memory. EMBO J **35**: 162–175

Lee JE, Neumann M, Duro DI, Schmid M (2019) CRISPR-based tools for targeted transcriptional and epigenetic regulation in plants. PLoS One **14**: e0222778

Liu C, Lu F, Cui X, Cao X (2010) Histone methylation in higher plants. Ann Rev Plant Biol **61**: 395–420

Liu F, Quesada V, Crevillen P, Bäurle I, Swiezewski S, Dean C (2007) The Arabidopsis RNA-binding protein FCA requires a lysine-specific demethylase 1 homolog to downregulate FLC. Mol Cell **28**: 398–407

Liu HC, Lämke J, Lin SY, Hung MJ, Liu KM, Charng YY, Bäurle I (2018) Distinct heat shock factors and chromatin modifications mediate the organ-autonomous transcriptional memory of heat stress. Plant J **95**: 401–413

Liu P, Zhang S, Zhou B, Luo X, Zhou XF, Cai B, Jin YH, Niu D, Lin J, Cao X, et al. (2019) The histone H3K4 demethylase JMJ16 represses leaf senescence in Arabidopsis. Plant Cell **31**: 430–443

Liu W, Gallego-Bartolomé J, Zhou Y, Zhong Z, Wang M, Wongpalee SP, Gardiner J, Feng S, Kuo PH, Jacobsen SE (2021) Ectopic targeting of CG DNA methylation in Arabidopsis with the bacterial SssI methyltransferase. Nat Commun **12**: 3130

Lowder LG, Zhang D, Baltes NJ, Paul JW, Tang X, Zheng X, Voytas DF, Hsieh T-F, Zhang Y, Qi Y (2015) A CRISPR/Cas9 Toolbox for Multiplexed Plant Genome Editing and Transcriptional Regulation. Plant Physiol **169**: 971–985

Lu F, Cui X, Zhang S, Liu C, Cao X (2010) JMJ14 is an H3K4 demethylase regulating flowering time in Arabidopsis. Cell Res **20**: 387–390

Morita S, Noguchi H, Horii T, Nakabayashi K, Kimura M, OkamuraK, Sakai A, Nakashima H, Hata K, Nakashima K, et al. (2016) Targeted DNA demethylation in vivo using dCas9–peptide repeat and scFv–TET1 catalytic domain fusions. Nat Biotechnol **34**: 1060–1065

Ng HH, Robert F, Young RA, Struhl K (2003) Targeted recruitment of Set1 histone methylase by elongating Pol II provides a localized mark and memory of recent transcriptional activity. Mol Cell **11**: 709–719

Nover L, Bharti K, Doring P, Mishra SK, Ganguli A, Scharf KD (2001) Arabidopsis and the heat stress transcription factor world: how many heat stress transcription factors do we need? Cell Stress Chaperones **6**: 177–189

Oberkofler V, Pratx L, Bäurle I (2021) Epigenetic regulation of abiotic stress memory: maintaining the good things while they last. Curr Opin Plant Biol **61**: 102007

Ohama N, Sato H, Shinozaki K, Yamaguchi-Shinozaki K (2017) Transcriptional regulatory network of plant heat stress response. Trends Plant Sci **22**: 53–65

Papikian A, Liu W, Gallego-Bartolomé J, Jacobsen SE (2019) Site-specific manipulation of Arabidopsis loci using CRISPR-Cas9SunTag systems. Nat Commun **10**: 729

Pelayo MA, Yamaguchi N, Ito T (2021) One factor, many systems: the floral homeotic protein AGAMOUS and its epigenetic regulatory mechanisms. Curr Opin Plant Biol **61**: 102009

Roca Paiẋao JF, Gillet FX, Ribeiro TP, Bournaud C, Lourenço-Tessutti IT, Noriega DD, de Melo BP, de Almeida-Engler J, Grossi-de-Sa MF (2019) Improved drought stress tolerance in Arabidopsis by CRISPR/dCas9 fusion with a Histone AcetylTransferase. Sci Rep **9**: 8080

Sadowski I, Ma J, Triezenberg S, Ptashne M (1988) GAL4-VP16 is an unusually potent transcriptional activator. Nature **335**: 563–564

Samo N, Ebert A, Kopka J, Mozgová I (2021) Plant chromatin, metabolism and development-an intricate crosstalk. Curr Opin Plant Biol **61**: 102002

Sani E, Herzyk P, Perrella G, Colot V, Amtmann A (2013) Hyperosmotic priming of Arabidopsis seedlings establishes a long-term somatic memory accompanied by specific changes of the epigenome. Genome Biol **14**: R59

Schramm F, Ganguli A, Kiehlmann E, Englich G, Walch D, von Koskull-Doring P (2006) The heat stress transcription factor HsfA2 serves as a regulatory amplifier of a subset of genes in the heat stress response in Arabidopsis. Plant Mole Biol **60**: 759–772

Smaczniak C, Immink RG, Muino JM, Blanvillain R, Busscher M, Busscher-Lange J, Dinh QD, Liu S, Westphal AH, Boeren S, et al. (2012) Characterization of MADS-domain transcription factor complexes in Arabidopsis flower development. Proc Natl Acad Sci USA **109**: 1560–1565

Song Z, Zhang L, Han J, Zhou M, Liu J (2021) Histone H3K4 methyltransferases SDG25 and ATX1 maintain heat-stress gene expression during recovery in Arabidopsis. Plant J **105**: 1326–1338

Sparkes IA, Runions J, Kearns A, Hawes C (2006) Rapid, transient expression of fluorescent fusion proteins in tobacco plants and generation of stably transformed plants. Nat Protocol **1**: 2019–2025

Stief A, Altmann S, Hoffmann K, Pant BD, Scheible W-R, Bäurle I (2014) Arabidopsis miR156 Regulates Tolerance to Recurring Environmental Stress through SPL Transcription Factors. The Plant Cell **26**: 1792–1807

Tanenbaum ME, Gilbert LA, Qi LS, Weissman JS, Vale RD (2014) A protein-tagging system for signal amplification in gene expression and fluorescence imaging. Cell **159**: 635–646

Ueda M, Seki M (2020) Histone modifications form epigenetic regulatory networks to regulate abiotic stress response. Plant Physiol **182**: 15–26

Wang ZP, Xing HL, Dong L, Zhang HY, Han CY, Wang XC, Chen QJ (2015) Egg cell-specific promoter-controlled CRISPR/Cas9 efficiently generates homozygous mutants for multiple target genes in Arabidopsis in a single generation. Genome Biol **16**: 144

Xiao J, Jin R, Wagner D (2017) Developmental transitions: integrating environmental cues with hormonal signaling in the chromatin landscape in plants. Genome Biol **18**: 88

Yang H, Han Z, Cao Y, Fan D, Li H, Mo H, Feng Y, Liu L, Wang Z, Yue Y, et al. (2012a) A companion cell-dominant and developmentally regulated H3K4 demethylase controls flowering time in Arabidopsis via the repression of FLC expression. PLoS Genet **8**: e1002664

Yang H, Mo H, Fan D, Cao Y, Cui S, Ma L (2012b) Overexpression of a histone H3K4 demethylase, JMJ15, accelerates flowering time in Arabidopsis. Plant Cell Rep **31**: 1297–308

Acknowledgements

Manuscript 3: Promoter and domain swap analysis between *Arabidopsis* HSFA1D and HSFA2 gives insight into the requirements for HS memory HSFs

Vicky Oberkofler[1], Witold Szymanski[2,3] & Isabel Bäurle[1]

[1] Institute for Biochemistry and Biology, University of Potsdam, Potsdam, Germany

[2] Max-Planck-Institute for Terrestrial Microbiology, Marburg, Germany

[3] Philipps University of Marburg, Marburg, Germany

V.O. and I.B. conceived and designed research, V.O. and W.S. performed experiments, V.O., W.S. and I.B. analyzed experiments, and V.O. wrote the manuscript with input from I.B.

Manuscript status: Expected to be ready for submission in 2022

Abstract

Exposure to moderate heat stress (HS) primes plants in order to better withstand future exposure to more severe HS conditions. In Arabidopsis, acquired thermotolerance is actively maintained for several days (HS memory). Out of the 21 Arabidopsis HEAT SHOCK TRANSCRIPTION FACTORS (HSFs), HSFA2 and HSFA3 are known to be positive regulators of HS memory by jointly mediating transcriptional memory of a subset of HS-inducible genes. Here, we report the findings of a promoter and domain swap analysis between HSFA2 and HSFA1D, a general regulator of the heat stress response (HSR), aimed to uncover which are the requirements for HS memory HSFs. We find that conferring the transcriptional pattern of *HSFA2* to HSFA1D is not sufficient to restore HS memory. In chimeric HSFA1D/A2 HSFs, the presence of a HSFA1D repression domain abrogates HS memory, while the C-terminal regions and the DNA-binding domains (DBDs) of the two HSFs are interchangeable. Interestingly, the oligomerization domain (OD) of HSFA1D does not replace its HSFA2 counterpart in physiological HS memory, but the respective chimeric HSF hyper-induces memory genes after a single mild HS. In summary, our work gives insight into the degree of specificity of single HSF domains with which they mediate molecular processes underlying HS memory and provides useful information for designing efficient memory HSFs.

Introduction

For plants, external stimuli that negatively affect metabolism, growth, and/or development, are considered stressors (Lichtenthaler, 1998). Exposure to mild stress triggers modified responses to a stress event which recurs after a recovery period. Priming of the stress response has been described in plants and other organisms after exposure to abiotic and biotic stressors (Hilker *et al.*, 2016; Mauch-Mani *et al.*, 2017). In plants, priming of the stress response has been associated with enhanced re-induction of transcription of subsets of stress-responsive genes after repeated stress exposure, as well as with chromatin modifications that are established at these loci upon priming and remain in place for longer than the duration of the stress stimulus. More precisely, histone H3 lysine 4 (H3K4) trimethylation (H3K4me3) and Polymerase II phosphorylated at serine 5 (Ser5P Pol II) accumulate at *RESPONSIVE TO DESICCATION 29B* (*RD29B*) and *RESPONSIVE TO ABA 18* (*RAB18*) in response to drought/dehydration stress (Ding, Fromm and Avramova, 2012; Kim *et al.*, 2012). In response to salt/hyperosmotic stress, enhanced re-induction of *HIGH-AFFINITY K+ TRANSPORTER 1* (*HKT1*) is accompanied by loss of histone H3 lysine 27 (H3K27) trimethylation (H3K27me3) (Sani *et al.*, 2013), and H3K4me3 accumulates at *DELTA1-PYRROLINE-5-CARBOXYLATE SYNTHASE 1* (*P5CS1*) (Feng *et al.*, 2016). Local pathogen infection primes *WRKY DNA-BINDING PROTEIN 29* (*WRKY29*) for future transcriptional activation, and induces tri- and dimethylation of H3K4 at this locus (Jaskiewicz, Conrath and Peterhänsel, 2011).

Exposure to elevated temperature is among the main abiotic stressors of plants. Plant responses to heat stress (HS) include basal and acquired thermotolerance (Mittler, Finka and Goloubinoff, 2012; Yeh *et al.*, 2012). Basal thermotolerance (bTT) is defined as tolerance towards severe HS without prior exposure to elevated temperature. Acquired thermotolerance (aTT) refers to better survival to severe HS conferred by prior exposure to moderate HS. After acquisition of thermotolerance, *Arabidopsis thaliana* (Arabidopsis) remains in a primed state for several days (Charng *et al.*, 2006; Stief *et al.*, 2014; Friedrich *et al.*, 2021). This maintenance of acquired thermotolerance (maTT), or heat stress memory, is genetically separable from acquisition of thermotolerance and several specific factors have been characterized (Charng *et al.*, 2006, 2007; Meiri and Breiman, 2009; Qu *et al.*, 2013; Brzezinka *et al.*, 2016; Lämke *et al.*, 2016; Brzezinka, Altmann and Bäurle, 2019; Urrea Castellanos *et al.*, 2020; Friedrich *et al.*, 2021). The general HS

response (HSR) is evolutionarily conserved in eukaryotes (Anckar and Sistonen, 2011) and heat shock transcription factors (HSFs), which bind to and transcriptionally activate target genes, are key factors of HSR (Wu, 2000; Nover, Bharti and Scharf, 2001). Activation of HSFs upon HS is generally explained by the chaperone titration model (Richter, Haslbeck and Buchner, 2010): in response to HS, chaperone proteins progressively dissociate from HSFs, activating the latter.

The number of HSFs in the plant kingdom is notably higher than in other groups of organisms. For example, yeast has a single HSF and vertebrates have 4 HSFs (Scharf *et al.*, 2012), while the number of plant HSFs has increased during evolution to an average of almost 30 HSFs in monocot and eudicot species (Wang *et al.*, 2018). Arabidopsis has 21 HSFs (Nover, Bharti and Scharf, 2001) which are divided into three classes (A, B, and C) and fourteen groups (A1-A9, B1-B4, C1) (Nover, Bharti and Scharf, 2001; Scharf *et al.*, 2012). HSFs are modularly organized (Åkerfelt, Morimoto and Sistonen, 2010). At the N-terminus, they contain two evolutionarily conserved domains: the DNA-binding domain (DBD), consisting of 3 α-helices and one β-sheet, which binds to conserved DNA sequence motifs called heat stress elements (HSEs); and the oligomerization domain (OD), consisting of two heptameric repeats of hydrophobic amino acids which form a coiled-coil-like structure (Peteranderl and Nelson, 1992; Peteranderl *et al.*, 1999; Scharf *et al.*, 2012), for oligomerization with other HSFs. At the C-terminus, most HSFs contain nuclear localization signal (NLS) and nuclear export signal (NES) for shuttling between cytosol and nucleus; and one or more AHA (aromatic and large hydrophobic amino acids embedded in an acidic context) activator motifs which are crucial for transcriptional activation of target genes and interact with components of the basal transcriptional machinery (Döring *et al.*, 2000).

Several Arabidopsis HSFs have been characterized regarding their involvement in different aspects of the HSR. Class A1 HSFs, in particular HSFA1A, HSFA1B, and HSFA1D, are master regulators of the HSR (Ohama *et al.*, 2017) and act partially redundantly to mediate immediate responses to HS by direct transcriptional activation of target genes and transcriptional (co)activators (Liu, Liao and Charng, 2011; Nishizawa-Yokoi *et al.*, 2011; Yoshida *et al.*, 2011; Ohama *et al.*, 2017). They are constitutively expressed and regulated through post-translational modification. For HSFA1D an additional regulatory domain was recently characterized (Ohama *et al.*, 2016). It was shown that the temperature-dependent regulatory domain (TDR) region,

located C-terminally to its NLS, functions as a negative regulator of HSFA1D activity under non-HS conditions through interaction with chaperones of the HEAT SHOCK PROTEIN (HSP) 70/90 families. This region was further subdivided into five partial sequences for deletion analyses. Partial deletions of TDR resulted in constitutive nuclear localization of the deletion constructs and transactivation of a subset of HS-responsive genes (Ohama *et al.*, 2016). HSFB1 and HSFB2B act as transcriptional repressors and are positive regulators of aTT (Kumar *et al.*, 2009; Ikeda, Mitsuda and Ohme-Takagi, 2011). In contrast, HSFA2 and HSFA3 are positive regulators specifically of HS memory (Charng *et al.*, 2007; Lämke *et al.*, 2016; Friedrich *et al.*, 2021) and are HS-inducible. Upon HS, transcription of *HSFA2* is directly induced by HSFA1s (Liu, Liao and Charng, 2011; Nishizawa-Yokoi *et al.*, 2011), while induction of *HSFA3* is mediated by several DEHYDRATION-RESPONSIVE ELEMENT BINDING PROTEIN 2 (DREB2) isoforms which are in turn induced by HSFA1s (Schramm *et al.*, 2007; Yoshida *et al.*, 2008), leading to delayed induction kinetics of *HSFA3* compared to *HSFA2* (Friedrich *et al.*, 2021).

In Arabidopsis, HS memory correlates with two types of transcriptional signatures of partially overlapping subsets of HS-responsive genes, termed memory genes: type I transcriptional memory or sustained induction, which is defined as sustained gene expression above non-stressed baseline expression levels for a prolonged time after stress exposure has ceased (Lämke and Bäurle, 2017; Bäurle, 2018), and type II transcriptional memory, in particular enhanced re-induction, which describes increased gene expression levels upon repeated exposure to HS of identical intensity and duration, after return to baseline expression levels during a stress free recovery period (Lämke and Bäurle, 2017; Bäurle, 2018). HSFA2 and HSFA3 jointly regulate type I transcriptional memory by direct binding to target genes. They form heteromeric complexes with each other together with other members of the HSF family (Friedrich *et al.*, 2021). Only HSFA2, but not HSFA3, is required for enhanced re-induction of type II memory genes, although promoter swap experiments between *HSFA2* and *HSFA3* have shown that HSFA3 partially rescues enhanced re-induction if expressed under control of *HSFA2* promoter in *hsfa2* background (Lämke *et al.*, 2016; Liu *et al.*, 2018; Friedrich *et al.*, 2021). For a subset of memory genes, transcriptional memory correlates with sustained enrichment of H3K4 methylation, in particular trimethylation (Lämke *et al.*, 2016; Liu *et al.*, 2018; Friedrich *et al.*, 2021; Oberkofler and Bäurle, 2022). H3K4 methylation is jointly

mediated by HSFA2 and HSFA3 (Lämke *et al.*, 2016; Friedrich *et al.*, 2021) through an as of yet unknown mechanism.

Here, we asked which properties characterize a memory HSF and enable it to mediate HS memory in Arabidopsis. We first aimed to complement the *hsfa2* allele, which is defective in HS memory, by HS-inducible expression of FLAG-tagged HSFA1D under control of the *HSFA2* promoter. Conferring HS-inducibility to *HSFA1D* was insufficient to mediate HS memory. We then generated a series of chimeric HSF proteins, in which single domains of HSFA1D substitute their HSFA2 counterpart, or, in the case of the TDR region, are added to HSFA2, and analyzed their ability to function as positive regulators of HS memory. We found that presence of the TDR region abrogated HS memory, while the C-terminal regions and DBDs of HSFA1D and HSFA2 interchangeably mediated physiological HS memory. The OD of HSFA1D did not replace its HSFA2 counterpart and conferred a distinct transcriptional profile to type II transcriptional memory genes. In summary, our work provides further insight into the molecular mechanisms at the base of HS memory and provides useful information to identify and/or design efficient HS memory transcription factors.

Results

HSFA1D does not replace HSFA2 in HS memory. To ask whether HSFA1D can replace HSFA2 function in HS memory if expressed in a suitable pattern, we created stable transgenic lines expressing triple FLAG-tagged (from here on referred to as FLAG) genomic *HSFA1D* (**Fig 1a, Table S1, Fig S1a**) under control of a 561 bp *HSFA2* promoter fragment (*pA2::FLAG-HSFA1D*) in the *hsfa2* background. This promoter fragment has been previously used successfully to generate a *pA2::FLAG-HSFA2* complementation line of the *hsfa2* allele (Friedrich *et al.*, 2021). Homozygous progeny of two independent lines (*pA2::FLAG-HSFA1D* # 3 and # 6) were tested for physiological HS memory (maTT). 4 d-old seedlings were exposed to a 2-step acclimation treatment (ACC; 1 h 37 ºC, 1.5 h 23 ºC recovery, 45 min 44 ºC) and, three days later, to HS of 44 ºC for 80-90 min (**Fig 2a**). These assays revealed lack of complementation of the *hsfa2* phenotype (**Fig 2b-c**) which is in line with previous experiments that showed that *FLAG-HSFA1D* expressed under control of a *HSFA3* promoter fragment did not complement the *hsfa3* allele (Friedrich *et al.*, 2021). Immunoblot analysis confirmed HS-specific accumulation of FLAG-HSFA1D after ACC treatment (**Fig 2d**). To assess functionality of FLAG-HSFA1D, we created stable transgenic lines expressing *FLAG-HSFA1D* under control of a 1,580 bp *HSFA1D* promoter fragment (*pA1D::FLAG-HSFA1D*) in the *hsfa1a/b/d* background. The *hsfa1a/b/d* mutant is defective in bTT and aTT (Liu *et al.*, 2011). In contrast, the *hsfa1a/b* mutant does not show major thermotolerance defects (Lohmann *et al.*, 2004). Homozygous progeny of two independent lines (*pA1D::FLAG-HSFA1D* # 9 and # 10) were subjected to HS assays probing bTT and aTT. We found that the *hsfa1a/b/d* phenotype was complemented both in bTT (**Fig S2a, c-d**) and aTT (**Fig S2b, e-f**) assays. Taken together, these results indicate that FLAG-HSFA1D is functional, but not able to replace HSFA2 as positive mediator of HS memory, and suggest that a specific protein function in HSFA2 is required for HS memory.

We next asked whether the specific function of HSFA2 in HS memory can be attributed to any one, or a combination, of its functional domains. We therefore investigated interchangeability of individual HSFA1D/HSFA2 domains. To this aim, we created a series of stable transgenic lines that express, under control of *pA2*, FLAG-tagged chimeric HSF proteins in which a single modular HSFA2 domain is substituted with its

HSFA1D counterpart, or where the TDR region of HSFA1D, which is absent in HSFA2, was added. Precisely, we created the following constructs: *FLAG-DBD(A1D)* (**Fig 1c, Table S1**), in which the DBD of HSFA1D substitutes the DBD of HSFA2; *FLAG-OD(A1D)* (**Fig 1d, Table S1**), in which the OD and NLS of HSFA1D substitute their HSFA2 counterparts; *FLAG-CTDΔ(A1D)* (**Fig 1e, Table S1**), where the C-terminal region of HSFA1D, including subregion 5 of the TDR, replace the C-terminal region of HSFA2; *FLAG-A2+TDR(A1D)* (**Fig 1f, Table S1**), where full-length TDR of HSFA1D was inserted into HSFA2; and *FLAG-CTD(A1D)* (**Fig 1g, Table S1**), where the C-terminal region of HSFA1D, including full-length TDR, replaces the C-terminal region of HSFA2. From here on, we refer to these lines without explicit mention of the FLAG tag. Lines harboring these constructs were established in the *hsfa2* background either in presence or absence of the previously described *pHSA32::HSA32-LUC* reporter construct in which the type I transcriptional memory marker gene *HEAT-STRESS-ASSOCIATED 32* (*HSA32*) is translationally fused to *LUCIFERASE (LUC)* coding sequence (Brzezinka *et al.*, 2016). This allows luciferin-based screening of type I transcriptional memory of the reporter gene.

The TDR region of HSFA1D abrogates HS memory, while the C-terminus of HSFA1D can functionally replace that of HSFA2. To investigate the regulatory role of the TDR region of HSFA1D, we tested sustained induction of the *pHSA32::HSA32-LUC* reporter gene for three days after ACC treatment in three different types of transgenic lines: *CTDΔ(A1D)*, *A2+TDR(A1D)*, and *CTD(A1D)* (**Fig 1e-g**). After initial luciferin-based screening for sustained induction of *HSA32-LUC* in the T2 generation (n ≥ 12), two representative independent transgenic lines for each of these constructs were selected for detailed characterization and propagated. For *A2+TDR(A1D)* and *CTD(A1D)*, both of which contain full-length TDR region of HSFA1D, we observed partial rescue of sustained induction of *HSA32-LUC* 1 day (d) after ACC treatment. However, at later time points, most clearly 3 d after ACC treatment, and more evident for *CTD(A1D)* than for *A2+TDR(A1D)*, LUC activity is markedly lower than in the parental line and more closely resembles the *hsfa2* line (**Fig S3a**). The *A2+TDR(A1D)* and *CTD(A1D)* lines also did not complement *hsfa2* in physiological HS memory assays (**Fig S3b-d**). In contrast, *CTDΔ(A1D)* lines # 20 and # 29, in which only subregion 5 of the HSFA1D TDR region is present, fully complemented sustained induction of *HSA32-LUC* over the observed time course (**Fig 3a**) and largely complemented the *hsfa2* allele in physiological HS memory assays (**Fig 3b-c**). Importantly, the comparison of transgene protein levels in whole

seedlings by immunoprecipitation and immunoblot showed that *CTDΔ(A1D)* line # 29, *A2+TDR(A1D)* line # 4, and *CTD(A1D)* line # 2 accumulate comparable levels of tagged proteins after ACC treatment (**Fig S4**). However, different protein levels of *A2+TDR(A1D)* line # 4 compared to line # 3 and of *CTD(A1D)* line # 2 compared to line # 1 did not correlate with observed differences in sustained induction of *HSA32-LUC* or performance in HS memory assays (**Fig S3**). Overall, these results suggest that the presence of the full-length TDR region of HSFA1D negatively affects HS memory, in accordance with its role as a negative regulator of HSFA1D activity (Ohama *et al.*, 2016).

As *CTDΔ(A1D)* largely complemented *hsfa2* in physiological HS memory assays, we were curious to investigate to which extent this is reflected by the underlying molecular processes. First, we assessed type I transcriptional memory of memory genes in *CTDΔ(A1D)* by reverse transcription- quantitative PCR (RT-qPCR). We investigated expression of type I memory genes *HSA32*, *ASCORBATE PEROXIDASE 2* (*APX2*), *HSP21*, *HSP22*, and of non-memory HS-inducible gene *HSP101* for 3 d after ACC treatment (**Fig 4**). Sustained induction of type I memory genes, but not induction of *HSP101*, is dependent on HSFA2 (Lämke *et al.*, 2016), which is reflected by lower sustained induction of *HSA32*, *APX2*, *HSP21*, and *HSP22* in *hsfa2* than in wild type. *CTDΔ(A1D)* lines # 20 and # 29 mediated rescue of sustained expression of these genes for up to 3 d after ACC treatment, while no effects on *HSP101* expression were observed (**Fig 4a**). To check whether rescue of sustained induction is due to promotion of transcription or transcript stability, we quantified levels of unspliced transcripts for intron-containing genes as a proxy for transcriptional activity. Indeed, *CTDΔ(A1D)* complemented nascent transcript levels of type I memory genes for up to 2 d after ACC treatment (**Fig 4b**).

Next, we asked whether *CTDΔ(A1D)* was able to mediate enhanced re-induction of type II transcriptional memory genes. To assess enhanced re-induction, gene expression was compared by RT-qPCR between seedlings that were either exposed to mild HS (1 h 37 ºC) 6 d after germination (triggering HS, T), or both 4 d and 6 d after germination (priming and triggering HS, P + T) (**Fig 5a**). Gene expression was tested for *APX2* and *MYO-INOSITOL-1-PHOSPHATE SYNTHASE 2* (*MIPS2*), which are induced above baseline expression levels both after T and P + T treatments and are therefore classified as +/++ memory genes (Liu *et al.*, 2018); for *LYSOPHOSPHATIDYL ACYLTRANSFERASE 5* (*LPAT5*) and *LONG CHAIN ACYL-COA SYNTHETASE 9*

(*LACS9*), which are induced above baseline expression levels only after P + T treatment and are therefore classified as 0/+ memory genes (Liu *et al.*, 2018); and for non-memory HS-inducible gene *HSP101*. *CTDΔ(A1D)* complemented type II transcriptional memory defects of *hsfa2* for all analyzed genes (**Fig 5b**). We asked if *CTDΔ(A1D)* mediates type II transcriptional memory by direct binding of CTDΔ(A1D) to target genes and performed chromatin immunoprecipitation followed by qPCR (ChIP-qPCR) of FLAG-tagged HSFA2 (**Fig 1b, Table S1, Fig S1**) and CTDΔ(A1D) proteins. For this analysis we selected genes *APX2*, *MIPS2*, *LPAT5*, and *HSP101*. We found similar enrichment of both HSFA2 and CTDΔ(A1D) at T and P + T at these loci (**Fig 5c**). For *APX2* and *MIPS2*, where amplicons both up- and downstream of the transcriptional start site (TSS) were tested, enrichment peaks upstream of the TSS. We next compared protein levels of HSFA2 and CTDΔ(A1D) 1 h and 49 h after priming HS (P) of 1 h 37 ºC 4 d after germination by immunoprecipitation and immunoblot. We detected both proteins 1 h and 49 h after P, although protein levels were decreased 49 h after HS. CTDΔ(A1D) accumulated to a lesser extent than HSFA2 (**Fig S5**). Finally, we investigated whether binding of CTDΔ(A1D) to *APX2* correlated with sustained H3K4 trimethylation. We found that both HSFA2 and CTDΔ(A1D) mediate sustained H3K4 trimethylation of the promoter and intragenic region of *APX2* for at least 2 d after P HS (**Fig 5d**). Taken together, these experiments show that in absence of the negative regulatory function of the TDR region, the C-terminal region of HSFA1D functionally replaces that of HSFA2 in all investigated molecular aspects that are associated with HS memory.

The DBD of HSFA1D mediates type I transcriptional memory and physiological HS memory. Next, we tested the ability of the DBD of HSFA1D to replace its HSFA2 counterpart. First, we checked type I transcriptional memory of the *HSA32-LUC* reporter gene in two independent transgenic lines of *DBD(A1D)* and found that both investigated lines (# 11 and # 54) complemented the defective sustained induction of *HSA32-LUC* observed in *hsfa2* after ACC treatment (**Fig 6a**). In physiological HS memory assays, both lines complemented the phenotype of *hsfa2* seedlings fully (# 54) or partially (# 11) (**Fig 6b-c**). For both lines, we performed RT-qPCR analysis of type I transcriptional memory genes *HSA32*, *APX2*, *HSP21*, *HSP22*, and non-memory gene *HSP101* (**Fig 4**). Similar to what was observed for *CTDΔ(A1D)*, we found that *DBD(A1D)* significantly upregulated transcripts of memory genes for up to 3 d after ACC treatment (**Fig 4a**), and unspliced transcripts were significantly upregulated for up to 2 d after ACC treatment compared to *hsfa2* (**Fig 4b**). We compared protein accumulation of DBD(A1D) in line #

54 to that of CTDΔ(A1D) in line # 29 by immunoprecipitation and immunoblot after ACC treatment. Both transgenic proteins were detected 4 h, 28 h, and 52 h after ACC treatment, with overall comparable levels (**Fig S6**). In conclusion, the DBD domain of HSFA1D mediates physiological HS memory and type I transcriptional memory, functionally replacing the DBD of HSFA2.

The OD of HSFA1D does not functionally replace that of HSFA2; it hyper-induces gene expression after priming HS. Finally, we compared the ODs of HSFA1D and HSFA2. We first selected two transgenic *OD(A1D)* lines (# 12 and # 13) containing the *HSA32-LUC* reporter gene in the *hsfa2* background and investigated type I transcriptional memory of *HSA32-LUC* in LUC activity assays. We found that LUC activity in the selected transgenic lines overall did not match those of the parental line and were more similar to the *hsfa2* background (**Fig S7a**). However, these *OD(A1D)* lines also expressed comparatively lower levels of transgenic protein already at the earliest assessed time point in a type I transcriptional memory set-up (4 h after end of ACC treatment) compared to *CTDΔ(A1D)* # 29 and *DBD(A1D)* # 54, which were shown above to return *HSA32-LUC* expression to wild type-like levels (**Fig S6**, **Fig 3a**, **Fig 6a**). For subsequent analyses, we therefore used two *OD(A1D)* lines (# 1 and # 2) in the *hsfa2* background without the reporter gene, in which synthesis of transgenic proteins is comparable to that of the above two lines at 4 h after ACC (**Fig S6**). Performance assessment of transgenic lines *OD(A1D)* # 1 and # 2 in the *hsfa2* background in physiological HS memory assays revealed that they did not complement the *hsfa2* phenotype (**Fig S7b-c**). Next, we tested expression of type I transcriptional memory genes in *OD(A1D)* by RT-qPCR. *OD(A1D)* expression in the *hsfa2* background resulted in significantly elevated expression levels of *APX2* and *HSP21* for 2 d after ACC treatment, while expression of *HSA32* and *HSP22* was significantly upregulated for only 1 d after ACC treatment (**Fig S8a**). For *HSP21*, unspliced transcript levels were also upregulated for 2 d after ACC treatment (**Fig S8b**). These results are in accordance with protein levels of OD(A1D) after ACC treatment: while CTDΔ(A1D) and DBD(A1D) are detected for up to 52 h after ACC treatment, OD(A1D) in both line # 1 and # 2 is only present at comparable levels immediately after end of ACC treatment (ACC + 4 h), while it could not anymore be detected at 28 h and 52 h after ACC treatment (**Fig S6**). We conclude that protein turn-over of OD(A1D) is increased compared to CTDΔ(A1D) and DBD(A1D), resulting in failure to sustain expression of type I memory genes at later time points after ACC treatment. We next tested whether *OD(A1D)* was normally induced

after priming HS (1 h 37 ºC). We compared OD(A1D) protein levels in transgenic lines # 1 and # 2 by immunoprecipitation and immunoblot to protein levels of HSFA2 and CTDΔ(A1D) line # 29 (**Fig S5**). 1 h after priming HS, OD(A1D) is present at comparable levels to CTDΔ(A1D), and both proteins are less abundant than HSFA2. 49 h after priming HS, OD(A1D) is not anymore detectable, but CTDΔ(A1D) and HSFA2 still are. This supports the hypothesis that protein turn-over of OD(A1D) is increased.

As both *HSFA2* and *CTDΔ(A1D)* rescue type II transcriptional memory defects of *hsfa2* (**Fig 5b, Fig S9**) to wild type-like extent, we investigated whether this was also the case for *OD(A1D)*. In addition to *APX2*, *MIPS2*, *LPAT5* and *LACS9*, we included 0/+ memory genes *DIGALACTOSYL DIACYLGLYCEROL DEFICIENT 1 (DGD1) SUPPRESSOR 1* (*DGS1*) and *TETRATRICOPEPTIDE REPEAT 1* (*TPR1*) in the RT-qPCR analysis. Surprisingly, we found that *OD(A1D)* hyper-induces gene expression of all analyzed type II memory genes after triggering HS (T) (**Fig 7a**). For *MIPS2* and *LACS9*, hyper-induction at T is so high that it is not statistically different from induction at P + T. Thus, in *OD(A1D)* lines, *MIPS2* and *LACS9* do not fulfill anymore the criteria of a type II memory gene (statistically significant higher induction at P + T than at T) and their transcriptional profile is similar to that of non-memory HS-inducible gene *HSP101* (**Fig 7a**). Overall, these data indicate that *OD(A1D)* maintains the ability to mediate type II transcriptional memory and has an intrinsically higher ability to promote gene expression of type II memory genes after a single mild HS.

We were interested to see whether this difference between ODs of HSFA1D and HSFA2 was reflected in their HSF interaction partners. We performed immunoprecipitation of either FLAG-tagged HSFA2 or OD(A1D) and mass spectrometry analysis of their HSF interacting partners (Co-IP/MS) 1 h and 4 h after priming HS (1 h 37 ºC) and non-HS conditions. The number of unique peptides found in HSFA2 samples was higher than that of OD(A1D) in the corresponding samples, which was also reflected in an overall higher number of unique peptides of other HSFs for HSFA2 samples (**Fig 7b**, **Table S2**). This is consistent with higher detected levels of HSFA2 than OD(A1D) at 1 h after P HS in immunoprecipitation and immunoblot experiments (**Fig S5**). For HSFA2, we identified all four HSFA1s, HSFA3, HSFA6B, HSFA7A, HSFA7B, HSFA4A, and HSFC1 as interaction partners (**Fig 7b**), in line with previous analyses (Friedrich *et al.*, 2021). The highest numbers of unique peptides at P + 1 h were found for HSFA1B, HSFA7A, and HSFA7B. At P + 4 h, HSFA3 peptides make up a larger share of total

co-immunoprecipitated peptides, possibly reflecting transcription kinetics of *HSFA3* after HS (Friedrich *et al.*, 2021). For OD(A1D), we identified all four HSFA1s, HSFA3, HSFA6B, and HSFA7A as potential interaction partners (**Fig 7b**). Given the overall lower numbers of identified unique peptides for OD(A1D) samples compared to HSFA2 samples and the low count of HSFA4A and HSFC1 peptides in the latter, we think that absence of HSFA4A and HSFC1 peptides in OD(A1D) samples may reflect technical limitations rather than interaction specificity. In contrast, HSFA7B peptides, which are among the most frequent HSF peptides in HSFA2 samples, are completely absent from OD(A1D) samples. Thus, the HSFA1D OD may have an intrinsically lower or absent affinity for HSFA7B. However, follow-up experiments are needed to test this hypothesis. Overall, peptides deriving from HSFA1s make up a higher proportion of OD(A1D) co-immunoprecipitated peptides than of HSFA2 co-immunoprecipitated peptides, and this is more evident at P + 4 h than at P + 1 h (**Fig 7b, Table S2**). This suggests that OD(A1D) may have higher affinity for the ODs of other HSFA1s than HSFA2. Amino acid sequence alignment between the OD of HSFA2 and the corresponding region from HSFA1D with which it was replaced to generate OD(A1D), does not reveal major differences in conserved amino acid residues in the bipartite heptad motif (**Fig S1b**) or in the hydrophobicity between these two sequences (**Fig S1c**). Interestingly however, HSFA1D but not HSFA2 contains two amino acid stretches that are classified as having prion-like amino acid composition (**Fig S1d**) (Lancaster *et al.*, 2014). Both of these sequences are fully located in the part of HSFA1D that was used to generate FLAG-OD(A1D) (**Fig S1b**).

Discussion

Here, we investigated which characteristics are required for a heat shock transcription factor to mediate HS memory in Arabidopsis. Of the 21 Arabidopsis HSFs, so far two have been described as having a specific role in HS memory, HSFA2 and HSFA3 (Charng *et al.*, 2007; Lämke *et al.*, 2016; Friedrich *et al.*, 2021). Transcription of both HSFs is strongly induced by HS; *HSFA2* expression peaks earlier than that of *HSFA3* (Schramm *et al.*, 2007; Swindell, Huebner and Weber, 2007; Friedrich *et al.*, 2021). HSFA2 and HSFA3 interact with each other and with other HSFs to form multimeric complexes (Friedrich *et al.*, 2021). They jointly regulate type I transcriptional memory and mediate H3K4me3 deposition at memory genes. Only HSFA2 is required *in vivo* for type II transcriptional memory, although HSFA3 can partially restore type II memory defects of *HSFA2* if expressed under promoter of *HSFA2*, indicating that overall these two HSFs share very similar molecular functions (Friedrich *et al.*, 2021). We asked whether conferring early and strong HS-inducibility to a HSF protein is a sufficient criterion to mediate HS memory and selected HSFA1D as candidate HSF as it has a well-documented function in the general HSR (Liu, Liao and Charng, 2011) and its domain organization is particularly well characterized (Ohama *et al.*, 2016). We found that HS-induced HSFA1D could not replace HSFA2 (**Fig 2**), suggesting that HSFA1D differs from HSFA2 at the protein level. At the level of domain organization, the most obvious difference between these two HSFs is the presence of the TDR region in HSFA1D, which is absent from HSFA2 (**Fig S1a**). The TDR region was characterized as a negative regulatory domain of HSFA1D. In Arabidopsis protoplasts, deletion of certain subregions of the TDR caused a shift of subcellular localization of mutated HSFA1D from a mixed distribution between cytoplasm and nucleus to nuclear localization and conferred constitutive transcriptional activity to mutated HSFA1D at ambient temperatures (Ohama *et al.*, 2016). This was most evident if subregions 1-4 were deleted, which is why we deleted those regions in the *CTDΔ(A1D)* lines. It was also shown that interaction with HSP70/90 chaperones is decreased in the mutated versions of HSFA1D (Ohama *et al.*, 2016). We included the TDR region in two of the five created chimeric HSF proteins: A2+TDR(A1D), in which the full-length TDR region was placed into *HSFA2 CDS*, and CTD(A1D), in which the C-terminal region of HSFA1D, including full-length TDR, replaces that of HSFA2. Failure to complement *hsfa2* in sustained

induction of *HSA32-LUC* and in physiological HS memory assays was observed for both lines (**Fig S3**) although transgenic proteins were detected for up to 52 h after ACC treatment (**Fig S4**). Thus, the presence of the full-length TDR in a HSF likely determines its gradual inactivation after HS through interaction with HSP70/90 chaperones and changes in subcellular localization.

The first surprising finding of this work is that the C-termini of HSFA1D and HSFA2 are fully interchangeable (**Fig 3, Fig 4, Fig 5**) although they are the least conserved in their amino acid sequence (**Fig S1a**). Of particular interest is the apparent absence of AHA motifs, conserved activating motifs that interact with basal transcription machinery (Döring *et al.*, 2000), in the C-terminus of HSFA1D. It may be that the C-terminal domain of HSFA1D has intrinsic ability to recruit basal transcriptional machinery through other, non-characterized motifs, or that its presence in a multimeric HSFA3-containing complex is sufficient to reconstitute overall function of a HS memory HSF complex. Similar considerations apply to the deposition of H3K4me3 at memory genes. In plants, H3K4 methyltransferases act as part of the evolutionarily conserved COMPLEX PROTEINS ASSOCIATED WITH SET1 (COMPASS)-like complex which contains subunits ARABIDOPSIS ASH2 RELATIVE (ASH2R), HUMAN WDR5 (WD40 REPEAT) HOMOLOG A (WDR5A), and RBBP5 (Jiang *et al.*, 2011). It is neither clear which are the methyltransferase enzymes that catalyze H3K4 methylation in response to HS, nor if they are directly recruited to loci of interest by specific HSFs or indirectly through basal transcriptional machinery. Transcription factors bZIP28 and bZIP60, master regulators of the unfolded protein response in the endoplasmic reticulum (Iwata and Koizumi, 2005; Liu *et al.*, 2007), were shown to interact with ASH2R and RBBP5 (Song *et al.*, 2015). It would be interesting to evaluate complementation of the *hsfa2,3* double mutant by HS-inducible expression of two chimeric HSFs, one HSFA2-, the other HSFA3-based, in which both C-terminal domains have been replaced by the HSFA1D C-terminus. If HS memory is rescued in such a context, this would further argue that the C-terminal regions of memory and non-memory HSFs are functionally equivalent in their co-factor recruitment.

The second surprising finding is the two-fold observed functional discrepancy between the OD domains of HSFA1D and HSFA2, even though they show the highest degree of sequence conservation (**Fig S1a**): On one hand, *OD(A1D)* is induced normally at ACC + 4 h, but the protein was not anymore detected at 28 h or 52 h after ACC treatment (**Fig

S6), which sets it apart from all other assessed chimeric HSFs. On the other hand, OD(A1D), which is induced comparably to CTDΔ(A1D) and less abundant than HSFA2 after mild HS (**Fig S5**), mediated higher transcription rates of type II memory genes after the same mild HS (**Fig 7a**). We compared interaction partners of HSFA2 and OD(A1D) by mass spectrometry and indeed found that OD(A1D) preferentially interacts with other class A1 HSFs and, in contrast to HSFA2, we did not find any co-immunoprecipitated HSFA7B peptides (**Fig 7b, Table S2**). These findings support the idea of formation of higher amounts of multimeric HSF complexes more suited to mediate faster/stronger transcriptional activation of gene response after acute HS, rather than functioning as HS memory complexes. However, further experiments are needed to verify this. One known example of specific interaction among Arabidopsis HSFs mediated by the OD is that of HSFA5 and HSFA4B (Baniwal *et al.*, 2007). *HSFA7B* is induced by HS (Schramm *et al.*, 2007; Swindell, Huebner and Weber, 2007; Friedrich *et al.*, 2021) and is a positive regulator of salt stress tolerance (Zang *et al.*, 2019), but whether it has a role in the HSR is so far unknown. If HSFA7B were a regulator of HS memory interacting with the OD of HSFA2 in wild type plants, absence of the OD of HSFA2 in *OD(A1D)* lines could further shift HSF complex equilibrium towards complexes specialized in the immediate response to HS. Amino acid sequence comparison (**Fig S1b**) and assessment of hydrophobicity (**Fig S1c**) of the region harboring core bipartite heptad repeats, implied in formation of a coiled-coil like structure (Peteranderl and Nelson, 1992; Peteranderl *et al.*, 1999), does not give obvious indications about functional specification. With one exception, positions of hydrophobic amino acids in the repeats are shared among HSFA1D and HSFA2, and hydrophobicity pattern is very similar. Successful crystallization of HSFs is usually restricted to the DBD (Neudegger *et al.*, 2016; Feng *et al.*, 2021), making predictions on the potential effect of replacement of single amino acids in the OD domain on overall structure or changes in affinity to other HSFs difficult. A major difference between the regions of HSFA1D and HSFA2 that were used to generate OD(A1D) is the identification of two stretches of prion-like domain (PrLD)-like amino acid sequences in HSFA1D via the PLAAC algorithm (Lancaster *et al.*, 2014), spanning amino acids 131-149 and 184-239 of endogenous HSFA1D (**Fig S1d**). Systematic discovery of prion-like proteins (PrLPs) in plants is a relatively new field (Chakrabortee *et al.*, 2016; Garai *et al.*, 2021), and there are few examples of functional characterization. Noteworthy is the discovery of a PrLD in Arabidopsis EARLY FLOWERING 3 (ELF3), which confers responsiveness to warm temperatures assessed

by early flowering phenotype (Jung *et al.,* 2020). The temperature shift assessed in this work (23 ºC to 37/44 ºC for 2-step ACC treatment) is greater than in (Jung *et al.,* 2020) (22 ºC to 27 ºC), but a putative regulatory role of the PrLD sequences, such as conferring greater/faster thermal responsiveness to *OD(A1D)* that would be reflected in faster/stronger transcriptional activation, can be hypothesized. Likewise, the question of why protein turn-over of OD(A1D) is increased with respect to all other chimeric HSFs remains unanswered. Protein turn-over of OD(A1D) appears to be higher than that of HSFA1D assessed in the complementation line (**Fig 1d**), indicating that other sequences deriving from *HSFA2* may exacerbate the phenomenon, or that the TDR region of HSFA1D may protect it from degradation through interaction with HSP chaperones. Although Phyre^2-based (Kelley *et al.,* 2015) secondary and tertiary structure predictions of OD(A1D) did not indicate obvious differences compared to HSFA2, we cannot exclude that protein misfolding of OD(A1D) may contribute to its fast turn-over.

In general, our work confirms previous observations about the strong correlation between physiological HS memory and duration of sustained induction of type I transcriptional memory genes (Stief *et al.,* 2014; Brzezinka *et al.,* 2016; Lämke *et al.,* 2016; Friedrich *et al.,* 2021). *DBD(A1D)* and *CTDΔ(A1D)*, both of which largely rescue the *hsfa2* phenotype in physiological HS memory assays, mediate sustained induction of gene expression for up to 3 d after ACC above baseline levels (**Fig 4**). In contrast, failure of *OD(A1D)* to complement *hsfa2* in physiological HS memory assays is reflected by overall lower sustained induction, especially at the 3 d after ACC (**Fig S8**). A total of 156 type I transcriptional memory genes which are upregulated for at least 52 h after ACC have previously been identified by RNA-seq (Friedrich *et al.,* 2021). Lower sustained induction of several of these genes by *OD(A1D)* compared to *DBD(A1D)* and *CTDΔ(A1D)* may result in the observed large cumulative effect at the physiological level.

It is less clear whether type II transcriptional memory contributes to physiological HS memory. To our best knowledge, no regulator of HS memory with a specific defect in type II, but not type I, transcriptional memory, has so far been identified. In *hsfa3*, only type I transcriptional memory is affected, while *hsfa2* is both deficient in type I and type II transcriptional memory, and the physiological phenotype of *hsfa2* is more severe than that of *hsfa3* (Friedrich *et al.,* 2021). However, *hsfa2* also shows stronger effects on type I transcriptional memory than *hsfa3* (Friedrich *et al.,* 2021). While *OD(A1D)* rescues type II transcriptional memory (**Fig 7a**), this is insufficient to complement *hsfa2* at the

physiological level (**Fig S7b-c**). Overall, our findings suggest a dominant importance of type I transcriptional memory to predict performance in physiological HS memory assays.

In summary, our work has given insight on the characteristics of memory HSFs at the level of individual protein domains. To function as a memory HSF, the absence of the TDR region is essential, as this presumably prevents inactivation after HS. This suggests in turn that active forms of HSFs are required in the memory lag phase to efficiently mediate physiological HS memory. Additionally, the OD shows a surprising degree of specificity considering high levels of amino acid sequence homology. The OD of memory HSFs may favor specific HSF-HSF interactions that facilitate formation of memory-specific HSF complexes, and may also confer elevated protein stability. Based on the findings of this work, it is for example expected that a HS-inducible chimeric HSF based on HSFA1D, from which subregions 1-4 of the TDR are deleted, and in which the OD from HSFA1D is replaced with the OD from HSFA2, will function as a memory HSF. Customized HSFs may be a useful tool to fine-tune and optimize stress responses and stress memory in a changing environment.

Material and Methods

Plant materials, growth conditions and HS treatments. The *hsfa2* allele used in this study is SALK_008978 and has been characterized previously (Charng *et al.*, 2007; Lämke *et al.*, 2016). The *pHSA32::HSA32-LUC* reporter line in *hsfa2* background was obtained by crossing *hsfa2* to the previously characterized *pHSA32::HSA32-LUC* reporter line (Brzezinka *et al.*, 2016). The *hsfa1a/b/d* triple mutant has previously been described (Liu, Liao and Charng, 2011). Primers for genotyping are listed in **Table S3**. Seedlings were grown on GM medium (1 % [w/v] glucose) under 16 h/ 8 h light/ dark cycle at 23 °C/ 21 °C. For maTT, 4 d-old seedlings were exposed to 3-step ACC treatment (1 h 37 °C, 1.5 h 23 °C, 45 min 44 °C), and, 3 d later, to HS of 44 °C for 80-90 min (**Fig 2a**). For bTT, 4 d-old seedlings were exposed to HS of 44 °C for 15-25 min (**Fig S2d**). For aTT, 4 d-old seedlings were exposed to 37 °C for 1 h, recovered at 23 °C for 1.5 h, and then exposed to HS of 44 °C for 140-180 min (**Fig S2f**). Seedlings were imaged and evaluated 18 d after germination. To statistically evaluate seedling performance in HS assays, Fisher's 2 x 4 exact probability test was used (http://vassarstats.net/fisher2x4.html).

Construction of transgenic lines. Constructs *pA2::FLAG-HSFA1D*, *pA1D::FLAG-HSFA1D*, and *pA2::FLAG-HSFA2* were generated by restriction enzyme-based cloning of Phusion DNA polymerase (Thermo Fisher Scientific) amplified fragments. 5' UTR and promoter regions were flanked by *Asc*I and *Age*I restriction sites while coding sequence and 3' UTR were flanked by *Age*I and *Not*I restriction sites. The triple FLAG epitope and a short linker sequence were added to the N-terminus of coding regions by primer-based amplification. Primer sequences used for creation of these constructs are listed in **Table S3**. Subsequently, constructs *pA2::FLAG-DBD(A1D)*, *pA2::FLAG-OD(A1D)*, *pA2::FLAG-CTDΔ(A1D)*, *pA2::FLAG-A2+TDR(A1D)*, and *pA2::FLAG-CTD(A1D)* were obtained by In-Fusion based cloning (Takara Bio) according to the manufacturer's protocol. In short, single fragments corresponding to desired parts of the coding sequence were amplified from either *HSFA2* or *HSFA1D* and joined to create chimeric coding sequences. For all constructs, 5' UTR derives from *HSFA2*, while 3' UTR region derives from *HSFA2* if the C-terminal domain derives from *HSFA2* and from *HSFA1D* if the C-terminal domain derives from *HSFA1D*. Amino acid sequences of domain swap constructs and of endogenous HSFA1D and HSFA2 are listed in **Table S1**.

For generation of stable transgenic lines, all constructs were cloned into binary vector *pGreenII* (NK43) and introduced into *Agrobacterium tumefaciens* GV3101. Plants were transformed using the floral dip method (Clough and Bent, 1998).

LUC imaging. Chemiluminescence emitted by luciferase was measured with NightOWL II LB 983 *in vivo* imaging system (Berthold Technologies). Seedlings were abundantly sprayed with 2 mM beetle luciferin (Promega) right before imaging. For data acquisition, signal acquisition time was set to 2 min. Data processing was done with Indigo Software for *in vivo* imaging (Berthold Technologies). Signal thresholds were set to the same interval for the whole length of the analyzed time series.

Total protein extraction, immunoprecipitation and immunoblotting. For immunoblotting, total protein was extracted from whole seedlings (Smaczniak *et al.*, 2012). Total protein was quantified by Bradford protein assay (Bradford, 1976). For immunoblot of total protein extract, 40 µg of total protein were separated by SDS-PAGE on a 12 % gel. FLAG signal was assessed with anti-FLAG antibody (F1804, Sigma) followed by secondary anti-mouse antibody (926-32210, LI-COR Biosciences). H3 signal was assessed with anti-histone H3 antibody (ab1791, Abcam) followed by secondary anti-rabbit antibody (926-32211, LI-COR Biosciences). For isolation of FLAG-tagged proteins and their interactors by immunoprecipitation, 500 µg of total protein were used as input material for processing with µMACS DYKDDDDK isolation kit (Miltenyi Biotec). 15 µl of 50 µl total eluate were used for assessment of FLAG signal, while 20 µg of total protein input were used for assessment of H3 signal.

Protein mass spectrometry. Sample preparation for mass spectrometry was based on a modified protocol by (Wiśniewski, 2018). Total protein was extracted from ca. 1g whole seedlings and FLAG-tagged bait protein was immunoprecipitated with µMACS DYKDDDDK isolation kit (Miltenyi Biotec) and samples were eluted in 8 M urea. In-solution protein digestion with Trypsin/LysC (Promega) was performed as follows: ammonium bicarbonate (AmBic) and DTT were added to the eluate to a final concentration of 50 mM and 5 mM, respectively, and samples were incubated at RT for 30 min. Iodoacetamide was added to a final concentration of 15 mM and samples were incubated at RT in the dark for 30 min. For in-solution protein digestion, 0.1 µg Trypsin/LysC mix resuspended in 50 mM AmBic was added. Samples were brought to 100 µl volume with 50 mM AmBic and digested at 37 °C for 4 h. Samples were brought to 400 µl with 50 mM AmBic and were incubated at 37 °C over night. Samples were

118

acidified by addition of trifluoroacetic acid (TFA) to a final concentration of 1 %. For desalting, Sep-Pak C18 96 well plates, 40 mg sorbent (Waters), were used. Wells were calibrated by addition of 1 mL 100 % methanol, once by addition of 1 mL Solution B (80 % acetonitrile, 0.1 % TFA), and twice by addition of 1 mL Solution A (0.1 % TFA). Samples were loaded and washed twice by addition of 1 mL Solution A. Each of these steps was followed by centrifugation at RT for 1 min at 100 g. Samples were eluted by adding 600 µl Solution C (60 % acetonitrile, 0.1 % TFA) followed by centrifugation, dried in a SpeedVac and stored at -20 °C.

RT-qPCR. RNA was extracted from snap-frozen tissue by hot-phenol extraction. Tissue was ground to a fine powder and resuspended in 500 µl RNA extraction buffer (100 mM Tris-HCl pH 8.5, 5 mM EDTA, 100 mM NaCl, 0.5 % SDS), 250 µl phenol, and 5 µl β-mercaptoethanol. Samples were incubated at 60 °C for 15 min. 250 µl chloroform was added and samples were incubated at RT for 15 min, followed by centrifugation at RT for 10 min at 16,000 g. 550 µl of the aqueous phase were recovered and mixed with 550 µl phenol:chloroform:isoamyl alcohol (25:24:1), incubated and centrifuged as above. 500 µl of the aqueous phase was recovered and mixed with 400 µl isopropanol and 50 µl 3 M sodium acetate and precipitated at -80 °C for 15 min, followed by centrifugation at 4 °C for 30 min at 20,500 g. RNA was precipitated overnight at 4 °C in 2 M LiCl. RNA was pelleted by centrifugation at 4 °C for 30 min at 20,500 g, washed in 80 % ethanol, dried, and resuspended in 40 µl H_2O. For RT-qPCR, total RNA was treated with TURBO DNA-free (Ambion) and reverse transcribed with SuperScript III (Invitrogen) according to manufacturer's instructions. For each 13.33 µl RT-qPCR reaction, 0.167 µl cDNA was used with GoTaq qPCR Master Mix (Promega) on a LightCycler480 II system (Roche). All analyzed transcripts were normalized to reference gene *At4g26410* (Czechowski *et al.*, 2005) using the comparative Cq method (Schmittgen and Livak, 2008). Primer sequences are listed in **Table S3**. To perform multiple comparison of gene expression results between transgenic lines, one-way ANOVA with post-hoc Tukey's HSD analysis (confidence level = 0.95) were performed using the TukeyHSD() function of the R package   multcompView (https://cran.r-project.org/web/packages/multcompView/index.html). To perform pair-wise comparison of gene expression results within one transgenic line between two time points,   independent   *t*   tests   were   performed (https://www.graphpad.com/quickcalcs/ttest1.cfm).

ChIP-qPCR. Samples for FLAG ChIP were cross-linked under vacuum in ice-cold MC buffer with 1 % (v/v) formaldehyde for 2 x 10 min; samples for H3K4me3 ChIP were cross-linked as above for 2 x 5 min. Chromatin was extracted as follows (Kaufmann *et al.*, 2010): snap-frozen tissue was ground to a fine powder, resuspended in 25 ml M1 buffer, filtered through Miracloth mesh (Merck), washed 5 times in 5 ml M2 buffer, and washed once in 5 ml M3 buffer, with a centrifugation step at 4 °C, 10 min, 1,000 g in between washes. The resulting chromatin pellet was resuspended in 1 ml Sonication buffer and sheared with a Bioruptor Pico (Diagenode) for 17 cycles (30 sec on/ 30 sec off) on low-intensity settings. Equal chromatin amounts of chromatin from each sample were immunoprecipitated over night at 4 °C using antibodies against FLAG (F1804, Sigma-Aldrich), H3 (ab1791, Abcam), or H3K4me3 (ab8580, Abcam). Immunoprecipitated DNA was quantified by qPCR on a LightCycler480 II system (Roche). Primer sequences are listed in **Table S3**. To statistically evaluate FLAG and H3K4me3 enrichment, independent *t* tests were performed (https://www.graphpad.com/quickcalcs/ttest1.cfm).

Main figures and tables
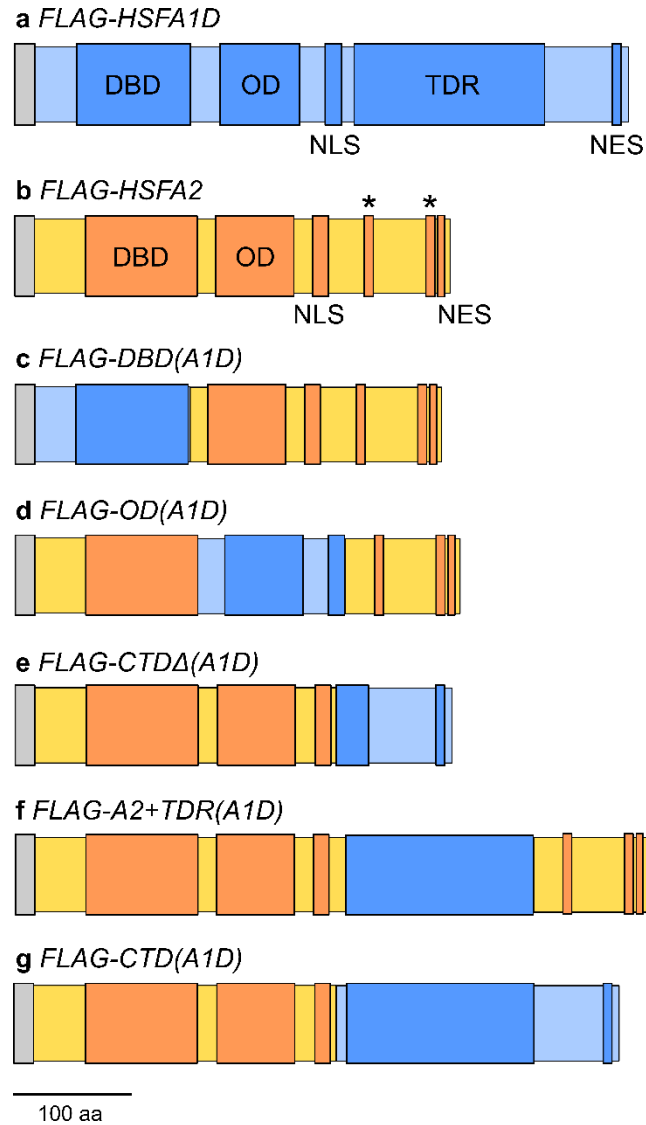
Fig. 1: Transgenic constructs for promoter and domain swap analysis of *HSFA1D* and *HSFA2*. All constructs are triple FLAG epitope-tagged (grey bar). The *FLAG-HSFA1D* construct (**a**) was expressed under control of a 561 bp *HSFA2* promoter fragment in the *hsfa2* background or under control of a 1,580 bp *HSFA1D* promoter fragment in the *hsfa1a/b/d* background. All other constructs (**b-g**) are expressed under control of a 561 bp *HSFA2* promoter fragment in the *hsfa2* background in presence or absence of the *pHSA32::HSA32-LUC* reporter construct. **a, b**) Modular domain organization of HSFA1D (**a**) and HSFA2 (**b**). From N-terminal to C-terminal, DNA-binding domain (DBD), oligomerization domain (OD), NLS (nuclear localization signal), NES (nuclear export signal). AHA (aromatic and large hydrophobic amino acids embedded in acidic context) motifs of HSFA2 are indicated with asterisks. Domain annotations from <u>uniprot.org</u>. HSFA1D contains a region encompassing a TDR (temperature-dependent regulatory domain) region (Ohama *et al.*, 2016). **c**) In *FLAG-DBD(A1D)*, DBD is from HSFA1D, while the remaining amino acid sequence is from HSFA2. **d**) In *FLAG-OD(A1D)*, OD and NLS are from HSFA1D, while the remaining amino acid sequences are from HSFA2. **e**) In *FLAG-CTDΔ(A1D)*, the C-terminal region, including subregion 5 of the TDR region (Ohama *et al.*, 2016), is from

121

HSFA1D, while the remaining amino acid sequence are from HSFA2. **f**) In *FLAG-A2+TDR(A1D)*, the TDR region of HSFA1D was inserted into HSFA2 at a position equivalent to its position in endogenous HSFA1D. **g**) In *FLAG-CTD(A1D)*, the C-terminal region, including the full-length TDR region, is from HSFA1D, while the remaining amino acid sequence is from HSFA2. Amino acid sequences of transgenic constructs are listed in **Table S1**.
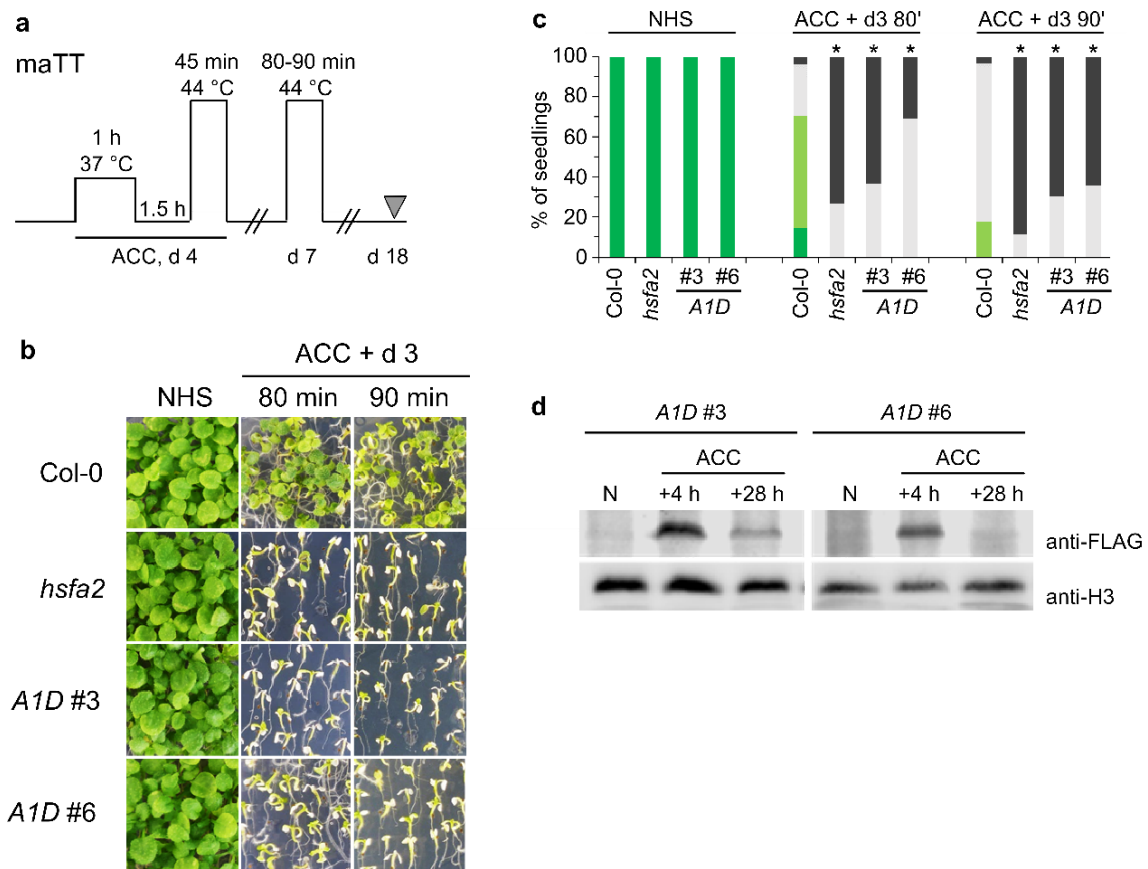
Fig. 2: *HSFA1D* does not complement *hsfa2* in physiological HS memory. a) Experimental set-up for physiological HS memory assay (maTT). 4 d-old seedlings are exposed to a 2-step acclimation treatment (ACC; 1 h 37 °C, 1.5 h 23 °C, 45 min 44 °C) and 3 d later, to severe HS of 44 °C for 80-90 min. All seedlings are imaged 18 d after germination. **b**) maTT assay of Col-0, *hsfa2*, and two independent transgenic lines (# 3 and # 6) of *FLAG-HSFA1D* in the *hsfa2* background (indicated as *A1D* #3 and #6). NHS, non-heat-stressed control. One representative of three independent experiments is shown. **c**) Quantification of observed phenotype categories of seedlings subjected to maTT assay depicted in (**a**) (dark green, unaffected; light green, slightly affected; grey, severely affected; dark grey, dead). Statistical significance was assessed with Fisher's exact probability test (*, *p* < 0.01 as compared to Col-0; n ≥ 23 for each genotype and time point). **d**) *HSFA1D* expression in *FLAG-HSFA1D* lines # 3 and # 6 assessed by immunoblot of total protein extract from seedlings 4 h and 28 h after ACC or in absence of HS (N). N samples were taken in parallel with ACC + 4 h samples. Histone H3 is blotted as loading control. One representative of two independent experiments is shown.
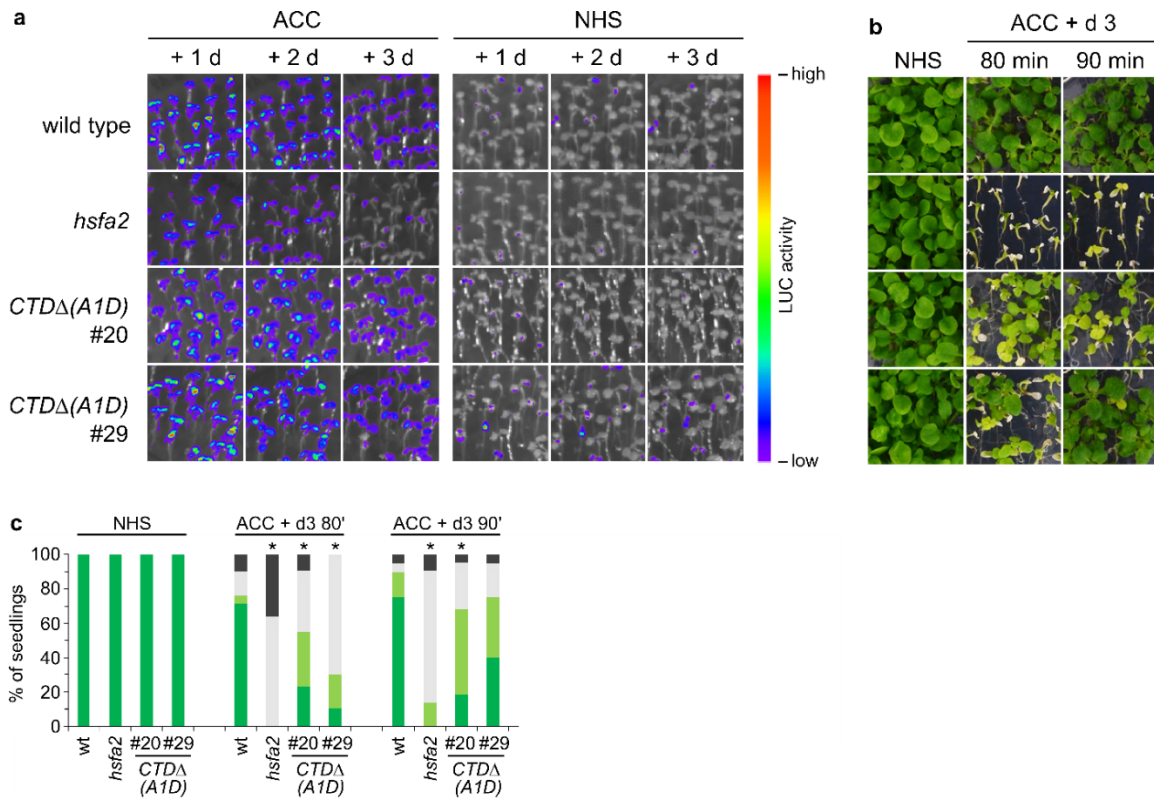
Fig. 3: *CTDΔ(A1D)* complements *hsfa2* fully in LUC activity-based type I transcriptional memory assay and largely in physiological HS memory. a) LUC activity assay of the *pHSA32::HSA32-LUC* reporter line (wild type), reporter line crossed to *hsfa2* (*hsfa2*), and two independent transgenic *CTDΔ(A1D)* lines (# 20 and # 29) in the *pHSA32::HSA32-LUC* x *hsfa2* background (indicated as *CTDΔ(A1D)* #20 and #29). 4 d-old seedlings were exposed to ACC treatment (**Fig 2a**) and LUC activity was quantified 1 d, 2 d, and 3 d later. Non-heat stressed (NHS) seedlings were imaged in parallel. One representative of three experiments is shown. **b**) maTT assay of the same genotypes as in (**a**), genotypes in the same order. HS treatments as in **Fig 2a**. NHS, non-heat-stressed control. One representative of three independent experiments is shown. **c**) Quantification of observed phenotype categories of seedlings subjected to maTT assay depicted in (**b**) (dark green, unaffected; light green, slightly affected; grey, severely affected; dark grey, dead). Statistical significance was assessed with Fisher's exact probability test (*, *p* < 0.01 as compared to wild type; n ≥ 20 for each genotype and time point). wt, wild type.
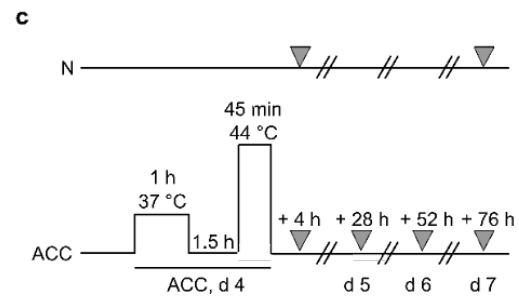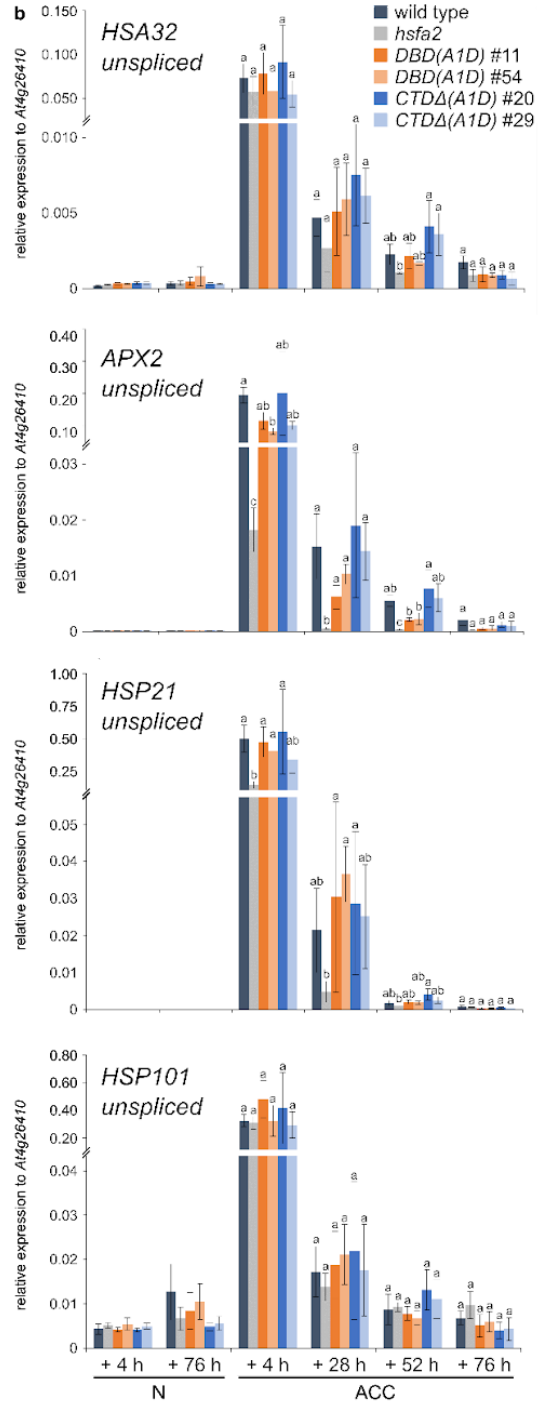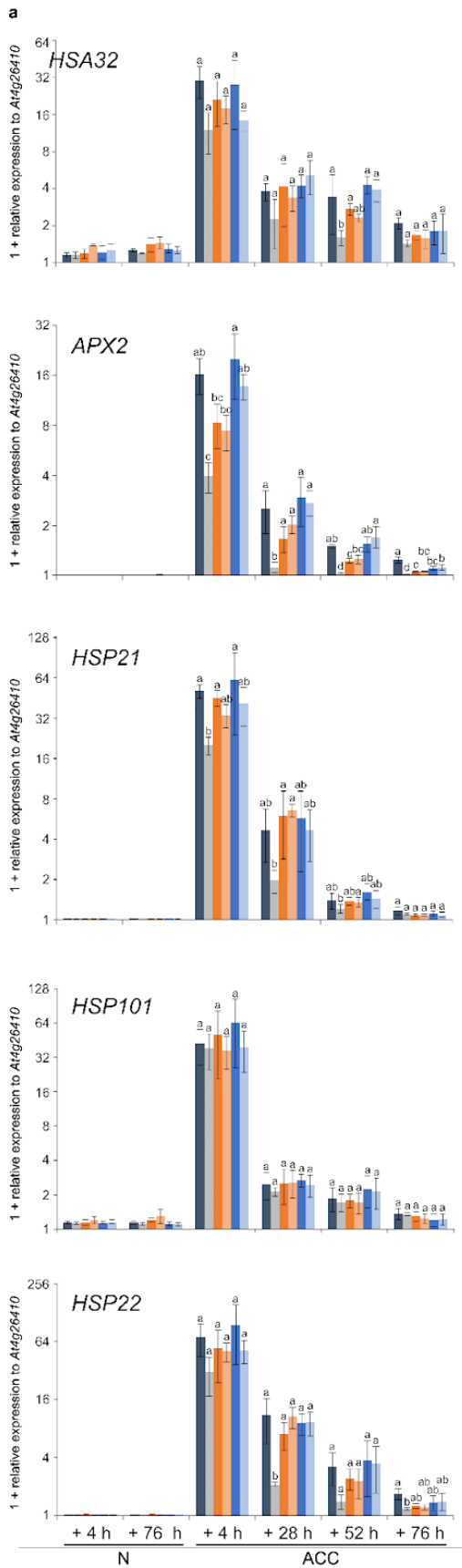
Fig. 4: *DBD(A1D)* and *CTDΔ(A1D)* mediate type I transcriptional memory. RT-qPCR analysis of transcript levels of type I transcriptional memory genes *HSA32*, *APX2*, *HSP21*, *HSP22*, and of non-memory gene *HSP101* in *pHSA32::HSA32-LUC* reporter line (wild type), reporter line crossed to *hsfa2* (*hsfa2*), and two independent transgenic *DBD(A1D)* lines (# 11 and # 54) and two independent transgenic *CTDΔ(A1D)* lines (# 20 and # 29), all in the *pHSA32::HSA32-LUC* x *hsfa2* background. **a**) Expression level of processed transcripts in $\log_2$ scale. **b**) Expression level of intron-containing transcripts. For **a**) and **b**), expression is relative to *At4g26410*. Data are mean ± SD of three independent experiments. Transcript levels were statistically evaluated for all genotypes within each time point after ACC by ANOVA followed by Tukey's HSD ($p < 0.05$). Genotypes are assigned one or more letters based on their statistical group. Genotypes sharing one letter are not significantly different. **c**) Experimental set-up. Samples were taken 4 h, 28 h, 52 h, and 76 h after ACC treatment. Non-heat stressed (N) samples were taken at 4 h and 76 h.
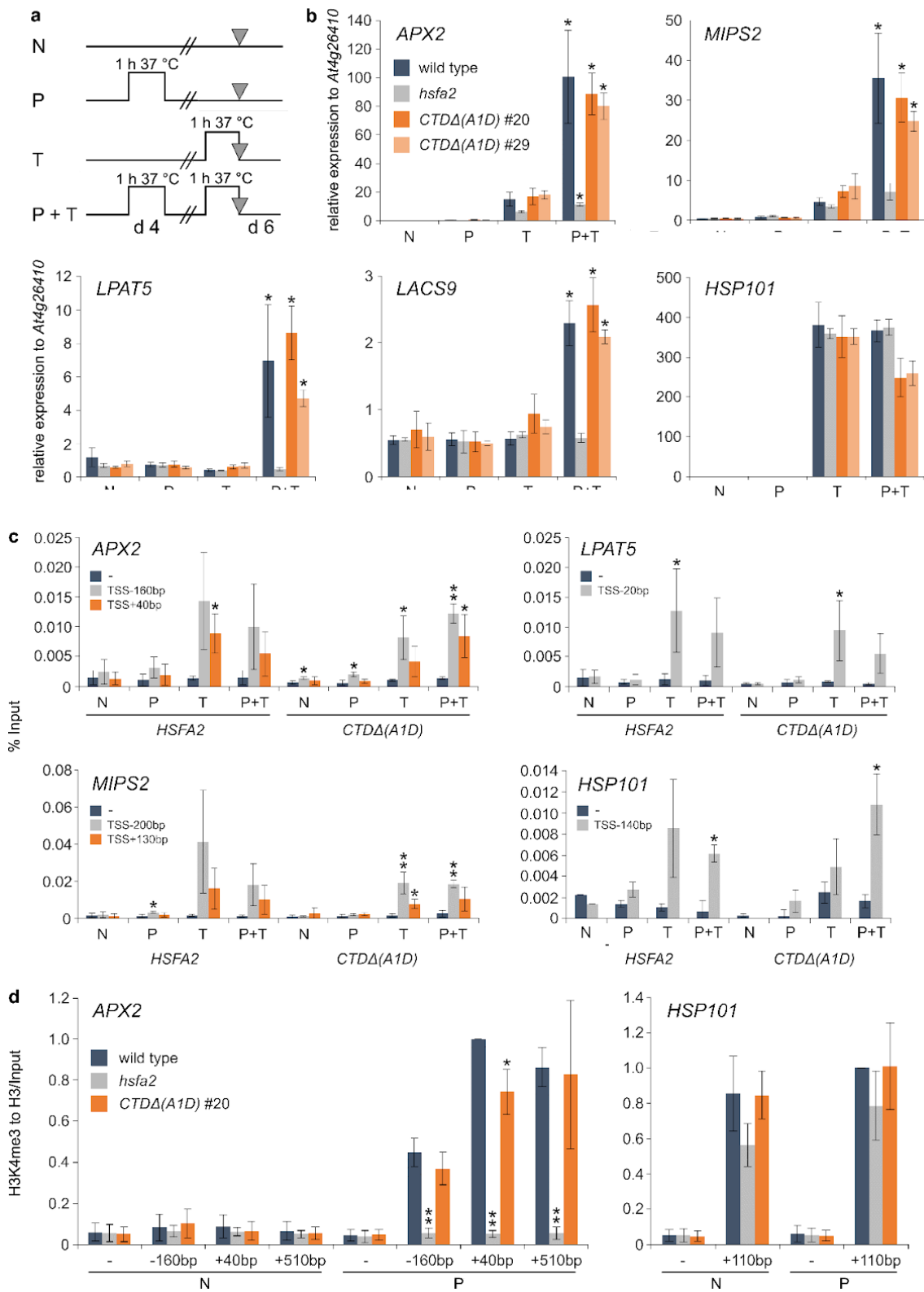
Fig. 5: ***CTDΔ(A1D)* mediates type II transcriptional memory, binds directly to target genes and mediates sustained H3K4 methylation. a**) Experimental set-up for type II transcriptional memory-related processes. 4 d-old seedlings were either not exposed to HS (N), exposed to mild HS of 37 °C for 1 h on d 4 (priming, P), exposed to mild HS of 37 °C for 1 h on d 6 (triggering, T), or exposed to mild HS of 37 °C on d 4 and again on d 6 (priming and triggering P + T). For RT-qPCR, all samples were taken on d 6 at the end of d 6 HS treatment. For ChIP-qPCR, P and N samples were taken on d 6 at a time point corresponding to 45 min after end of d 6 HS treatment. **b**) RT-qPCR analysis of transcript levels of +/++ type II transcriptional memory genes *APX2* and *MIPS2*, of 0/+ type II transcriptional memory genes *LPAT5* and *LACS9*, and of non-memory gene *HSP101* in *pHSA32::HSA32-LUC* reporter line (wild type), reporter line crossed to *hsfa2* (*hsfa2*), and two independent transgenic *CTDΔ(A1D)* lines (# 20 and # 29) in the *pHSA32::HSA32-LUC* x *hsfa2* background. Sampling time points as in (**a**). Expression relative to *At4g26410*. Data are mean ± SD of three independent experiments. Asterisks indicate significant difference of transcript levels between P + T and T samples of a genotype (*, *p* < 0.01, unpaired *t* test). **c**) ChIP-qPCR analysis of binding of HSFA2 in *pA2::FLAG-HSFA2* complementation line #2 in *hsfa2* background (*HSFA2*) and of CTDΔ(A1D) in *CTDΔ(A1D)* line #29 (*CTDΔ(A1D)*)), to *APX2*, *MIPS2*, *LPAT5*, and *HSP101*. Sampling time points as in (**a**). Enrichment is relative to Input control. Asterisks indicate statistically significant enrichment compared to negative amplicon (*, *p* < 0.05, **, *p* < 0.01, unpaired *t* test). **d**) ChIP-qPCR analysis of H3K4me3 enrichment in *pHSA32::HSA32-LUC* reporter line (wild type), reporter line crossed to *hsfa2* (*hsfa2*), and *CTDΔ(A1D)* line #20 at *APX2* and *HSP101*. Sampling time points as in (**a**). Enrichment is relative to H3 and Input control and is normalized to H3K4me3 enrichment of wild type at P. Asterisks indicate statistically significant differences of enrichment compared to wild type (*, *p* < 0.05, **, *p* < 0.01, unpaired *t* test). For **c**) and **d**), amplicons are described based on their distance from TSS. - refers to negative control amplicon located ca. 3 kbp upstream of TSS.
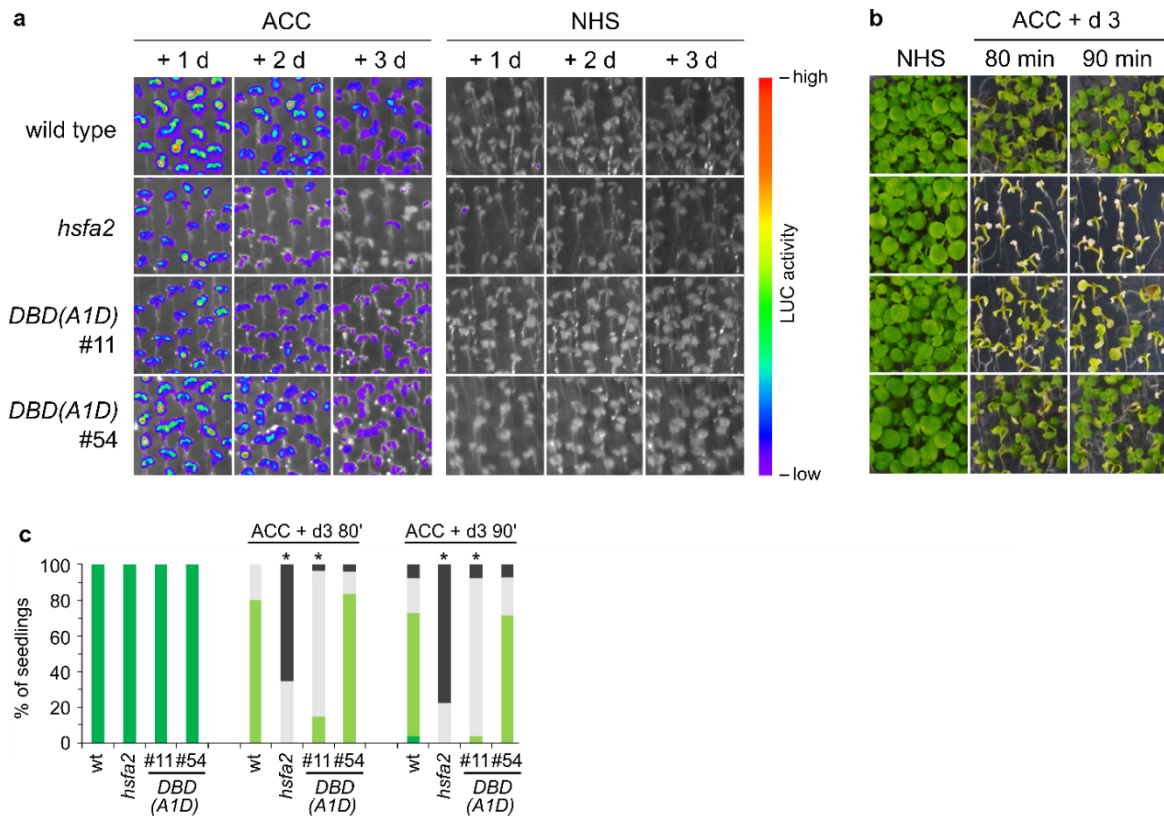
Fig. 6: *DBD(A1D)* complements *hsfa2* fully in LUC activity-based type I transcriptional memory assay and largely in physiological HS memory. a) LUC activity assay of the *pHSA32::HSA32-LUC* reporter line (wild type), reporter line crossed to *hsfa2* (*hsfa2*), and two independent transgenic *DBD(A1D)* lines (# 11 and # 54) in the *pHSA32::HSA32-LUC* x *hsfa2* background (indicated as *DBD(A1D)* #11 and #54). 4 d-old seedlings were exposed to ACC treatment (**Fig 2a**) and LUC activity was quantified 1 d, 2 d, and 3 d later. Non-heat stressed (NHS) seedlings were imaged in parallel. One representative of three experiments is shown. **b**) maTT assay of the same genotypes as in (**a**), genotypes in the same order. HS treatments as in **Fig 2a**. NHS, non-heat-stressed control. One representative of three independent experiments is shown. **c**) Quantification of observed phenotype categories of seedlings subjected to maTT assay depicted in (**b**) (dark green, unaffected; light green, slightly affected; grey, severely affected; dark grey, dead). Statistical significance was assessed with Fisher's exact probability test (*, *p* < 0.01 as compared to wild type; n ≥ 24 for each genotype and time point). wt, wild type.
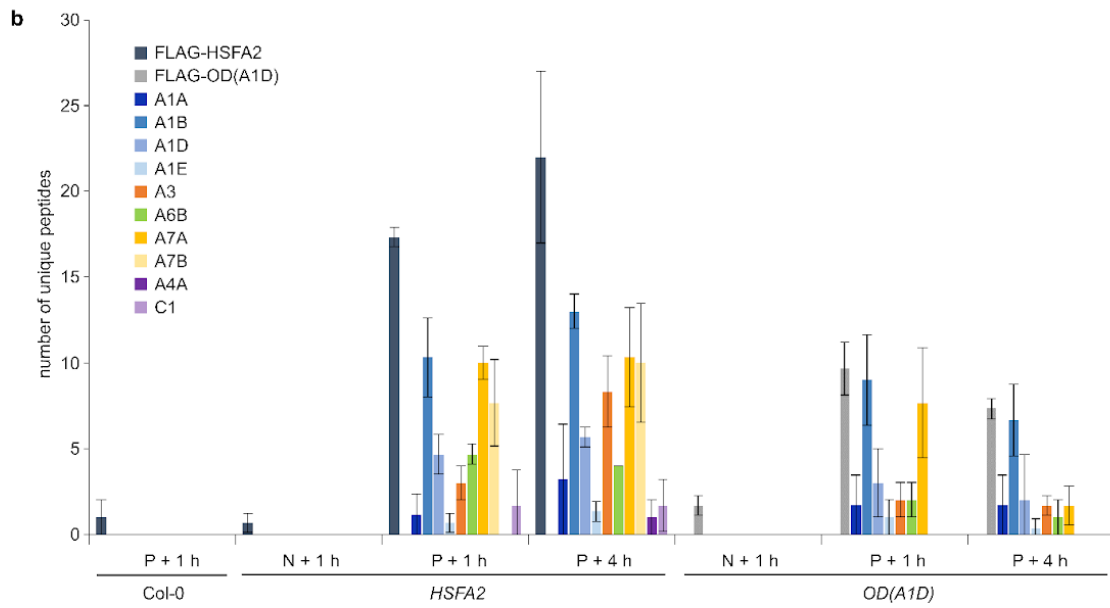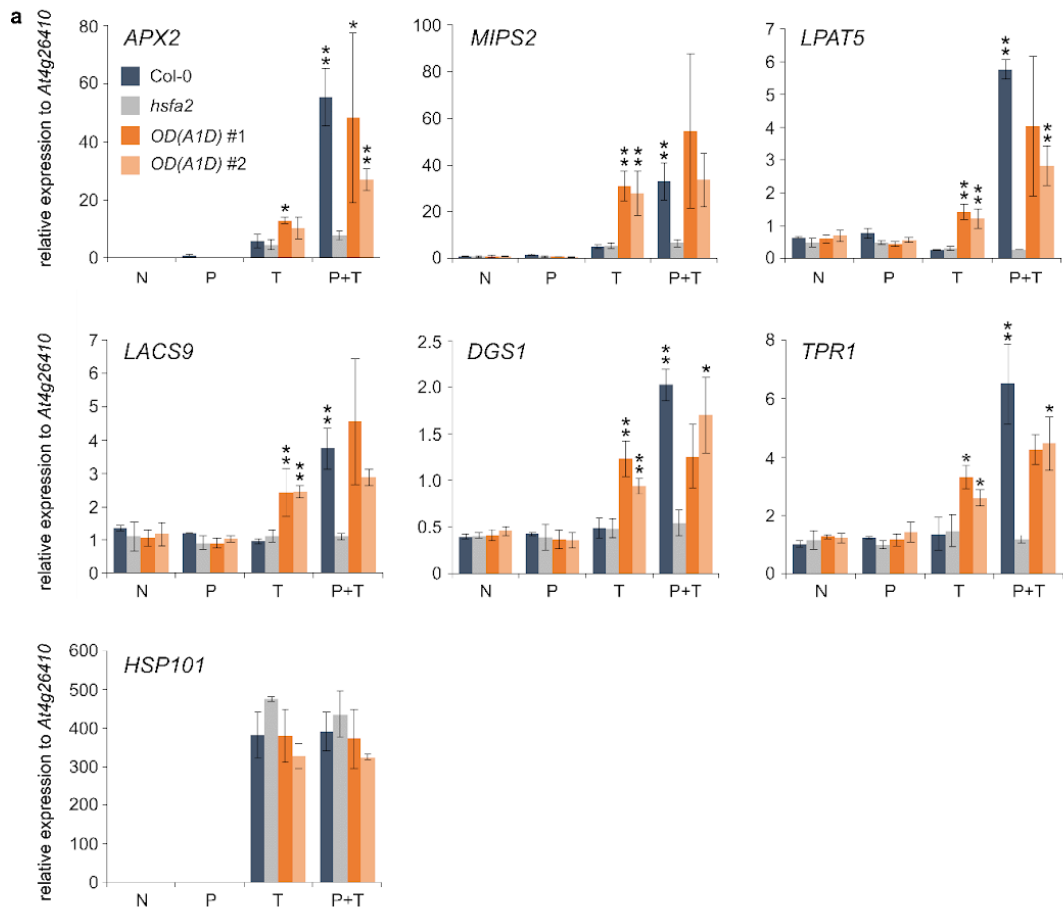
Fig. 7: *OD(A1D)* mediates hyper-induction of type II transcriptional memory genes after triggering HS; HSF interaction partners of HSFA2 and OD(A1D) after triggering HS. a) RT-qPCR analysis of transcript levels of +/++ type II transcriptional memory genes *APX2* and *MIPS2*, of 0/+ type II transcriptional memory genes *LPAT5*, *LACS9*, *DGS1*, and *TPR1*, and of non-memory gene *HSP101* in Col-0, *hsfa2*, and two independent transgenic *OD(A1D)* lines (# 1 and # 2) in the *hsfa2* background. Experimental set-up as in **Fig 5a**. Expression relative to *At4g26410*. Data are mean ± SD of three independent experiments. Asterisks at P + T samples indicate significant difference of transcript levels between P + T and T samples of a genotype (*, *p* < 0.05, **, *p* < 0.01, unpaired *t* test). Asterisks at T samples indicate significant difference of transcript levels between T and N samples of a genotype (*, *p* < 0.05, **, *p* < 0.01, unpaired *t* test). **b**) HSF interaction partners of FLAG-HSFA2 and FLAG-OD(A1D) after triggering HS assessed by Co-IP/MS performed on co-immunoprecipitated peptides using FLAG-HSFA2 bait protein deriving from *pA2::FLAG-HSFA2* line # 2 in *hsfa2* background (*HSFA2*) or FLAG-OD(A1D) bait protein deriving from *OD(A1D)* line #2 in *hsfa2* background (*OD(A1D)*). Samples were harvested 1 h or 4 h after priming (P) HS (1 h of 37 °C). Non-heat stressed control samples (N) were harvested at the same time as P + 1 h samples. Col-0 samples were harvested at P + 1 h as additional negative control. Number of unique peptides attributed to individual HSFs is indicated. Data are mean ± SD of three independent experiments. For bait proteins FLAG-HSFA2 and FLAG-OD(A1D) and for endogenous HSFA1D, peptides deriving from the OD were excluded from the count from all samples as in *OD(A1D)* samples they could derive either from endogenous HSFA1D or from FLAG-OD(A1D).
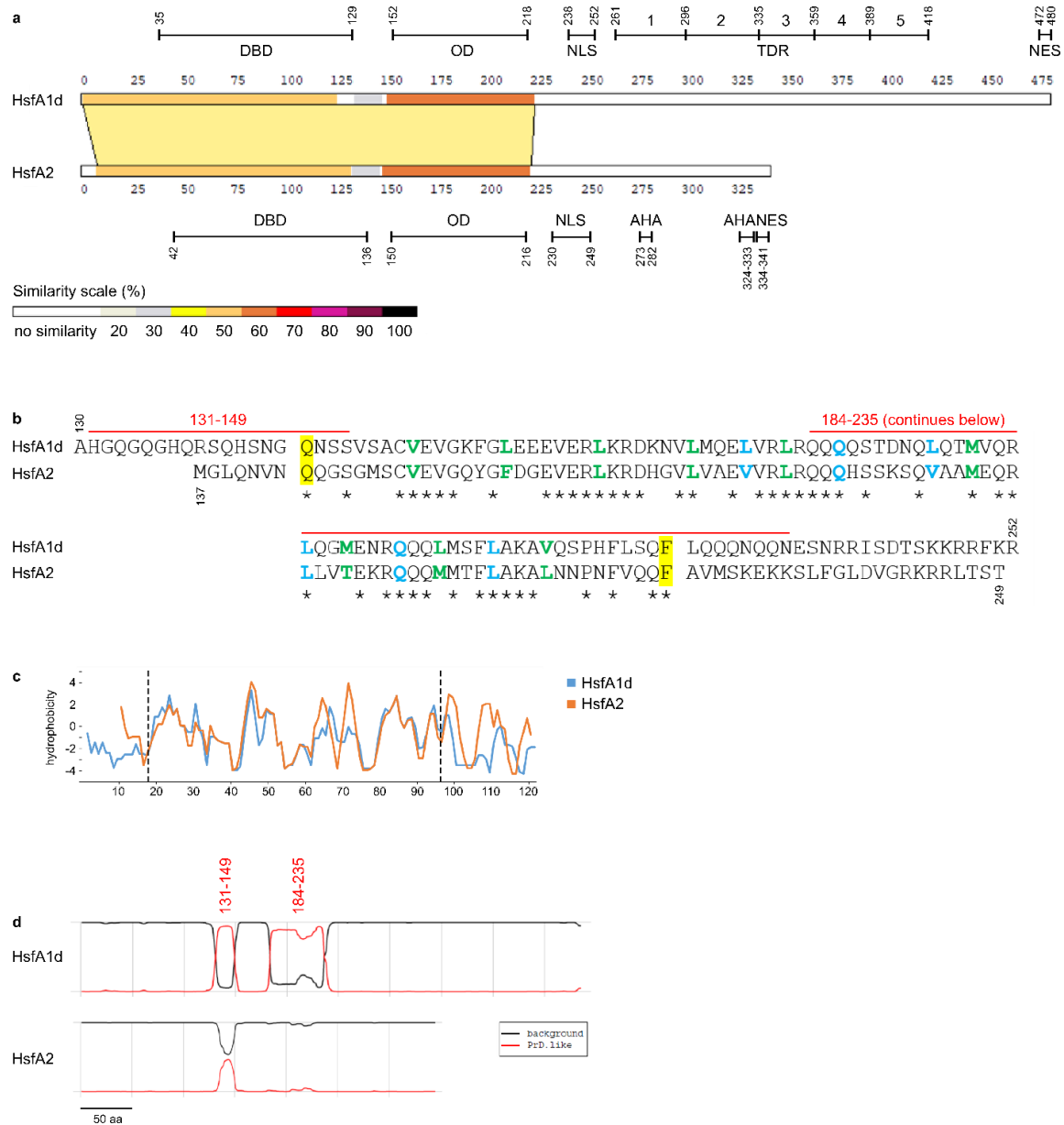
Supplementary material

Fig. S1: Amino acid sequence alignments between HSFA1D and HSFA2 and their respective oligomerization domains. a) Amino acid sequence alignment between full-length endogenous HSFA1D and HSFA2 with Expasy SIM alignment tool (https://web.expasy.org/sim/). LALNVIEWER (Duret, Gasteiger and Perrièe, 1996) was used for graphical representation. Positions of functional domains identified by uniprot.org and (Ohama *et al.*, 2016) are indicated. **b**) Sequence alignment of oligomerization domains of HSFA1D and HSFA2 as utilized for generation of FLAG-OD(A1D) domain swap construct, generated with Expasy SIM alignment tool. Amino acids 137-249 of HSFA2 were replaced with amino acids 130-252 of HSFA1D to generate FLAG-OD(A1D). Start and end of aligned region are indicated in yellow. Asterisks within the aligned regions indicate identical amino acids between HSFA1D and HSFA2. Amino acids in

green and blue indicate positions of hydrophobic amino acid residues within the bi-partite heptad repeats which characterize OD. Amino acids 131-149 and 184-235 of HSFA1D were identified as prion-like by PLAAC algorithm. **c**) Kyte & Doolittle hydrophobicity scale of amino acid sequences 130-252 of HSFA1D and 137-249 of HSFA2 generated with Expasy ProtScale tool (https://web.expasy.org/protscale/). y-axis, hydrophobicity value, x-axis, amino acid position. Amino acid sequences were aligned as in (**b**). Region in between the dashed vertical lines corresponds to core aligned region as shown in (**b**). **d**) PLAAC algorithm (Lancaster *et al.*, 2014) applied to analysis of full-length HSFA1D and HSFA2 proteins reveals two prion-like amino acid sequences within HSFA1D (amino acids 131-149 and 184-235). These sequences are within the HSFA1D amino acid region used to generate OD(A1D) construct (amino acids 130-252; see (**b**)).
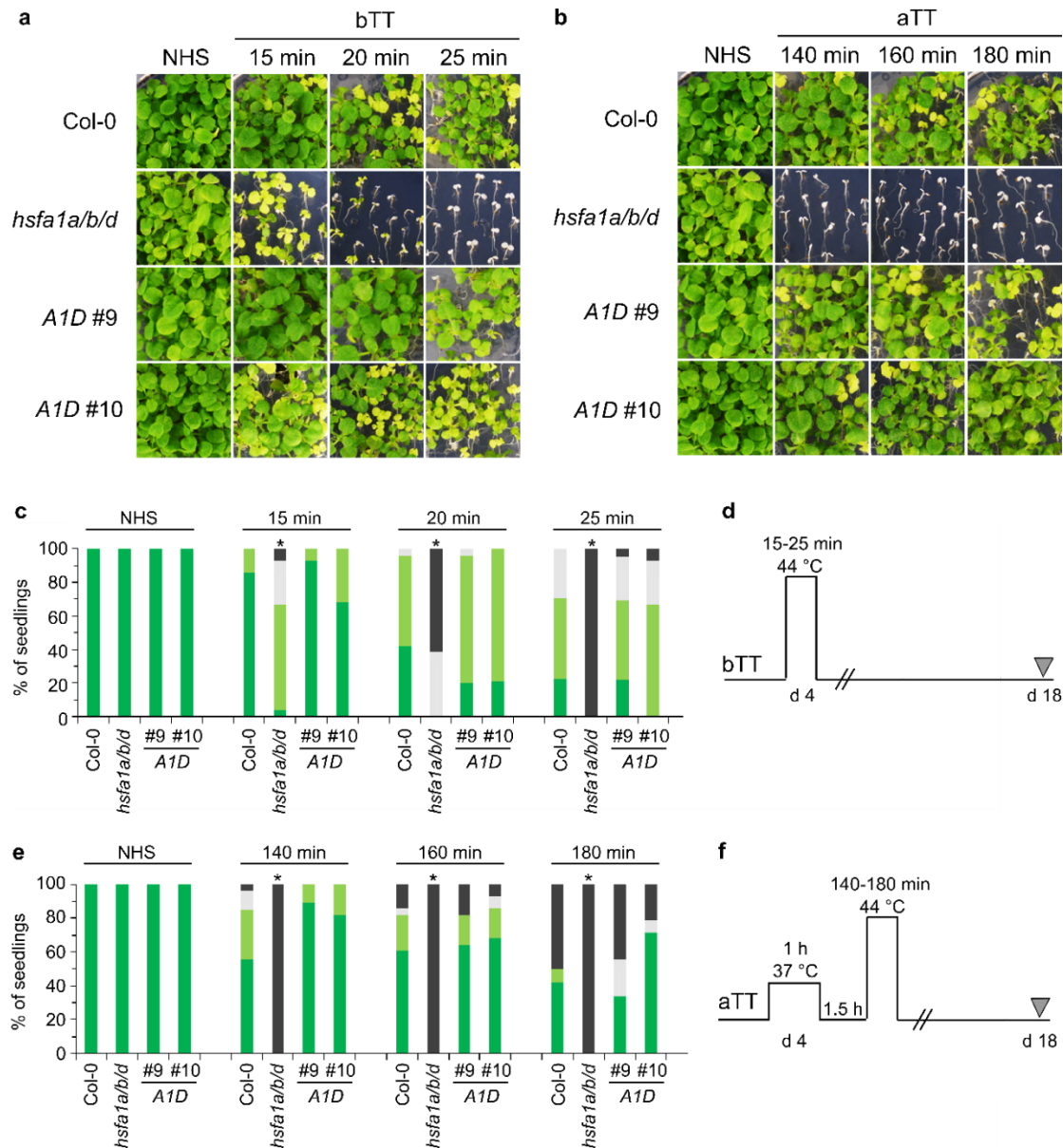
Fig. S2: *HSFA1D* complements *hsfa1a/b/d* in bTT and aTT. a) bTT assay of Col-0, *hsfa1a/b/d*, and two independent transgenic lines (# 9 and # 10) of *pA1D::FLAG-HSFA1D* in *hsfa1a/b/d* background (indicated as *A1D* #9 and #10). HS treatments as in (**d**). One representative of three independent experiments is shown. **b**) aTT assay of the same genotypes as indicated in (**a**). HS treatments as in (**f**). One representative of three independent experiments is shown. **c**, **e**) Quantification of observed phenotype categories of seedlings subjected to bTT assay (**c**) depicted in (**a**) and aTT assay (**e**) depicted in (**b**) (dark green, unaffected; light green, slightly affected; grey, severely affected; dark grey, dead). Statistical significance was assessed with Fisher's exact probability test (*, $p < 0.01$ as compared to Col-0; n ≥ 23 for each genotype and time point in bTT; n ≥ 25 for each genotype and time point in aTT;). **d**, **f**) Experimental set-ups for physiological bTT (**d**) and aTT (**f**) assays. For bTT assays, 4 d-old seedlings were exposed to severe HS of 44 °C for 15-25 min. For aTT assays, 4 d-old seedlings were exposed to mild HS of 37 °C for 1 h, recovered at 23 °C for 1.5 h, and were then exposed to severe HS of 44 °C HS for 140-180 min. All seedlings were imaged 18 d after germination.
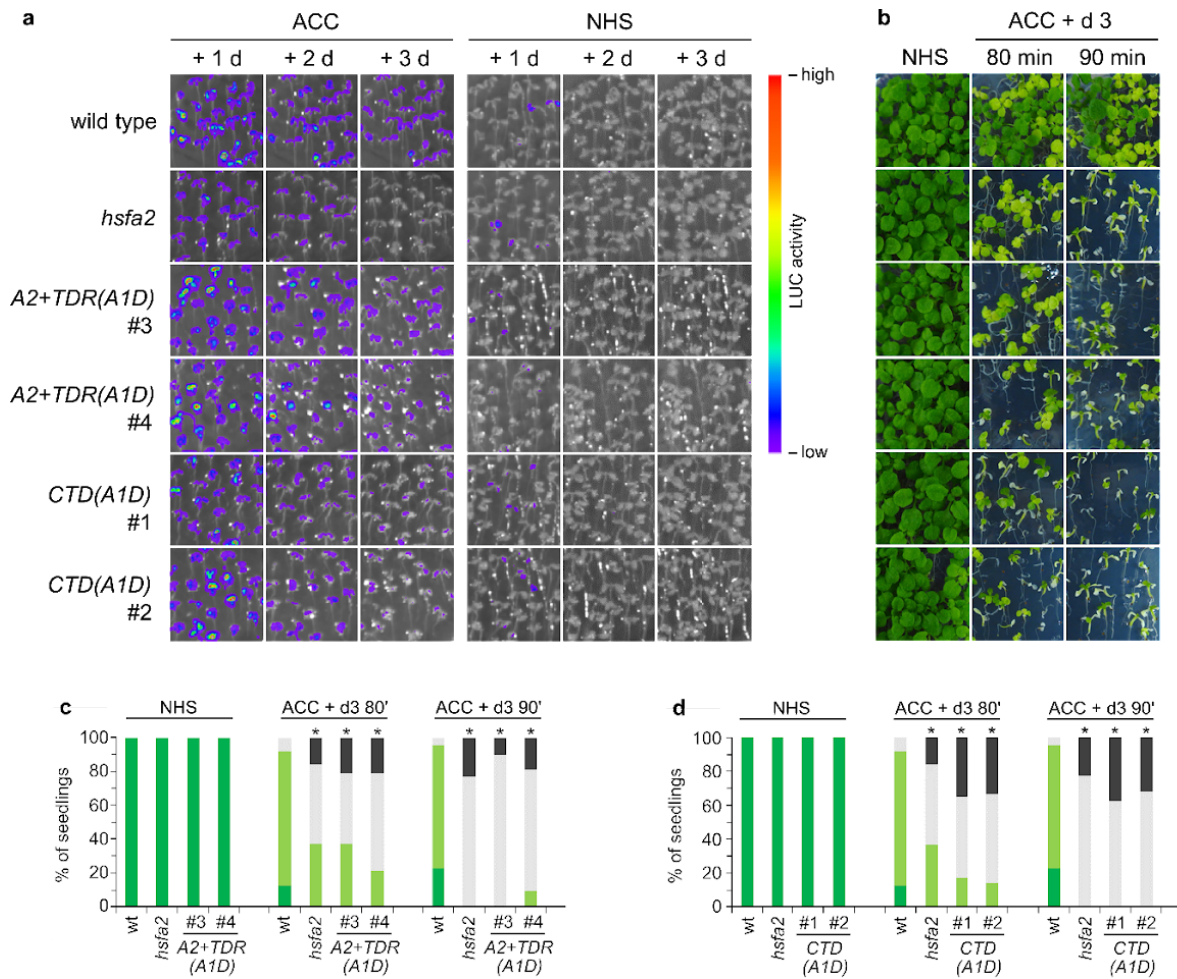
Fig. S3: *A2+TDR(A1D)* and *CTD(A1D)* do not complement *hsfa2* in LUC activity-based type I transcriptional memory assay and do not complement *hsfa2* in physiological HS memory.
a) LUC activity assay of the *pHSA32::HSA32-LUC* reporter line (wild type), reporter line crossed to *hsfa2* (*hsfa2*), and two independent transgenic *A2+TDR(A1D)* lines (# 3 and # 4) and two independent transgenic *CTD(A1D)* lines (# 1 and # 2), all in the *pHSA32::HSA32-LUC* x *hsfa2* background. 4 d-old seedlings were exposed to ACC treatment (**Fig 2a**) and LUC activity was quantified 1 d, 2 d, and 3 d later. Non-heat stressed (NHS) seedlings were imaged in parallel. One representative of three experiments is shown. **b**) maTT assay of the same genotypes as in (**a**), genotypes in the same order. HS treatments as in **Fig 2a**. NHS, non-heat stressed control. One representative of three independent experiments is shown. **c**, **d**) Quantification of observed phenotype categories of *A2+TDR(A1D)* (**c**) and *CTD(A1D)* (**d**) seedlings subjected to maTT assay depicted in (**b**) (dark green, unaffected; light green, slightly affected; grey, severely affected; dark grey, dead). Statistical significance was assessed with Fisher's exact probability test (*, *p* < 0.01 as compared to wild type; n ≥ 14 for each genotype and time point).
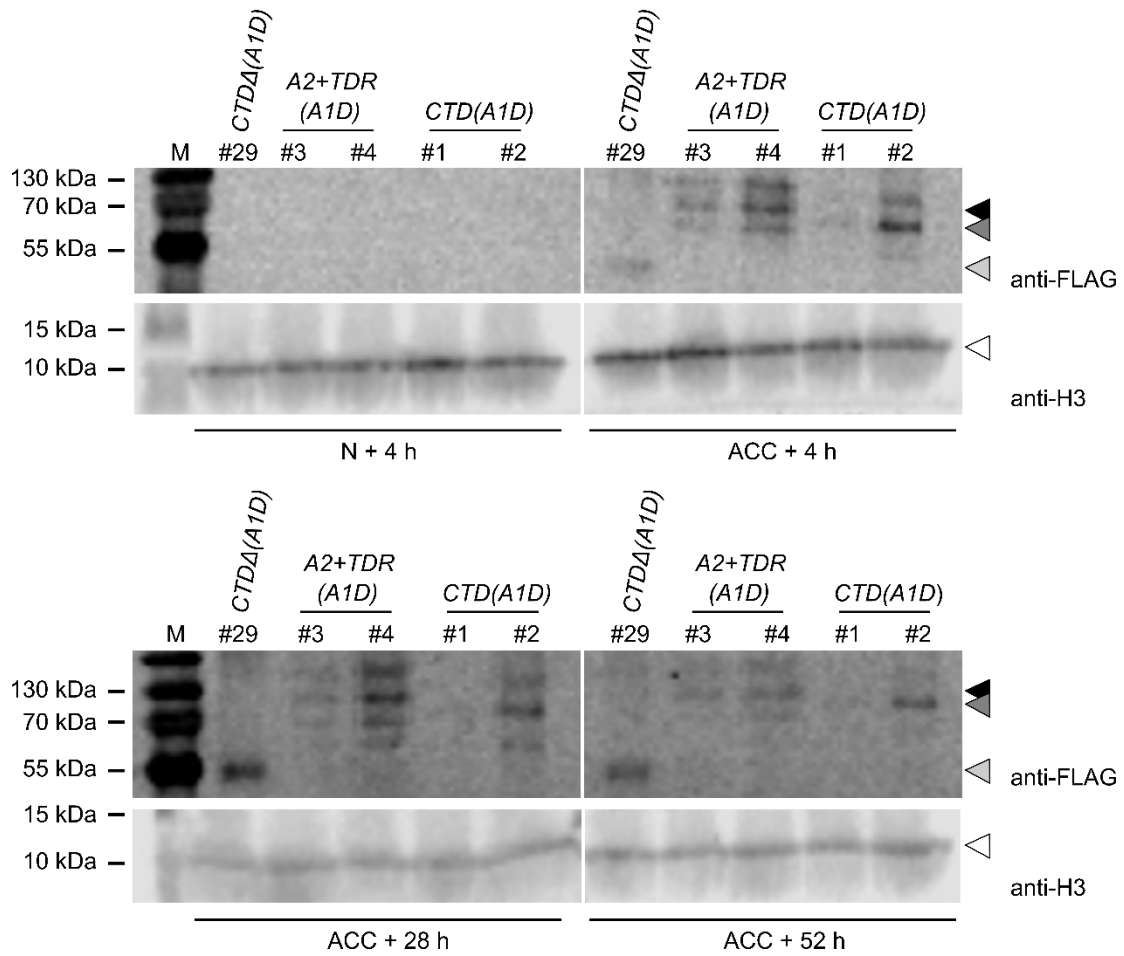
Fig. S4: Protein expression of CTDΔ(A1D), A2+TDR(A1D), and CTD(A1D) after ACC assessed by immunoprecipitation followed by immunoblot. Samples of transgenic lines *CTDΔ(A1D)* #29, *A2+TDR(A1D)* #3 and #4, and *CTD(A1D)* #1 and #2 were harvested 4 h, 28 h, and 52 h after ACC (**Fig 2a**). Non-heat stressed samples (N) were harvested at the same time as ACC + 4 h samples. Presence of transgenic proteins is assessed with anti-FLAG antibody. Histone H3 is blotted as loading control and assessed with anti-H3 antibody. M, protein ladder. Experiment is representative of two independent replicates. Expected positions of proteins are indicated by arrows (black: A2+TDR(A1D); dark grey: CTD(A1D); light grey: CTDΔ(A1D); white: H3).
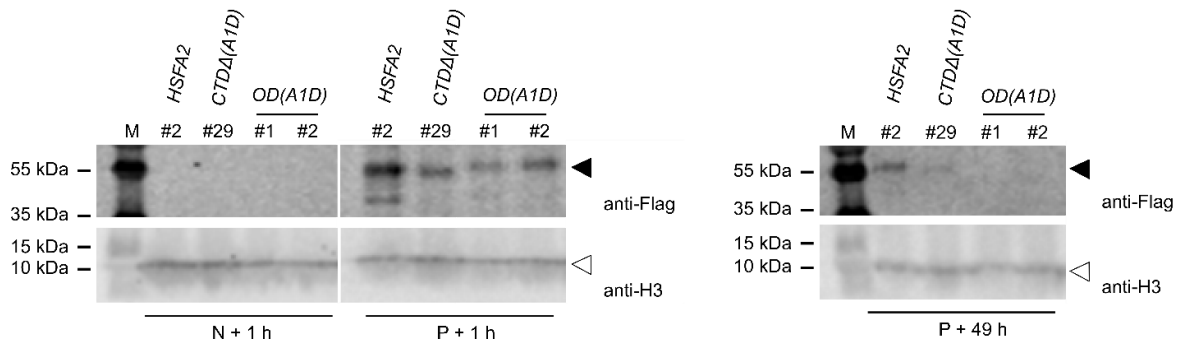
Fig. S5: Protein expression of HSFA2, CTDΔ(A1D), and OD(A1D) after priming HS assessed by immunoprecipitation followed by immunoblot. Samples of transgenic lines *HSFA2* #2, *CTDΔ(A1D)* #29, and *OD(A1D)* #1 and #2 were harvested 1 h and 49 h after priming treatment (P) of 1 h at 37° C. Non-heat stressed samples (N) were harvested at the same time as P + 1 h samples. Presence of transgenic proteins is assessed with anti-FLAG antibody. Histone H3 is blotted as loading control and assessed with anti-H3 antibody. M, protein ladder. Experiment is representative of two independent replicates. Expected positions of proteins are indicated by arrows (black: HSFA2, CTDΔ(A1D), OD(A1D); white: H3).
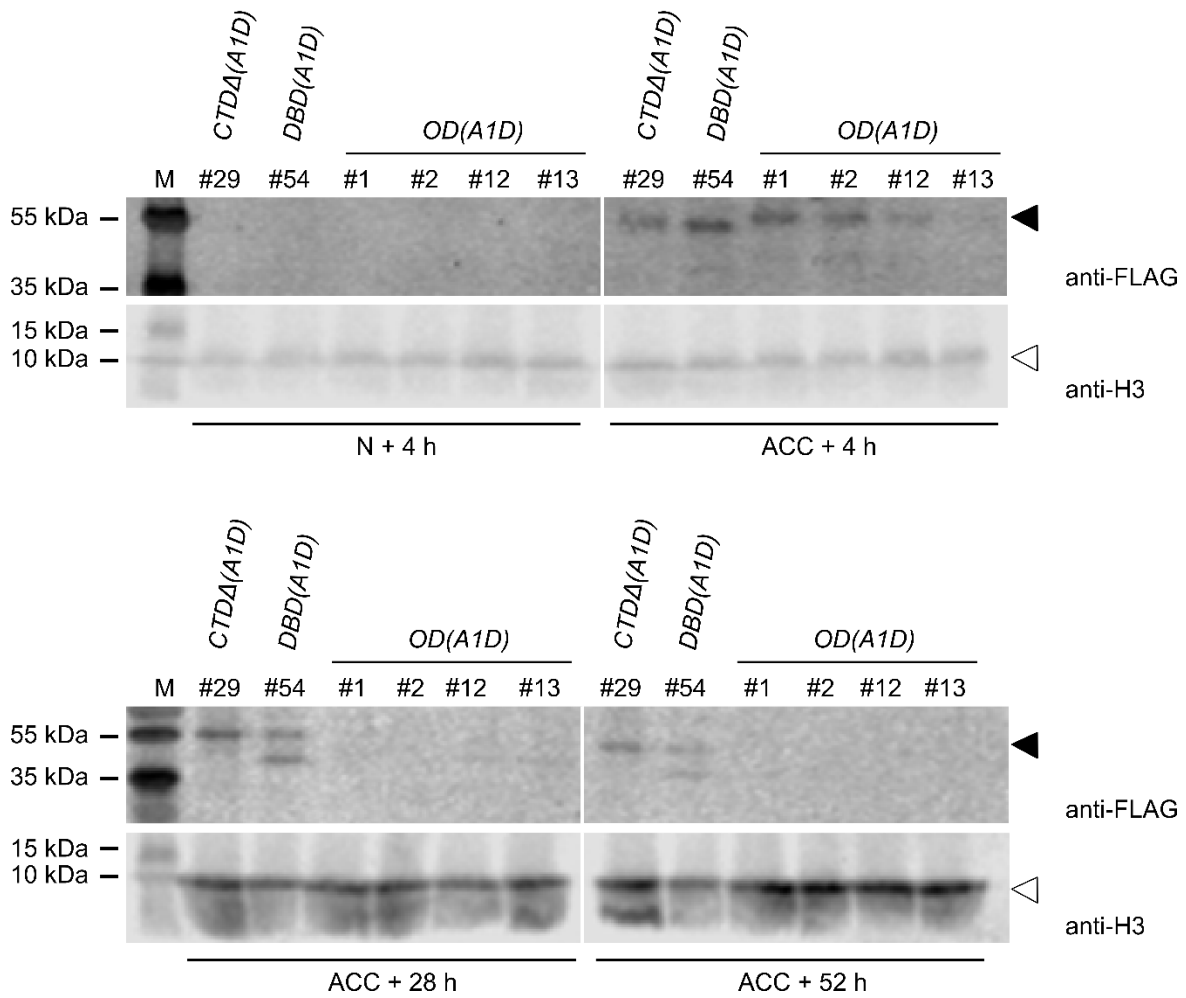
Fig. S6: Protein expression of CTDΔ(A1D), DBD(A1D), and OD(A1D) after ACC assessed by immunoprecipitation followed by immunoblot. Samples of transgenic lines *CTDΔ(A1D)* #29, *DBD(A1D)* #54, and *OD(A1D)* #1 and #2 (both in *hsfa2* background), #12, and #13 (both in *pHSA32::HSA32-LUC* x *hsfa2* background) were harvested 4 h, 28 h, and 52 h after ACC (**Fig 2a**). Non-heat stressed samples (N) were harvested at the same time as ACC + 4 h samples. Presence of transgenic proteins is assessed with anti-FLAG antibody. Histone H3 is blotted as loading control and assessed with anti-H3 antibody. M, protein ladder. Experiment is representative of two independent replicates. Expected positions of proteins are indicated by arrows (black: CTDΔ(A1D), DBD(A1D), OD(A1D); white: H3).
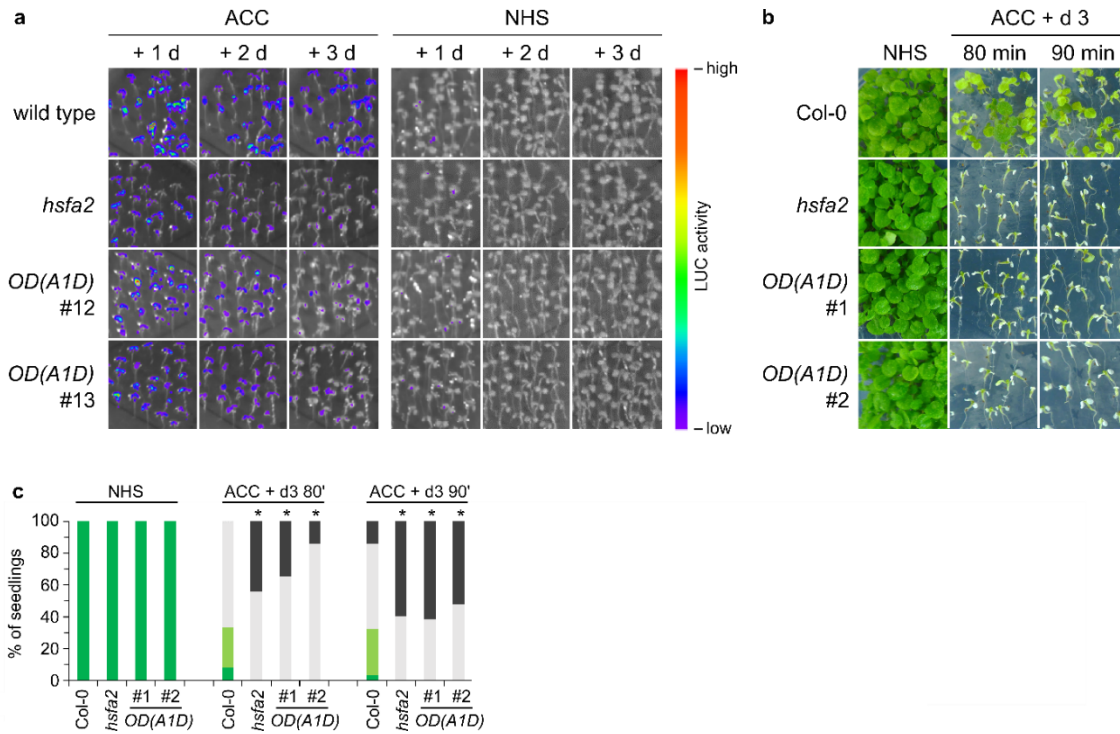
Fig. S7: ***OD(A1D)* does not complement *hsfa2* in physiological HS memory. a**) LUC activity assay of the *pHSA32::HSA32-LUC* reporter line (wild type), reporter line crossed to *hsfa2* (*hsfa2*), and two independent transgenic *OD(A1D)* lines (# 12 and # 13) in the *pHSA32::HSA32-LUC* x *hsfa2* background (indicated as *OD(A1D)* #12 and #13). 4 d-old seedlings were exposed to ACC treatment (**Fig 2a**) and LUC activity was quantified 1 d, 2 d, and 3 d later. Non-heat stressed (NHS) seedlings were imaged in parallel. One representative of three experiments is shown. **b**) maTT assay of Col-0, *hsfa2*, and two independent transgenic *OD(A1D)* lines (# 1 and # 2) in the *hsfa2* background (indicated as *OD(A1D)* #1 and #2). HS treatments as in **Fig 2a**. NHS, non-heat stressed control. One representative of three independent experiments is shown. **c**) Quantification of observed phenotype categories of seedlings subjected to maTT assay depicted in (**b**) (dark green, unaffected; light green, slightly affected; grey, severely affected; dark grey, dead). Statistical significance was assessed with Fisher's exact probability test (*, $p < 0.01$ as compared to wild type; n ≥ 21 for each genotype and time point).
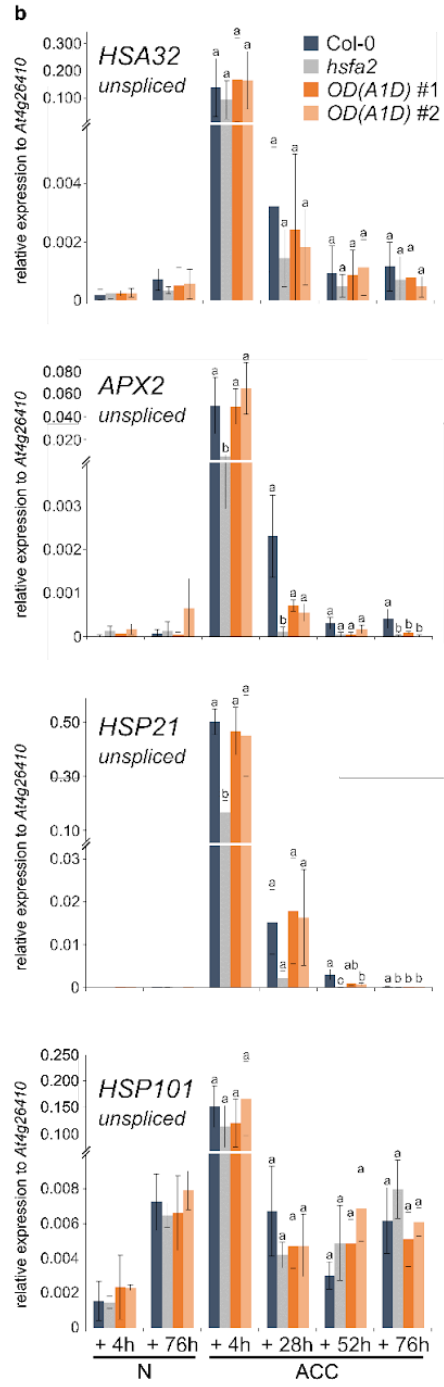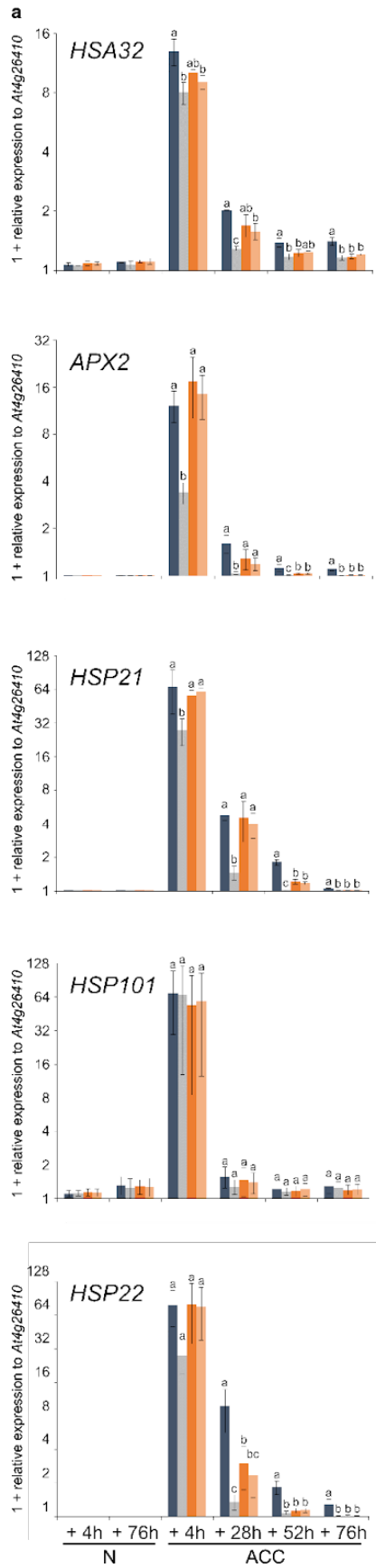
Fig. S8: Type I transcriptional memory in *OD(A1D)* transgenic lines. RT-qPCR analysis **of** transcript levels of type I transcriptional memory genes *HSA32*, *APX2*, *HSP21*, *HSP22*, and of non-memory gene *HSP101* in Col-0, *hsfa2*, and two independent transgenic *OD(A1D)* lines (# 1 and # 2) in *hsfa2* background (indicated as *OD(A1D)* #1 and #2). Experimental set-up as in **Fig 4c**. **a**) Expression level of processed transcripts in $\log_2$ scale. **b**) Expression level of intron-containing transcripts. For **a**) and **b**), expression is relative to *At4g26410*. Data are mean ± SD of three independent experiments. Transcript levels were statistically evaluated for all genotypes within each time point after ACC by ANOVA followed by Tukey's HSD ($p < 0.05$). Genotypes are assigned one or more letters based on their statistical group. Genotypes sharing one letter are not significantly different.
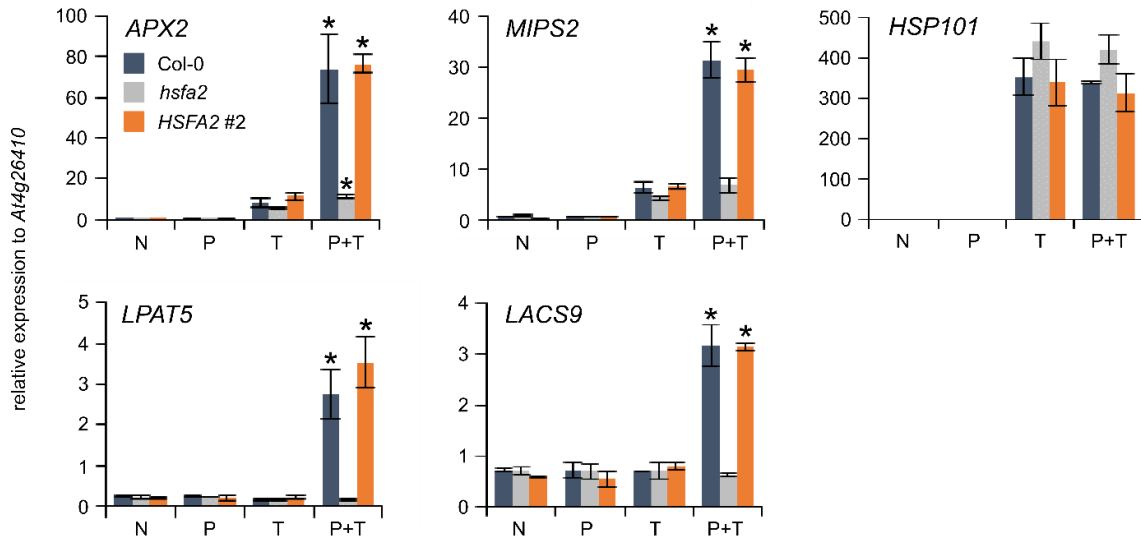
Fig. S9: *FLAG-HSFA2* **mediates type II transcriptional memory.** RT-qPCR analysis of transcript levels of +/++ type II transcriptional memory genes *APX2* and *MIPS2*, of 0/+ type II transcriptional memory genes *LPAT5* and *LACS9*, and of non-memory gene *HSP101* in Col-0, *hsfa2*, and of complementation line *pA2::FLAG-HSFA2* # 2 in *hsfa2* background (indicated as *HSFA2* #2). Experimental set-up as in **Fig 5a**. Expression relative to *At4g26410*. Data are mean ± SD of three independent experiments. Asterisks at P + T samples indicate significant difference of transcript levels between P + T and T samples of a genotype (*, *p* < 0.01, unpaired *t* test).

Table S1: Amino acid sequences of FLAG-HSFA1D, FLAG-HSFA2, and chimeric HSFs. Bold sequence corresponds to FLAG-GAGA epitope tag and linker and is common to all listed proteins. For the remaining amino acid sequences, underlined sequences derive from HSFA1D, while non-underlined sequences derive from HSFA2.

protein	amino acid sequence (N-terminus to C-terminus)
FLAG-HSFA1D	**MDYKDHDGDYKDHDIDYKDDDDKGAGA**<u>MDVSKVTTSDGGGDSMETKP</u><u>SPQPQPAAILSSNAPPPFLSKTYDMVDDHNTDSIVSWSANNNSFIVWKPP</u><u>EFARDLLPKNFKHNNFSSFVRQLNTYGFRKVDPDRWEFANEGFLRGQKH</u><u>LLQSITRRKPAHGQGQGHQRSQHSNGQNSSVSACVEVGKFGLEEEVERL</u><u>KRDKNVLMQELVRLRQQQQSTDNQLQTMVQRLQGMENRQQQLMSFLAK</u><u>AVQSPHFLSQFLQQQNQQNESNRRISDTSKKRRFKRDGIVRNNDSATPD</u><u>GQIVKYQPPMHEQAKAMFKQLMKMEPYKTGDDGFLLGNGTSTTEGTEM</u><u>ETSSNQVSGITLKEMPTASEIQSSSPIETTPENVSAASEATENCIPSPDDLTL</u><u>PDFTHMLPENNSEKPPESFMEPNLGGSSPLLDPDLLIDDSLSFDIDDFPMD</u><u>SDIDPVDYGLLERLLMSSPVPDNMDSTPVDNETEQEQNGWDKTKHMDNL</u><u>TQQMGLLSPETLDLSRQNP</u>-
FLAG-HSFA2	**MDYKDHDGDYKDHDIDYKDDDDKGAGA**MEELKVEMEEETVTFTGSVAASSSVGSSSSPRPMEGLNETGPPPFLTKTYEMVEDPATDTVVSWSNGRNSFVVWDSHKFSTTLLPRYFKHSNFSSFIRQLNTYGFRKIDPDRWEFANEGFLAGQKHLLKNIKRRRNMGLQNVNQQGSGMSCVEVGQYGFDGEVERLKRDHGVLVAEVVRLRQQQHSSKSQVAAMEQRLLVTEKRQQQMMTFLAKALNNPNFVQQFAVMSKEKKSLFGLDVGRKRRLTSTPSLGTMEENLLHDQEFDRMKDDMEMLFAAAIDDEANNSMPTKEEQCLEAMNVMMRDGNLEAAALDVKVEDLVGSPLDWDSQDLHDMVDQMGFLGSEP-
FLAG-DBD(A1D)	**MDYKDHDGDYKDHDIDYKDDDDKGAGA**<u>MDVSKVTTSDGGGDSMETKP</u><u>SPQPQPAAILSSNAPPPFLSKTYDMVDDHNTDSIVSWSANNNSFIVWKPP</u><u>EFARDLLPKNFKHNNFSSFVRQLNTYGFRKVDPDRWEFANEGFLRGQKH</u><u>LLQSITRRKP</u>MGLQNVNQQGSGMSCVEVGQYGFDGEVERLKRDHGVLVAEVVRLRQQQHSSKSQVAAMEQRLLVTEKRQQQMMTFLAKALNNPNFVQQFAVMSKEKKSLFGLDVGRKRRLTSTPSLGTMEENLLHDQEFDRMKDDMEMLFAAAIDDEANNSMPTKEEQCLEAMNVMMRDGNLEAAALDVKVEDLVGSPLDWDSQDLHDMVDQMGFLGSEP-
FLAG-OD(A1D)	**MDYKDHDGDYKDHDIDYKDDDDKGAGA**MEELKVEMEEETVTFTGSVAASSSVGSSSSPRPMEGLNETGPPPFLTKTYEMVEDPATDTVVSWSNGRNSFVVWDSHKFSTTLLPRYFKHSNFSSFIRQLNTYGFRKIDPDRWEFANEGFLAGQKHLLKNIKRRRN<u>AHGQGQGHQRSQHSNGQNSSVSACVEVGKFGLE</u><u>EEVERLKRDKNVLMQELVRLRQQQQSTDNQLQTMVQRLQGMENRQQQL</u><u>MSFLAKAVQSPHFLSQFLQQQNQQNESNRRISDTSKKRRFKR</u>PSLGTMEENLLHDQEFDRMKDDMEMLFAAAIDDEANNSMPTKEEQCLEAMNVMMRDGNLEAAALDVKVEDLVGSPLDWDSQDLHDMVDQMGFLGSEP-

FLAG-CTDΔ(A1D)	**MDYKDHDGDYKDHDIDYKDDDDKGAGA**MEELKVEMEEETVTFTGSVAASSSVGSSSSPRPMEGLNETGPPPFLTKTYEMVEDPATDTVVSWSNGRNSFVVWDSHKFSTTLLPRYFKHSNFSSFIRQLNTYGFRKIDPDRWEFANEGFLAGQKHLLKNIKRRRNMGLQNVNQQGSGMSCVEVGQYGFDGEVERLKRDHGVLVAEVVRLRQQQHSSKSQVAAMEQRLLVTEKRQQQMMTFLAKALNNPNFVQQFAVMSKEKKSLFGLDVGRKRRLTST<u>LGGSSPLLDPDLLIDDSLSFDIDDFPMDSDIDPVDYGLLERLLMSSPVPDNMDSTPVDNETEQEQNGWDKTKHMDNLTQQMGLLSPETLDLSRQNP</u>-
FLAG-A2+TDR(A1D)	**MDYKDHDGDYKDHDIDYKDDDDKGAGA**MEELKVEMEEETVTFTGSVAASSSVGSSSSPRPMEGLNETGPPPFLTKTYEMVEDPATDTVVSWSNGRNSFVVWDSHKFSTTLLPRYFKHSNFSSFIRQLNTYGFRKIDPDRWEFANEGFLAGQKHLLKNIKRRRNMGLQNVNQQGSGMSCVEVGQYGFDGEVERLKRDHGVLVAEVVRLRQQQHSSKSQVAAMEQRLLVTEKRQQQMMTFLAKALNNPNFVQQFAVMSKEKKSLFGLDVGRKRRLTST<u>DGIVRNNDSATPDGQIVKYQPPMHEQAKAMFKQLMKMEPYKTGDDGFLLGNGTSTTEGTEMETSSNQVSGITLKEMPTASEIQSSSPIETTPENVSAASEATENCIPSPDDLTLPDFTHMLPENNSEKPPESFMEPNLGGSSPLLDPDLLIDDSLSFDIDDFPMDSP</u>SLGTMEENLLHDQEFDRMKDDMEMLFAAAIDDEANNSMPTKEEQCLEAMNVMMRDGNLEAALDVKVEDLVGSPLDWDSQDLHDMVDQMGFLGSEP-
FLAG-CTD(A1D)	**MDYKDHDGDYKDHDIDYKDDDDKGAGA**MEELKVEMEEETVTFTGSVAASSSVGSSSSPRPMEGLNETGPPPFLTKTYEMVEDPATDTVVSWSNGRNSFVVWDSHKFSTTLLPRYFKHSNFSSFIRQLNTYGFRKIDPDRWEFANEGFLAGQKHLLKNIKRRRNMGLQNVNQQGSGMSCVEVGQYGFDGEVERLKRDHGVLVAEVVRLRQQQHSSKSQVAAMEQRLLVTEKRQQQMMTFLAKALNNPNFVQQFAVMSKEKKSLFGLDVGRKRRLTST<u>DGIVRNNDSATPDGQIVKYQPPMHEQAKAMFKQLMKMEPYKTGDDGFLLGNGTSTTEGTEMETSSNQVSGITLKEMPTASEIQSSSPIETTPENVSAASEATENCIPSPDDLTLPDFTHMLPENNSEKPPESFMEPNLGGSSPLLDPDLLIDDSLSFDIDDFPMDSDIDPVDYGLLERLLMSSPVPDNMDSTPVDNETEQEQNGWDKTKHMDNLTQQMGLLSPETLDLSRQNP</u>-

Table S2: Unique peptide counts of HSF interactors of FLAG-HSFA2 and FLAG-OD(A1D) evaluated by Co-IP/MS. All HSFs of which at least one unique peptide was found in at least one sample are reported. Sample identities are as follows: HSFA2 refers to FLAG-HSFA2 used as bait protein; OD(A1D) refers to FLAG-OD(A1D) used as bait protein (Table S1). Peptide counts of FLAG-HSFA2 in OD(A1D) samples and of FLAG-OD(A1D) in HSFA2 samples were manually set to 0 as the respective other bait protein is not present in those samples. For HSF interactors FLAG-HSFA2, FLAG-OD(A1D), and A1D, peptides that were exclusively located in the regions that were swapped between HSFA2 and HSFA1D to obtain OD(A1D) were excluded from the count.

	HSF interactors											
	FLAG-HSFA2			FLAG-OD(A1D)			A1A			A1B		
	rep 1	rep 2	rep 3	rep 1	rep 2	rep 3	rep 1	rep 2	rep 3	rep 1	rep 2	rep 3
Col_+1h	1	2	0	0	0	0	0	0	0	0	0	0
A2_N	1	1	0	0	0	0	0	0	0	0	0	0
A2_+1h	17	18	17	0	0	0	4	4	6	9	9	13
A2_+4h	27	22	17	0	0	0	8	7	2	14	13	12
OD_N	0	0	0	2	1	2	0	0	0	0	0	0
OD_+1h	0	0	0	8	10	11	2	5	5	6	10	11
OD_+4h	0	0	0	8	7	7	2	2	5	6	5	9

	HSF interactors											
	A1D			A1E			A3			A6B		
	rep 1	rep 2	rep 3	rep 1	rep 2	rep 3	rep 1	rep 2	rep 3	rep 1	rep 2	rep 3
Col_+1h	0	0	0	0	0	0	0	0	0	0	0	0
A2_N	0	0	0	0	0	0	0	0	0	0	0	0
A2_+1h	4	4	6	0	1	1	2	4	3	4	5	5
A2_+4h	6	6	5	2	1	1	10	9	6	4	4	4
OD_N	0	0	0	0	0	0	0	0	0	0	0	0
OD_+1h	1	3	5	0	1	2	1	2	3	1	3	2
OD_+4h	0	1	5	0	0	1	1	2	2	0	1	2

	HSF interactors											
	A7A			A7B			A4A			C1		
	rep 1	rep 2	rep 3	rep 1	rep 2	rep 3	rep 1	rep 2	rep 3	rep 1	rep 2	rep 3
Col_+1h	0	0	0	0	0	0	0	0	0	0	0	0
A2_N	0	0	0	0	0	0	0	0	0	0	0	0
A2_+1h	10	11	9	8	5	10	0	0	0	4	0	1
A2_+4h	12	12	7	12	12	6	0	2	1	3	2	0
OD_N	0	0	0	0	0	0	0	0	0	0	0	0
OD_+1h	4	10	9	0	0	0	0	0	0	0	0	0
OD_+4h	1	1	3	0	0	0	0	0	0	0	0	0

Table S3: Oligonucleotides used in this work

Cloning		
primer	**sequence (5' – 3')**	**product**
2624/pHSFA2-AscI-F	AGGCGCGCCCTGTTTGGTTATCGGGTGAGAGAAAAATTG	*pA2*
2625/pHSFA2-AgeI-R	TACCGGTTTTCGTTGTTTATCTCAAATCCATAAGCTCAG	
3327/AscI-pHSFA1D_F	AAGGCGCGCCTAGTTACGACAAATTTGTATGTGG	*pA1D*
3328/AgeI-pHSFA1D_R	TACCGGTTCGGATTTTTGATTCCAAGTC	
2810/FLAG-HSFA1DF	AACCGGTATGGACTACAAAGACCATGACGGTGATTATAAAGATCATGATATCGATTACAAGGATGACGATGACAAGGGAGCAGGAGCAATGGATGTGAGCAAAGTAACCACAA	*HSFA1D CDS + 3' UTR*
2811/HSFA1D-3rev	TGCGGCCGCATTAGTCTCGGTTTGGTTTTCAGGG	
3268/AgeI-FLAG-gHSFA2-NotI_F	AACCGGTATGGACTACAAAGACCATGACGGTGATTATAAAGATCATGATATCGATTACAAGGATGACGATGACAAGGGAGCAGGAGCAATGGAAGAACTGAAAGTGGAAATGG	*HSFA2 CDS + 3' UTR*
3269/AgeI-FLAG-gHSFA2-NotI_R	TGCGGCCGCATTTCTCTTTCTTATCCTTAAAATCCC	
Genotyping		
primer	**sequence (5' – 3')**	**locus**
2628/HSFA2genoI	AAACCACCCCAGTACATTAAAAACGTCC	*HSFA2*
2629/HSFA2genoforward	AATCTTGGAATGATAAGTAAGGACTCTGCC	
2630/HSFA2geno R	GAACGTCATCATCTGCTGCTGTCTC	
1874/HSFA1A-5	AAGAAGATAAGCCGGAGAAAATCT	*HSFA1A*
1875/HSFA1A-6	ACAAAGTTGCAACCGTACTACTGA	
1876/JL-202_HSFA1A	CATTTTATAATAACGCTGCGGACATCTAC	
1877/HSFA1b-5	CCAGCTTCGTCAGACAGTTAAATA	*HSFa1b*
1878/HSFA1b-6	TAGGAAACTGTCAGGATTGTTTGA	
1879/LB_of *HSFa1b*	GATGCACTCGAAATCAGCCAATTTTAGAC	
1881/HSFA1D-6	AGGTTTTCGCCTAGTTATTGATTG	*HSFA1D*
2044/HSFA1D_newRP	ATGTTGGGCACTATTTGAAGC	
1266/Lba_SALK	TTGGGTGATGGTTCACGTAGTGGG	
RT-qPCR		
primer	**sequence (5' – 3')**	**target**
1547/F-AT4G26410	GAGCTGAAGTGGCTTCAATGAC	*At4g26410*
1548/R-AT4G26410	GGTCCGACATACCCATGATCC	
352/LP-Hsa32	ctgatgcgaagttggttgag	*HSA32*
353/RP_Hsa32	GCACATAACATCAGACACATACGA	

315/Hsa32uspl_F	TATGCTTACTGTGAGAATGCCTTTGT	HSA32 unspliced
653/HSA32-3UTR	Ttcttacagcatcaaagaagca	
633/AT3G09640 REV	ACTCCTTGTCAGCAAACCCGAG	APX2
634/AT3G09640 FOR	CTTGATGATCCTCTCTTTCTCCCA	
634/AT3G09640 FOR	CTTGATGATCCTCTCTTTCTCCCA	APX2 unspliced
2210/APX2_unspliced_R	AGAAGGCATCCTCATCCTGAGAG	
363/AT4G27670_qPCR_F	TGGACGTCTCTCCTTTCGGATTGT	HSP21
364/AT4G27670_qPCR_R	TGCACGAATCTCTGACACTCCACT	
2302/Hsp21_unspliced_transcript_F	TTAATCTAACCACAGGATTGTTGGATC	HSP21 unspliced
364/AT4G27670_qPCR_R	TGCACGAATCTCTGACACTCCACT	
637/AT4G10250 REV	TTCAGGAGATAGTTTCGTGAGGTTA	HSP22
638/AT4G10250 FOR	ATTCTGGAGACAGTTCAAGCTACCT	
267/HSP101F	ATGACCCGGTGTATGGTGCTAG	HSP101
268/HSP101R	CGCCTGCATCTATGTAAACAGTG	
2725/HSP101_unsp_F	CTGACTCTTGTGGTTGCTTTCT	HSP101 unspliced
268/HSP101R	CGCCTGCATCTATGTAAACAGTG	
2938/At2g22240-1f	GTAGCTAGTAATGGCATCCTCTTTGA	MIPS2
2939/At2g22240-1r	ATCCGCAACATATGGCACATAC	
4156/LPAT5-F	AGGGCACAGATTACACAGAGGCTA	LPAT5
4157/LPAT5-R	AAGTGAGCAACTCAGTTCTTGCAAGC	
4150/LACS9-F	CACGAAAGAGCAAGCCGTGAAAG	LACS9
4151/LACS9-R	ATCGTGATTGTTTAGCCGCCTTC	
4154/DGS1-F	GAGCAACCGACGAGTGGGATTTAG	DGS1
4155/DGS1-R	TTTGCTGCTGTGGCCTTCCTAAC	
4158/TPR1-F	ACGACGGATCAAACAAGGAGAAAGC	TPR1
4159/TPR1-R	TATGGATCGAAGCTCTATAGACTCAGG	

ChIP-qPCR

primer	sequence (5' – 3')	amplicon
1857/APX2_Tss-3261_F	GGATATCAAACCCAACTTGAAGAGAG	APX2 -
1858/APX2_Tss-3261_R	ATAATCTGAGCAAAAGATAAAACACGG	
1239/APX2_HRE1_2-F	ACGTGGTGTGTATCTGTTGGA	APX2 TSS -160 bp
1240/APX2_HRE1_2-R	AGTCTTCTTTTGGAGATGGACGGT	
1854/APX2_Tss+40_F	TCGATAGGTTCTCCATTCTCTTTAGG	APX2 TSS + 40 bp
1855/APX2_Tss+40_R	TTCCTCTTGCATCTCTGAACAGC	
1869/APX2_Tss+510_F	CTGTTCCCTATTCTGTCATATGCTG	APX2 TSS + 510 bp
1870/APX2_Tss+510_R	ACCCTTGATTCTATGGTTCTACCTC	
2898/Mips2_negative_F	CATGCAGATCCGTGATAGTATGAAGTA	MIPS2 -
2899/Mips2_negative_R	GGGTTTATTACTTAATTTGTGTAAACATGC	
2904/Mips2_TSS-200_F	TCGGGTGTCTTCGAGTGTGTTC	MIPS2 TSS - 200 bp
2905/Mips2_TSS-200_R	GGACGAGAACCACTAAAAGAGTCG	
2906/Mips2_Tss+130_F	CGAGATCACACACACAACCACC	MIPS2 TSS + 130 bp
2907/Mips2_Tss+130_R	CTGTTGTTTCGTAATCGTACACCG	

5203/LPAT5_ChIP_neg_2_F	tttagcctttctccccgtacg	*LPAT5 -*
5204/LPAT5_ChIP_neg_2_R	ATTGAAACTTGACGAGCTGC	
5189/LPAT5_ChIP_5'_1_F	tacgagaagtggcatagacc	*LPAT5 TSS - 200 bp*
5190/LPAT5_ChIP_5'_1_R	agcttaccatggaactgagc	
2518/HSP101_TSS-3,2kb_F	CTCTCAAAAAGTGTACCTCCA	*HSP101 -*
2519/HSP101_TSS-3,2kb_R	GAGCTCCAAGAAAAGGCCAT	
2671/HSP101_TSS -136_F	ACATCTACCTGTCGGATCAA	*HSP101 TSS - 140 bp*
2672/HSP101_TSS -136_R	TCTGGAAAGATAGAGAACTA	
2675/HSP101_TSS _112_F	TCTGCTTGATTCTCTGCAA	*HSP101 TSS + 110 bp*
2676/HSP101_TSS _112_R	ACACACAAATGAGAACAAGA	

References

Åkerfelt, M., Morimoto, R.I. and Sistonen, L. (2010) Heat shock factors: integrators of cell stress, development and lifespan. *Nature Reviews Molecular Cell Biology*, **11**(8), pp. 545–555. doi:10.1038/nrm2938

Anckar, J. and Sistonen, L. (2011) Regulation of HSF1 Function in the Heat Stress Response: Implications in Aging and Disease. *Annual Review of Biochemistry*, **80**(1), pp. 1089–1115. doi:10.1146/annurev-biochem-060809-095203

Baniwal, S.K. *et al.* (2007) Role of Heat Stress Transcription Factor HsfA5 as Specific Repressor of HsfA4. *Journal of Biological Chemistry*, **282**(6), pp. 3605–3613. doi:10.1074/jbc.M609545200

Bäurle, I. (2018) Can't remember to forget you: Chromatin-based priming of somatic stress responses. *Seminars in Cell & Developmental Biology*, **83**, pp. 133–139. doi:10.1016/j.semcdb.2017.09.032

Bradford, M.M. (1976) A Rapid and Sensitive Method for the Quantitation of Microgram Quantities of Protein Utilizing the Principle of Protein-Dye Binding. *Analytical Biochemistry*, **72**, pp. 248-254. doi: 10.1006/abio.1976.9999

Brzezinka, K. *et al.* (2016) Arabidopsis FORGETTER1 mediates stress-induced chromatin memory through nucleosome remodeling. *eLife*, **5**, e17061. doi:10.7554/eLife.17061

Brzezinka, K., Altmann, S. and Bäurle, I. (2019) BRUSHY1/TONSOKU/MGOUN3 is required for heat stress memory. *Plant, Cell & Environment*, **42**(3), pp. 771–781. doi:10.1111/pce.13365

Chakrabortee, S. *et al.* (2016) Luminidependens (LD) is an Arabidopsis protein with prion behavior. *Proceedings of the National Academy of Sciences*, **113**(21), pp. 6065–6070. doi:10.1073/pnas.1604478113

Charng, Y. *et al.* (2006) Arabidopsis Hsa32, a Novel Heat Shock Protein, Is Essential for Acquired Thermotolerance during Long Recovery after Acclimation. *Plant Physiology*, **140**(4), pp. 1297–1305. doi:10.1104/pp.105.074898

Charng, Y. *et al.* (2007) A Heat-Inducible Transcription Factor, HsfA2, Is Required for Extension of Acquired Thermotolerance in Arabidopsis. *Plant Physiology*, **143**(1), pp. 251–262. doi:10.1104/pp.106.091322

Clough, S.J. and Bent, A.F. (1998) Floral dip: a simplified method for Agrobacterium-mediated transformation of Arabidopsis thaliana. *The Plant Journal*, **16**(6), pp. 735–743. doi:10.1046/j.1365-313x.1998.00343.x

Czechowski, T. *et al.* (2005) Genome-Wide Identification and Testing of Superior Reference Genes for Transcript Normalization in Arabidopsis. *Plant Physiology*, **139**(1), pp. 5–17. doi:10.1104/pp.105.063743

Ding, Y., Fromm, M. and Avramova, Z. (2012) Multiple exposures to drought "train" transcriptional responses in Arabidopsis. *Nature Communications*, **3**(1), 740. doi:10.1038/ncomms1732

Döring, P. *et al.* (2000) The Role of AHA Motifs in the Activator Function of Tomato Heat Stress Transcription Factors HsfA1 and HsfA2. *The Plant Ce*ll, **12**(2), pp. 265-278. PMID: 10662862; PMCID: PMC139763

Duret, L., Gasteiger, E. and Perrièe, G. (1996) LALNVIEW: a graphical viewer for pairwise sequence alignments. *Bioinformatics*, **12**(6), pp. 507–510. doi:10.1093/bioinformatics/12.6.507

Feng, N. *et al.* (2021) Structures of heat shock factor trimers bound to DNA. *iScience*, **24**(9), 102951. doi:10.1016/j.isci.2021.102951

Feng, X.J. *et al.* (2016) Light affects salt stress-induced transcriptional memory of P5CS1 in Arabidopsis. *Proceedings of the National Academy of Sciences*, **113**(51). doi:10.1073/pnas.1610670114

Friedrich, T. *et al.* (2021) Heteromeric HSFA2/HSFA3 complexes drive transcriptional memory after heat stress in Arabidopsis. *Nature Communications*, **12**(1), 3426. doi:10.1038/s41467-021-23786-6

Garai, S. *et al.* (2021) Complex Networks of Prion-Like Proteins Reveal Cross Talk Between Stress and Memory Pathways in Plants. *Frontiers in Plant Science*, **12**, 707286. doi:10.3389/fpls.2021.707286

Hilker, M. *et al.* (2016) Priming and memory of stress responses in organisms lacking a nervous system: Priming and memory of stress responses. *Biological Reviews*, **91**(4), pp. 1118–1133. doi:10.1111/brv.12215

Ikeda, M., Mitsuda, N. and Ohme-Takagi, M. (2011) Arabidopsis HsfB1 and HsfB2b Act as Repressors of the Expression of Heat-Inducible Hsfs But Positively Regulate the Acquired Thermotolerance. *Plant Physiology*, **157**(3), pp. 1243–1254. doi:10.1104/pp.111.179036

Iwata, Y. and Koizumi, N. (2005) An Arabidopsis transcription factor, AtbZIP60, regulates the endoplasmic reticulum stress response in a manner unique to plants. *Proceedings of the National Academy of Sciences*, **102**(14), pp. 5280–5285. doi:10.1073/pnas.0408941102

Jaskiewicz, M., Conrath, U. and Peterhänsel, C. (2011) Chromatin modification acts as a memory for systemic acquired resistance in the plant stress response. *EMBO Reports*, **12**(1), pp. 50–55. doi:10.1038/embor.2010.186

Jiang, D. *et al.* (2011) Arabidopsis COMPASS-Like Complexes Mediate Histone H3 Lysine-4 Trimethylation to Control Floral Transition and Plant Development. *PLoS Genetics*, **7**(3), e1001330. doi:10.1371/journal.pgen.1001330

Jung, J.-H. *et al.* (2020) A prion-like domain in ELF3 functions as a thermosensor in Arabidopsis. *Nature*, **585**(7824), pp. 256–260. doi:10.1038/s41586-020-2644-7

Kaufmann, K. *et al.* (2010) Chromatin immunoprecipitation (ChIP) of plant transcription factors followed by sequencing (ChIP-SEQ) or hybridization to whole genome arrays (ChIP-CHIP). *Nature Protocols*, **5**(3), pp. 457–472. doi:10.1038/nprot.2009.244

Kelley, L.A. *et al.* (2015) The Phyre2 web portal for protein modeling, prediction and analysis. *Nature Protocols*, **10**(6), pp. 845–858. doi:10.1038/nprot.2015.053

Kim, J.-M. *et al.* (2012) Transition of Chromatin Status During the Process of Recovery from Drought Stress in Arabidopsis thaliana. *Plant and Cell Physiology*, **53**(5), pp. 847–856. doi:10.1093/pcp/pcs053

Kumar, M. *et al.* (2009) Heat Shock Factors HsfB1 and HsfB2b Are Involved in the Regulation of Pdf1.2 Expression and Pathogen Resistance in Arabidopsis. *Molecular Plant*, **2**(1), pp. 152–165. doi:10.1093/mp/ssn095

Lämke, J. *et al.* (2016) A hit-and-run heat shock factor governs sustained histone methylation and transcriptional stress memory. *The EMBO Journal*, **35**(2), pp. 162–175. doi:10.15252/embj.201592593

Lämke, J. and Bäurle, I. (2017) Epigenetic and chromatin-based mechanisms in environmental stress adaptation and stress memory in plants. *Genome Biology*, **18**(1), 124. doi:10.1186/s13059-017-1263-6

Lancaster, A.K. *et al.* (2014) PLAAC: a web and command-line application to identify proteins with prion-like amino acid composition. *Bioinformatics*, **30**(17), pp. 2501–2502. doi:10.1093/bioinformatics/btu310

Lichtenthaler, H.K. (1998) The Stress Concept in Plants: An Introduction. Annals of the New York Academy of Sciences, **851**(1), pp. 187–198. doi:10.1111/j.1749-6632.1998.tb08993.x

Liu, H. *et al.* (2018) Distinct heat shock factors and chromatin modifications mediate the organ-autonomous transcriptional memory of heat stress. *The Plant Journal*, **95**(3), pp. 401–413. doi:10.1111/tpj.13958

Liu, H.-C., Liao, H.-T. and Charng, Y.-Y. (2011) The role of class A1 heat shock factors (HSFA1s) in response to heat and other stresses in Arabidopsis. *Plant, Cell & Environment*, **34**(5), pp. 738–751. doi:10.1111/j.1365-3040.2011.02278.x

Liu, J.-X. *et al.* (2007) An Endoplasmic Reticulum Stress Response in Arabidopsis Is Mediated by Proteolytic Processing and Nuclear Relocation of a Membrane-Associated Transcription Factor, bZIP28. *The Plant Cell*, **19**(12), pp. 4111–4119. doi:10.1105/tpc.106.050021

Lohmann, C. *et al.* (2004) Two different heat shock transcription factors regulate immediate early expression of stress genes in Arabidopsis. *Molecular Genetics and Genomics*, **271**(1), pp. 11–21. doi:10.1007/s00438-003-0954-8

Mauch-Mani, B. *et al.* (2017) Defense Priming: An Adaptive Part of Induced Resistance. *Annual Review of Plant Biology*, **68**(1), pp. 485–512. doi:10.1146/annurev-arplant-042916-041132

Meiri, D. and Breiman, A. (2009) Arabidopsis ROF1 (FKBP62) modulates thermotolerance by interacting with HSP90.1 and affecting the accumulation of HsfA2-regulated sHSPs. *The Plant Journal*, **59**(3), pp. 387–399. doi:10.1111/j.1365-313X.2009.03878.x

Mittler, R., Finka, A. and Goloubinoff, P. (2012) How do plants feel the heat?. *Trends in Biochemical Sciences*, **37**(3), pp. 118–125. doi:10.1016/j.tibs.2011.11.007

Neudegger, T. *et al.* (2016) Structure of human heat-shock transcription factor 1 in complex with DNA. *Nature Structural & Molecular Biology*, **23**(2), pp. 140–146. doi:10.1038/nsmb.3149

Nishizawa-Yokoi, A. *et al.* (2011) HsfA1d and HsfA1e Involved in the Transcriptional Regulation of HsfA2 Function as Key Regulators for the Hsf Signaling Network in Response to Environmental Stress. *Plant and Cell Physiology*, **52**(5), pp. 933–945. doi:10.1093/pcp/pcr045

Nover, L., Bharti, K. and Scharf, K.-D. (2001) Arabidopsis and the heat stress transcription factor world: how many heat stress transcription factors do we need?. *Cell Stress Chaperones*, **6**(3), pp. 177-189. doi: 10.1379/1466-1268(2001)006<0177:aathst>2.0.co;2

Oberkofler, V. and Bäurle, I. (2022) Inducible epigenome editing probes for the role of histone H3K4 methylation in Arabidopsis heat stress memory. *Plant Physiology*, kiac113. doi:10.1093/plphys/kiac113

Ohama, N. *et al.* (2016) The Transcriptional Cascade in the Heat Stress Response of Arabidopsis Is Strictly Regulated at the Level of Transcription Factor Expression. *The Plant Cell*, **28**(1), pp. 181–201. doi:10.1105/tpc.15.00435

Ohama, N. *et al.* (2017) Transcriptional Regulatory Network of Plant Heat Stress Response. *Trends in Plant Science*, **22**(1), pp. 53–65. doi:10.1016/j.tplants.2016.08.015

Peteranderl, R. *et al.* (1999) Biochemical and Biophysical Characterization of the Trimerization Domain from the Heat Shock Transcription Factor. *Biochemistry*, **38**(12), pp. 3559–3569. doi:10.1021/bi981774j

Peteranderl, R. and Nelson, H.C.M. (1992) Trimerization of the heat shock transcription factor by a triple-stranded alpha-helical coiled-coil. *Biochemistry*, **31**(48), pp. 12272–12276. doi:10.1021/bi00163a042

Qu, A.-L. *et al.* (2013) Molecular mechanisms of the plant heat stress response. *Biochemical and Biophysical Research Communications*, **432**(2), pp. 203–207. doi:10.1016/j.bbrc.2013.01.104

Richter, K., Haslbeck, M. and Buchner, J. (2010) The Heat Shock Response: Life on the Verge of Death. *Molecular Cell*, **40**(2), pp. 253–266. doi:10.1016/j.molcel.2010.10.006

Sani, E. *et al.* (2013) Hyperosmotic priming of Arabidopsis seedlings establishes a long-term somatic memory accompanied by specific changes of the epigenome. *Genome Biology*, **14**(6), R59. doi:10.1186/gb-2013-14-6-r59

Scharf, K.-D. *et al.* (2012) The plant heat stress transcription factor (Hsf) family: Structure, function and evolution. *Biochimica et Biophysica Acta*, **1819**(2), pp. 104–119. doi:10.1016/j.bbagrm.2011.10.002

Schmittgen, T.D. and Livak, K.J. (2008) Analyzing real-time PCR data by the comparative CT method. *Nature Protocols*, **3**(6), pp. 1101–1108. doi:10.1038/nprot.2008.73

Schramm, F. *et al.* (2007) A cascade of transcription factor DREB2A and heat stress transcription factor HsfA3 regulates the heat stress response of Arabidopsis: Role of Arabidopsis HsfA3. *The Plant Journal*, **53**(2), pp. 264–274. doi:10.1111/j.1365-313X.2007.03334.x

Smaczniak, C. *et al.* (2012) Proteomics-based identification of low-abundance signaling and regulatory protein complexes in native plant tissues. *Nature Protocols*, **7**(12), pp. 2144–2158. doi:10.1038/nprot.2012.129

Song, Z.-T. *et al.* (2015) Transcription factor interaction with COMPASS-like complex regulates histone H3K4 trimethylation for specific gene expression in plants. *Proceedings of the National Academy of Sciences*, **112**(9), pp. 2900–2905. doi:10.1073/pnas.1419703112

Stief, A. *et al.* (2014) Arabidopsis miR156 Regulates Tolerance to Recurring Environmental Stress through SPL Transcription Factors. *The Plant Cell*, **26**(4), pp. 1792–1807. doi:10.1105/tpc.114.123851

Swindell, W.R., Huebner, M. and Weber, A.P. (2007) Transcriptional profiling of Arabidopsis heat shock proteins and transcription factors reveals extensive overlap between heat and non-heat stress response pathways. *BMC Genomics*, **8**(1), p. 125. doi:10.1186/1471-2164-8-125

Urrea Castellanos, R. *et al.* (2020) FORGETTER2 protein phosphatase and phospholipase D modulate heat stress memory in Arabidopsis. *The Plant Journal*, **104**(1), pp. 7–17. doi:10.1111/tpj.14927

Wang, X. *et al.* (2018) Evolutionary Origin, Gradual Accumulation and Functional Divergence of Heat Shock Factor Gene Family with Plant Evolution. *Frontiers in Plant Science*, **9**, 71. doi:10.3389/fpls.2018.00071

Wiśniewski, J.R. (2018) Filter-Aided Sample Preparation for Proteome Analysis. In Becher, D. (ed.) Microbial Proteomics. New York, NY: Springer New York (Methods in Molecular Biology), pp. 3–10. doi:10.1007/978-1-4939-8695-8_1

Wu, C. (1995) Heat Shock Transcription Factors: Structure and Regulation. *Annual Review of Cell and Developmental Biology*, **11**, pp. 441-469. doi: 10.1146/annurev.cb.11.110195.002301

Yeh, C.-H. *et al.* (2012) Some like it hot, some like it warm: Phenotyping to explore thermotolerance diversity. *Plant Science*, **195**, pp. 10–23. doi:10.1016/j.plantsci.2012.06.004

Yoshida, T. *et al.* (2008) Functional analysis of an Arabidopsis heat-shock transcription factor HsfA3 in the transcriptional cascade downstream of the DREB2A stress-regulatory system. *Biochemical and Biophysical Research Communications*, **368**(3), pp. 515–521. doi:10.1016/j.bbrc.2008.01.134

Yoshida, T. *et al.* (2011) Arabidopsis HsfA1 transcription factors function as the main positive regulators in heat shock-responsive gene expression. *Molecular Genetics and Genomics*, **286**(5–6), pp. 321–332. doi:10.1007/s00438-011-0647-7

Zang, D. *et al.* (2019) Arabidopsis heat shock transcription factor HSFA7b positively mediates salt stress tolerance by binding to an E-box-like motif to regulate gene expression. *Journal of Experimental Botany*, **70**(19), pp. 5355–5374. doi:10.1093/jxb/erz261

General Discussion

Maintenance of acquired thermotolerance or HS memory in *Arabidopsis* is one of the best studied examples of how organisms prime their response to recurring stress events. The identification of several novel components and factors specifically involved in HS memory in recent years suggests that HS memory is a complex process that involves multiple cellular pathways ranging from the epigenetic to the metabolic level (reviewed in Friedrich *et al.*, 2019; Oberkofler, Pratx and Bäurle, 2021; Balazadeh, 2022).

The contribution of transcriptional memory to HS memory is well studied and several specific regulators, which include TFs and chromatin remodelers, have been identified and characterized. TFs HSFA2 and HSFA3 directly promote transcriptional memory and sustained H3K4 hyper-methylation (Charng *et al.*, 2007; Lämke *et al.*, 2016; H. Liu *et al.*, 2018, **Man. 1**). Chromatin remodeler FGT1 promotes low nucleosome occupancy and therefore an open chromatin structure at memory genes (Brzezinka *et al.*, 2016). BRU1 also contributes to sustained induction of memory genes after HS (Brzezinka, Altmann and Bäurle, 2019), although its mechanism of action remains unclear. The mammalian orthologue of BRU1 is involved in DNA replication (Saredi *et al.*, 2016) and in *Arabidopsis*, BRU1 was shown to be involved in DNA damage repair and gene silencing (Takeda *et al.*, 2004). It is tempting to speculate that BRU1 may contribute to maintaining the open and hyper-methylated chromatin state of memory genes throughout cell division events. Maintenance of specific chromatin features associated with transcriptional memory across several mitotic divisions has been reported in yeast (Brickner *et al.*, 2007; Kundu, Horn and Peterson, 2007) and human cell cultures (Boehm *et al.*, 1997; Gialitakis *et al.*, 2010; Light *et al.*, 2013).

In addition to transcriptional regulation of HS memory, the levels of some HS memory factors are regulated by protein stabilization and degradation. For example, HSFA2 stability is controlled by HSP90 and ROF1, and the formation of these HSF-chaperone complexes guarantees long-lasting expression of *HSP* genes (Meiri and Breiman, 2009). The gene product of type I memory gene *HSP21* is negatively regulated by the metalloprotease FTSH6 (Sedaghatmehr, Mueller-Roeber and Balazadeh, 2016) as well as by autophagy (Sedaghatmehr *et al.*, 2021).

Protein phosphatase PP2C and its interactor phospholipase PLDα2 are positive regulators of HS memory (Urrea Castellanos *et al.*, 2020). The PP2C-PLDα2 module

may represent a link between post-translational regulation of protein activity and lipid metabolism. Additionally, carbohydrate metabolism has also been implicated in HS memory in two recent publications (Sharma *et al.*, 2019; Olas *et al.*, 2021). Both works show that high sugar levels are required for memory gene expression. This may be linked to maintenance of high H3K4me3 levels at memory genes promoted by HIKESHI-LIKE PROTEIN 1 (HLP1) (Sharma *et al.*, 2019).

My work has yielded new insights on the transcriptional regulation of HS memory. In this section, I discuss the key findings of the three presented manuscripts in a comprehensive manner by outlining the principal emerging questions and suggesting possible experimental approaches to address them.

How many memory HSFs are there and how do they interact functionally?

This work has contributed to the functional characterization of a second *Arabidopsis* HSF with a specific function in HS memory, HSFA3 (**Man. 1**). Although the *hsfa2,3* double mutant is severely defective in physiological HS memory assays compared to wild type seedlings, HS memory is not completely abolished as evidenced by the fact that after priming, *hsfa2,3* seedlings still partially survive severe HS of 44 °C of up to 80 min length (**Man. 1 Fig 3d**), which exceeds their basal thermotolerance (**Man. 1 Fig S4**). This indicates that there likely exist additional positive regulators of HS memory that act independently of HSFA2/HSFA3, and some of these factors could be HSFs. RNA-seq analysis of Col-0, *hsfa2*, *hsfa3*, and *hsfa2,3* seedlings revealed the existence of 156 type I transcriptional memory genes in Col-0 that are significantly upregulated for at least 52 h after ACC compared to non-HS baseline expression levels (**Man. 1 Fig 6**). While HSFA2 and HSFA3 are important for their sustained induction especially at later time points, the expression of 25.6 % of these genes remains unaffected 52 h after ACC in *hsfa2,3*. This supports the hypothesis of the existence of other positive transcriptional regulators, and argues against residual activity of truncated HSFA2/HSFA3 proteins. *HSFA2* and *HSFA3* are both induced by HS (**Man. 1 Fig 3a-b**), additional memory HSFs may share this characteristic. Early genome-wide transcriptional analyses have identified several additional HS-inducible HSFs, among which *HSFB1*, *HSFB2A*, *HSFB2B*, *HSFA7A*, and *HSFA7B* (Schramm *et al.*, 2007; Swindell, Huebner and Weber, 2007). The reported

data are less consistent for *HSFA8*, which may be induced in the recovery phase after HS (Schramm *et al.*, 2007), and for *HSFA1E* and *HSFA6B*, which may peak in their expression during HS (Swindell, Huebner and Weber, 2007). Our RNA-seq dataset shows HS-induced expression of *HSFA7A*, *HSFA7B*, *HSFA1E*, and *HSFA6B* 4 h after ACC (**Man. 1 Dataset S1**). Indeed, HSFA6B, HSFA7A, and HSFA7B were also identified as interaction partners of HSFA2 (**Man. 1 Fig 7e**, **Man. 3 Fig 7b**) and may therefore contribute to the formation of HSFA2- and/or HSFA3-containing memory HSF complexes. Interestingly, while HSFA6B and HSFA7A were also co-immunoprecipitated with HSFA3 and the chimeric OD(A1D) HSF in which the OD of HSFA1D substitutes its HSFA2 counterpart (**Man. 3 Fig 1d**), HSFA7B was neither pulled down by HSFA3 (**Man. 1 Fig 7d, Table S3**) or OD(A1D) (**Man. 3 Fig 7b**). Further experiments such as *in vitro* pull-down or bimolecular fluorescence complementation (BiFC) assays are needed to investigate whether the ODs of HSFA2 and HSFA7B specifically interact. One example of specific and exclusive interaction between *Arabidopsis* HSFs was reported for HSFA4 and HSFA5 (Baniwal *et al.*, 2007). This specificity is mediated by the OD of these HSFs but no causative amino acid residues were identified (Baniwal *et al.*, 2007). It was hypothesized that the formation of HSFA4/A5 heterooligomers leads to repression of HSFA4 transcriptional activity (Baniwal *et al.*, 2007). HSFA7B has been characterized as a positive regulator of salinity stress tolerance and, secondarily, as a potential positive regulator of thermotolerance (Zang *et al.*, 2019). Interestingly, ChIP-seq analysis of the genomic targets of HSFA7B revealed that it not only binds HSEs, but also other types of sequence motifs, among which a series of novel E-box-like motifs (Zang *et al.*, 2019). Induction of *HSFA3* is mediated by DREB2A, which is activated by HSFA1s and induced by drought and salinity stress (Sakuma *et al.*, 2006; Schramm *et al.*, 2007; Yoshida *et al.*, 2008), representing a possible node of cross-talk between responses to different abiotic stresses. Similarly, it would be interesting to uncover the salinity stress regulatory network of *HSFA7B*, potential overlaps with its HSR regulatory network, and whether it is a regulator of HS memory.

Related to the interaction network between HSFs is the question of whether there is any specificity at the level of DNA sequence for the target genes of memory HSFs. It is possible that memory HSF complexes target different DNA sequences based on the presence of individual HSFs in the complex that confer a certain degree of sequence specificity, e.g., presence of HSFA7B may favor binding of E-box-like motifs. Interestingly, ChIP-seq analysis has revealed that HSFA1B binds genes that contain

HSEs, MADS box, LEAFY, and G-Box promoter motifs (Albihlal *et al.*, 2018). Additionally, another open question is if memory genes have common *cis*-regulatory sequence elements which contribute to establishing transcriptional memory and distinguish them from HS-inducible non-memory genes. To begin to address these questions, we identified in **Man. 1** the target genes of HSFA2 and HSFA3 by RNA-seq in a genome-wide manner and found that they are largely overlapping (**Man. 1 Fig 6**), arguing that at least HSFA2/HSFA3 predominantly function in the context of heterooligomeric complexes. To begin asking whether transcriptional regulation by HSFA2/HSFA3 is mediated by their direct binding to target genes on the genome-wide level, and whether direct binding of HSFA2/HSFA3 is favored by specific sequence composition, spacing, and/or arrangement of HSEs in the memory target gene promoters or other sequence features, we have prepared a ChIP-seq dataset that is currently being evaluated. In this experiment, we immunoprecipitated FLAG-HSFA2 and FLAG-HSFA3 from the *pA2::FLAG-HSFA2* in *hsfa2* and *pA3::FLAG-HSFA3* in *hsfa3* complementation lines generated for **Man. 1** at 4 h, 28 h, and 52 h after ACC. The integration of the previously obtained RNA-seq dataset (**Man. 1**), the FLAG-HSFA2 and FLAG-HSFA3 ChIP-seq dataset, and published ChIP-seq datasets that investigated genome-wide H3K4me3 enrichment before (Liu *et al.*, 2020) and 3 d after HS (Yamaguchi *et al.*, 2021), respectively, will hopefully allow us to investigate the above-mentioned questions and to screen for distinct memory-specific chromatin environments before and after HS.

What is the contribution of H3K4 hyper-methylation to transcriptional memory?

H3K4 hyper-methylation is one of the most commonly reported features of transcriptional memory across different organisms and in response to different stressors (Jaskiewicz, Conrath and Peterhänsel, 2011; Ding, Fromm and Avramova, 2012; Kim *et al.*, 2012; Light *et al.*, 2013; D'Urso *et al.*, 2016; Feng *et al.*, 2016; Lämke *et al.*, 2016; H. Liu *et al.*, 2018; Yamaguchi *et al.*, 2021, **Man. 1**). However, attributing causality is experimentally challenging as this would ideally require to interfere exclusively with a specific type of hyper-methylation (di- or trimethylation), at a specific locus, and specifically in the memory phase. Often, HKMT and HKDM enzymes lack specificity regarding their substrate and their target loci (Cheng *et al.*, 2019; Ueda and Seki, 2020), which complicates approaches aimed at generating mutants of one or more HKMT/HKDM

enzymes or pharmacological inhibition of H3K4 (de)methylation. In fact, the identity of the HKMT enzyme(s) driving H3K4 hyper-methylation after HS in *Arabidopsis* remains elusive. Initially, I contributed to the generation and characterization of single and higher-order mutants of HKMT and HKDM enzymes, which were investigated for altered phenotypes in physiological HS memory compared to wild type plants. It gradually became clear that there was likely an elevated degree of genetic redundancy between these enzymes, as even the most promising (combinations of) mutants showed weak and/or unspecific phenotypes (**Table S1**). One possible limit to our approach was that we focused on creating higher-order mutants within the same enzyme families. It was for example recently shown that ATX1 and SDG25, which belong to different HKMT families, contribute to H3K4 hyper-methylation of several target genes in response to chronic HS, and, importantly, that the double mutants are much more severely negatively affected by HS than either single mutant (Song *et al.*, 2020), implying cross-family redundancy of these HKMTs. Similarly, the *jmj11/12/30/32* HKDM quadruple mutant was more severely affected by HS after acclimatizing treatment than either of the respective single mutants or the *jmj30/32* double mutant (Yamaguchi *et al.*, 2021).

In parallel to the HKMT/HKDM mutant screen, I developed a dCas9-based, targeted approach aimed at interfering with H3K4 hyper-methylation in a locus-specific manner at the memory gene *APX2* (**Man. 2, Fig 1**). In this setup, dCas9 was translationally fused to either the active, or presumably inactive, catalytic JmjC domain of JMJ18 ((d)JMJ). The dCas9-(d)JMJ protein was expressed under control of the HS-inducible *HSP21* promoter in order to avoid targeting of the fusion protein to the locus of interest in absence of HS. Targeting to the *APX2* promoter was achieved by co-expression, under a suitable constitutive promoter, of sequence-specific sgRNAs. In order to verify the efficiency of different combinations of sgRNAs, I developed a transient co-expression assay in *Nicotiana benthamiana* leaves. Here, dCas9 translationally fused to the transcriptional activator VP64 was co-expressed with the sgRNAs that needed to be tested, as well as with a *pAPX2::LUC* reporter construct (**Man. 2, Fig 1**). In order to observe increased luciferase activity, two conditions must be fulfilled: first, sgRNAs must target dCas9-VP64 to *pAPX2*; second, dCas9-VP64 must be targeted close enough to the transcriptional start site to be able to mediate transcriptional activity. Of the two sgRNA combinations that I tested, only the more TSS-proximal sgRNAs could mediate increased LUC activity (**Man. 2 Fig 2**), indicating that both necessary conditions were fulfilled. The

corresponding sgRNAs were located up to -206 bp from the TSS (**Man. 2 Table 1**). The second set of sgRNAs was located between -238 and -387 bp from the TSS and did not mediate increased LUC activity (**Man. 2 Fig 2**), but it is not known whether this is due to lack of sgRNA targeting efficiency, or because the distance of correctly targeted dCas9-VP64 to the TSS is too big. This is an important consideration for the future use of this transient system, as it limits the range of promoter regions to be investigated for sgRNA binding efficiency, and possibly also the range at which sgRNAs can be targeted to investigate functional effects.

I could show that dCas9-(d)JMJ proteins bind to the *APX2* promoter after HS with a binding peak that corresponds to the localization of the sgRNA binding sequences (**Man. 2 Fig 5**), and that this correlates with reduced type II transcriptional memory of *APX2* (**Man. 2 Fig 3**-**4**) as well as with reduced levels of H3K4 hyper-methylation at the locus (**Man. 2 Fig 6**), and that these effects were overall stronger with JMJ than with dJMJ. Residual activity of dJMJ could be explained by a scaffolding function through which it interacts with, and recruits, catalytically active JMJs to the locus, or by steric interference of the dCas9-dJMJ fusion protein with recruitment of general and/or specific transcriptional regulators. In conclusion, this work confirms the previously observed tight connection between transcriptional memory in response to HS and H3K4 hyper-methylation (Lämke *et al.*, 2016; H. Liu *et al.*, 2018, **Man. 1**) although it does not provide a definitive answer on the importance of H3K4 hyper-methylation for transcriptional memory of the *APX2* locus. Additionally, it presents a general framework on how to investigate functionality of chromatin modifications in a locus-specific manner. This could be applied to other HS memory genes, other stresses, and also to developmental genes which show distinct chromatin profiles over time, e.g. the role of H3K27me3 at flowering time regulating genes (Kinoshita and Richter, 2020). Future experiments that address these questions need to be carefully designed and several controls should be included, including catalytically inactive versions of the chromatin modifying enzyme and, ideally, also an unrelated enzyme of comparable molecular weight to investigate steric hindrance. Fluorescent marker proteins might be suitable, as they provide the additional benefit of easy monitoring of their expression (pattern).

How is H3K4 hyper-methylation established at memory genes?

The observation that H3K4 hyper-methylation is established and sustained at memory genes raises several questions regarding the underlying molecular mechanisms. Importantly, it is not yet clear which percentage of type I or type II HS memory genes is subjected to H3K4 hyper-methylation, as previous analyses have focused on H3K4me3/2 ChIP-qPCR assays targeted at individual candidate loci (Lämke *et al.*, 2016; H. Liu *et al.*, 2018). For type I transcriptional memory, the RNA-seq dataset generated for **Man. 1**, combined with publically available data sets on H3K4 trimethylation (Liu *et al.*, 2020; Yamaguchi *et al.*, 2021), will hopefully provide answers to this question. Additionally, if this analysis reveals that only a certain subset of memory genes is characterized by sustained H3K4 hyper-methylation in the memory phase, it would be interesting to look for the underlying causes. These memory genes may have distinct *cis*-elements in their promoters, or could be characterized by particular chromatin environments before and/or after HS, which may favor recruitment of the COMPASS-like complex which then catalyzes H3K4 methylation. How specificity of the interplay between sequence-specific chromatin components, such as TFs, basal transcriptional machinery, and/or COMPASS-like complex subunits is achieved, is an open, interesting, and complex question. An interesting case study of transcriptional memory requiring complex interactions between cis-specific sequence elements and several conserved protein complexes, is that of the yeast *INOSITOL-1-PHOSPHATE SYNTHASE* (*INO1*) gene. *INO1* is induced by inositol starvation; *INO1* transcriptional memory refers to its repression after the end of these unfavorable conditions and its distinct localization at the nuclear membrane, where it remains primed for reactivation (Light et al., 2010). *INO1* transcriptional memory is mediated by a cis-located sequence motif in its promoter, which is bound by SUPPRESSOR GENE FOR FLOCCULATION 1 (SFL1) (Light *et al.*, 2010; D'Urso *et al.*, 2016). SFL1 promotes targeting of *INO1* to the nuclear membrane (D'Urso *et al.*, 2016) which depends on specific subunits of the nuclear pore complex (NPC) (Light *et al.*, 2010). Additionally, primed *INO1* is characterized by incorporated H2A.Z (Light *et al.*, 2010) and requires H3K4me2 (Light *et al.*, 2013), which is maintained by a COMPASS-like complex with specific composition, i.e. lacking SUBUNIT OF COMPASS (SET1C), PHD FINGER PROTEIN (SPP1) (D'Urso *et al.*, 2016). In Arabidopsis, one example of direct interaction between sequence specific TFs and components of the COMPASS-like complex is that of bZIP28 and bZIP60 which interact with two subunits of the COMPASS-like complex, ASH2R and WDR5A (Song *et al.*, 2015). In HS memory, several empirical observations argue that there is some

degree of redundancy regarding (direct or indirect) interactions between HSFs and the COMPASS-like complex. First, HSFA2 and HSFA3 redundantly mediate sustained H3K4 trimethylation 28 h and 52 h after ACC at memory genes *HSP22* and *APX2*. While *hsfa2* and *hsfa3* single mutants show lower levels of H3K4me3 at these genes, only the double mutant completely lacks ability to mediate H3K4me3 enrichment (**Man. 1 Fig 9**). Second, the chimeric HSF CTDΔ(A1D) (**Man. 3 Fig 1e**), in which the C-terminal region of HSFA2 is replaced with that of HSFA1D, restores sustained H3K4me3 accumulation at *APX2* for at least 2 d after mild priming HS (1 h 37 °C) to wild type levels in the *hsfa2* background (**Man. 3 Fig 5d**). Loss of H3K4 hyper-methylation during the memory phase correlates therefore with overall abundance of (HS-inducible) HSFs. To test whether some HSFs are intrinsically more efficient than others in recruiting H3K4 hyper-methylation, it would be interesting to use the *hsfa2,3* double mutant background as starting point to express different combinations of two *HSFs* under the *HSFA2* and the *HSFA3* promoter, respectively. For example, it would be interesting to check if two copies of HSFA2 promote higher levels of H3K4 hyper-methylation than observed in the wild type background where one copy of HSFA2 and one copy of HSFA3 are present. Similarly, both HSFA2 and HSFA3 could be replaced by two copies of CTDΔ(A1D), to see whether both C-terminal domains are replaceable. These experiments could be extended to other members of the HSF family, especially those that are likely candidates to be additional memory HSFs. However, these experiments have to take into account that some HSFs may differ at the protein level from HSFA2/HSFA3 in their activity and/or their stability over the memory phase (**Man. 3**).

Our failure to identify strong and/or HS memory-specific phenotypes of single and multiple *hkmt* mutants (**Table S1**) argues either for elevated genetic redundancy or against a major contribution of H3K4 hyper-methylation to mediating transcriptional memory.

Which molecular mechanisms contribute to type I and type II transcriptional memory and to which degree do they overlap?

On the level of transcription, HS memory is associated with type I and type II transcriptional memory (reviewed in Lämke and Bäurle, 2017; Bäurle, 2018). Type II transcriptional memory is a conserved feature of plant priming in response to other stresses than HS (Jaskiewicz, Conrath and Peterhänsel, 2011; Ding, Fromm and

Avramova, 2012; Sani *et al.*, 2013; Ding *et al.*, 2014; Feng *et al.*, 2016). It has also been reported in other model systems, namely in yeast, where *INO1* and *GALACTOKINASE 1* (*GAL1*) show faster transcriptional re-activation after a period in which their expression was repressed (Brickner *et al.*, 2007; Kundu, Horn and Peterson, 2007), and in human cell cultures, where previous exposure to interferon gamma (IFN-γ) mediates faster and stronger re-induction of IFN-γ-inducible genes upon repeat exposure (Boehm *et al.*, 1997; Gialitakis *et al.*, 2010; Light *et al.*, 2013). To the best of my knowledge, type I transcriptional memory has so far only been observed in response to HS. This work has identified type I transcriptional memory genes of *Arabidopsis* on a genome-scale level (**Man. 1**). A genome-wide microarray-based identification of type II transcriptional memory genes previously reported the identification of 89 genes that show enhanced re-induction when triggered 3 d after a priming HS (H. Liu *et al.*, 2018). This analysis revealed further that enhanced re-induction of almost all type II memory genes is lost in *hsfa2* (H. Liu *et al.*, 2018), indicating that functional HSFA2 is essential for type II transcriptional memory in *Arabidopsis*. Our findings in **Man. 1** support a predominant role of HSFA2 as mediator of type II transcriptional memory, as *hsfa3* seedlings were unaffected in type II transcriptional memory of several assessed candidate genes (**Man. 1 Fig 5**). Interestingly, HSFA3 was able to mediate type II transcriptional memory if expressed under control of the *HSFA2* promoter in the *hsfa2* background (**Man. 1 Fig 10b**), suggesting that HSFA2 and HSFA3 are redundant on the protein level and correct timing of expression and total HSF protein levels may be more important properties. Importantly, *HSFA2* itself is induced to similar levels after both priming and triggering HS (H. Liu *et al.*, 2018). Additionally, our data indicate that type II transcriptional memory does not solely depend on residual HSFA2 that is still around at the time of the triggering HS, as the chimeric HSF OD(A1D), which is not detectable anymore at this time in contrast to HSFA2 (**Man. 3 Fig S5**), still mediates type II transcriptional memory (**Man. 3 Fig 7a**).

One possible hypothesis to explain enhanced re-induction upon recurrent HS would be the presence/activity of an additional transcriptional regulator that is absent/inactive upon the first HS.

Such a factor may have a (-/+) or (0/+) transcription pattern, i.e., it is repressed or not upregulated after single HS, but expressed after repeated HS. Therefore, the expression pattern of this factor may itself be a form of transcriptional memory. Additionally, transcription and/or activity of this additional factor has to depend directly or indirectly on

HSFA2. A similar scenario has been proposed for the expression of dehydration stress (+/-) memory genes. Their expression depends on MYC2, which is itself a (+/-) memory gene, but the reason for its transcriptional pattern is unclear (Liu *et al.*, 2014; Liu, Staswick and Avramova, 2016; Avramova, 2019). An alternative explanation for enhanced re-induction of HS memory genes is that HSFA2 may induce chromatin changes after priming HS that confer the hyper-inducibility. A combination of both mechanisms is also possible.

The *pAPX2::LUC* reporter line (H. Liu *et al.*, 2018) that I used in **Man. 2** is currently being employed in our lab to screen for, and eventually functionally characterize, mutants that are affected in type II transcriptional memory. It will be interesting to see if there are any TFs or Mediator complex subunits among the identified candidate genes, as this would suggest a conserved type II transcriptional memory mechanism in response to different abiotic stresses in plants. Secondly, it will also be interesting to see whether this screen yields any mutants that are specifically affected in type II, but not type I, transcriptional memory. As HSFA2 is the key regulator of type II transcriptional memory, for any candidate genes identified by this screen it must be carefully evaluated whether they exercise a regulatory function on *HSFA2* or act independently of it. Candidate genes encoding a negative regulator of *HSFA2* may however still give novel insight into the regulation of *HSFA2*.

It is known that the sets of type I and type II transcriptional memory genes are partially overlapping (*APX2*, for example, shows both types of transcriptional memory (Lämke *et al.*, 2016)). It would be interesting to explore this partial overlap in a genome-wide manner using the available datasets. In particular, it would be interesting to see to which extent type II transcriptional memory genes overlap with HSFA2- and HSFA3-regulated type I transcriptional memory genes. If genes exist where type II, but not type I, transcriptional memory depends on HSFA2, their study could shed light on the existence of independent molecular mechanisms mediating transcriptional memory that converge on the same set of genes.

Since as of now no specific regulator of type II transcriptional memory that does not also affect type I transcriptional memory is known, it is challenging to distinguish the individual contribution of type I and type II transcriptional memory to physiological HS memory. In our setup, physiological HS memory is investigated by exposing 4 d-old

seedlings first to a 2-step ACC treatment which is followed by exposure to severe HS 3 d later (see **Man. 3 Fig 2a**). Similarly, type I transcriptional memory is investigated in the memory phase after this same treatment (see **Man. 3 Fig 4c**), and numerous lines of evidence suggest that the two processes are tightly associated (**Man. 1**, **Man. 3**). Contrarily, type II transcriptional memory is commonly investigated by exposing 4 d-old seedlings to only a mild HS and then exposing them to the same stress on d 6 (see **Man. 3 Fig 5a**). These mild heat stresses are insufficient to interfere with growth and survival of seedlings (Hong, Lee and Vierling, 2003; Stief *et al.*, 2014). We have never investigated the transcription of genes in response to the severe triggering HS 3 d after ACC that is used to evaluate physiological HS memory, and we therefore do not know if type II memory genes, as defined by their transcription pattern in response to consecutive mild HS, would show a distinct transcriptional profile from type I transcriptional memory genes at this time point.

For HS, GO term enrichment analysis of *Arabidopsis* (+/++) type II memory genes revealed that these were overrepresented in genes involved in cellular lipid metabolic processes and carbohydrate metabolic processes (H. Liu *et al.*, 2018). Contrarily, (+/++) dehydration stress memory genes are associated with cell protective functions (Ding *et al.*, 2013). While this is true also for (+/++) dehydration stress memory genes in *Zea mays*, comparison of these two datasets revealed that homologous genes of the two species most often showed vastly different transcriptional profiles in response to repeated dehydration stress (Ding *et al.*, 2014).

Overall, our findings indicate that type I transcriptional memory is predominantly important for physiological HS memory. It is mediated by the concerted action of several processes, such as direct transcriptional regulation by memory HSFs and chromatin reassembly. Type II transcriptional memory has been reported in relation to several other stressors, and these and our findings support the hypothesis that there is an elevated degree of species- and stress-specificity of type II transcriptional memory. No specific regulators of type II transcriptional memory have been identified as of yet, and it will be interesting to see if there are any that are independent of the HS memory master regulator HSFA2.

Perspectives

The challenge of satisfying the increasing caloric needs of a steadily growing world population is multi-faceted (FAO, 2017). Among other aspects, climate change increases the frequency and intensity of extreme weather events such as drought and heat waves which will negatively influence crop yield (FAO, 2017; IPCC, 2021). Understanding the molecular mechanisms underlying priming of the plant response to heat stress is important, because it may allow targeted breeding or genetic engineering of crops that are more resistant to high temperature stress during their growing season, while at the same time minimally compromising their fitness in non-stressed conditions. The molecular mechanisms of HS memory in *Arabidopsis* have been partially elucidated and this thesis has contributed to their more detailed understanding.

In the near future it will be important to understand which are the most promising targets for biotechnological engineering. Since multiple abiotic stresses often occur at the same time, it is important to gain an understanding of potential cross-priming and cross-talk between different stress regulatory networks. Finally, knowledge obtained in model species must urgently be translated to agriculturally important crops.

Supplementary Material

Table S1: Results of mutant screen of HKMTs and HKDMs for altered physiological HS memory. Performance of the indicated mutant alleles in HS memory assays is reported as compared to their relative genetic background (Col-0 or Ws-0). ~, no difference to wild type; ↓, worse performance than wild type; ↑, better performance than wild type.

HKMTs				
mutant	**allele(s)**	**back-ground**	**physio-logical HS memory**	**additional information**
atx1-1	obtained from Zoya Avramova (reference: Alvarez-Venegas *et al.*, 2003; doi: 10.1016/S0960-9822(03)00243-4)	Ws-0	~	shoot apical meristem negatively affected; no obvious effect on seedling survival
sdg2-3	SALK_021008	Col-0	~	segregating; seedlings were genotyped after assay evaluation
sdg4-1	SALK_128444	Col-0	~	
sdg8-2	SALK_026442	Col-0	~	
sdg26-1	SALK_013895	Col-0	~	
sdg37-1	SALK_109558	Col-0	↓	unspecific phenotype: aTT also affected
atx1-2, sdg26-1	SALK_149002 (*atx1-2*), SALK_013895 (*sdg26-1*)	Col-0	~	
atx3-1, atx4-1, atx5-1	GK-128H01 (*atx3-1*), SALK_060156 (*atx4-1*), WiscDsLoxHs127_10D (*atx5-1*)	Col-0	↓	unspecific phenotype: aTT also affected
sdg2-3, sdg8-2	SALK_021008 (*sdg2-3*), SALK_026442 (*sdg8-2*)	Col-0	~	*sdg2-3* segregating; seedlings were genotyped after assay evaluation
sdg25-1, sdg26-1	SALK_149692 (*sdg25-1*), SALK_013895 (*sdg26-1*)	Col-0	~	
HKMDs				
mutant	**allele(s)**	**back-ground**	**physio-logical HS memory**	**additional information**
jmj14-1	SALK_135712	Col-0	~↓	low reproducibility of phenotype; weak phenotype

jmj15-1	GK-257F10	Col-0	~↓	low reproducibility of phenotype; weak phenotype
jmj16-1	SAIL_535_F09	Col-0	~	
jmj18-2	GK-649D05	Col-0	~↓	low reproducibility of phenotype; weak phenotype
jmj14-1, jmj15-1	SALK_135712 (*jmj14-1*), GK-257F10 (*jmj15-1*)	Col-0	↓	low reproducibility of phenotype; weak phenotype
jmj14-1, jmj18-2	SALK_135712 (*jmj14-1*), GK-649D05 (*jmj18-2*)	Col-0	↓	low reproducibility of phenotype; weak phenotype
jmj15-1, jmj18-2	GK-257F10 (*jmj15-1*), GK-649D05 (*jmj18-2*)	Col-0	↓	low reproducibility of phenotype; weak phenotype
jmj14-1, jmj15-1, jmj18-2	SALK_135712 (*jmj14-1*), GK-257F10 (*jmj15-1*), GK-649D05 (*jmj18-2*)	Col-0	↓	low reproducibility of phenotype; weak phenotype
ldl1-2	SALK_034869	Col-0	↑	low reproducibility of phenotype
ldl1-2, ldl2-2	SALK_034869 (*ldl1-2*), SALK_135831 (*ldl2-2*)	Col-0	↑	low reproducibility of phenotype
ldl1-2, ldl2-2, fld-1	SALK_034869 (*ldl1-2*), SALK_135831 (*ldl2-2*), *fld-1* was generated by CRISPR/Cas9-based mutagenesis of *ldl1-2, ldl2-2*	Col-0	~	

Bibliography

Here, all publications cited in the sections General Introduction, General Discussion, and Perspectives are listed alphabetically. Publications cited in the three presented manuscripts are excluded.

Albihlal, W.S. *et al.* (2018) Arabidopsis HEAT SHOCK TRANSCRIPTION FACTORA1b regulates multiple developmental genes under benign and stress conditions. *Journal of Experimental Botany*, **69**(11), pp. 2847–2862. doi:10.1093/jxb/ery142

Amasino, R. (2010) Seasonal and developmental timing of flowering. *The Plant Journal*, **61**(6), pp. 1001–1013. doi:10.1111/j.1365-313X.2010.04148.x

Avramova, Z. (2009) Evolution and pleiotropy of TRITHORAX function in Arabidopsis. *The International Journal of Developmental Biology*, **53**(2–3), pp. 371–381. doi:10.1387/ijdb.082664za

Avramova, Z. (2019) Defence-related priming and responses to recurring drought: Two manifestations of plant transcriptional memory mediated by the ABA and JA signalling pathways: dehydration stress memory and jasmonic acid priming. *Plant, Cell & Environment*, **42**(3), pp. 983–997. doi:10.1111/pce.13458

Balazadeh, S. (2022) A "hot" cocktail: The multiple layers of thermomemory in plants. *Current Opinion in Plant Biology*, **65**, 102147. doi:10.1016/j.pbi.2021.102147

Baniwal, S.K. *et al.* (2004) Heat stress response in plants: a complex game with chaperones and more than twenty heat stress transcription factors. *Journal of Biosciences*, **29**(4), pp. 471–487. doi:10.1007/BF02712120

Baniwal, S.K. *et al.* (2007) Role of Heat Stress Transcription Factor HsfA5 as Specific Repressor of HsfA4. *Journal of Biological Chemistry*, **282**(6), pp. 3605–3613. doi:10.1074/jbc.M609545200

Bäurle, I. (2018) Can't remember to forget you: Chromatin-based priming of somatic stress responses. *Seminars in Cell & Developmental Biology*, **83**, pp. 133–139. doi:10.1016/j.semcdb.2017.09.032

Bäurle, I. and Trindade, I. (2020) Chromatin regulation of somatic abiotic stress memory. *Journal of Experimental Botany*, **71**(17), pp. 5269-5279. doi:10.1093/jxb/eraa098

Berr, A. *et al.* (2009) SET DOMAIN GROUP25 Encodes a Histone Methyltransferase and Is Involved in FLOWERING LOCUS C Activation and Repression of Flowering. *Plant Physiology*, **151**(3), pp. 1476–1485. doi:10.1104/pp.109.143941

Bharti, K. *et al.* (2004) Tomato Heat Stress Transcription Factor HsfB1 Represents a Novel Type of General Transcription Coactivator with a Histone-Like Motif Interacting

with the Plant CREB Binding Protein Ortholog HAC1[W]. *The Plant Cell*, **16**(6), pp. 1521–1535. doi:10.1105/tpc.019927

Boehm, U. *et al.* (1997) CELLULAR RESPONSES TO INTERFERON-γ. *Annual Review of Immunology*, **15**(1), pp. 749–795. doi:10.1146/annurev.immunol.15.1.749

Brickner, D.G. *et al.* (2007) H2A.Z-Mediated Localization of Genes at the Nuclear Periphery Confers Epigenetic Memory of Previous Transcriptional State. *PLoS Biology*, **5**(4), e81. doi:10.1371/journal.pbio.0050081

Brzezinka, K. *et al.* (2016) Arabidopsis FORGETTER1 mediates stress-induced chromatin memory through nucleosome remodelling. *eLife*, **5**, e17061. doi:10.7554/eLife.17061

Brzezinka, K., Altmann, S. and Bäurle, I. (2019) BRUSHY1/TONSOKU/MGOUN3 is required for heat stress memory. *Plant, Cell & Environment*, **42**(3), pp. 771–781. doi:10.1111/pce.13365

Chan-Schaminet, K.Y. *et al.* (2009) Specific Interaction between Tomato HsfA1 and HsfA2 Creates Hetero-oligomeric Superactivator Complexes for Synergistic Activation of Heat Stress Gene Expression. *Journal of Biological Chemistry*, **284**(31), pp. 20848–20857. doi:10.1074/jbc.M109.007336

Charng, Y. *et al.* (2006) Arabidopsis Hsa32, a Novel Heat Shock Protein, Is Essential for Acquired Thermotolerance during Long Recovery after Acclimation. *Plant Physiology*, **140**(4), pp. 1297–1305. doi:10.1104/pp.105.074898

Charng, Y. *et al.* (2007) A Heat-Inducible Transcription Factor, HsfA2, Is Required for Extension of Acquired Thermotolerance in Arabidopsis. *Plant Physiology*, **143**(1), pp. 251–262. doi:10.1104/pp.106.091322

Chen, H. *et al.* (2010) Arabidopsis DREB2C functions as a transcriptional activator of HsfA3 during the heat stress response. *Biochemical and Biophysical Research Communications*, **401**(2), pp. 238–244. doi:10.1016/j.bbrc.2010.09.038

Chen, L.-Q. *et al.* (2017) ATX3, ATX4, and ATX5 Encode Putative H3K4 Methyltransferases and Are Critical for Plant Development. *Plant Physiology*, **174**(3), pp. 1795–1806. doi:10.1104/pp.16.01944

Chen, X., Hu, Y. and Zhou, D.-X. (2011) Epigenetic gene regulation by plant Jumonji group of histone demethylase. *Biochimica et Biophysica Acta*, **1809**(8), pp. 421–426. doi:10.1016/j.bbagrm.2011.03.004

Cheng, K. *et al.* (2019) Histone tales: lysine methylation, a protagonist in Arabidopsis development. *Journal of Experimental Botany*, **71**(3), pp. 793–807. doi:10.1093/jxb/erz435

Csorba, T. *et al.* (2014) Antisense COOLAIR mediates the coordinated switching of chromatin states at FLC during vernalization. *Proceedings of the National Academy of Sciences*, **111**(45), pp. 16160–16165. doi:10.1073/pnas.1419030111

Damberger, F.F. *et al.* (1994) Solution structure of the DNA-binding domain of the heat shock transcription factor determined by multidimensional heteronuclear magnetic resonance spectroscopy. *Protein Science*, **3**(10), pp. 1806–1821. doi:10.1002/pro.5560031020

De Vos, M. *et al.* (2005) Signal Signature and Transcriptome Changes of Arabidopsis During Pathogen and Insect Attack. *Molecular Plant-Microbe Interactions*, **18**(9), pp. 923–937. doi:10.1094/MPMI-18-0923

Ding, Y. *et al.* (2013) Four distinct types of dehydration stress memory genes in Arabidopsis thaliana. *BMC Plant Biology*, **13**(1), 229. doi:10.1186/1471-2229-13-229

Ding, Y. *et al.* (2014) Dehydration stress memory genes of Zea mays; comparison with Arabidopsis thaliana. *BMC Plant Biology*, **14**(1), 141. doi:10.1186/1471-2229-14-141

Ding, Y., Avramova, Z. and Fromm, M. (2011a) The Arabidopsis trithorax-like factor ATX1 functions in dehydration stress responses via ABA-dependent and ABA-independent pathways. *The Plant Journal*, **66**(5), pp. 735–744. doi:10.1111/j.1365-313X.2011.04534.x

Ding, Y., Avramova, Z. and Fromm, M. (2011b) Two Distinct Roles of ARABIDOPSIS HOMOLOG OF TRITHORAX1 (ATX1) at Promoters and within Transcribed Regions of ATX1-Regulated Genes. *The Plant Cell*, **23**(1), pp. 350–363. doi:10.1105/tpc.110.080150

Ding, Y., Fromm, M. and Avramova, Z. (2012) Multiple exposures to drought "train" transcriptional responses in Arabidopsis. *Nature Communications*, **3**(1), 740. doi:10.1038/ncomms1732

Döring, P. *et al.* (2000) The Role of AHA Motifs in the Activator Function of Tomato Heat Stress Transcription Factors HsfA1 and HsfA2. *The Plant Ce*ll, **12**(2), pp. 265-278. PMID: 10662862; PMCID: PMC139763

Doudna, J.A. and Charpentier, E. (2014) The new frontier of genome engineering with CRISPR-Cas9. *Science*, **346**(6213), 1258096. doi:10.1126/science.1258096

D'Urso, A. *et al.* (2016) Set1/COMPASS and Mediator are repurposed to promote epigenetic transcriptional memory. eLife, **5**, e16691. doi:10.7554/eLife.16691

Feng, X.J. *et al.* (2016) Light affects salt stress-induced transcriptional memory of P5CS1 in Arabidopsis. *Proceedings of the National Academy of Sciences*, **113**(51), pp. 8335-8343. doi:10.1073/pnas.1610670114

Food and Agriculture Organization of the United Nations (2017) The future of food and agriculture. Trends and challenges. Rome, 2017. ISSN: 2522-722X (online)

Friedrich, T. *et al.* (2019) Chromatin-based mechanisms of temperature memory in plants: Chromatin-based temperature memory in plants. *Plant, Cell & Environment*, **42**(3), pp. 762–770. doi:10.1111/pce.13373

Gallego-Bartolomé, J. *et al.* (2018) Targeted DNA demethylation of the Arabidopsis genome using the human TET1 catalytic domain. *Proceedings of the National Academy of Sciences*, **115**(9), pp. 2125-2134. doi:10.1073/pnas.1716945115

Gangloff, Y.-G. *et al.* (2001) The TFIID Components Human TAFII140 andDrosophila BIP2 (TAFII155) Are Novel Metazoan Homologues of Yeast TAFII47 Containing a Histone Fold and a PHD Finger. *Molecular and Cellular Biology*, **21**(15), pp. 5109–5121. doi:10.1128/MCB.21.15.5109-5121.2001

Ghoshal, B. *et al.* (2021) CRISPR-based targeting of DNA methylation in Arabidopsis thaliana by a bacterial CG-specific DNA methyltransferase. *Proceedings of the National Academy of Sciences*, **118**(23), e2125016118. doi:10.1073/pnas.2125016118

Gialitakis, M. *et al.* (2010) Gamma Interferon-Dependent Transcriptional Memory via Relocalization of a Gene Locus to PML Nuclear Bodies. *Molecular and Cellular Biology*, **30**(8), pp. 2046–2056. doi:10.1128/MCB.00906-09

Guo, L. *et al.* (2010) SET DOMAIN GROUP2 is the major histone H3 lysine 4 trimethyltransferase in Arabidopsis. *Proceedings of the National Academy of Sciences*, **107**(43), pp. 18557–18562. doi:10.1073/pnas.1010478107

Harrison, C.J., Bohm, A.A. and Nelson, H.C.M. (1994) Crystal Structure of the DNA Binding Domain of the Heat Shock Transcription Factor. *Science*, **263**(5144), pp. 224–227. doi:10.1126/science.8284672

Heo, J.B. and Sung, S. (2011) Vernalization-Mediated Epigenetic Silencing by a Long Intronic Noncoding RNA. *Science*, **331**(6013), pp. 76–79. doi:10.1126/science.1197349

Hilker, M. *et al.* (2016) Priming and memory of stress responses in organisms lacking a nervous system: Priming and memory of stress responses. *Biological Reviews*, **91**(4), pp. 1118–1133. doi:10.1111/brv.12215

Hong, E.-H. *et al.* (2009) Temporal and spatial expression patterns of nine Arabidopsis genes encoding Jumonji C-domain proteins. *Molecules and Cells*, **27**(4), pp. 481–490. doi:10.1007/s10059-009-0054-7

Hong, S.-W., Lee, U. and Vierling, E. (2003) Arabidopsis hot Mutants Define Multiple Functions Required for Acclimation to High Temperatures. *Plant Physiology*, **132**(2), pp. 757–767. doi:10.1104/pp.102.017145

van Hulten, M. *et al.* (2006) Costs and benefits of priming for defense in Arabidopsis. *Proceedings of the National Academy of Sciences*, **103**(14), pp. 5602–5607. doi:10.1073/pnas.0510213103

Hyun, K. *et al.* (2017) Writing, erasing and reading histone lysine methylations. *Experimental & Molecular Medicine*, **49**(4), e324. doi:10.1038/emm.2017.11

Ikeda, M., Mitsuda, N. and Ohme-Takagi, M. (2011) Arabidopsis HsfB1 and HsfB2b Act as Repressors of the Expression of Heat-Inducible Hsfs But Positively Regulate the Acquired Thermotolerance. *Plant Physiology*, **157**(3), pp. 1243–1254. doi:10.1104/pp.111.179036

Ikeda, M. and Ohme-Takagi, M. (2009) A Novel Group of Transcriptional Repressors in Arabidopsis. *Plant and Cell Physiology*, **50**(5), pp. 970–975. doi:10.1093/pcp/pcp048

IPCC (2021) Climate Change 2021: The Physical Science Basis. Contribution of Working Group I to the Sixth Assessment Report of the Intergovernmental Panel on Climate Change [Masson-Delmotte, V., P. Zhai, A. Pirani, S.L. Connors, C. Péan, S. Berger, N. Caud, Y. Chen, L. Goldfarb, M.I. Gomis, M. Huang, K. Leitzell, E. Lonnoy, J.B.R. Matthews, T.K. Maycock, T. Waterfield, O. Yelekçi, R. Yu, and B. Zhou (eds.)]. Cambridge University Press, Cambridge, United Kingdom and New York, NY, USA, In press. doi:10.1017/9781009157896

Iwata, Y. and Koizumi, N. (2005) An Arabidopsis transcription factor, AtbZIP60, regulates the endoplasmic reticulum stress response in a manner unique to plants. *Proceedings of the National Academy of Sciences*, **102**(14), pp. 5280–5285. doi:10.1073/pnas.0408941102

Jaskiewicz, M., Conrath, U. and Peterhänsel, C. (2011) Chromatin modification acts as a memory for systemic acquired resistance in the plant stress response. *EMBO Reports*, **12**(1), pp. 50–55. doi:10.1038/embor.2010.186

Jeong, J.-H. et al. (2009) Repression of FLOWERING LOCUS T Chromatin by Functionally Redundant Histone H3 Lysine 4 Demethylases in Arabidopsis. *PLoS ONE*, **4**(11), e8033. doi:10.1371/journal.pone.0008033

Jiang, D. *et al.* (2007) Arabidopsis Relatives of the Human Lysine-Specific Demethylase1 Repress the Expression of FWA and FLOWERING LOCUS C and Thus Promote the Floral Transition. *The Plant Cell*, **19**(10), pp. 2975–2987. doi:10.1105/tpc.107.052373

Jiang, D. *et al.* (2011) Arabidopsis COMPASS-Like Complexes Mediate Histone H3 Lysine-4 Trimethylation to Control Floral Transition and Plant Development. *PLoS Genetics*, **7**(3), e1001330. doi:10.1371/journal.pgen.1001330

Jinek, M. *et al.* (2012) A Programmable Dual-RNA–Guided DNA Endonuclease in Adaptive Bacterial Immunity. *Science*, **337**(6096), pp. 816–821. doi:10.1126/science.1225829

Kaplan, F. *et al.* (2004) Exploring the Temperature-Stress Metabolome of Arabidopsis. *Plant Physiology*, **136**(4), pp. 4159–4168. doi:10.1104/pp.104.052142

Kim, D.-H. and Sung, S. (2017) Vernalization-Triggered Intragenic Chromatin Loop Formation by Long Noncoding RNAs. *Developmental Cell*, **40**(3), pp. 302-312. doi:10.1016/j.devcel.2016.12.021

Kim, D.-H., Xi, Y. and Sung, S. (2017) Modular function of long noncoding RNA, COLDAIR, in the vernalization response. *PLOS Genetics*, **13**(7), e1006939. doi:10.1371/journal.pgen.1006939

Kim, J.-M. *et al.* (2012) Transition of Chromatin Status During the Process of Recovery from Drought Stress in Arabidopsis thaliana. *Plant and Cell Physiology*, **53**(5), pp. 847–856. doi:10.1093/pcp/pcs053

Kinoshita, A. and Richter, R. (2020) Genetic and molecular basis of floral induction in Arabidopsis thaliana. *Journal of Experimental Botany*, **71**(9), pp. 2490–2504. doi:10.1093/jxb/eraa057

Kotak, S. *et al.* (2007) Complexity of the heat stress response in plants. *Current Opinion in Plant Biology*, **10**(3), pp. 310–316. doi:10.1016/j.pbi.2007.04.011

Kumar, M. *et al.* (2009) Heat Shock Factors HsfB1 and HsfB2b Are Involved in the Regulation of Pdf1.2 Expression and Pathogen Resistance in Arabidopsis. *Molecular Plant*, **2**(1), pp. 152–165. doi:10.1093/mp/ssn095

Kumar, S.V. and Wigge, P.A. (2010) H2A.Z-Containing Nucleosomes Mediate the Thermosensory Response in Arabidopsis. *Cell*, **140**(1), pp. 136–147. doi:10.1016/j.cell.2009.11.006

Kumlehn, J. *et al.* (2018) The CRISPR/Cas revolution continues: From efficient gene editing for crop breeding to plant synthetic biology. *Journal of Integrative Plant Biology*, **60**(12), pp. 1127–1153. doi:10.1111/jipb.12734

Kundu, S., Horn, P.J. and Peterson, C.L. (2007) SWI/SNF is required for transcriptional memory at the yeast GAL gene cluster. *Genes & Development*, **21**(8), pp. 997–1004. doi:10.1101/gad.1506607

Lämke, J. *et al.* (2016) A hit-and-run heat shock factor governs sustained histone methylation and transcriptional stress memory. *The EMBO Journal*, **35**(2), pp. 162–175. doi:10.15252/embj.201592593

Lämke, J. and Bäurle, I. (2017) Epigenetic and chromatin-based mechanisms in environmental stress adaptation and stress memory in plants. *Genome Biology*, **18**, 124. doi:10.1186/s13059-017-1263-6

Lang-Mladek, C. *et al.* (2010) Transgenerational Inheritance and Resetting of Stress-Induced Loss of Epigenetic Gene Silencing in Arabidopsis. *Molecular Plant*, **3**(3), pp. 594–602. doi:10.1093/mp/ssq014

Larkindale, J. and Vierling, E. (2008) Core Genome Responses Involved in Acclimation to High Temperature. *Plant Physiology*, **146**(2), pp. 323–324. doi:10.1104/pp.107.112060

Lawit, S.J. *et al.* (2007) Yeast two-hybrid map of Arabidopsis TFIID. *Plant Molecular Biology*, **64**(1–2), pp. 73–87. doi:10.1007/s11103-007-9135-1

Lee, J.E. *et al.* (2019) CRISPR-based tools for targeted transcriptional and epigenetic regulation in plants. *PLoS ONE*, **14**(9), e0222778. doi:10.1371/journal.pone.0222778

Lee, K., Park, O.-S. and Seo, P.J. (2017) Arabidopsis ATXR2 deposits H3K36me3 at the promoters of LBD genes to facilitate cellular dedifferentiation. *Science Signaling*, **10**(507), eaan0316. doi:10.1126/scisignal.aan0316

Lee, K., Park, O.-S. and Seo, P.J. (2018) ATXR2 as a core regulator of de novo root organogenesis. *Plant Signaling & Behavior*, **13**(3), e1449543. doi:10.1080/15592324.2018.1449543

Lei, B. and Berger, F. (2020) H2A Variants in Arabidopsis: Versatile Regulators of Genome Activity. *Plant Communications*, **1**(1), 100015. doi:10.1016/j.xplc.2019.100015

Li, Q. *et al.* (2015) Understanding the Biochemical Basis of Temperature-Induced Lipid Pathway Adjustments in Plants. *The Plant Cell*, **27**(1), pp. 86–103. doi:10.1105/tpc.114.134338

Light, W.H. *et al.* (2010) Interaction of a DNA Zip Code with the Nuclear Pore Complex Promotes H2A.Z Incorporation and INO1 Transcriptional Memory. *Molecular Cell*, **40**(1), pp. 112–125. doi:10.1016/j.molcel.2010.09.007

Light, W.H. *et al.* (2013) A Conserved Role for Human Nup98 in Altering Chromatin Structure and Promoting Epigenetic Transcriptional Memory. *PLoS Biology*, **11**(3), e1001524. doi:10.1371/journal.pbio.1001524

Liu, C. *et al.* (2010) Histone Methylation in Higher Plants. *Annual Review of Plant Biology*, **61**(1), pp. 395–420. doi:10.1146/annurev.arplant.043008.091939

Liu, F. *et al.* (2007) The Arabidopsis RNA-Binding Protein FCA Requires a Lysine-Specific Demethylase 1 Homolog to Downregulate FLC. *Molecular Cell*, **28**(3), pp. 398–407. doi:10.1016/j.molcel.2007.10.018

Liu, H. *et al.* (2018) Distinct heat shock factors and chromatin modifications mediate the organ-autonomous transcriptional memory of heat stress. *The Plant Journal*, **95**(3), pp. 401–413. doi:10.1111/tpj.13958

Liu, H.-C., Liao, H.-T. and Charng, Y.-Y. (2011) The role of class A1 heat shock factors (HSFA1s) in response to heat and other stresses in Arabidopsis. *Plant, Cell & Environment*, **34**(5), pp. 738–751. doi:10.1111/j.1365-3040.2011.02278.x

Liu, H.-T. *et al.* (2007) Calmodulin-binding protein phosphatase PP7 is involved in thermotolerance in Arabidopsis. *Plant, Cell & Environment*, **30**(2), pp. 156–164. doi:10.1111/j.1365-3040.2006.01613.x

Liu, J.-X. *et al.* (2007) An Endoplasmic Reticulum Stress Response in Arabidopsis Is Mediated by Proteolytic Processing and Nuclear Relocation of a Membrane-Associated Transcription Factor, bZIP28. *The Plant Cell*, **19**(12), pp. 4111–4119. doi:10.1105/tpc.106.050021

Liu, J.-X. *et al.* (2008) An Endoplasmic Reticulum Stress Response in Arabidopsis Is Mediated by Proteolytic Processing and Nuclear Relocation of a Membrane-Associated Transcription Factor, bZIP28. *The Plant Cell*, **19**(12), pp. 4111–4119. doi:10.1105/tpc.106.050021

Liu, N. *et al.* (2014) Different gene-specific mechanisms determine the "revised-response" memory transcription patterns of a subset of A. thaliana dehydration stress responding genes. *Nucleic Acids Research*, **42**(9), pp. 5556–5566. doi:10.1093/nar/gku220

Liu, N. and Avramova, Z. (2016) Molecular mechanism of the priming by jasmonic acid of specific dehydration stress response genes in Arabidopsis. *Epigenetics & Chromatin*, **9**(1), 8. doi:10.1186/s13072-016-0057-5

Liu, N., Staswick, P.E. and Avramova, Z. (2016) Memory responses of jasmonic acid-associated Arabidopsis genes to a repeated dehydration stress: Transcriptional memory of JA genes to dehydration. *Plant, Cell & Environment*, **39**(11), pp. 2515–2529. doi:10.1111/pce.12806

Liu, P. *et al.* (2019) The Histone H3K4 Demethylase JMJ16 Represses Leaf Senescence in Arabidopsis. *The Plant Cell*, **31**(2), pp. 430–443. doi:10.1105/tpc.18.00693

Liu, Q. *et al.* (2020) The characterization of Mediator 12 and 13 as conditional positive gene regulators in Arabidopsis. *Nature Communications*, **11**(1), 2798. doi:10.1038/s41467-020-16651-5

Liu, Y. *et al.* (2018) Trithorax-group proteins ARABIDOPSIS TRITHORAX4 (ATX4) and ATX5 function in abscisic acid and dehydration stress responses. *New Phytologist*, **217**(4), pp. 1582–1597. doi:10.1111/nph.14933

Lu, F. *et al.* (2010) JMJ14 is an H3K4 demethylase regulating flowering time in Arabidopsis. *Cell Research*, **20**(3), pp. 387–390. doi:10.1038/cr.2010.27

Luger, K. (1997) Crystal structure of the nucleosome core particle at 2.8 Å resolution. *Nature*, **389**, pp. 251-260. doi: 10.1038/38444

Luo, X. and He, Y. (2020) Experiencing winter for spring flowering: A molecular epigenetic perspective on vernalization. *Journal of Integrative Plant Biology*, **62**(1), pp. 104–117. doi:10.1111/jipb.12896

Mahajan, S. and Tuteja, N. (2005) Cold, salinity and drought stresses: An overview. *Archives of Biochemistry and Biophysics*, **444**(2), pp. 139–158. doi:10.1016/j.abb.2005.10.018

Meiri, D. and Breiman, A. (2009) Arabidopsis ROF1 (FKBP62) modulates thermotolerance by interacting with HSP90.1 and affecting the accumulation of HsfA2-regulated sHSPs. *The Plant Journal*, **59**(3), pp. 387–399. doi:10.1111/j.1365-313X.2009.03878.x

Mittler, R., Finka, A. and Goloubinoff, P. (2012) How do plants feel the heat?. *Trends in Biochemical Sciences*, **37**(3), pp. 118–125. doi:10.1016/j.tibs.2011.11.007

Mizuguchi, G. *et al.* (2004) ATP-Driven Exchange of Histone H2AZ Variant Catalyzed by SWR1 Chromatin Remodeling Complex. *Science*, **303**(5656), pp. 343–348. doi:10.1126/science.1090701

Naumann, K. *et al.* (2005) Pivotal role of AtSUVH2 in heterochromatic histone methylation and gene silencing in Arabidopsis. *The EMBO Journal*, **24**(7), pp. 1418–1429. doi:10.1038/sj.emboj.7600604

Ng, D.W.-K. *et al.* (2007) Plant SET domain-containing proteins: Structure, function and regulation. *Biochimica et Biophysica Acta*, **1769**(5–6), pp. 316–329. doi:10.1016/j.bbaexp.2007.04.003

Ng, H.H. *et al.* (2003) Targeted Recruitment of Set1 Histone Methylase by Elongating Pol II Provides a Localized Mark and Memory of Recent Transcriptional Activity. *Molecular Cell*, **11**(3), pp. 709–719. doi:10.1016/S1097-2765(03)00092-3

Ning, Y.-Q. *et al.* (2015) Two novel NAC transcription factors regulate gene expression and flowering time by associating with the histone demethylase JMJ14. *Nucleic Acids Research*, **43**(3), pp. 1469–1484. doi:10.1093/nar/gku1382

Nishimura, N. *et al.* (2004) Isolation and Characterization of Novel Mutants Affecting the Abscisic Acid Sensitivity of Arabidopsis Germination and Seedling Growth. *Plant and Cell Physiology*, **45**(10), pp. 1485–1499. doi:10.1093/pcp/pch171

Nover, L., Bharti, K. and Scharf, K.-D. (2001) Arabidopsis and the heat stress transcription factor world: how many heat stress transcription factors do we need?. *Cell Stress Chaperones*, **6**(3), pp. 177-189. doi: 10.1379/1466-1268(2001)006<0177:aathst>2.0.co;2

Oberkofler, V., Pratx, L. and Bäurle, I. (2021) Epigenetic regulation of abiotic stress memory: maintaining the good things while they last. *Current Opinion in Plant Biology*, **61**, 102007. doi:10.1016/j.pbi.2021.102007

Ohama, N. *et al.* (2016) The Transcriptional Cascade in the Heat Stress Response of Arabidopsis Is Strictly Regulated at the Level of Transcription Factor Expression. *The Plant Cell*, **28**(1), pp. 181–201. doi:10.1105/tpc.15.00435

Ohama, N. *et al.* (2017) Transcriptional Regulatory Network of Plant Heat Stress Response. *Trends in Plant Science*, **22**(1), pp. 53–65. doi:10.1016/j.tplants.2016.08.015

Olas, J.J. *et al.* (2021) Primary carbohydrate metabolism genes participate in heat-stress memory at the shoot apical meristem of Arabidopsis thaliana. *Molecular Plant*, **14**(9), pp. 1508–1524. doi:10.1016/j.molp.2021.05.024

Pecinka, A. *et al.* (2010) Epigenetic Regulation of Repetitive Elements Is Attenuated by Prolonged Heat Stress in Arabidopsis. *The Plant Cell*, **22**(9), pp. 3118–3129. doi:10.1105/tpc.110.078493

Peteranderl, R. *et al.* (1999) Biochemical and Biophysical Characterization of the Trimerization Domain from the Heat Shock Transcription Factor. *Biochemistry*, **38**(12), pp. 3559–3569. doi:10.1021/bi981774j

Peteranderl, R. and Nelson, H.C.M. (1992) Trimerization of the heat shock transcription factor by a triple-stranded alpha-helical coiled-coil. *Biochemistry*, **31**(48), pp. 12272–12276. doi:10.1021/bi00163a042

Pfluger, J. and Wagner, D. (2007) Histone modifications and dynamic regulation of genome accessibility in plants. *Current Opinion in Plant Biology*, **10**(6), pp. 645–652. doi:10.1016/j.pbi.2007.07.013

Pontvianne, F., Blevins, T. and Pikaard, C.S. (2010) Arabidopsis Histone Lysine Methyltransferases. *Advances in Botanical Research* **53**, pp. 1–22. doi:10.1016/S0065-2296(10)53001-5

Qi, L.S. *et al.* (2013) Repurposing CRISPR as an RNA-Guided Platform for Sequence-Specific Control of Gene Expression. *Cell*, **152**(5), pp. 1173–1183. doi:10.1016/j.cell.2013.02.022

Qian, C. and Zhou, M.-M. (2006) SET domain protein lysine methyltransferases: Structure, specificity and catalysis. *Cellular and Molecular Life Sciences*, **63**(23), pp. 2755–2763. doi:10.1007/s00018-006-6274-5

Qin, X. and Zeevaart, J.A.D. (1999) The 9-cis-epoxycarotenoid cleavage reaction is the key regulatory step of abscisic acid biosynthesis in water-stressed bean. *Proceedings of the National Academy of Sciences*, **96**(26), pp. 15354–15361. doi:10.1073/pnas.96.26.15354

Reindl, A. *et al.* (1997) Phosphorylation by a Cyclin-Dependent Kinase Modulates DNA Binding of the Arabidopsis Heat-Shock Transcription Factor HSF1 in Vitro. *Plant Physiology*, **115**(1), pp. 93-100. doi: 10.1104/pp.115.1.93

Richter, K., Haslbeck, M. and Buchner, J. (2010) The Heat Shock Response: Life on the Verge of Death. *Molecular Cell*, **40**(2), pp. 253–266. doi:10.1016/j.molcel.2010.10.006

Roca Paixão, J.F. *et al.* (2019) Improved drought stress tolerance in Arabidopsis by CRISPR/dCas9 fusion with a Histone AcetylTransferase. *Scientific Reports*, **9**(1), 8080. doi:10.1038/s41598-019-44571-y

Rothbart, S.B. and Strahl, B.D. (2014) Interpreting the language of histone and DNA modifications. *Biochimica et Biophysica Acta*, **1839**(8), pp. 627–643. doi:10.1016/j.bbagrm.2014.03.001

Roudier, F. *et al.* (2011) Integrative epigenomic mapping defines four main chromatin states in Arabidopsis: Organization of the Arabidopsis epigenome. *The EMBO Journal*, **30**(10), pp. 1928–1938. doi:10.1038/emboj.2011.103

Sakuma, Y. *et al.* (2006) Dual function of an Arabidopsis transcription factor DREB2A in water-stress-responsive and heat-stress-responsive gene expression. *Proceedings of the National Academy of Sciences*, **103**(49), pp. 18822–18827. doi:10.1073/pnas.0605639103

Sani, E. *et al.* (2013) Hyperosmotic priming of Arabidopsis seedlings establishes a long-term somatic memory accompanied by specific changes of the epigenome. *Genome Biology*, **14**, R59. doi:10.1186/gb-2013-14-6-r59

Saredi, G. *et al.* (2016) H4K20me0 marks post-replicative chromatin and recruits the TONSL–MMS22L DNA repair complex. *Nature*, **534**(7609), pp. 714–718. doi:10.1038/nature18312

Scharf, K.-D. *et al.* (2012) The plant heat stress transcription factor (Hsf) family: Structure, function and evolution. *Biochimica et Biophysica Acta*, **1819**(2), pp. 104–119. doi:10.1016/j.bbagrm.2011.10.002

Scheid, R., Chen, J. and Zhong, X. (2021) Biological role and mechanism of chromatin readers in plants. *Current Opinion in Plant Biology*, **61**, 102008. doi:10.1016/j.pbi.2021.102008

Schramm, F. *et al.* (2007) A cascade of transcription factor DREB2A and heat stress transcription factor HsfA3 regulates the heat stress response of Arabidopsis: Role of Arabidopsis HsfA3. *The Plant Journal*, **53**(2), pp. 264–274. doi:10.1111/j.1365-313X.2007.03334.x

Sedaghatmehr, M. *et al.* (2021) Autophagy complements metalloprotease FtsH6 in degrading plastid heat shock protein HSP21 during heat stress recovery. *Journal of Experimental Botany*, **72**(21), pp. 7498–7513. doi:10.1093/jxb/erab304

Sedaghatmehr, M., Mueller-Roeber, B. and Balazadeh, S. (2016) The plastid metalloprotease FtsH6 and small heat shock protein HSP21 jointly regulate thermomemory in Arabidopsis. *Nature Communications*, **7**(1), 12439. doi:10.1038/ncomms12439

Sequeira-Mendes, J. *et al.* (2014) The Functional Topography of the Arabidopsis Genome Is Organized in a Reduced Number of Linear Motifs of Chromatin States. *The Plant Cell*, **26**(6), pp. 2351–2366. doi:10.1105/tpc.114.124578

Sharma, M. *et al.* (2019) Glucose-Regulated HLP1 Acts as a Key Molecule in Governing Thermomemory. *Plant Physiology*, **180**(2), pp. 1081–1100. doi:10.1104/pp.18.01371

Shen, Y. *et al.* (2014) Over-expression of histone H3K4 demethylase gene JMJ15 enhances salt tolerance in Arabidopsis. *Frontiers in Plant Science*, **5**, 290. doi:10.3389/fpls.2014.00290

Shi, Yujiang *et al.* (2004) Histone Demethylation Mediated by the Nuclear Amine Oxidase Homolog LSD1. *Cell*, **119**(7), pp. 941–953. doi:10.1016/j.cell.2004.12.012

Song, Z.-T. *et al.* (2015) Transcription factor interaction with COMPASS-like complex regulates histone H3K4 trimethylation for specific gene expression in plants. *Proceedings of the National Academy of Sciences*, **112**(9), pp. 2900–2905. doi:10.1073/pnas.1419703112

Song, Z.-T. *et al.* (2020) Histone H3K4 methyltransferases SDG25 and ATX1 maintain heat-stress gene expression during recovery in Arabidopsis. *The Plant Journal*, **105**(5), pp. 1326-1338. doi: 10.1111/tpj.15114

Stief, A. *et al.* (2014) Arabidopsis miR156 Regulates Tolerance to Recurring Environmental Stress through SPL Transcription Factors. *The Plant Cell*, **26**(4), pp. 1792–1807. doi:10.1105/tpc.114.123851

Swiezewski, S. *et al.* (2009) Cold-induced silencing by long antisense transcripts of an Arabidopsis Polycomb target. *Nature*, **462**(7274), pp. 799–802. doi:10.1038/nature08618

Swindell, W.R., Huebner, M. and Weber, A.P. (2007) Transcriptional profiling of Arabidopsis heat shock proteins and transcription factors reveals extensive overlap between heat and non-heat stress response pathways. *BMC Genomics*, **8**(1), 125. doi:10.1186/1471-2164-8-125

Takeda, S. *et al.* (2004) BRU1, a novel link between responses to DNA damage and epigenetic gene silencing in Arabidopsis. *Genes & Development*, **18**(7), pp. 782–793. doi:10.1101/gad.295404

Tamada, Y. *et al.* (2009) ARABIDOPSIS TRITHORAX-RELATED7 Is Required for Methylation of Lysine 4 of Histone H3 and for Transcriptional Activation of FLOWERING LOCUS C. *The Plant Cell*, **21**(10), pp. 3257–3269. doi:10.1105/tpc.109.070060

Tian, Y. *et al.* (2019) PRC2 recruitment and H3K27me3 deposition at FLC require FCA binding of COOLAIR. *Science Advances*, **5**, eaau7246. doi:10.1126/sciadv.aau7246

Tittel-Elmer, M. *et al.* (2010) Stress-Induced Activation of Heterochromatic Transcription. *PLoS Genetics*, **6**(10), e1001175. doi:10.1371/journal.pgen.1001175

Tsukada, Y. *et al.* (2006) Histone demethylation by a family of JmjC domain-containing proteins. *Nature*, **439**(7078), pp. 811–816. doi:10.1038/nature04433

Ueda, M. and Seki, M. (2020) Histone Modifications Form Epigenetic Regulatory Networks to Regulate Abiotic Stress Response. *Plant Physiology*, **182**(1), pp. 15–26. doi:10.1104/pp.19.00988

Urrea Castellanos, R. *et al.* (2020) FORGETTER2 protein phosphatase and phospholipase D modulate heat stress memory in Arabidopsis. *The Plant Journal*, **104**(1), pp. 7–17. doi:10.1111/tpj.14927

Vanderauwera, S. *et al.* (2011) Extranuclear protection of chromosomal DNA from oxidative stress. *Proceedings of the National Academy of Sciences*, **108**(4), pp. 1711–1716. doi:10.1073/pnas.1018359108

Vermeulen, M. *et al.* (2007) Selective Anchoring of TFIID to Nucleosomes by Trimethylation of Histone H3 Lysine 4. *Cell*, **131**(1), pp. 58–69. doi:10.1016/j.cell.2007.08.016

Vuister, G.W. *et al.* (1994) NMR evidence for similarities between the DNA-binding regions of Drosophila melanogaster heat shock factor and the helix-turn-helix and HNF-3/forkhead families of transcription factors. *Biochemistry*, **33**(1), pp. 10–16. doi:10.1021/bi00167a002

Wang, L. *et al.* (2014) Hydrogen Peroxide Acts Upstream of Nitric Oxide in the Heat Shock Pathway in Arabidopsis Seedlings. *Plant Physiology*, **164**(4), pp. 2184–2196. doi:10.1104/pp.113.229369

Wang, X. *et al.* (2018) Evolutionary Origin, Gradual Accumulation and Functional Divergence of Heat Shock Factor Gene Family with Plant Evolution. *Frontiers in Plant Science*, **9**, 71. doi:10.3389/fpls.2018.00071

Weng, M. *et al.* (2014) Histone chaperone ASF1 is involved in gene transcription activation in response to heat stress in A rabidopsis thaliana: AtASF1 in heat stress response. *Plant, Cell & Environment*, **37**(9), pp. 2128–2138. doi:10.1111/pce.12299

Wu, C. (1995) Heat Shock Transcription Factors: Structure and Regulation. *Annual Review of Cell and Developmental Biology*, **11**, pp. 441-469. doi: 10.1146/annurev.cb.11.110195.002301

Xiao, J., Lee, U.-S. and Wagner, D. (2016) Tug of war: adding and removing histone lysine methylation in Arabidopsis. *Current Opinion in Plant Biology*, **34**, pp. 41–53. doi:10.1016/j.pbi.2016.08.002

Xuan, Y. *et al.* (2010) Nitric Oxide Functions as a Signal and Acts Upstream of AtCaM3 in Thermotolerance in Arabidopsis Seedlings. *Plant Physiology*, **153**(4), pp. 1895–1906. doi:10.1104/pp.110.160424

Yamaguchi, N. *et al.* (2021) H3K27me3 demethylases alter HSP22 and HSP17.6C expression in response to recurring heat in Arabidopsis. *Nature Communications*, **12**(1), 3480. doi:10.1038/s41467-021-23766-w

Yang, H., Han, Z., *et al.* (2012) A Companion Cell–Dominant and Developmentally Regulated H3K4 Demethylase Controls Flowering Time in Arabidopsis via the Repression of FLC Expression. *PLoS Genetics*, **8**(4), e1002664. doi:10.1371/journal.pgen.1002664

Yang, H., Mo, H., *et al.* (2012) Overexpression of a histone H3K4 demethylase, JMJ15, accelerates flowering time in Arabidopsis. *Plant Cell Reports*, **31**(7), pp. 1297–1308. doi:10.1007/s00299-012-1249-5

Yang, W. *et al.* (2010) A plant-specific histone H3 lysine 4 demethylase represses the floral transition in Arabidopsis: Histone H3K4 demethylation and flowering. *The Plant Journal*, **62**(4), pp. 663–673. doi:10.1111/j.1365-313X.2010.04182.x

Yángüez, E. *et al.* (2013) Analysis of Genome-Wide Changes in the Translatome of Arabidopsis Seedlings Subjected to Heat Stress. *PLoS ONE*, **8**(8), e71425. doi:10.1371/journal.pone.0071425

Yeh, C.-H. *et al.* (2012) Some like it hot, some like it warm: Phenotyping to explore thermotolerance diversity. *Plant Science*, **195**, pp. 10–23. doi:10.1016/j.plantsci.2012.06.004

Yoshida, T. *et al.* (2006) ABA-Hypersensitive Germination3 Encodes a Protein Phosphatase 2C (AtPP2CA) That Strongly Regulates Abscisic Acid Signaling during Germination among Arabidopsis Protein Phosphatase 2Cs. *Plant Physiology*, **140**(1), pp. 115–126. doi:10.1104/pp.105.070128

Yoshida, T. *et al.* (2008) Functional analysis of an Arabidopsis heat-shock transcription factor HsfA3 in the transcriptional cascade downstream of the DREB2A stress-regulatory system. *Biochemical and Biophysical Research Communications*, **368**(3), pp. 515–521. doi:10.1016/j.bbrc.2008.01.134

Zang, D. *et al.* (2019) Arabidopsis heat shock transcription factor HSFA7b positively mediates salt stress tolerance by binding to an E-box-like motif to regulate gene expression. *Journal of Experimental Botany*, **70**(19), pp. 5355–5374. doi:10.1093/jxb/erz261

Zhang, S. *et al.* (2015) C-terminal domains of histone demethylase JMJ14 interact with a pair of NAC transcription factors to mediate specific chromatin association. *Cell Discovery*, **1**(1), 15003. doi:10.1038/celldisc.2015.3

Zhang, W. *et al.* (2009) Molecular and Genetic Evidence for the Key Role of AtCaM3 in Heat-Shock Signal Transduction in Arabidopsis. *Plant Physiology*, **149**(4), pp. 1773–1784. doi:10.1104/pp.108.133744

Zhang, X. *et al.* (2009) Genome-wide analysis of mono-, di- and trimethylation of histone H3 lysine 4 in Arabidopsis thaliana. *Genome Biology*, **10**, R62. doi:10.1186/gb-2009-10-6-r62